Look at the Earth's Interior with X-rays Through a Diamond Window

L. Dubrovinsky

BGI Bayerisches Geoinstitut

SPP 1236

ESRF

DESY

European Science Foundation

EuroMinScI
A EUROCORES PROGRAMME
EUROPEAN SCIENCE FOUNDATION COLLABORATIVE RESEARCH

ARGONNE NATIONAL LABORATORY

BGI Bayerisches Geoinstitut


nature
THE INTERNATIONAL WEEKLY JOURNAL OF SCIENCE
SIX NEW WORLDS

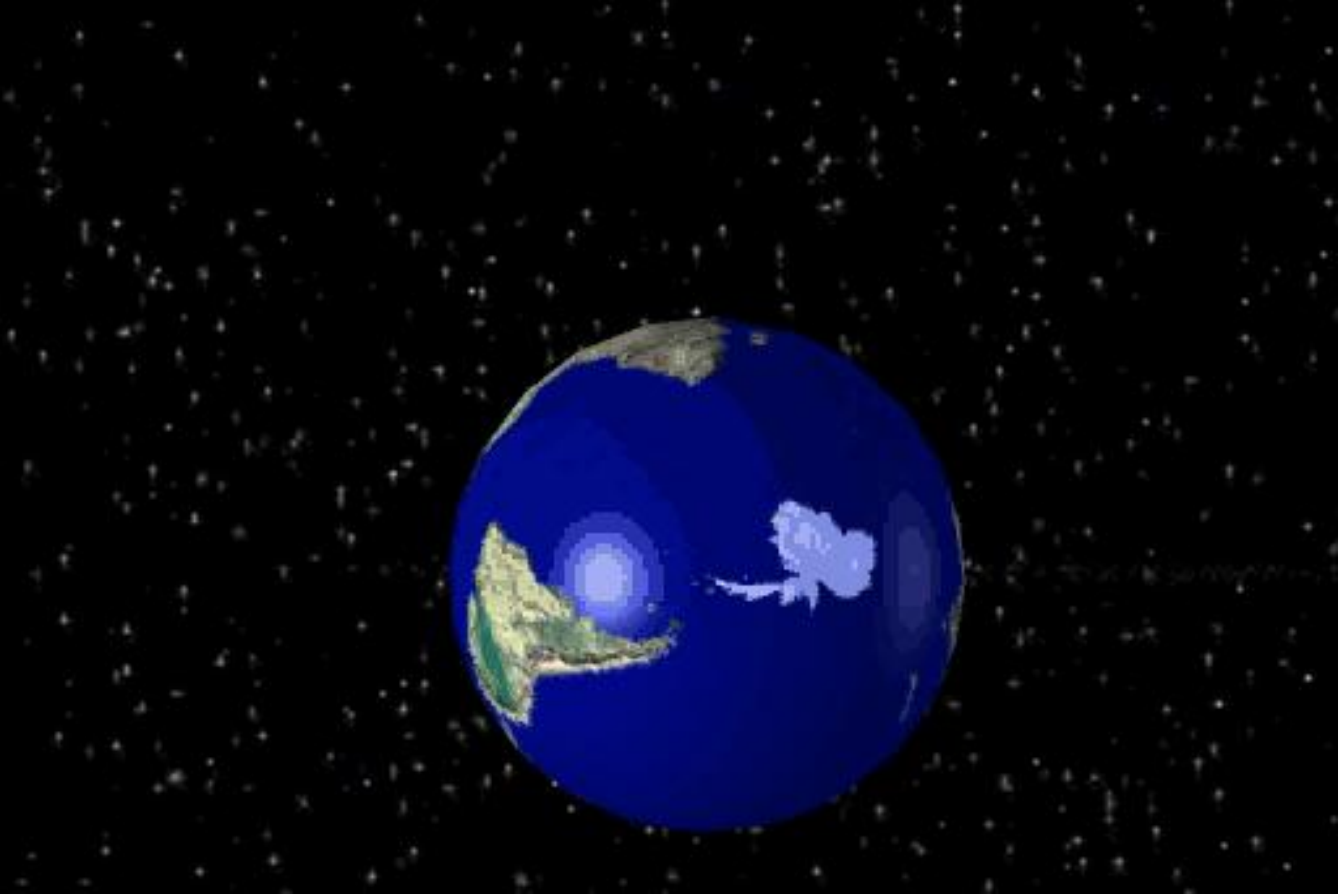

Looking deep into the Earth...

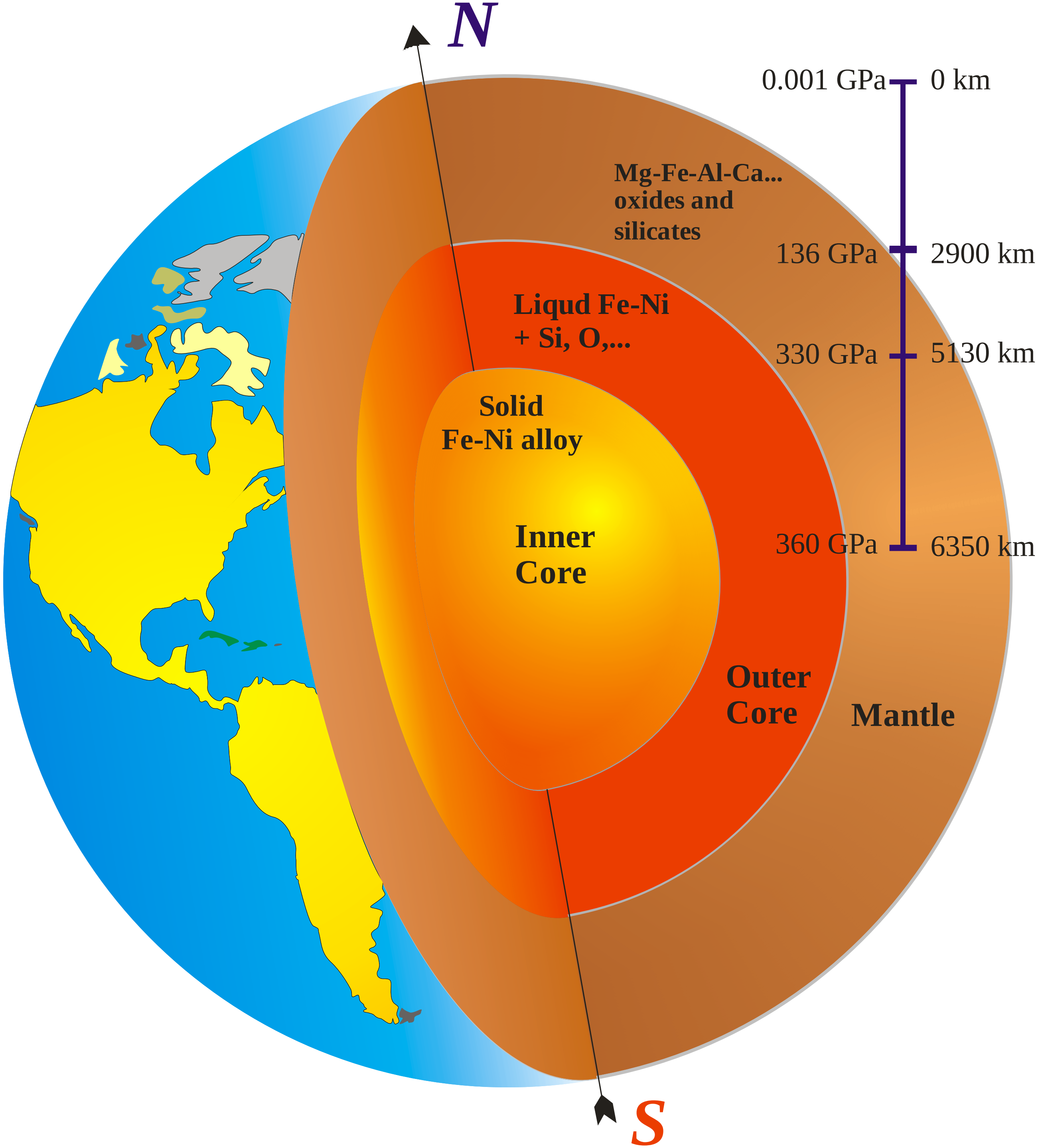

N
0.001 GPa
0 km
Mg-Fe-Al-Ca...
oxides and
silicates
136 GPa
2900 km
Liqud Fe-Ni
+ Si, O,...
330 GPa
5130 km
Solid
Fe-Ni alloy
Inner
Core
360 GPa
6350 km
Outer
Core
Mantle
S

P-and S-wave Pathways Through Earth

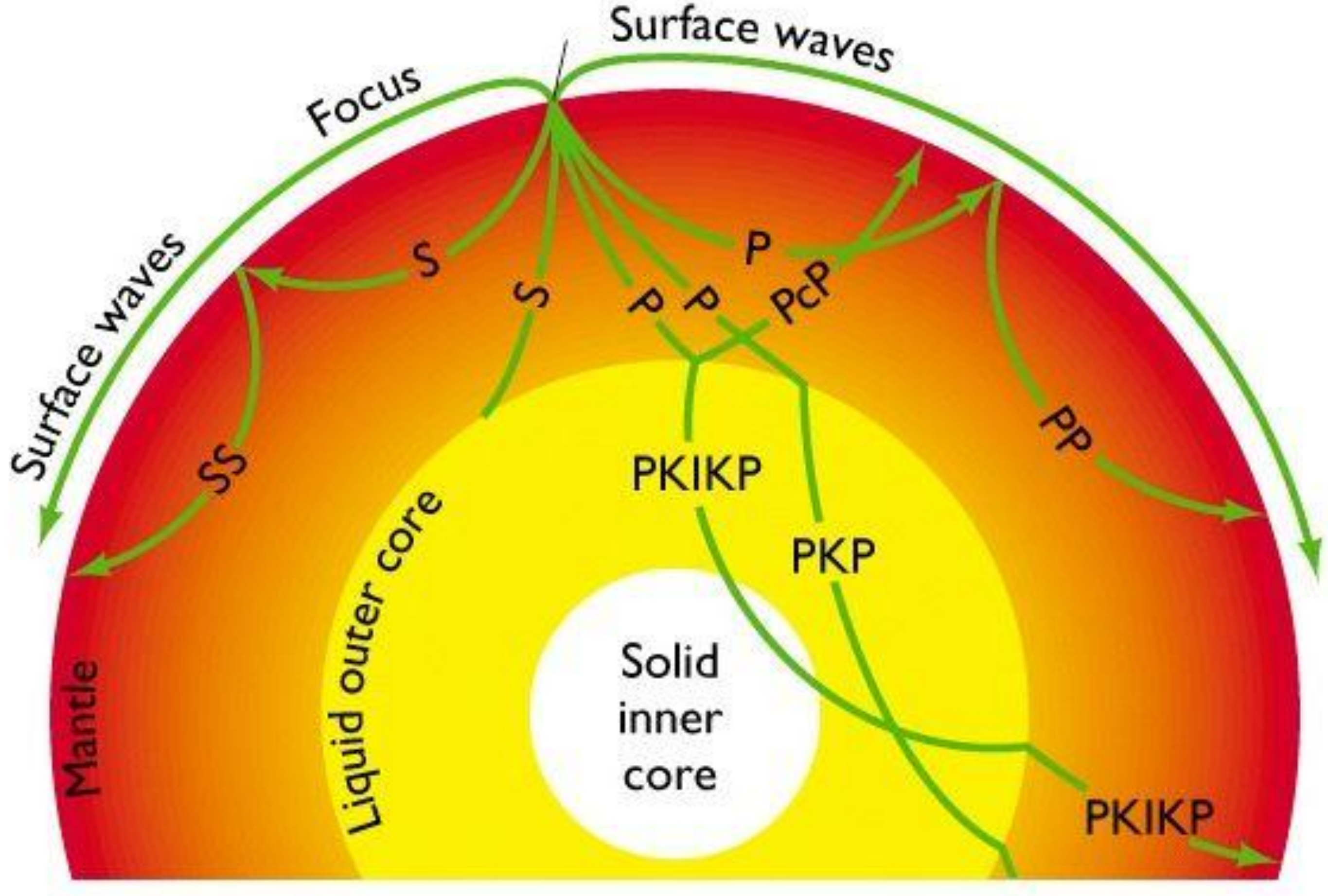

Fig. 19.3

Sequence of phase transitions in MgO-SiO_2 system at Earth mantle and transition zone

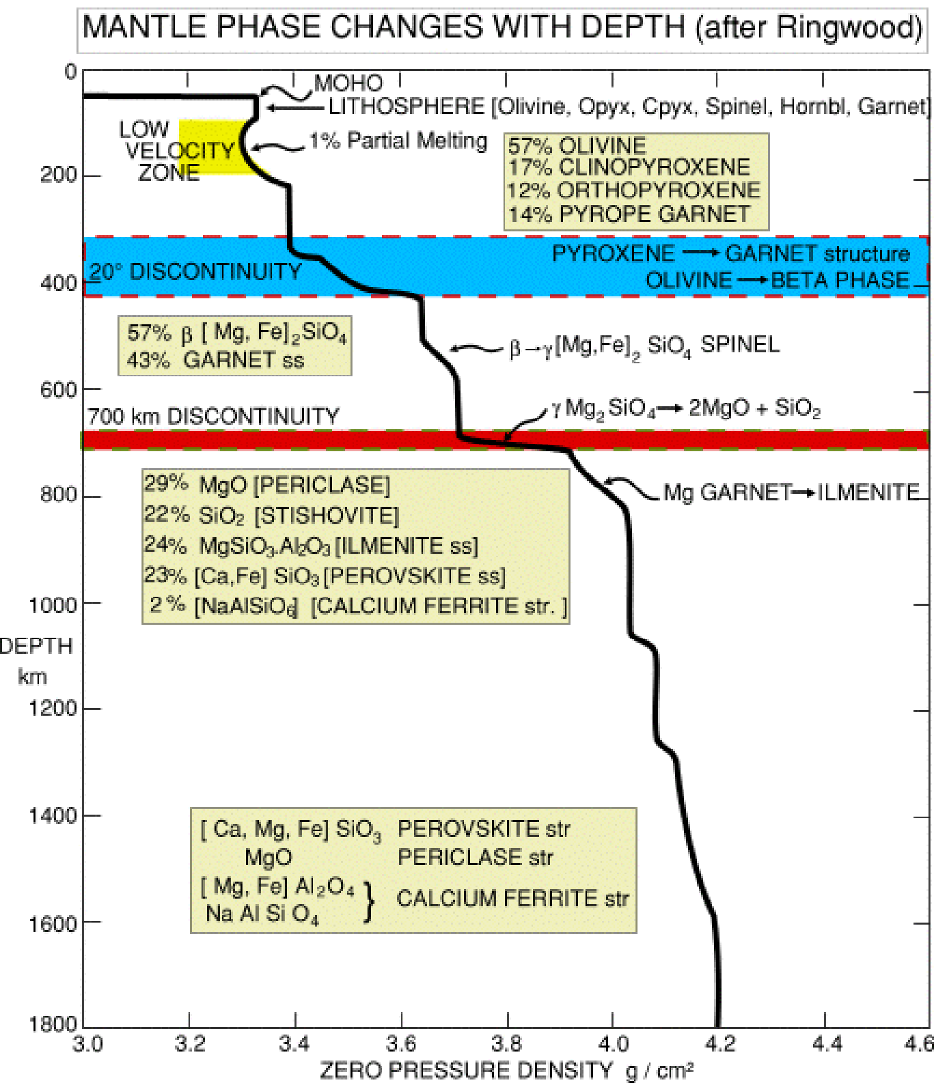

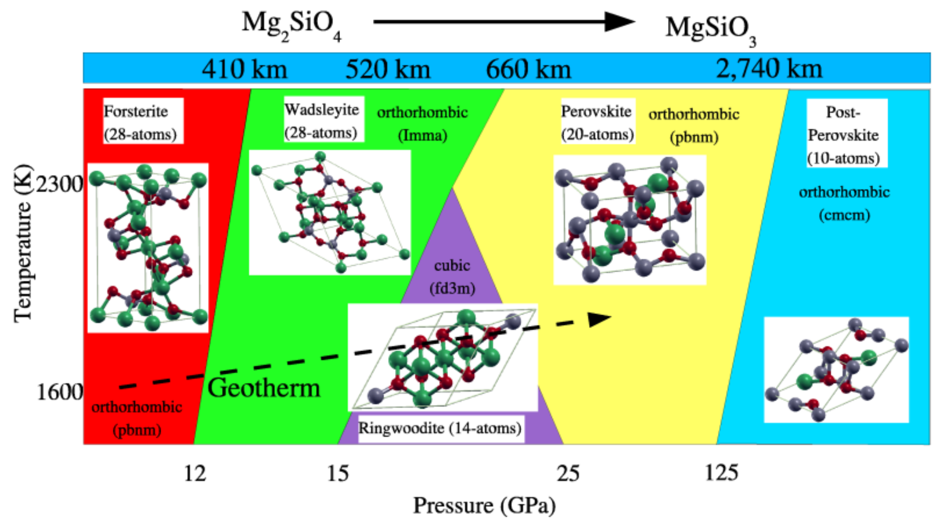

Iron content, valence and electronic state affect

- density of the phases
- sound velocity
- thermal conductivity
- electrical conductivity
- elements partitioning
- dynamics of the core and mantle

http://www.le.ac.uk/gl/art/gl209/Image12.gif http://www.physics.ohio-state.edu/~driver/research.html

Mantle velocity profiles and tomography

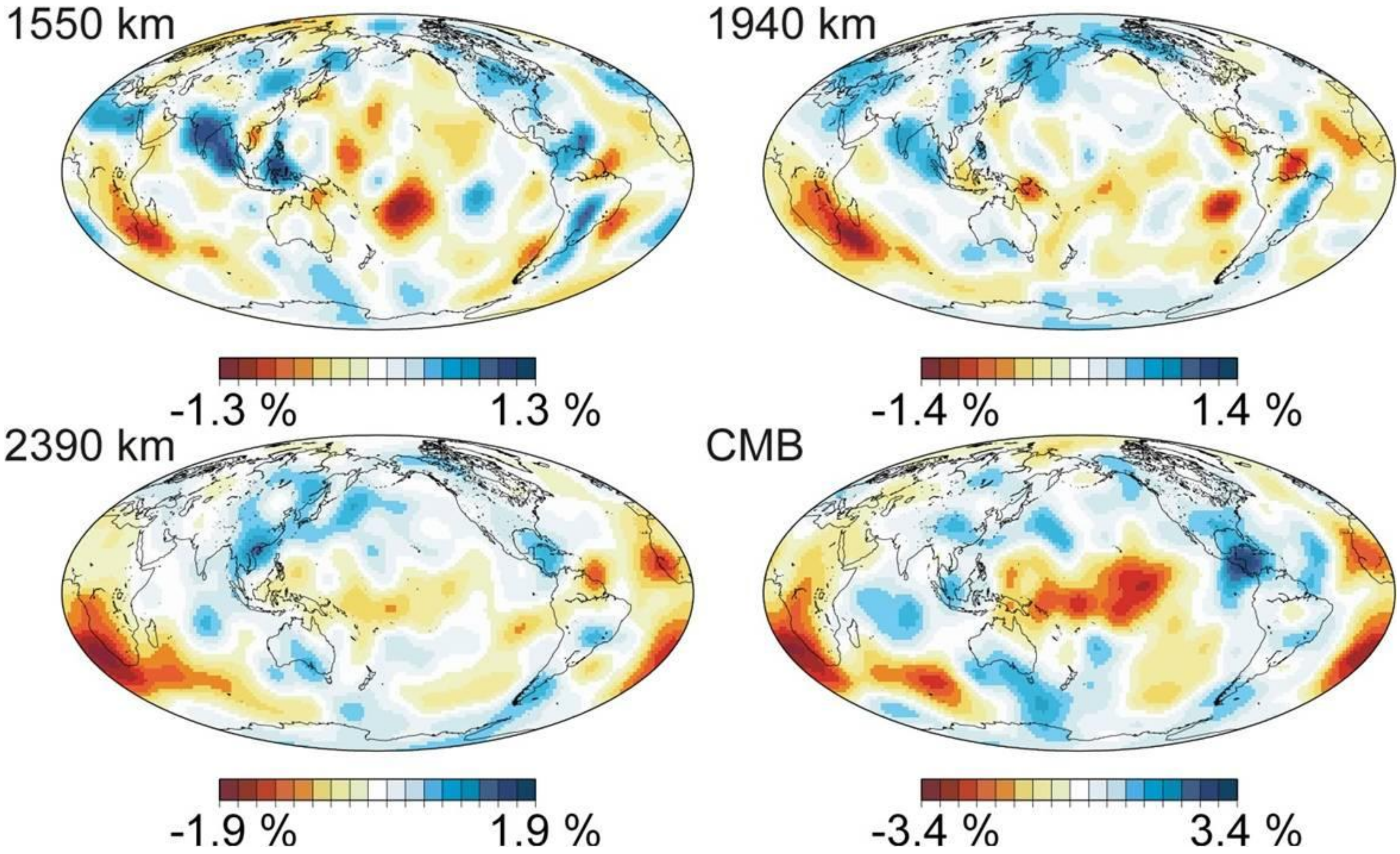

Takeuchi, N., 2007. J. Int., 169, 1153-1163

www.eri.u-tokyo.ac.jp/takeuchi/model/

Sequence of phase transitions in MgO-SiO_2 system at Earth mantle and transition zone

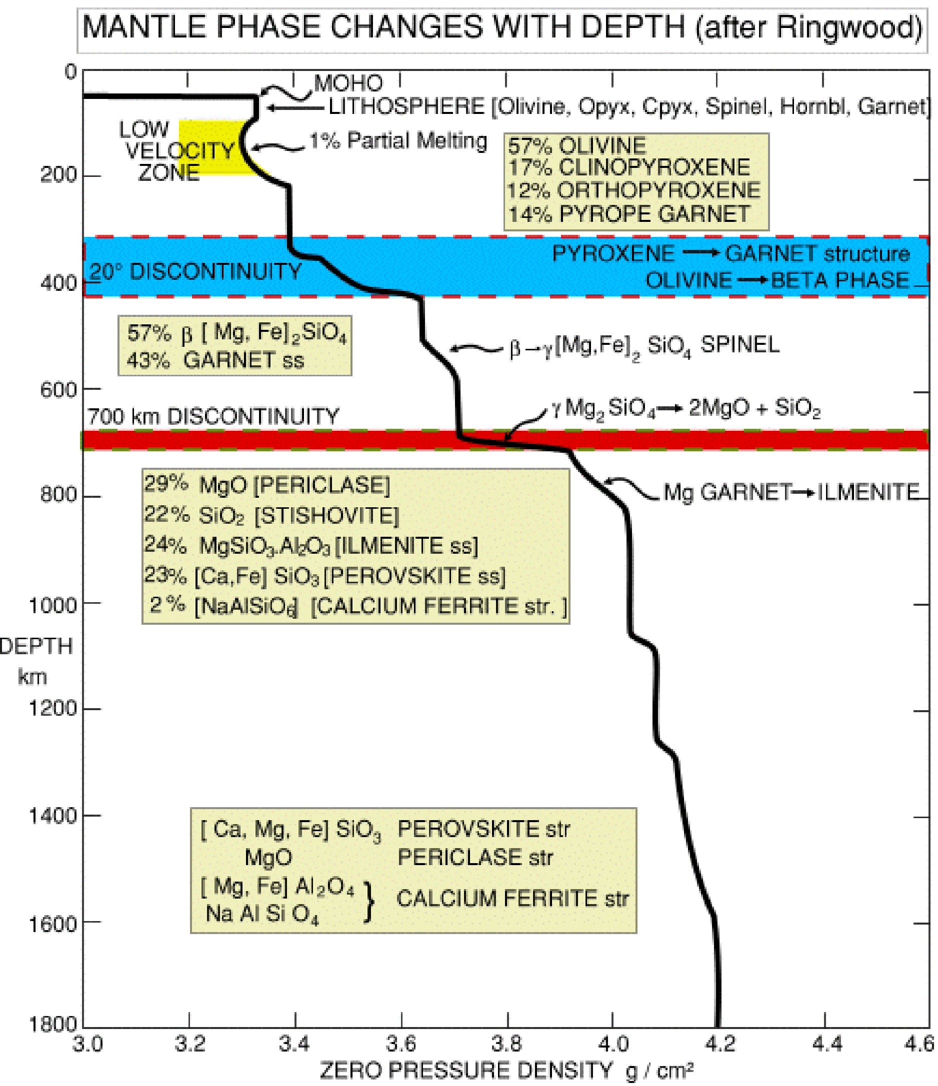

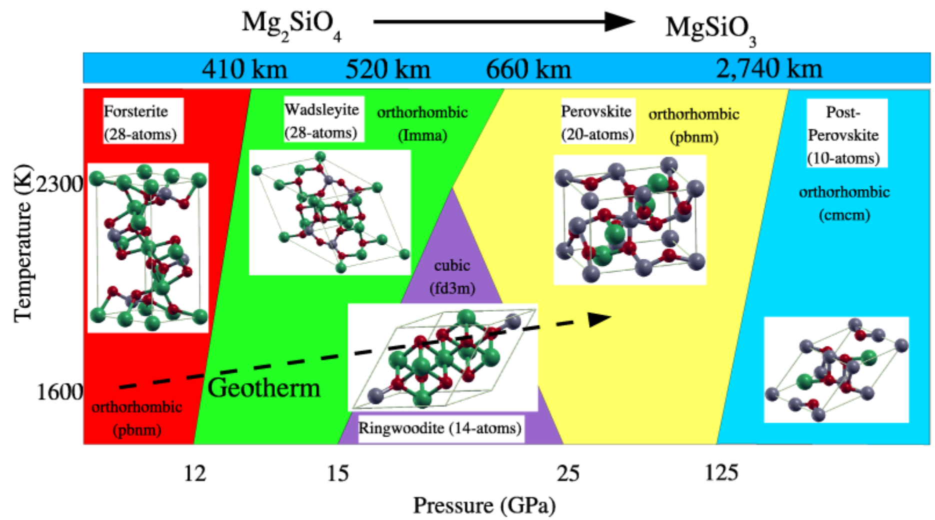

Iron content, valence and electronic state affect

- density of the phases
- sound velocity
- thermal conductivity
- electrical conductivity
- elements partitioning
- dynamics of the core and mantle

http://www.le.ac.uk/gl/art/gl209/Image12.gif http://www.physics.ohio-state.edu/~driver/research.html

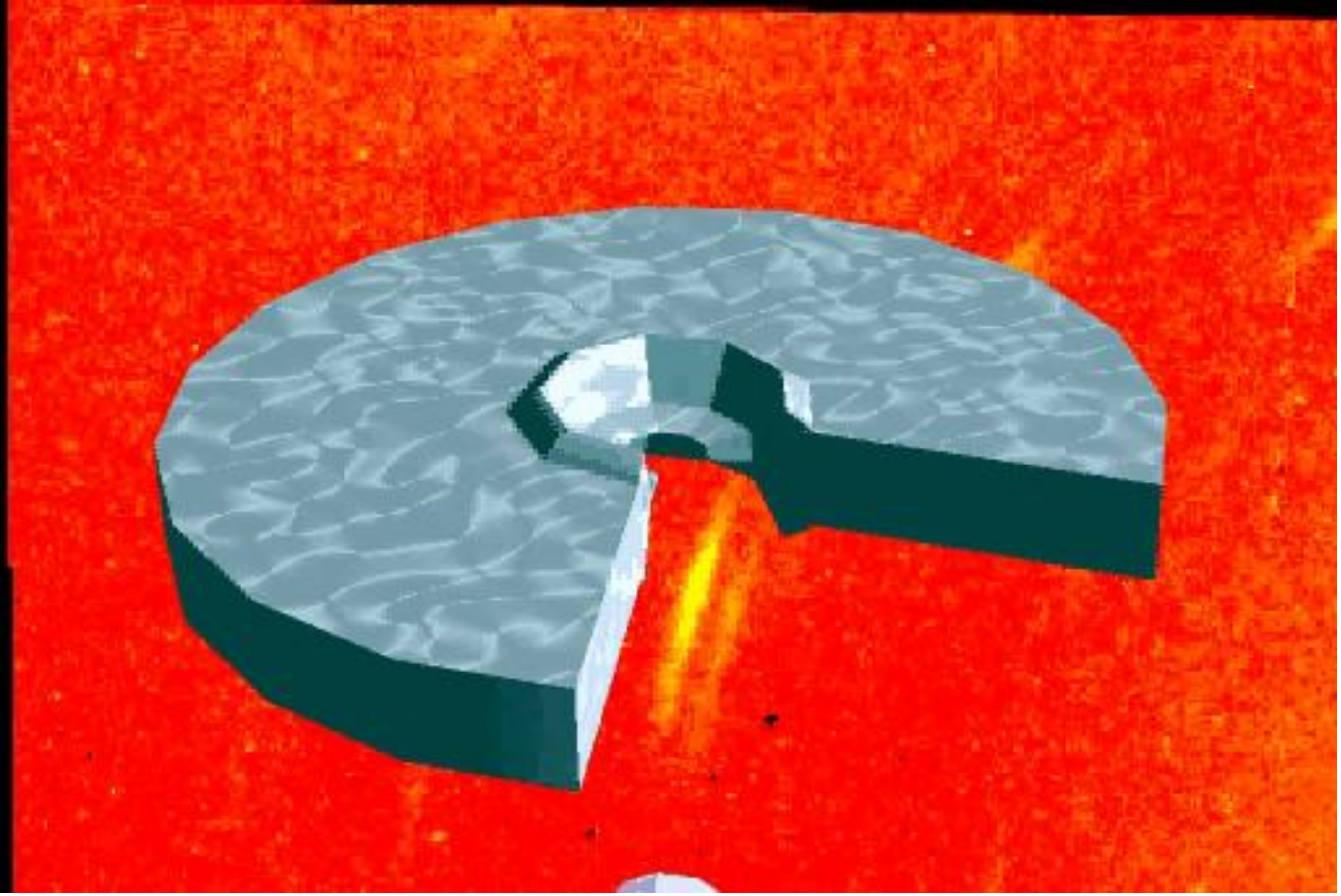

Diamond Anvil Cell Technique

DAC

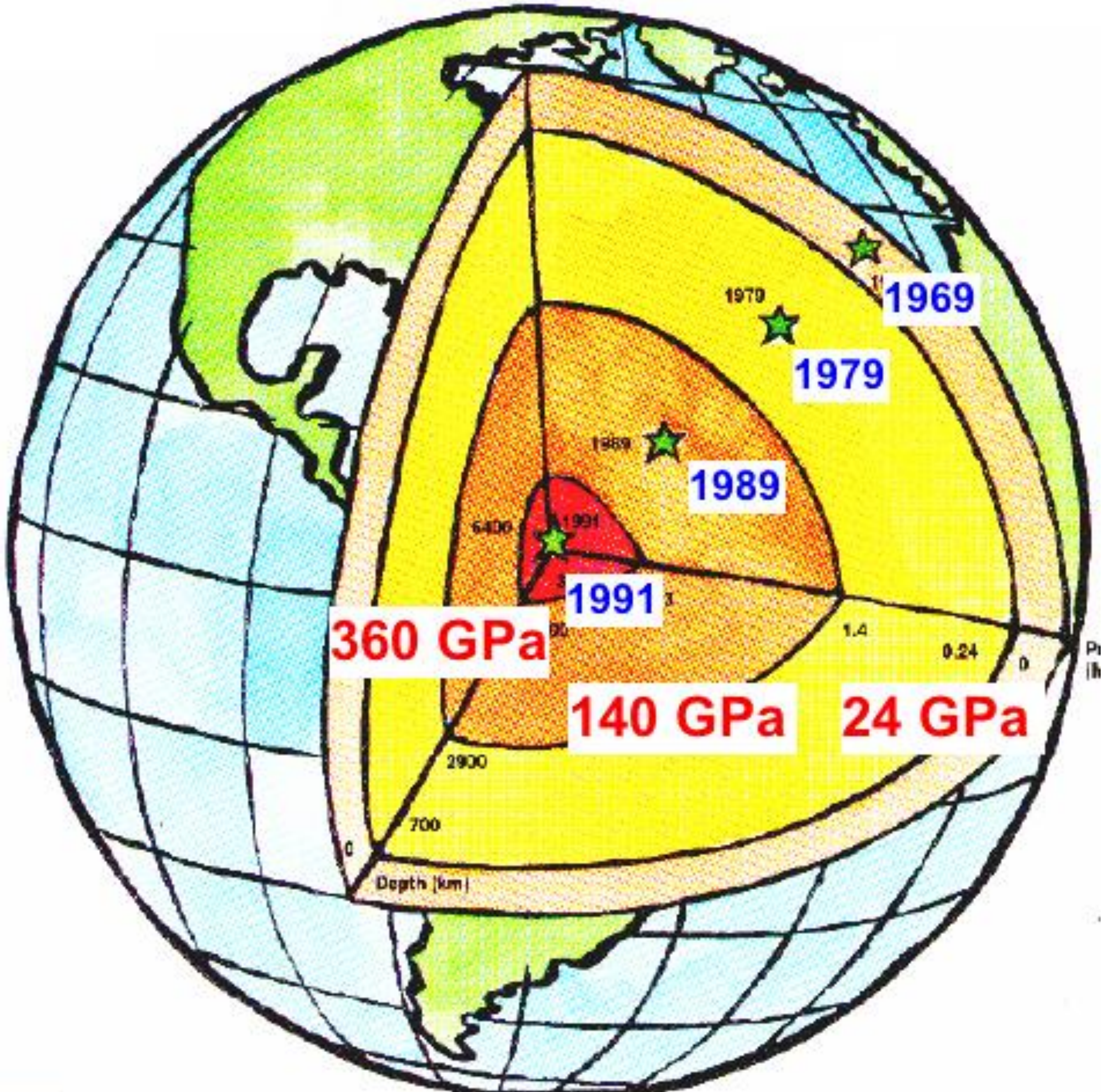
1969
1979
1989
1991
360 GPa
140 GPa
24 GPa
1979
1989
6400
1991
1.4
0.24
0
2900
700
0
Depth (km)

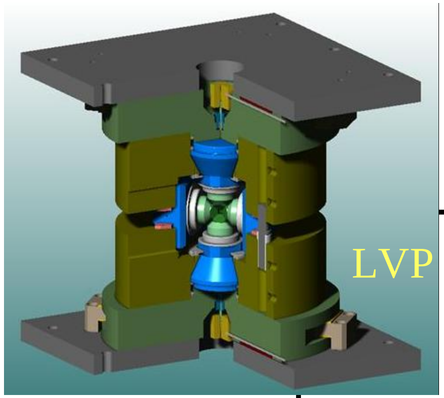

A geotherm together with accessible *P-T* ranges by static techniques

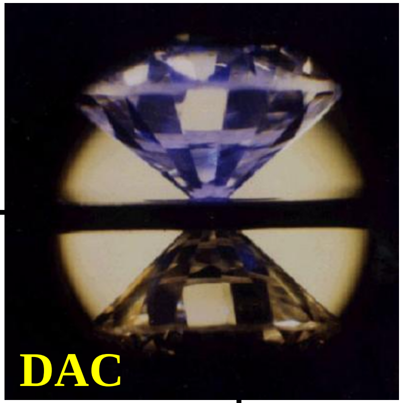

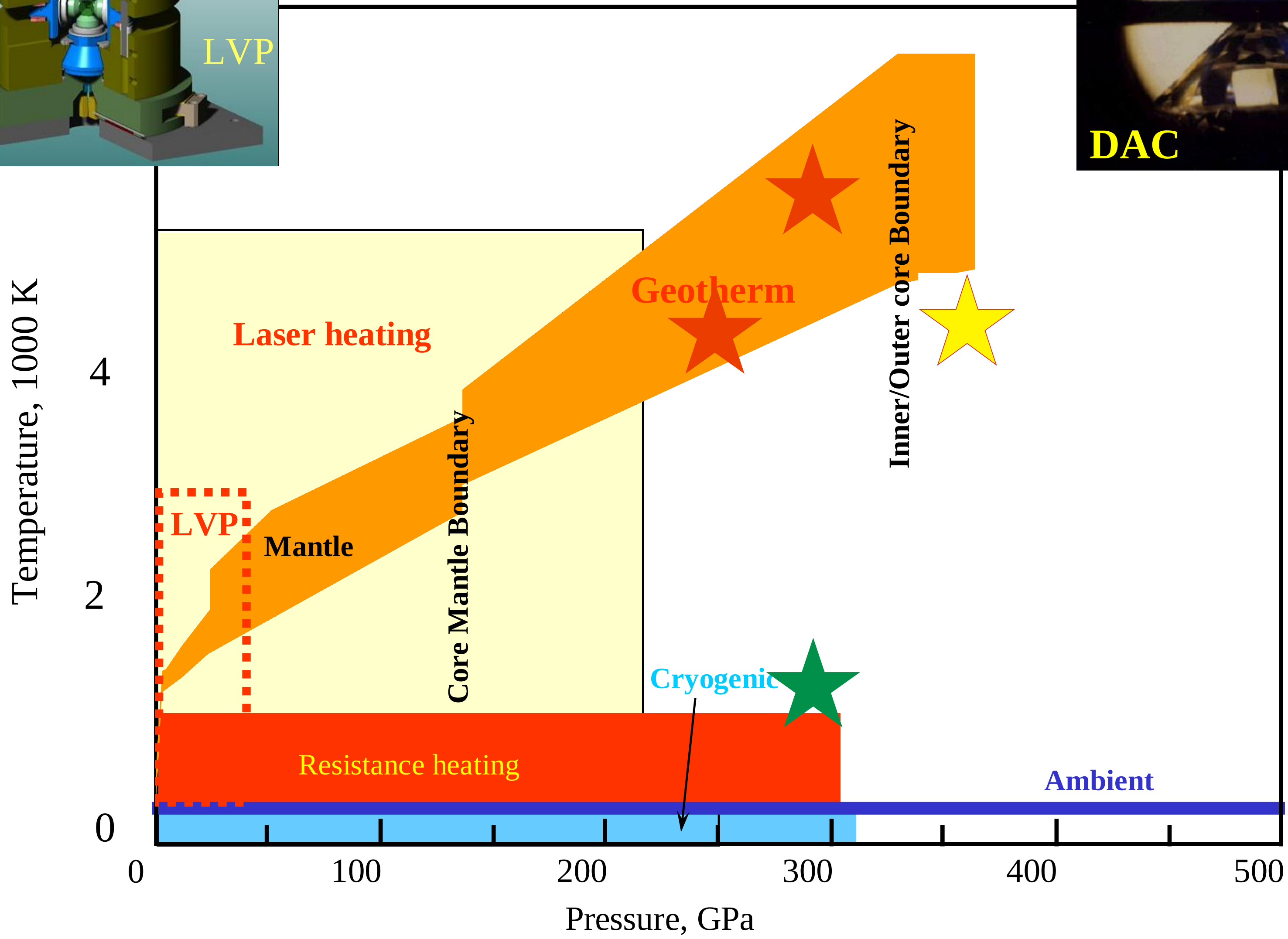

Courtesy of Guoyin Shen

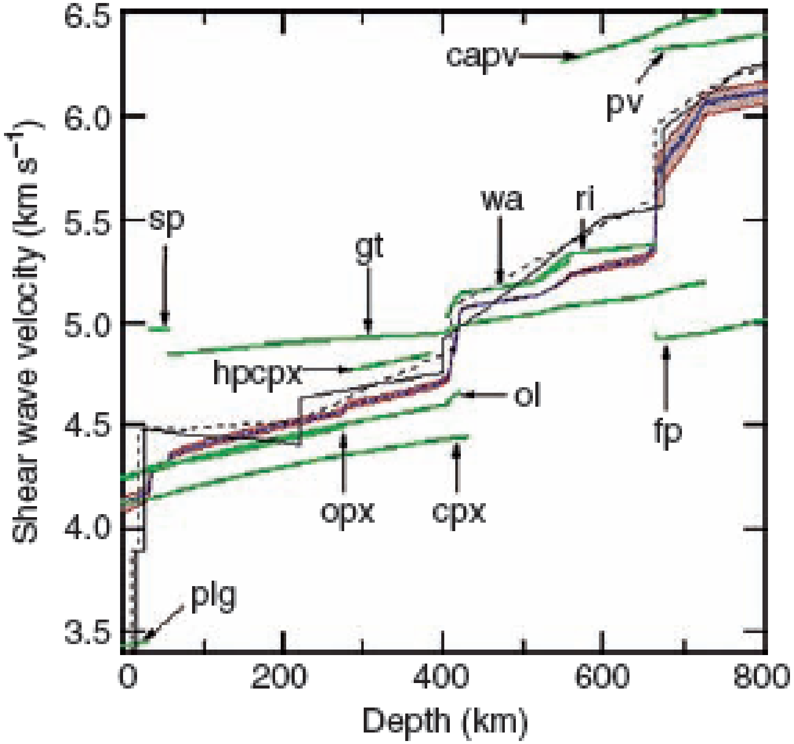

Figure 8 Computed shear-wave velocities of a model mantle composition (blue), and of the individual phases of the assemblage (green) along the 1600 K adiabat computed self-consistently with the phase equilibria and physical properties according to the method of Stixrude and Lithgow-Bertelloni (2005a). The Voigt–Reuss (red) and Hashin–Shtrikman (blue) bounds on the aggregate velocity are shown. Thin black lines are radial seismological models: (solid) PREM (Dziewonski and Anderson, 1981); (dashed) AK135 (Kennett and Engdahl, 1991). Adapted from Stixrude L and Lithgow-Bertelloni C (2005b) Thermodynamics of mantle minerals. I: Physical properties. *Geophysical Journal International* 162: 610–632.

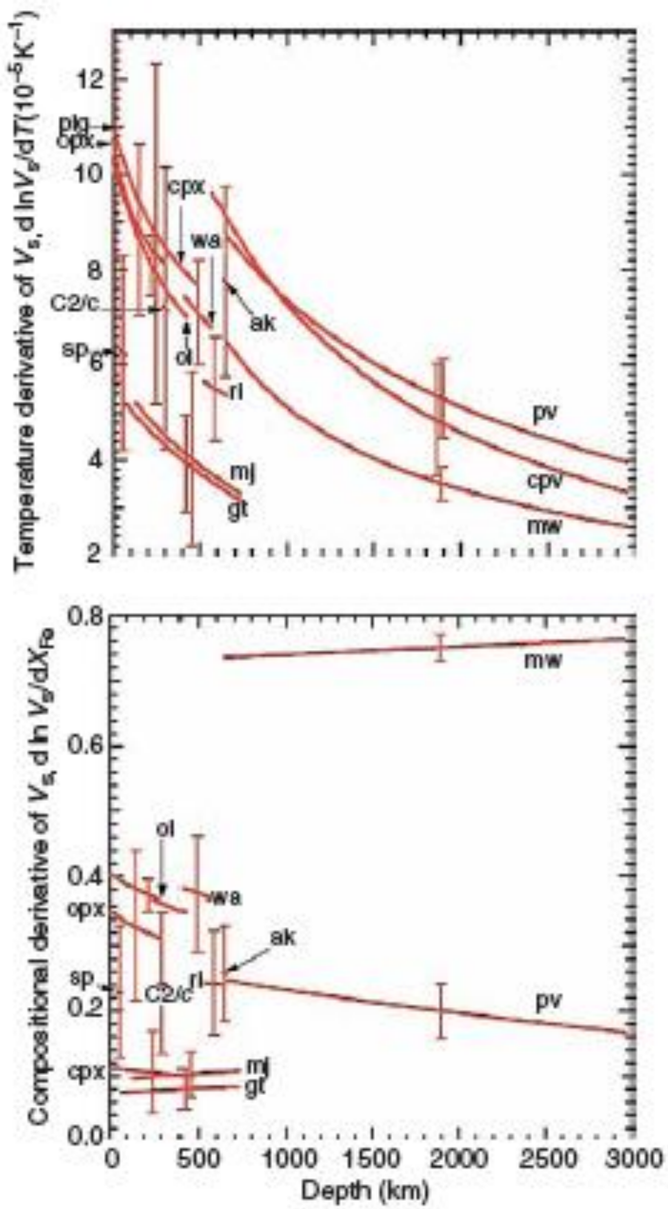

Figure 9 Variation of the shear-wave velocity with respect to (top) temperature and (bottom) composition. From Stixrude L and Lithgow-Bertelloni C (2005b) Thermodynamics of mantle minerals. I: Physical properties. *Geophysical Journal International* 162: 610–632.

Saikia et al., PEPI, 2009

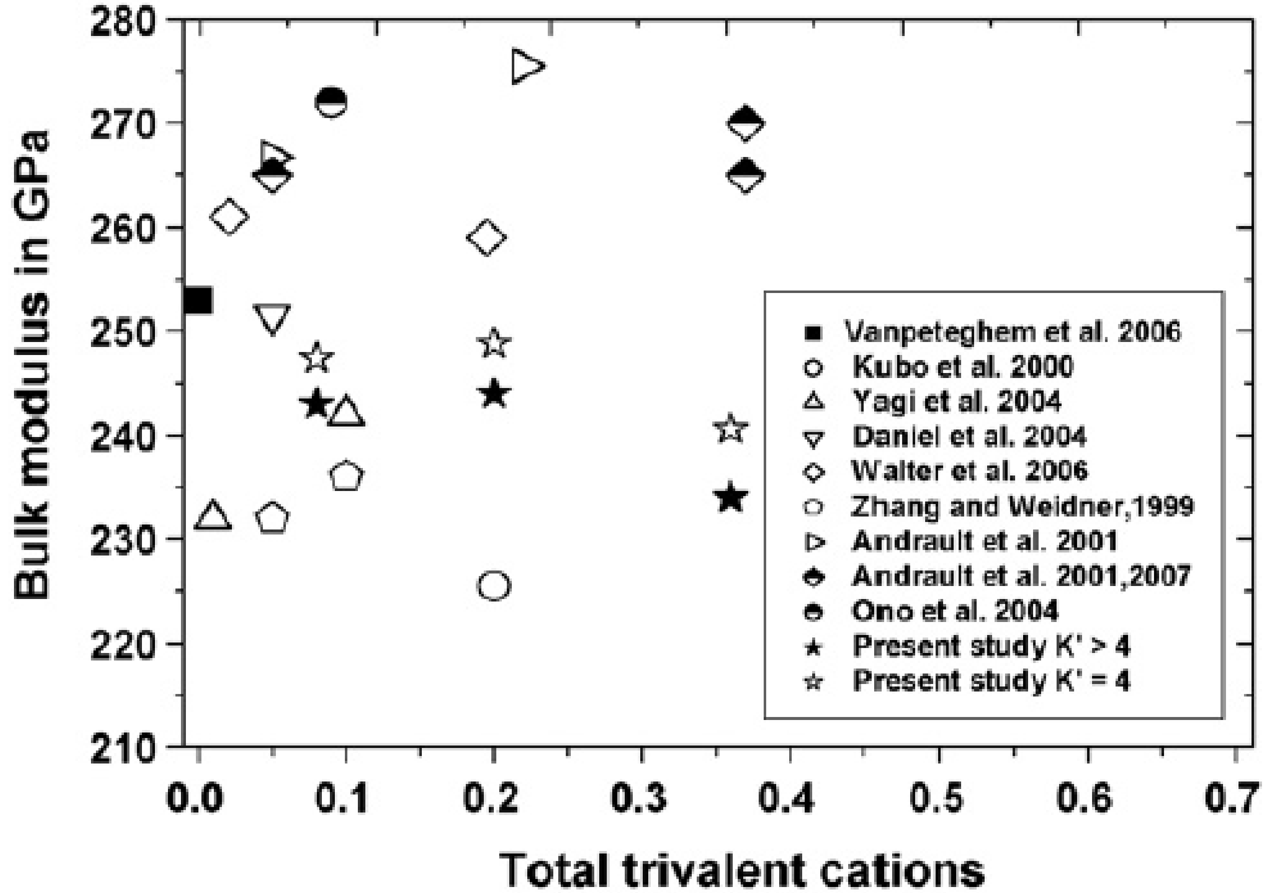

Fig. 9. The room pressure isothermal bulk moduli of Fe–Al-bearing MgSi(perovskite single crystals determined in this study using both 2nd ($K' = 4$; open sta and 3rd ($K' > 4$; filled stars) order Birch–Murnaghan equations of state, as a functi of total trivalent cation content (i.e., $Fe^{3+} + Al^{3+}$). The results of previous studies on bearing (open symbols) and Fe,Al-bearing powdered perovskite samples (half fill symbols) are shown for comparison. The bulk modulus for pure $MgSiO_3$ perovsk (filled square) is taken from the single crystal compression study of Vanpeteghe

A geotherm together with accessible *P-T* ranges by static techniques

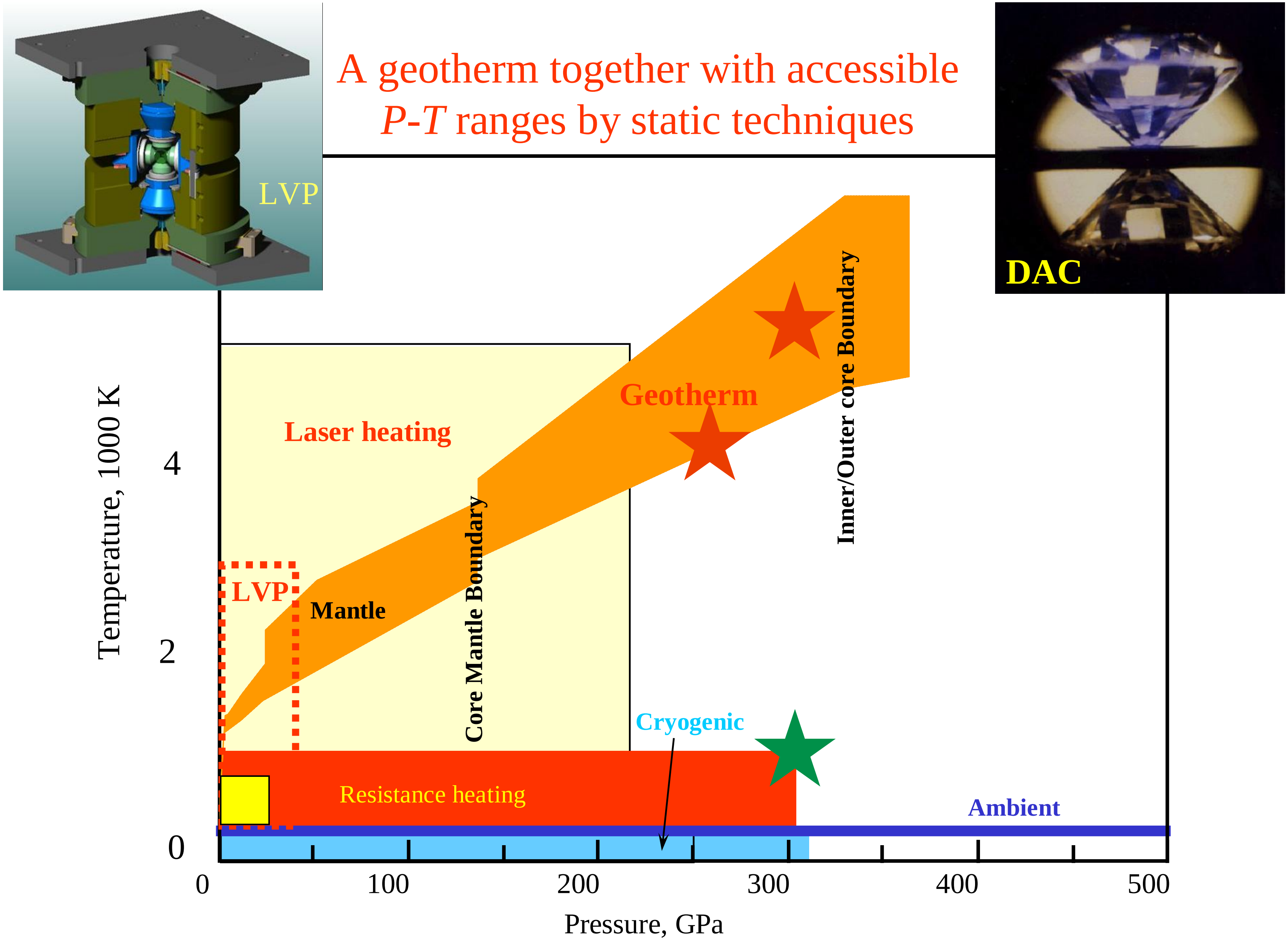

Courtesy of Guoyin Shen

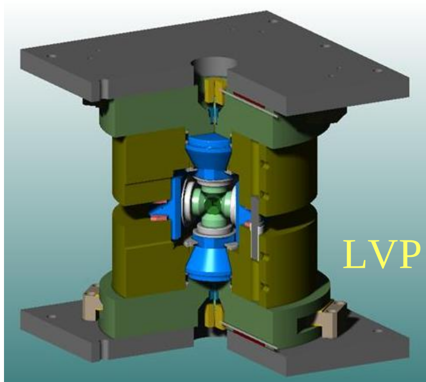

A geotherm together with accessible *P-T* ranges by static techniques

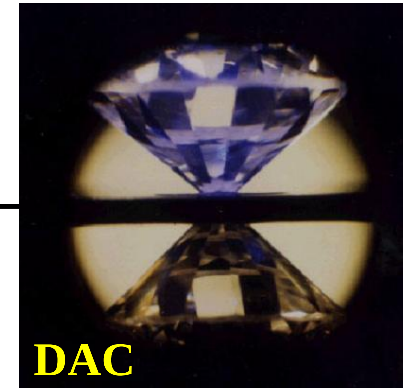

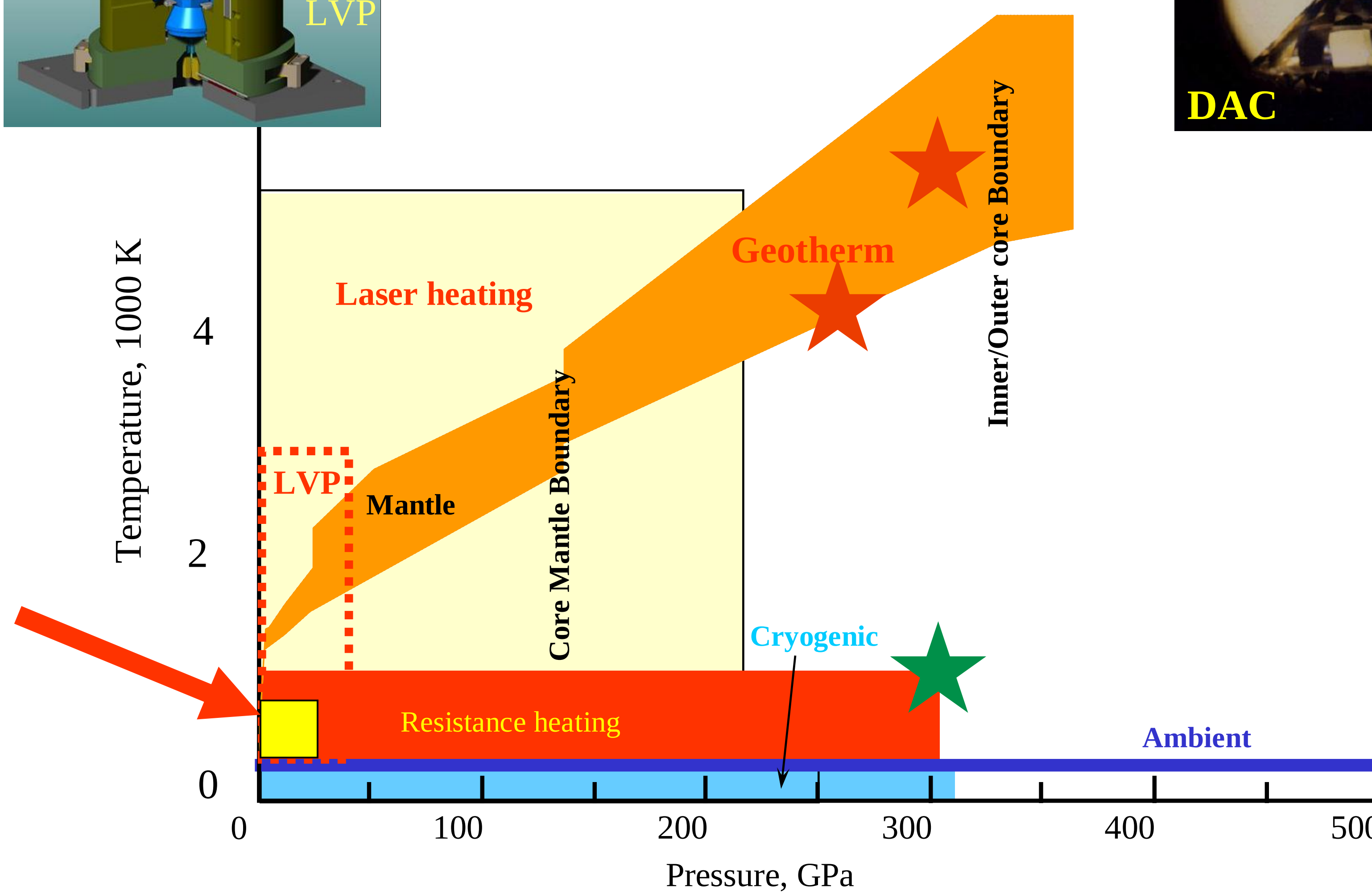

Courtesy of Guoyin Shen

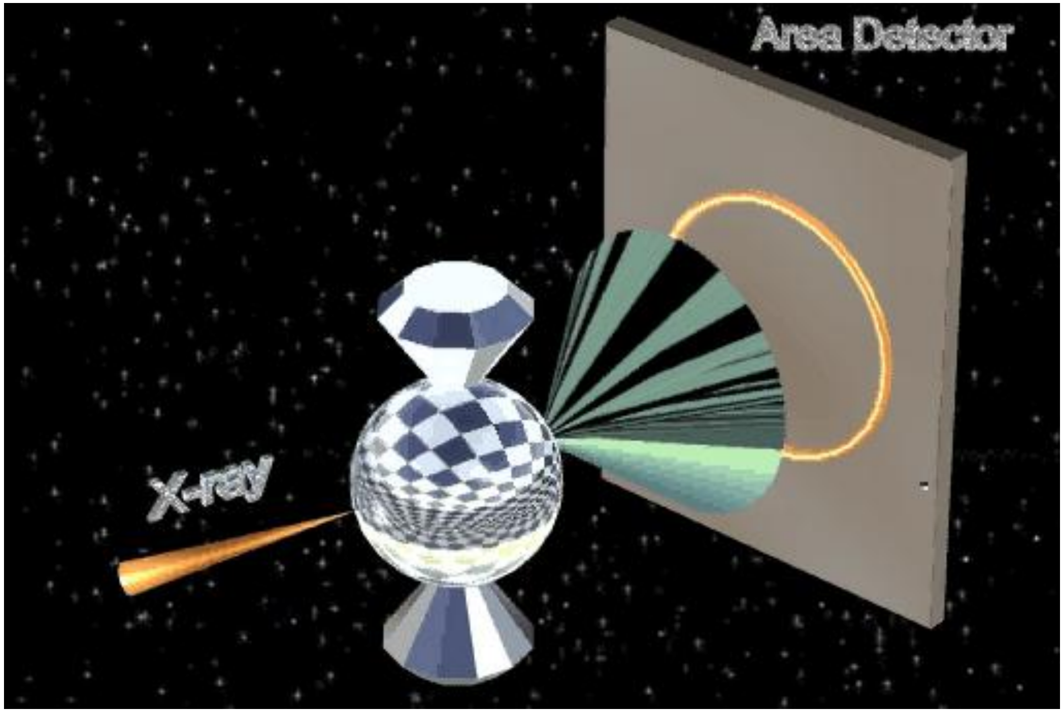

Large stresses in DACs tend to destroy crystals...

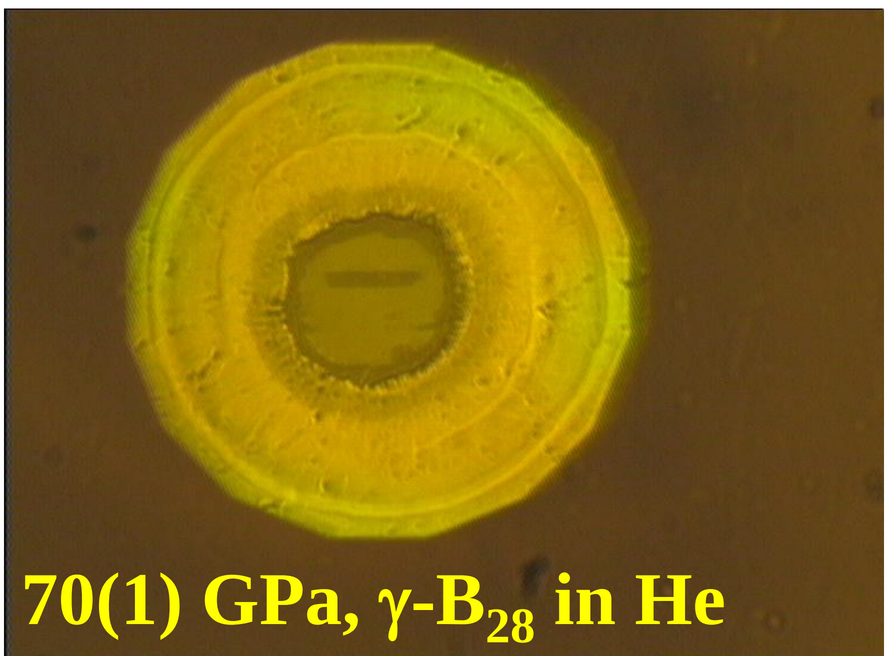

...but quasi-hydrostatic nobel gases (He, Ne) pressure transmitting media preserve them!

Zarechnaya et al., 2010

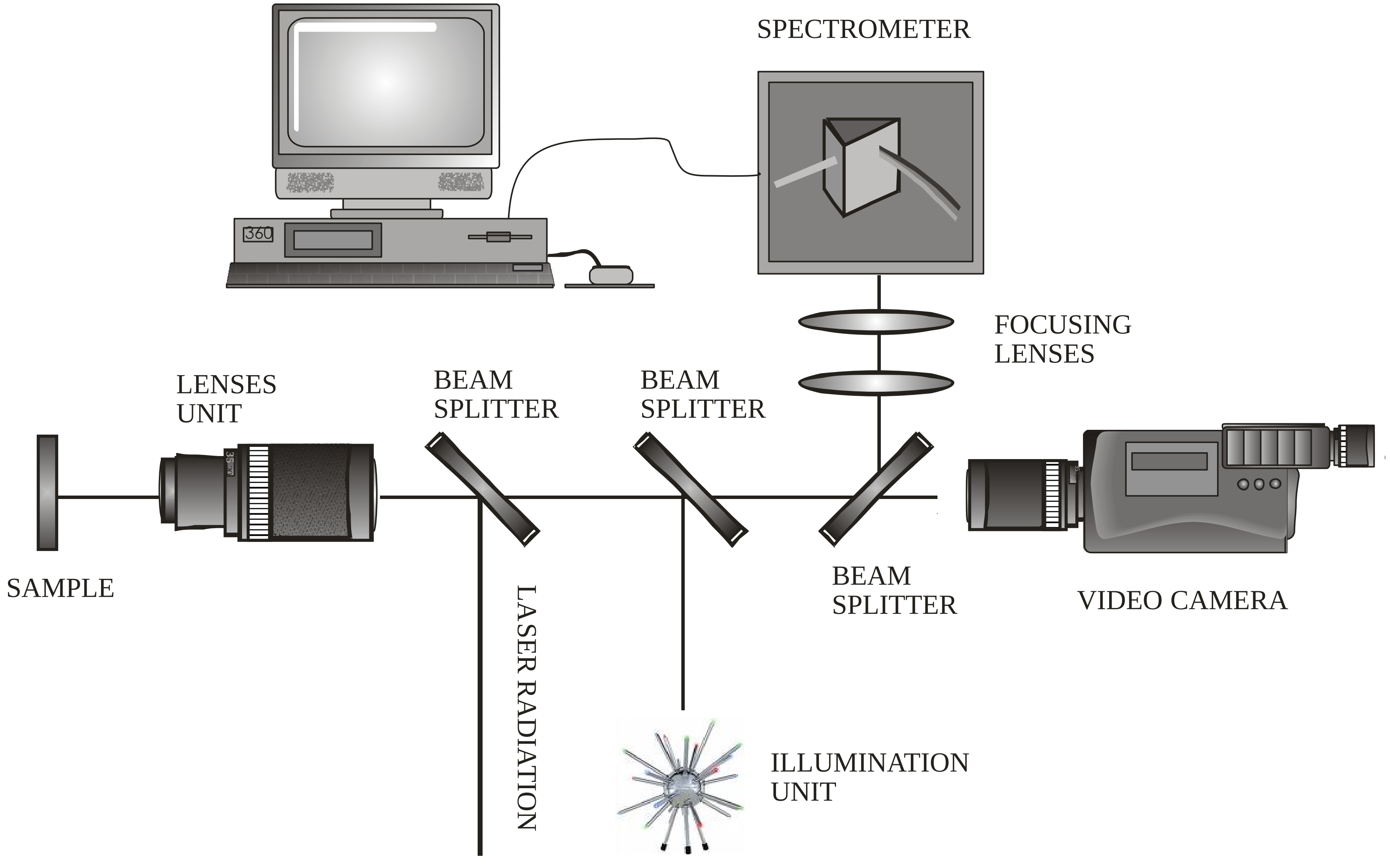

Dubrovinsky et al., 2004, 2009

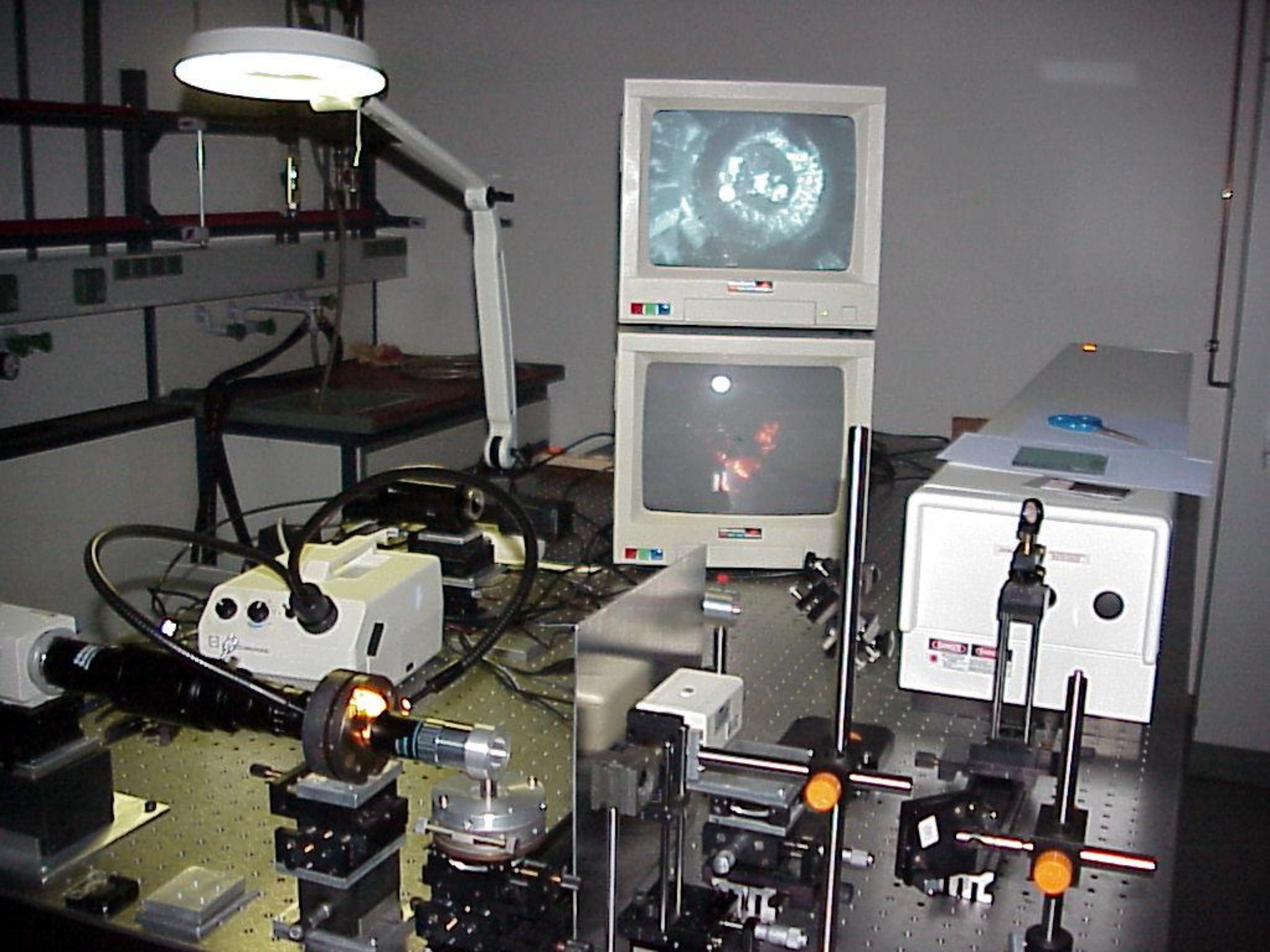

Single Crystal Diffraction in Diamond Anvil Cells

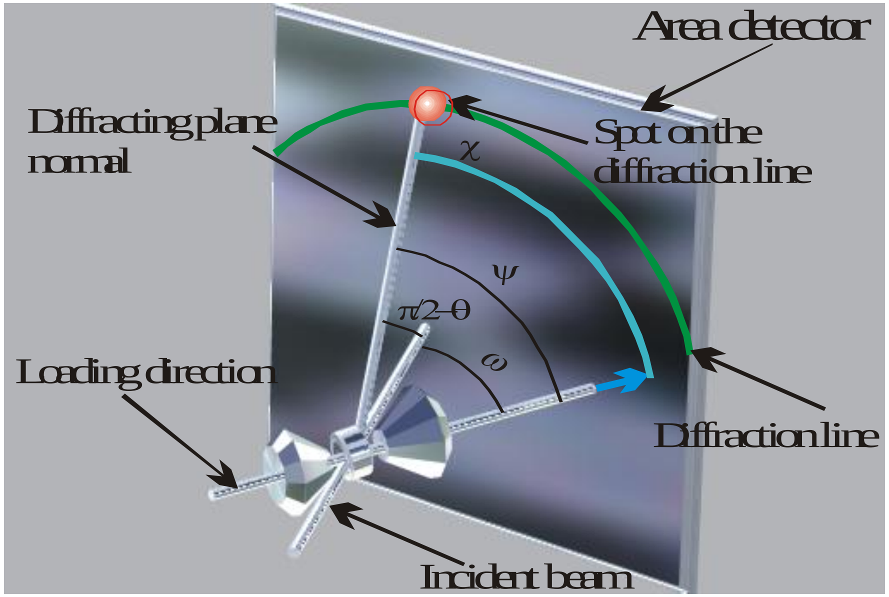

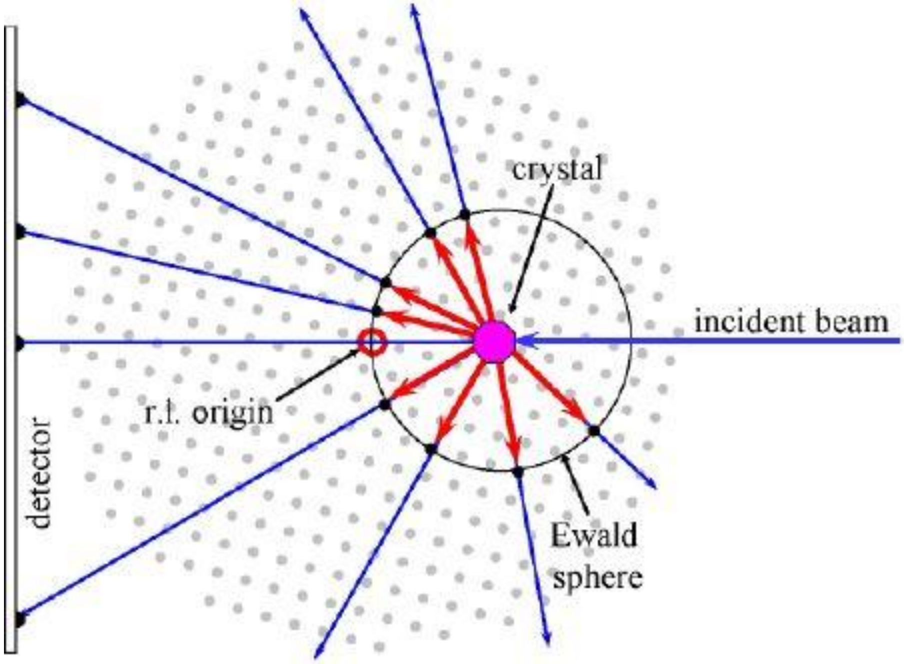

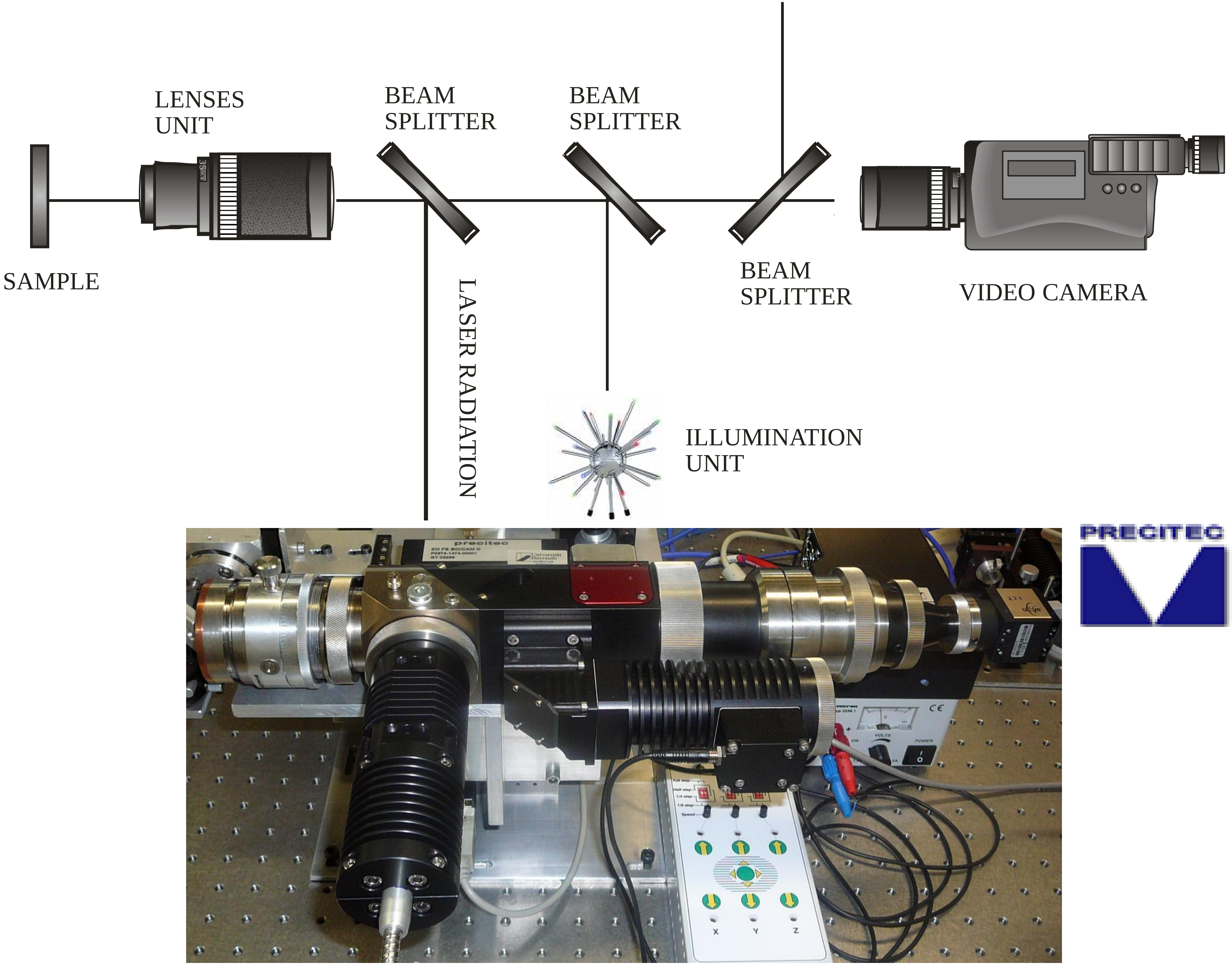
LENSES UNIT
BEAM SPLITTER
BEAM SPLITTER
SAMPLE
LASER RADIATION
BEAM SPLITTER
VIDEO CAMERA
ILLUMINATION UNIT
PRECITEC

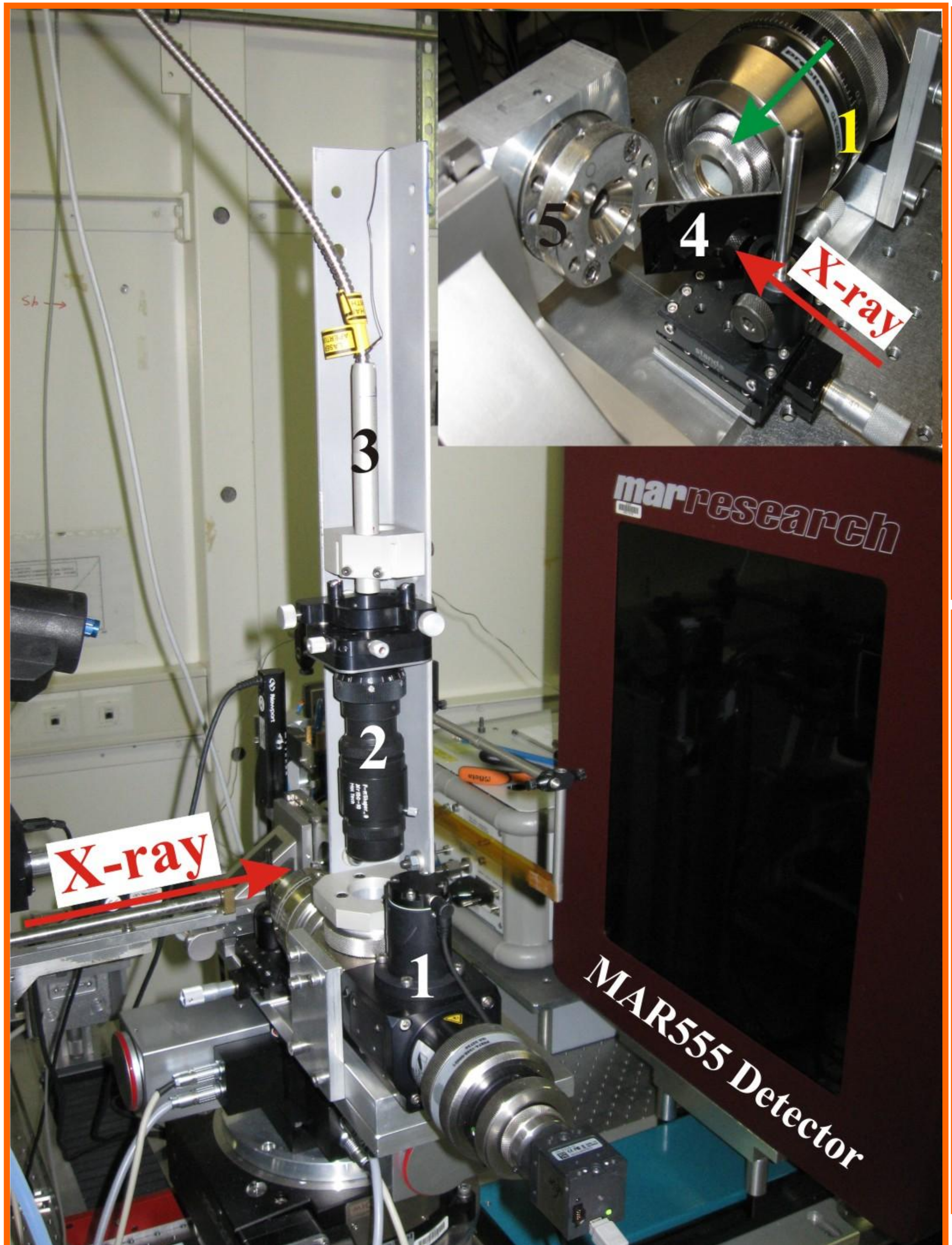

ESRF, ID09, 11.2011

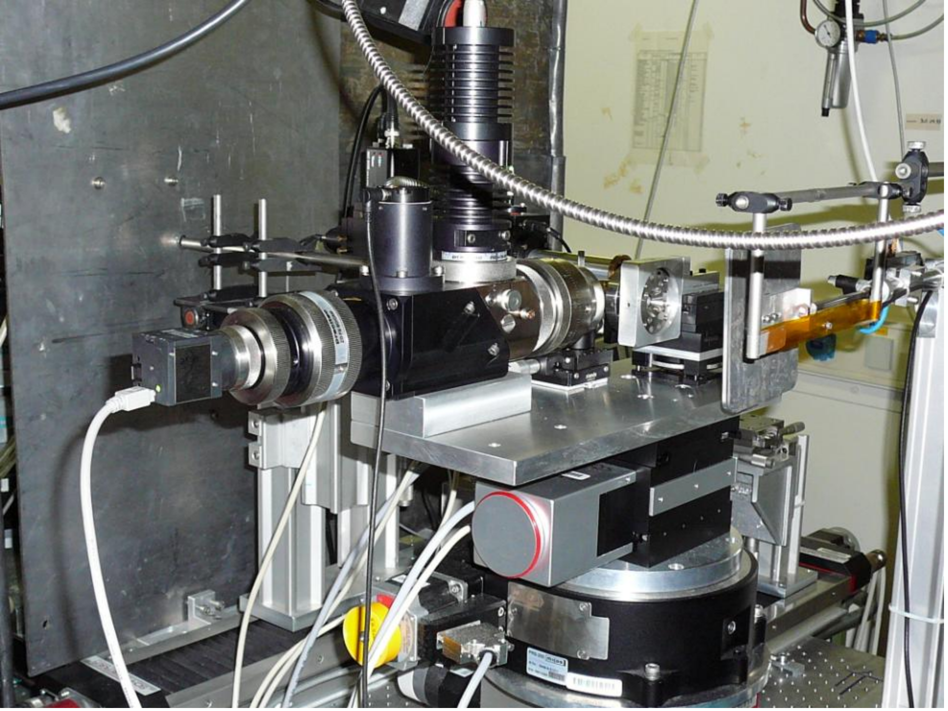

ID09a, ESRF
01.11.2011

ω scans -28 -:- 26º

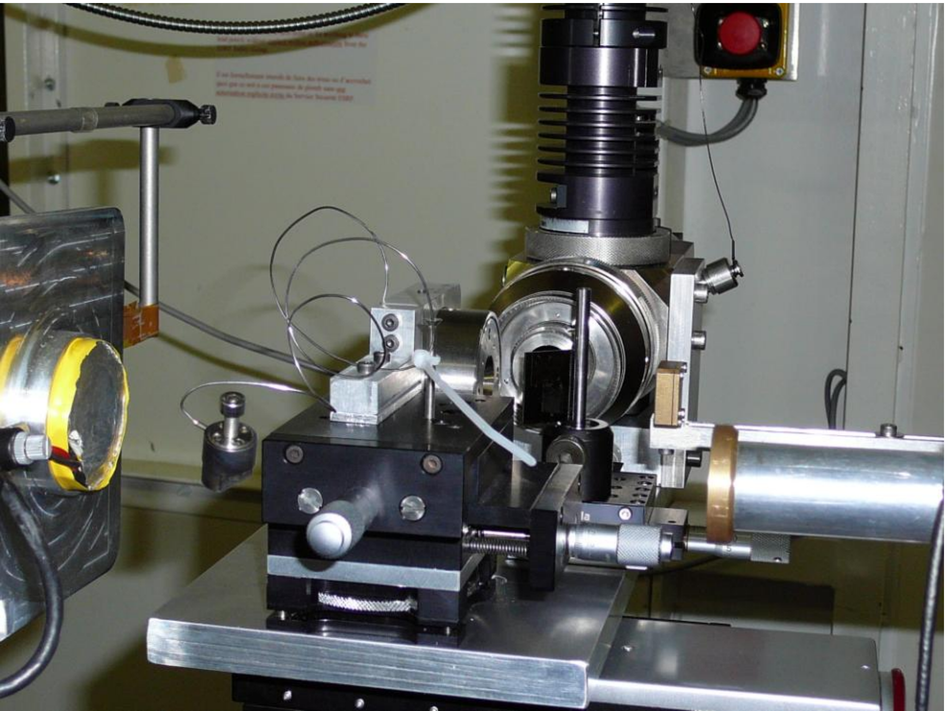

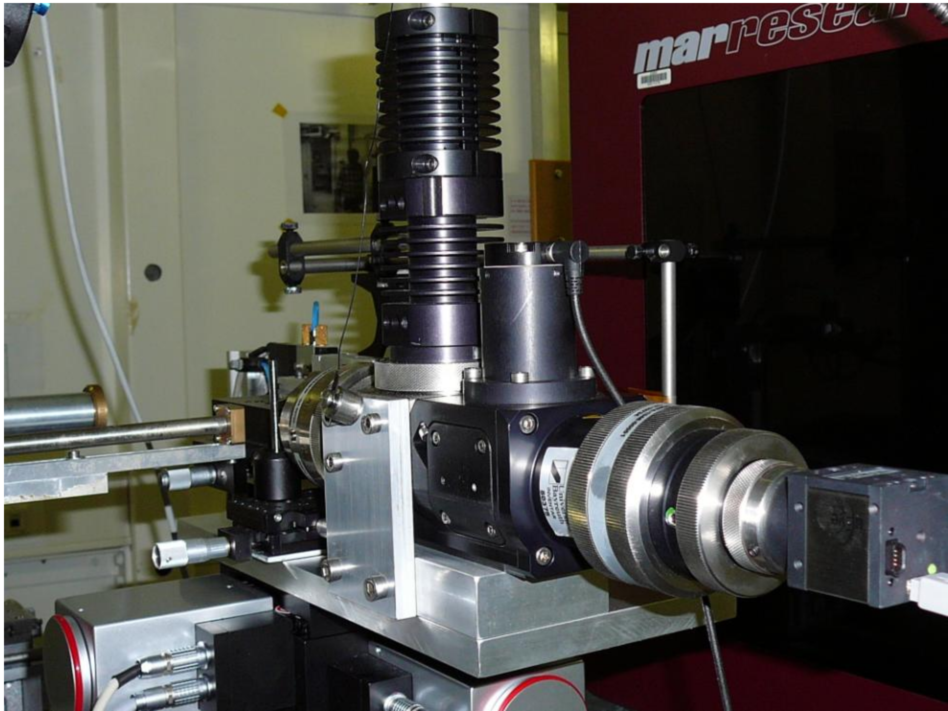

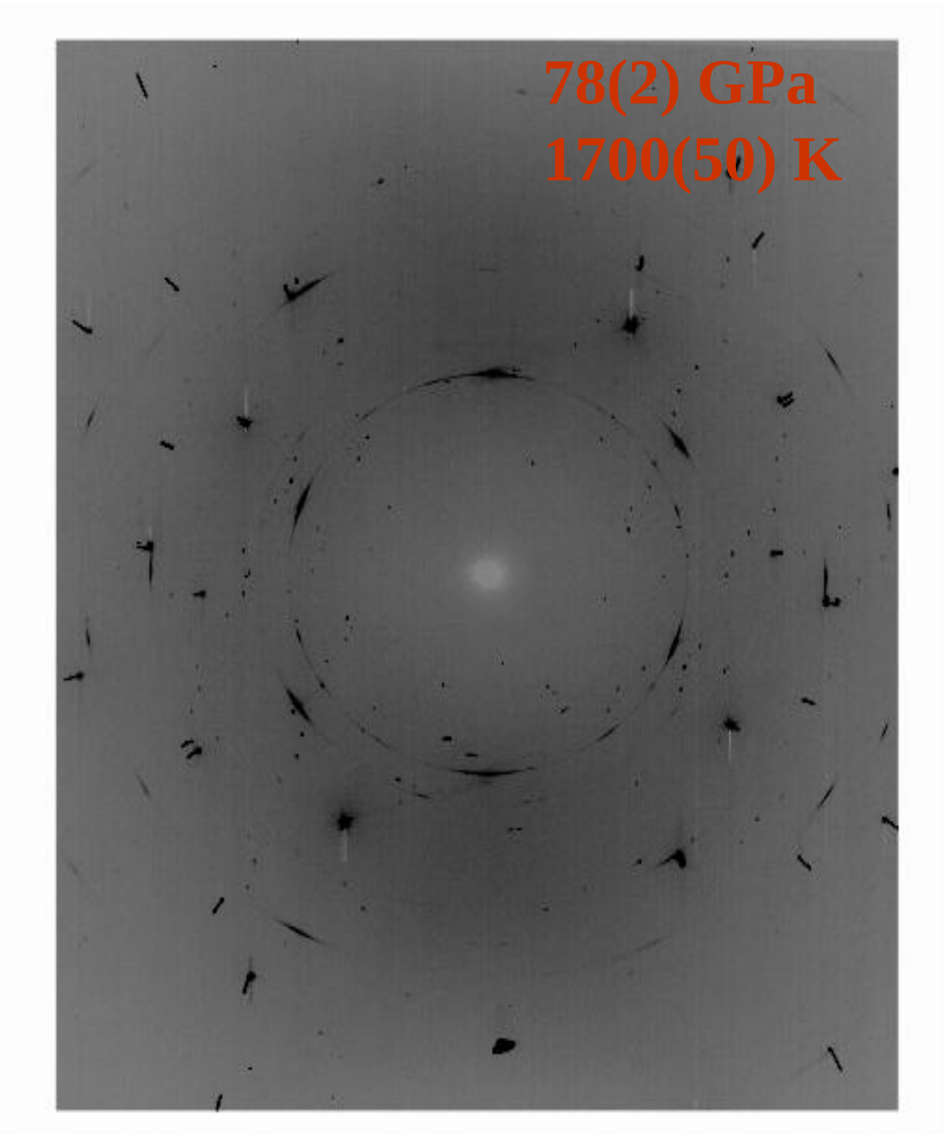

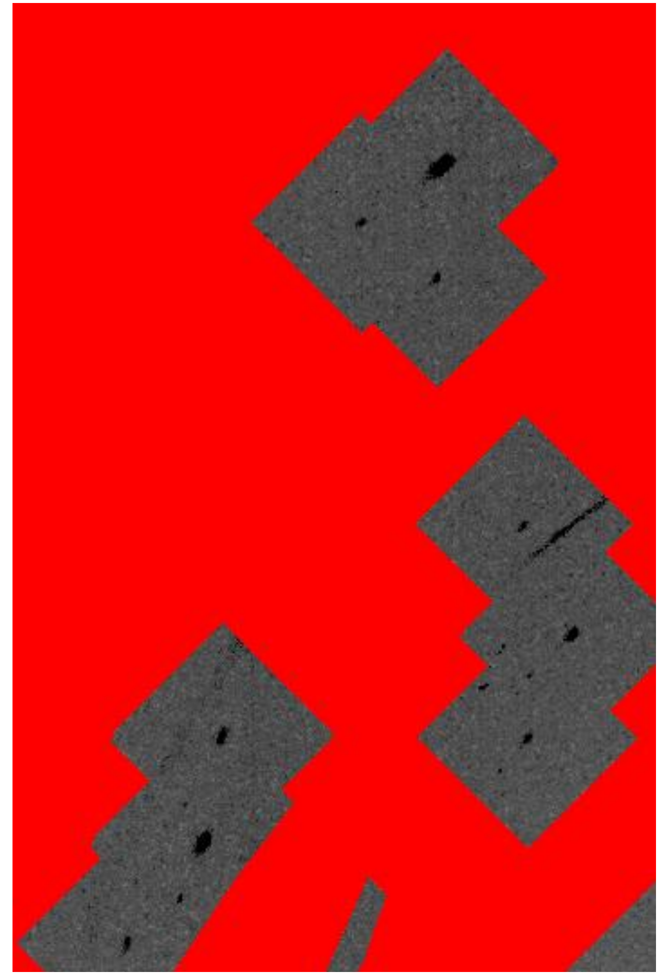

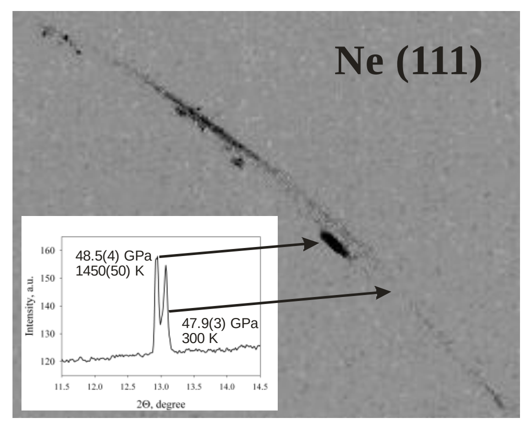

Silicate Perovskite

$(Mg_{0.63},Fe_{0.37})(Si_{0.63}Al_{0.37})O_3$

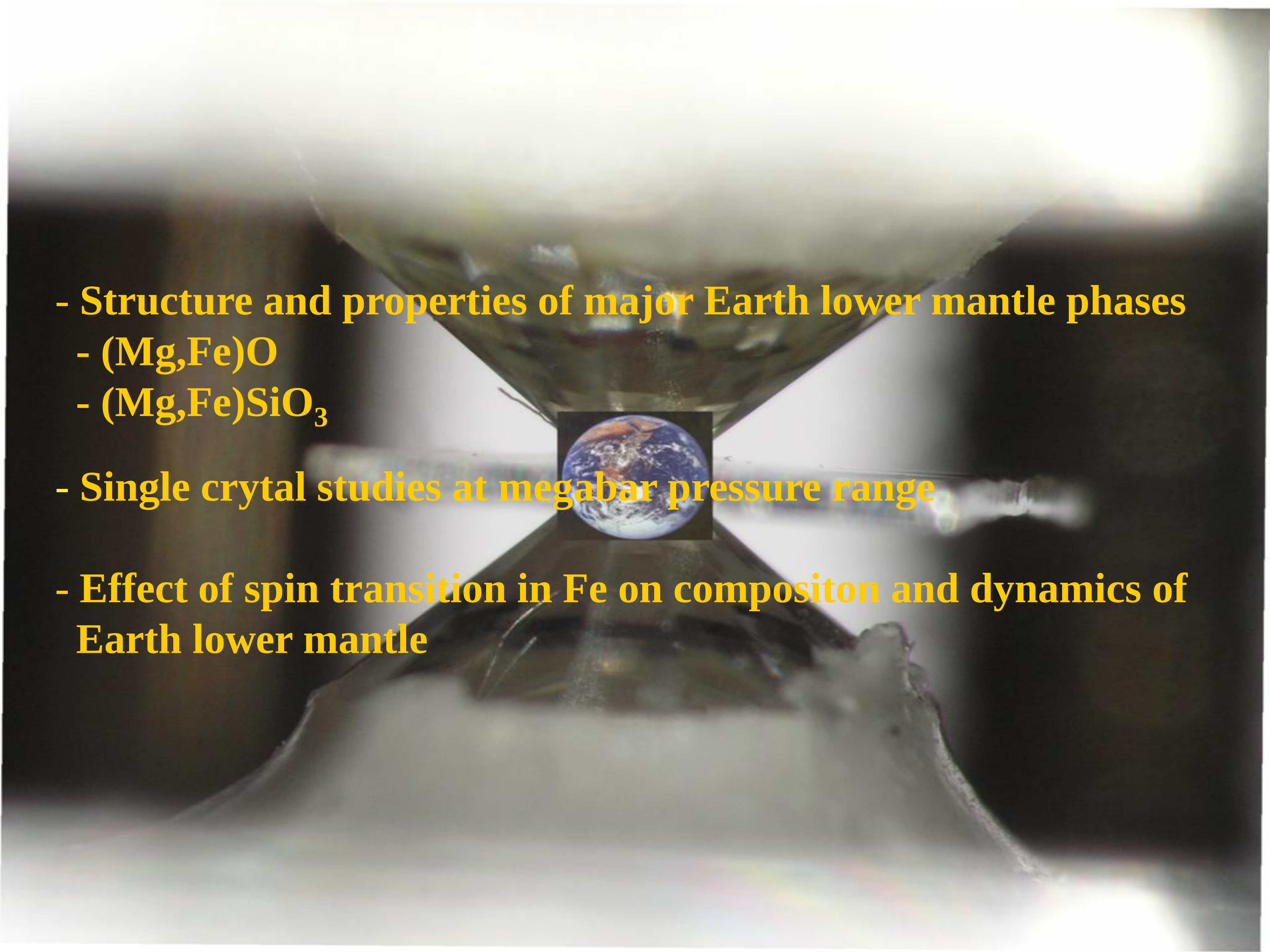

- Structure and properties of major Earth lower mantle phases
  - (Mg,Fe)O
  - $(Mg,Fe)SiO_3$

- Single crytal studies at megabar pressure range

- Effect of spin transition in Fe on compositon and dynamics of Earth lower mantle

Thermal EoS of Fp $(Mg_{0.8}Fe_{0.2})O$

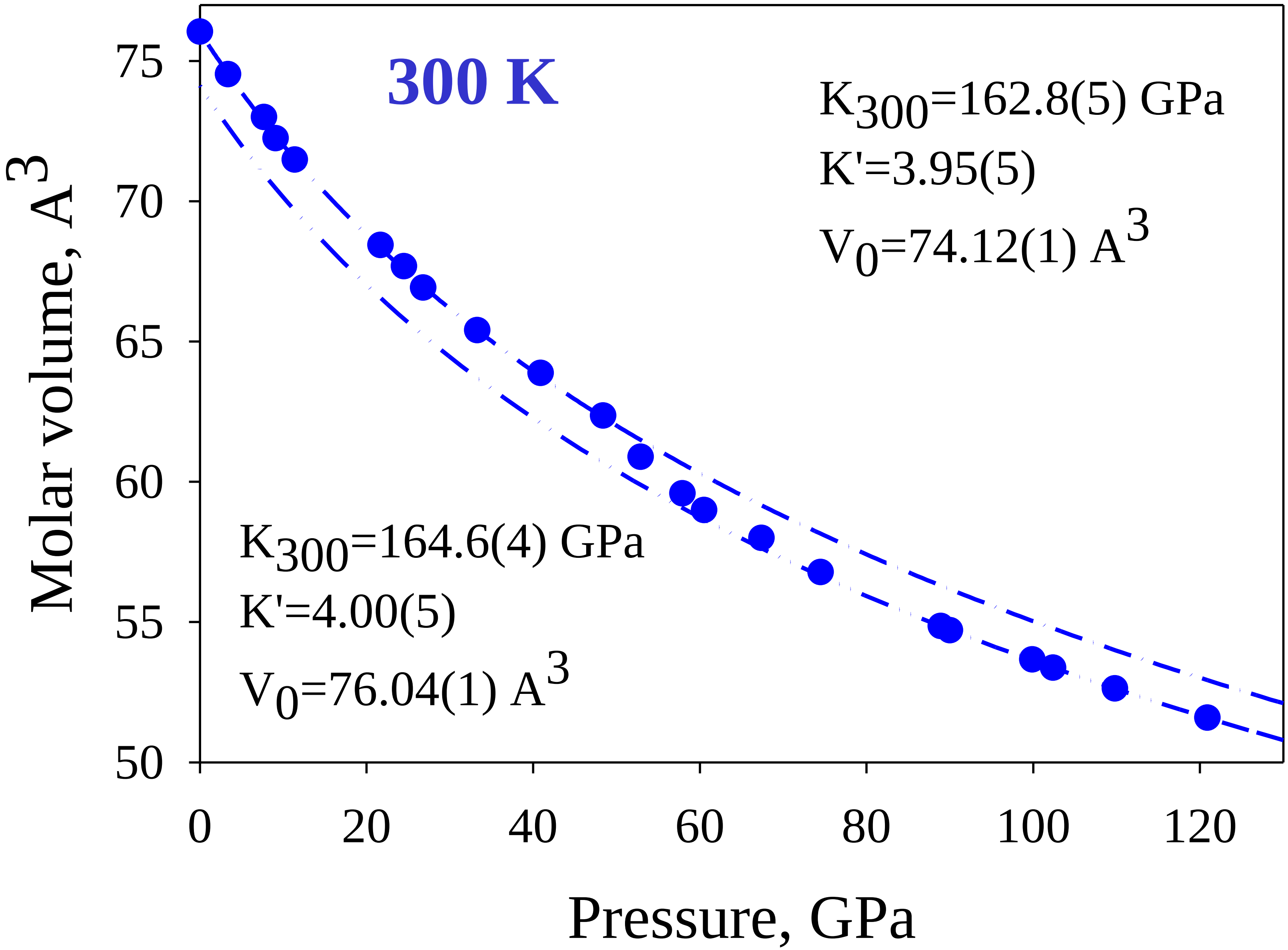

Iron electronic structure

Fe^{2+} (Ar)$3s^2 3p^6 3d^6$

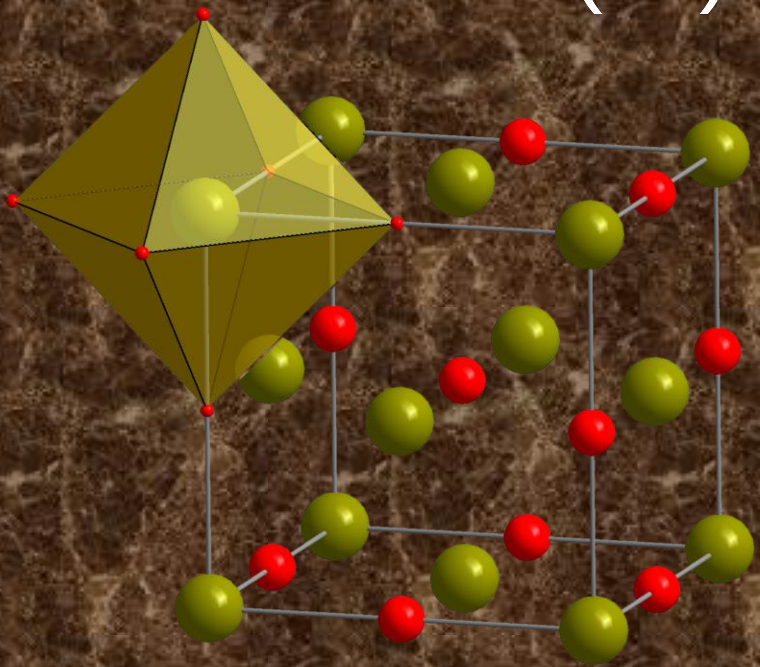

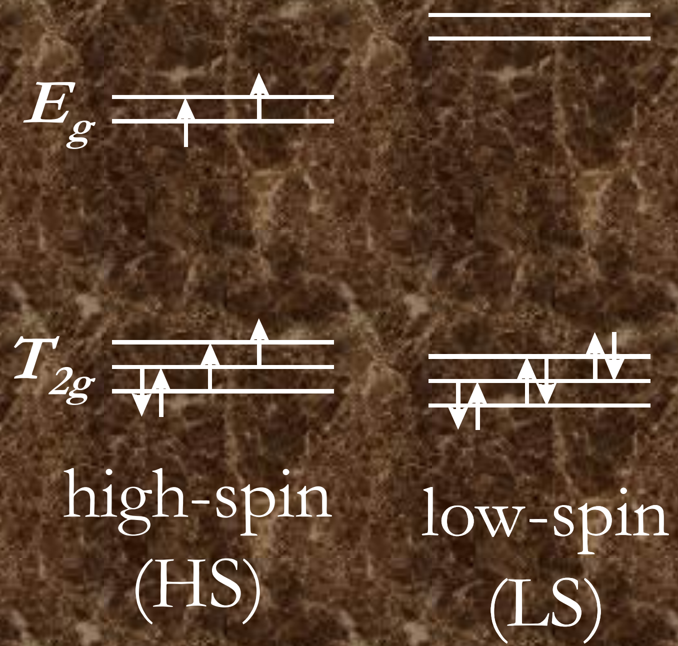

Possible effects of Fe^{2+} spin crossover important for geophysics and geochemistry

- Density increase – possible discontinuity in seismic profile of the mantle, changes in compressibility.

- Red shift of the absorption edge – possible decrease of radiative heat transfer in the mantle.

- Rapid change in Fe partitioning between major phases:
  (Mg,Fe)O ferropericlase and (Mg,Fe)SiO_3 perovskite.

Results: Mössbauer spectroscopy

I. Kantor et al., 2007; 2009

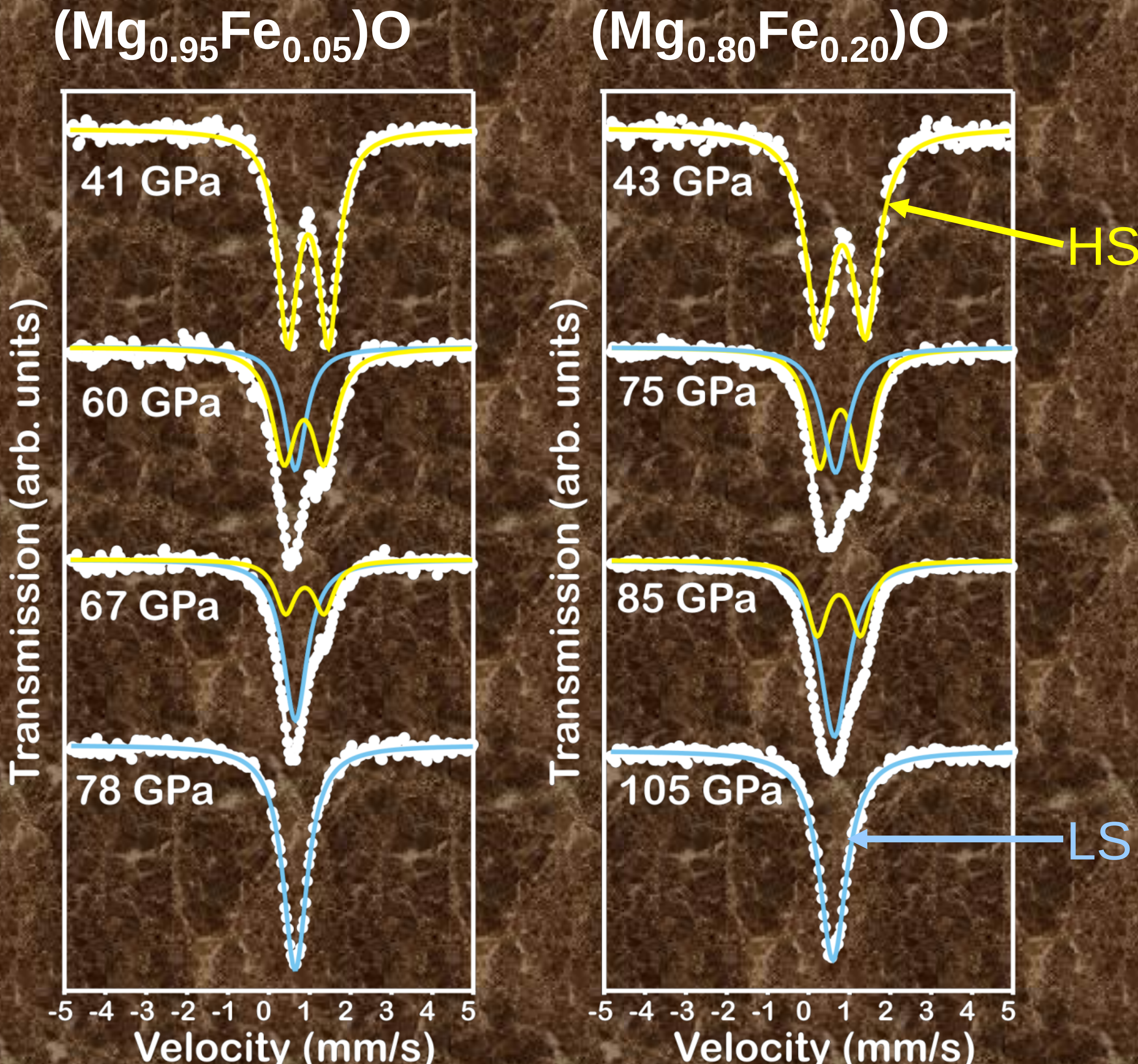

Thermal EoS of Fp $(Mg_{0.8}Fe_{0.2})O$

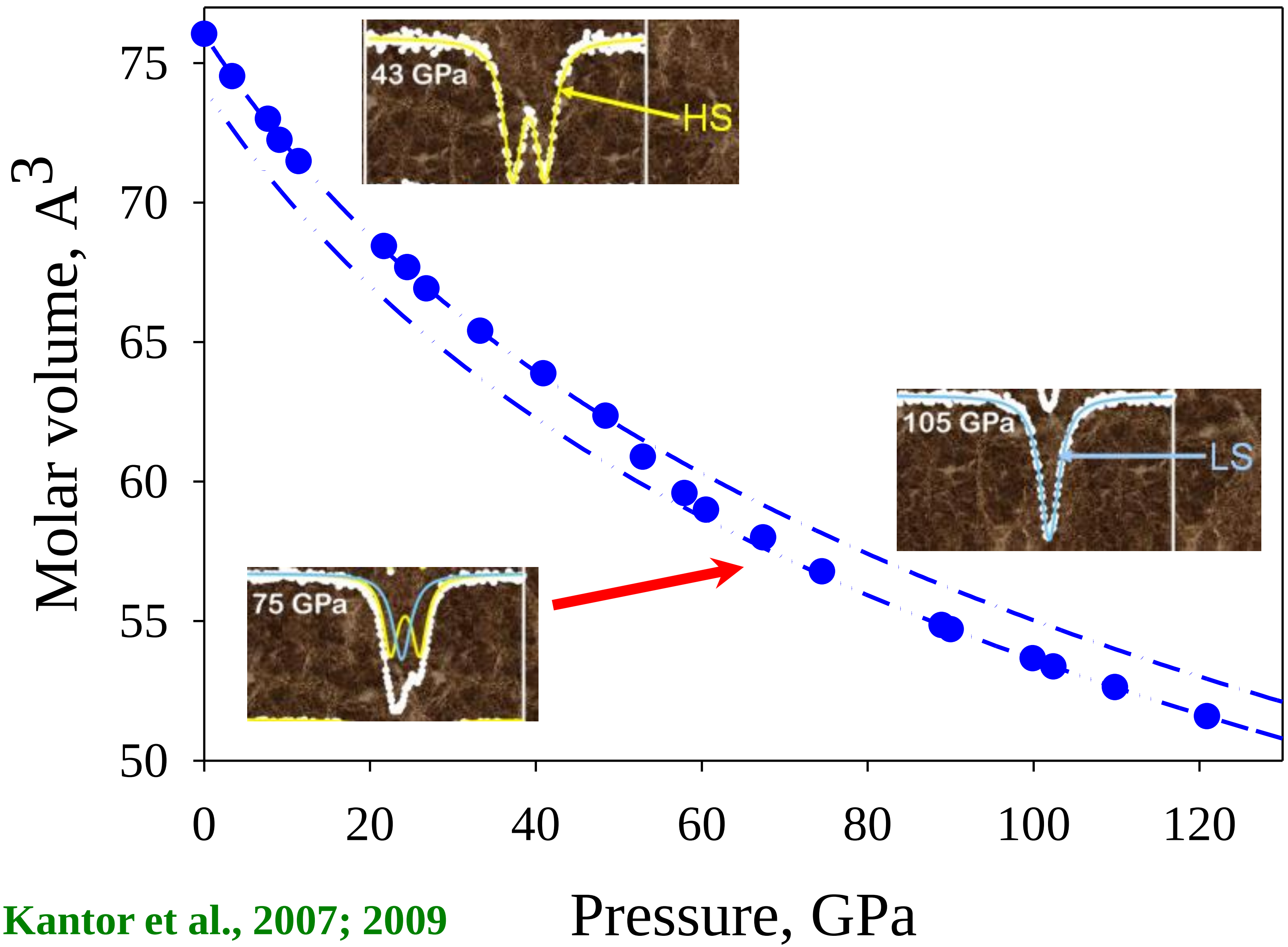

I. Kantor et al., 2007; 2009

Thermal EoS of Fp $(Mg_{0.8}Fe_{0.2})O$

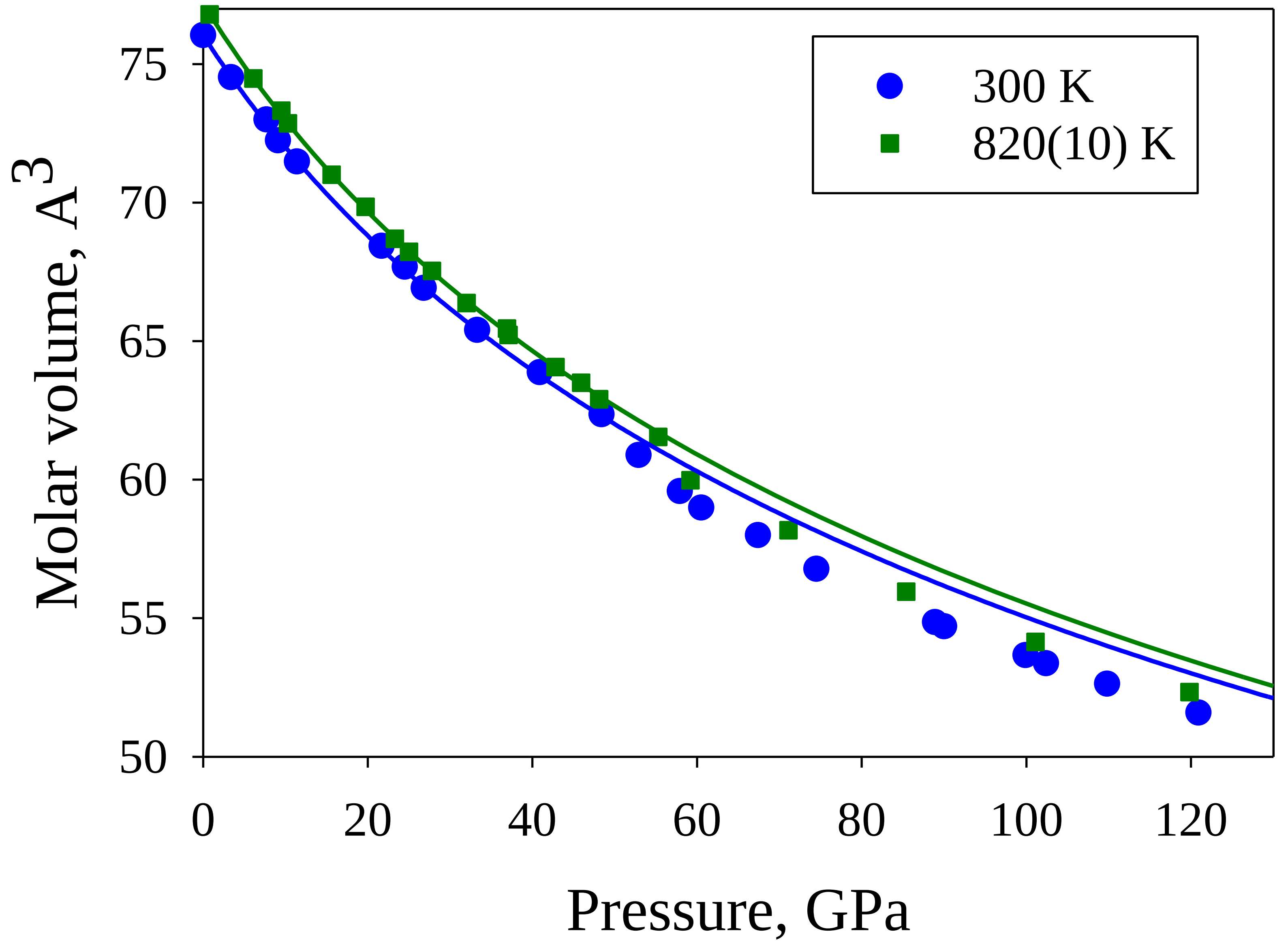

Thermal EoS of Fp $(Mg_{0.8}Fe_{0.2})O$

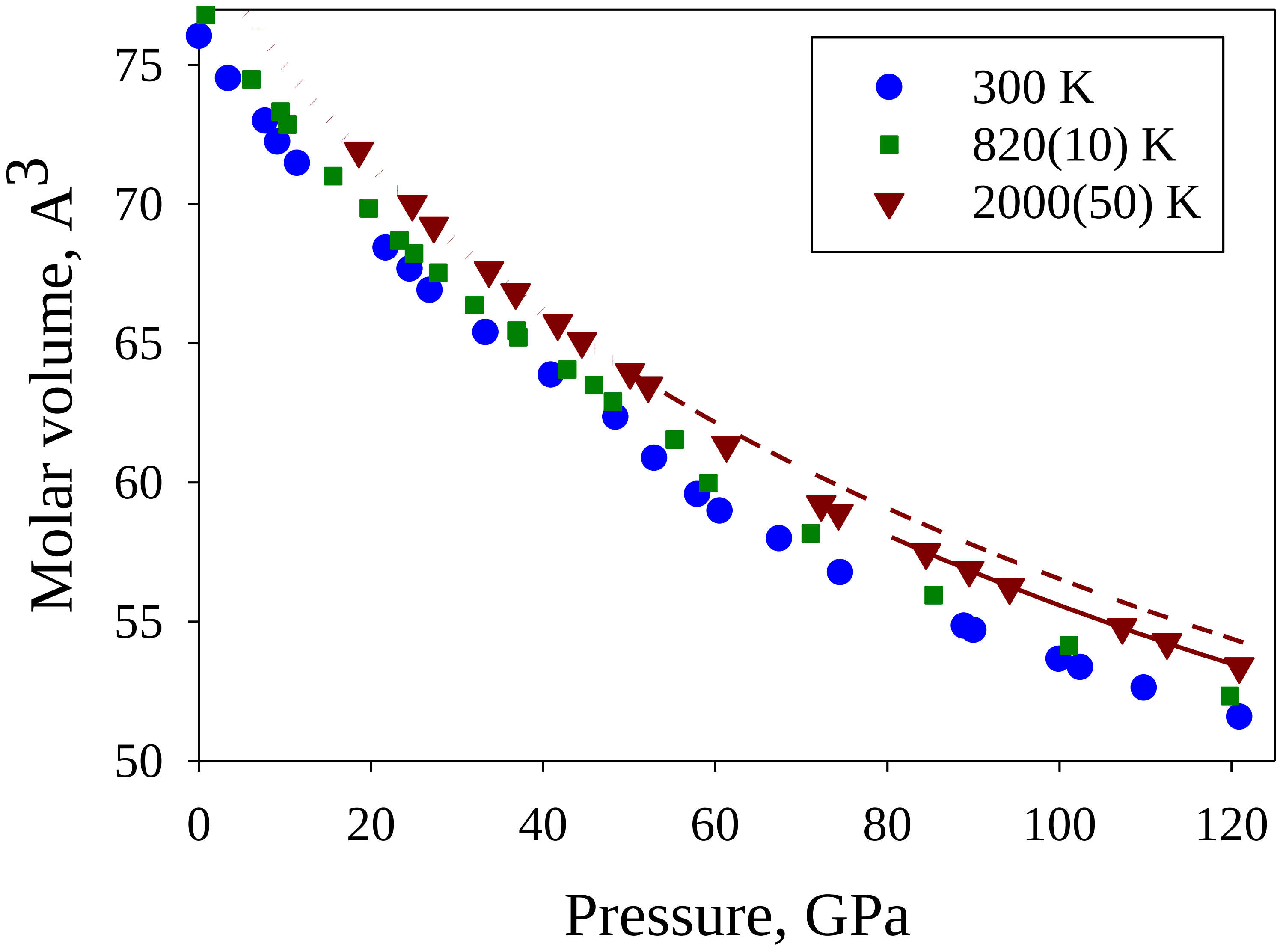

$(Mg_{0.95}Fe_{0.05})O$ $(Mg_{0.8}Fe_{0.2})O$

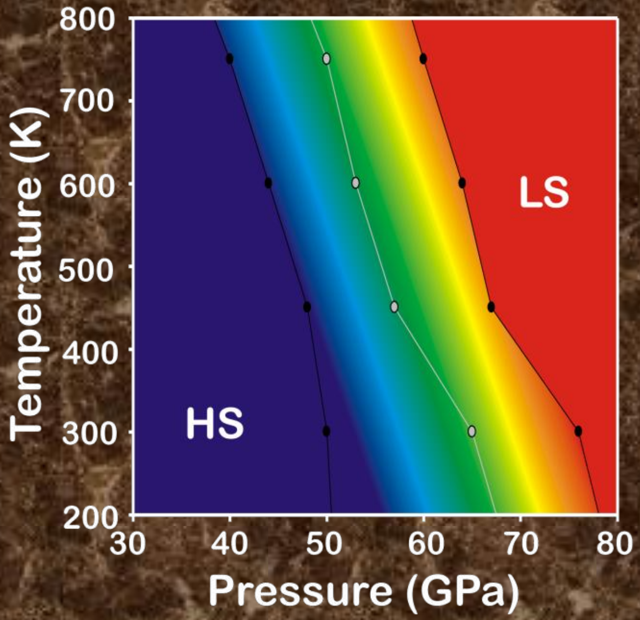

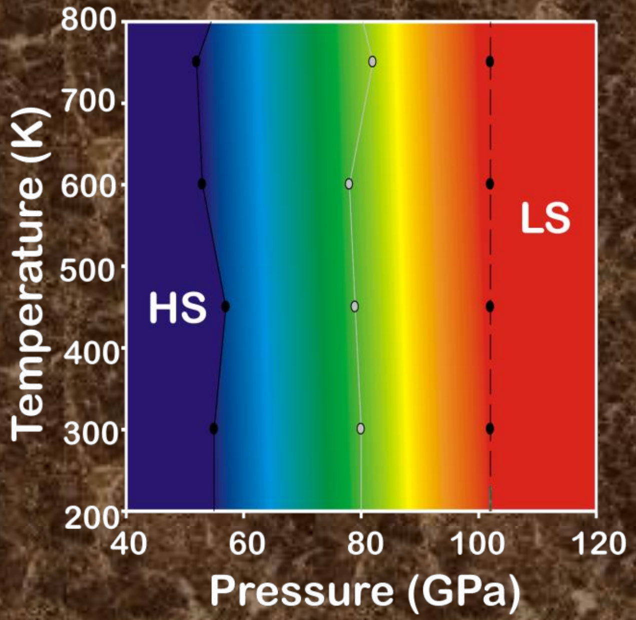

Kantor et al. 2007; 2008; 2009

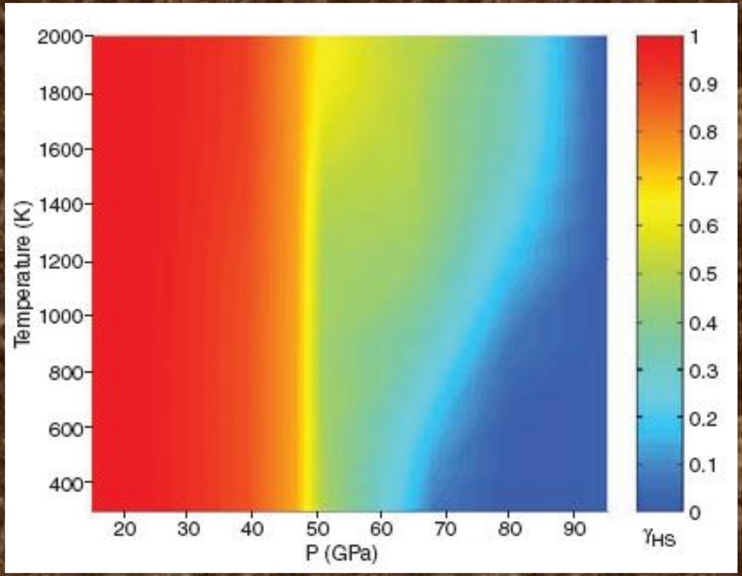

Lin et al., 2007

Mössbauer spectroscopy: Silicate Perovskites

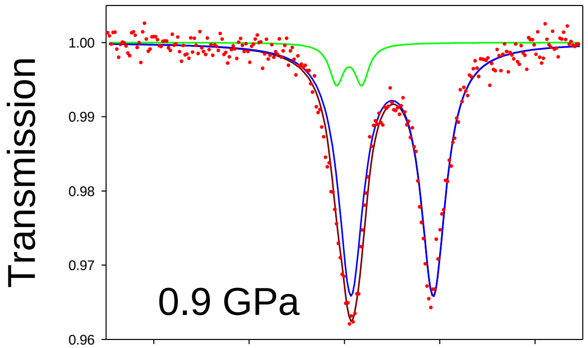

$(Mg_{0.88},Fe_{0.12})SiO_3$

$(Mg_{0.59},Fe_{0.41})(Si_{0.63}Al_{0.37})O_3$

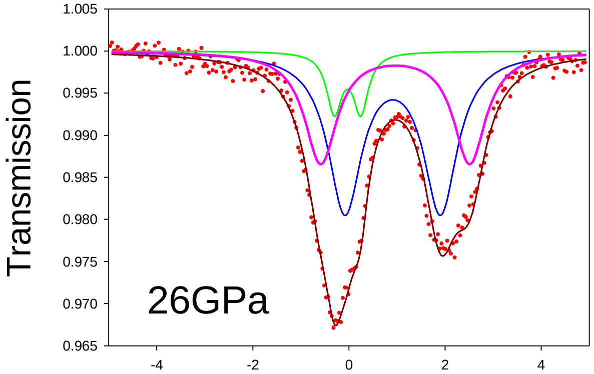

McCammon et al., 2008;
Narygina, 2009, 2010

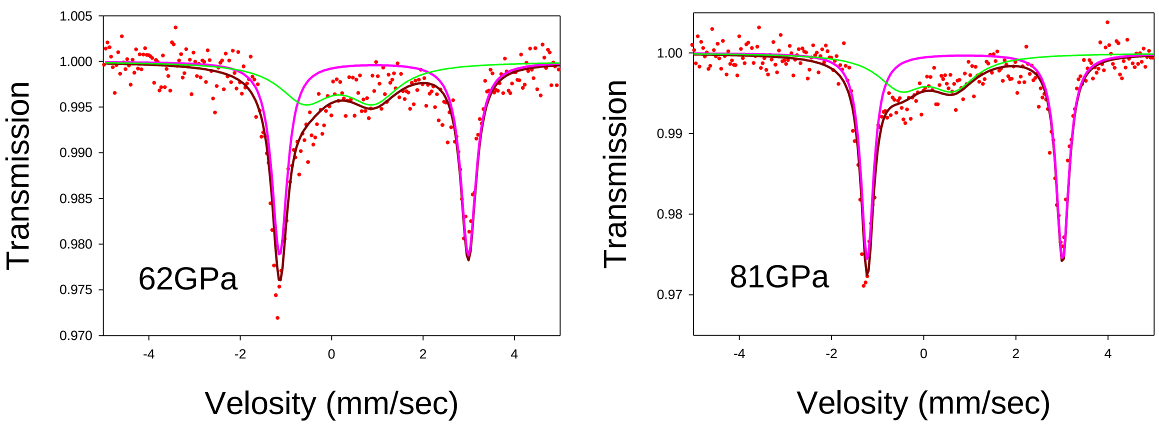

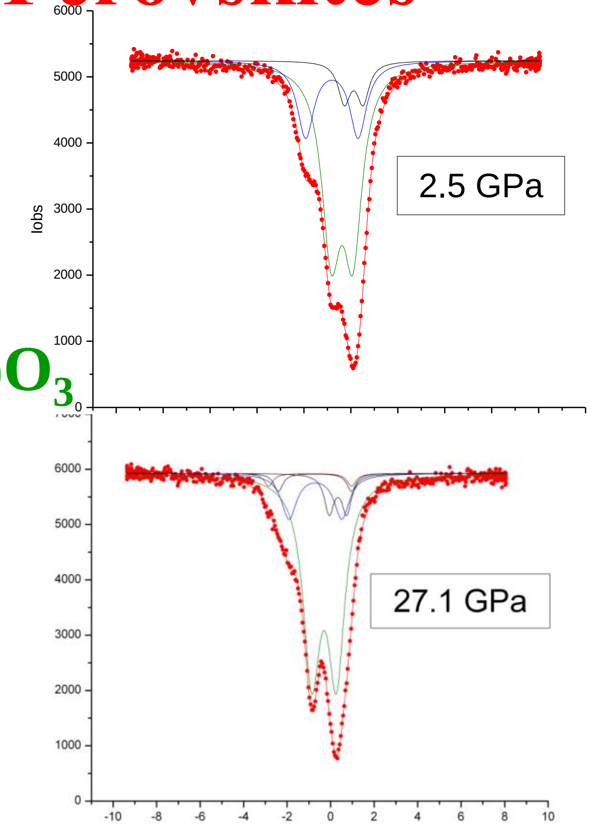

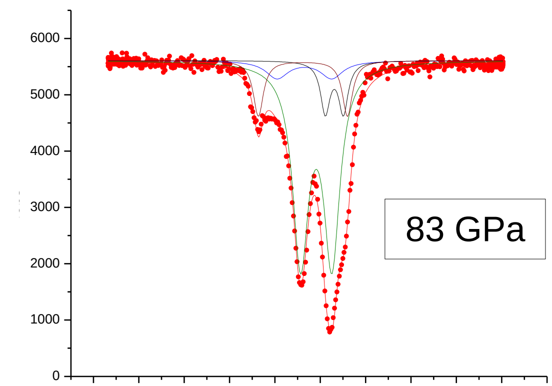

Potapkin et al., 2011

Electronic structure of the 3*d* orbitals of Fe^{2+} in eight-fold coordination

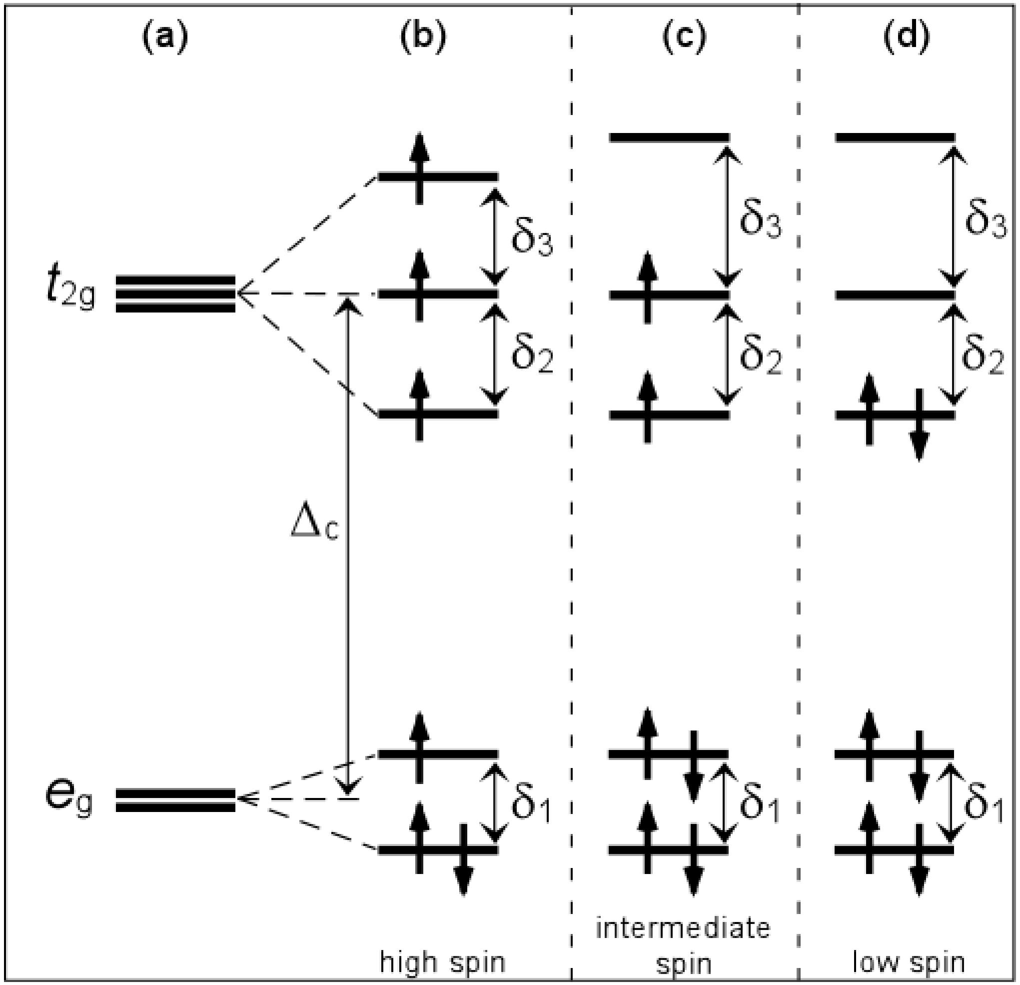

In a symmetrical ligand environment (a) the five *d* energy levels are split into three upper (t_{2g}) and two lower (e_g) levels, separated by the crystal field splitting (Δ_c). A distorted ligand environment further splits the t_{2g} and e_g energy levels, and depending on the relative magnitudes of Δ_c, the energy required to pair spins, and the splitting between individual e_g and t_{2g} levels (δ_1, δ_2 and δ_3), the six 3*d* electrons (arrows) are distributed in different spin states as follows: (b) high-spin Fe^{2+} with 4 unpaired electrons; (c) intermediate-spin Fe^{2+} with 2 unpaired electrons; and (d) low-spin Fe^{2+} with no unpaired electrons. The relative magnitudes of δ_2 and δ_3 and Δ_c can lead to the stabilisation of unusual spin states, such as intermediate-spin Fe^{2+}.

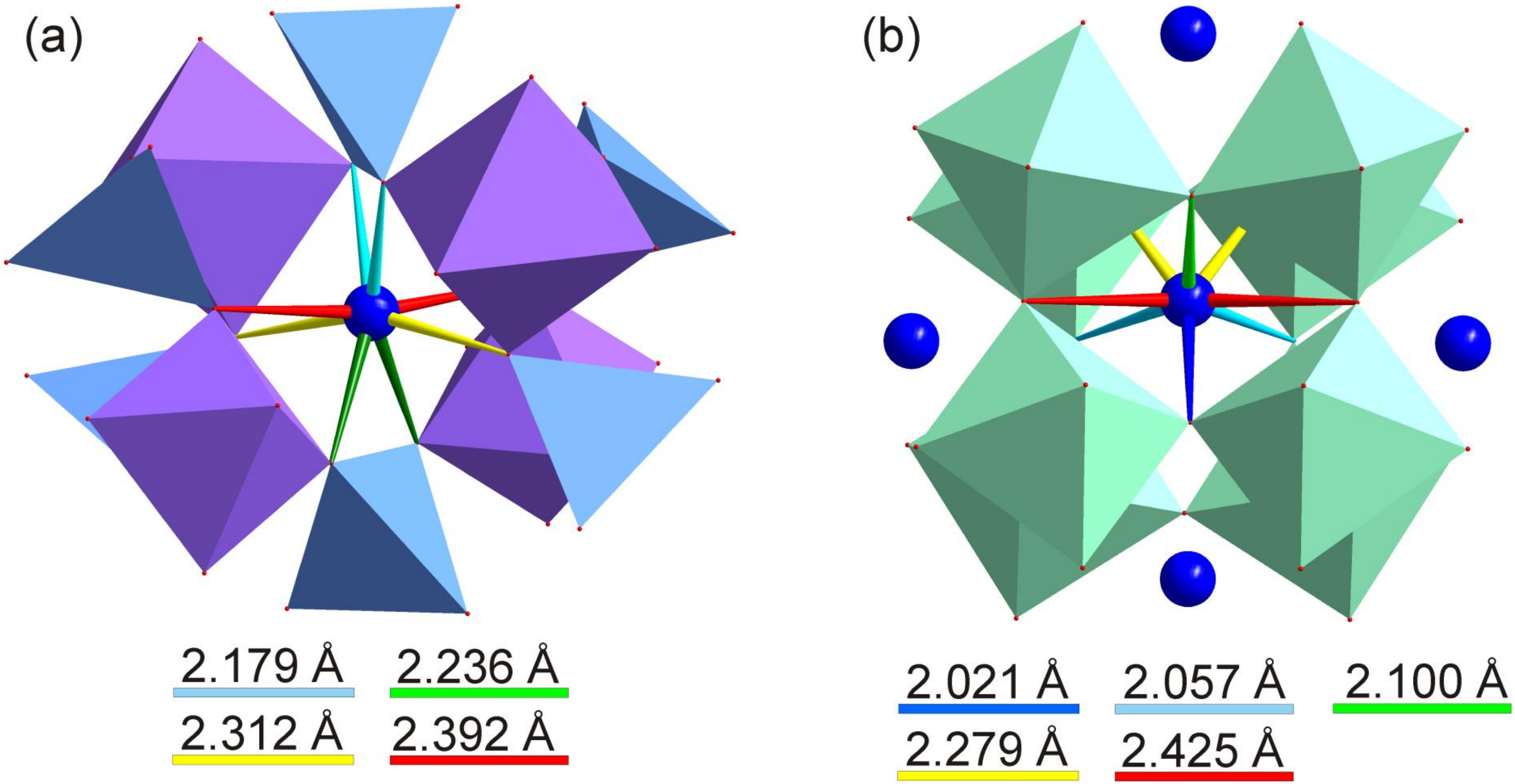

Majorite

Silicate Pv

Silicate Pv

Majorite

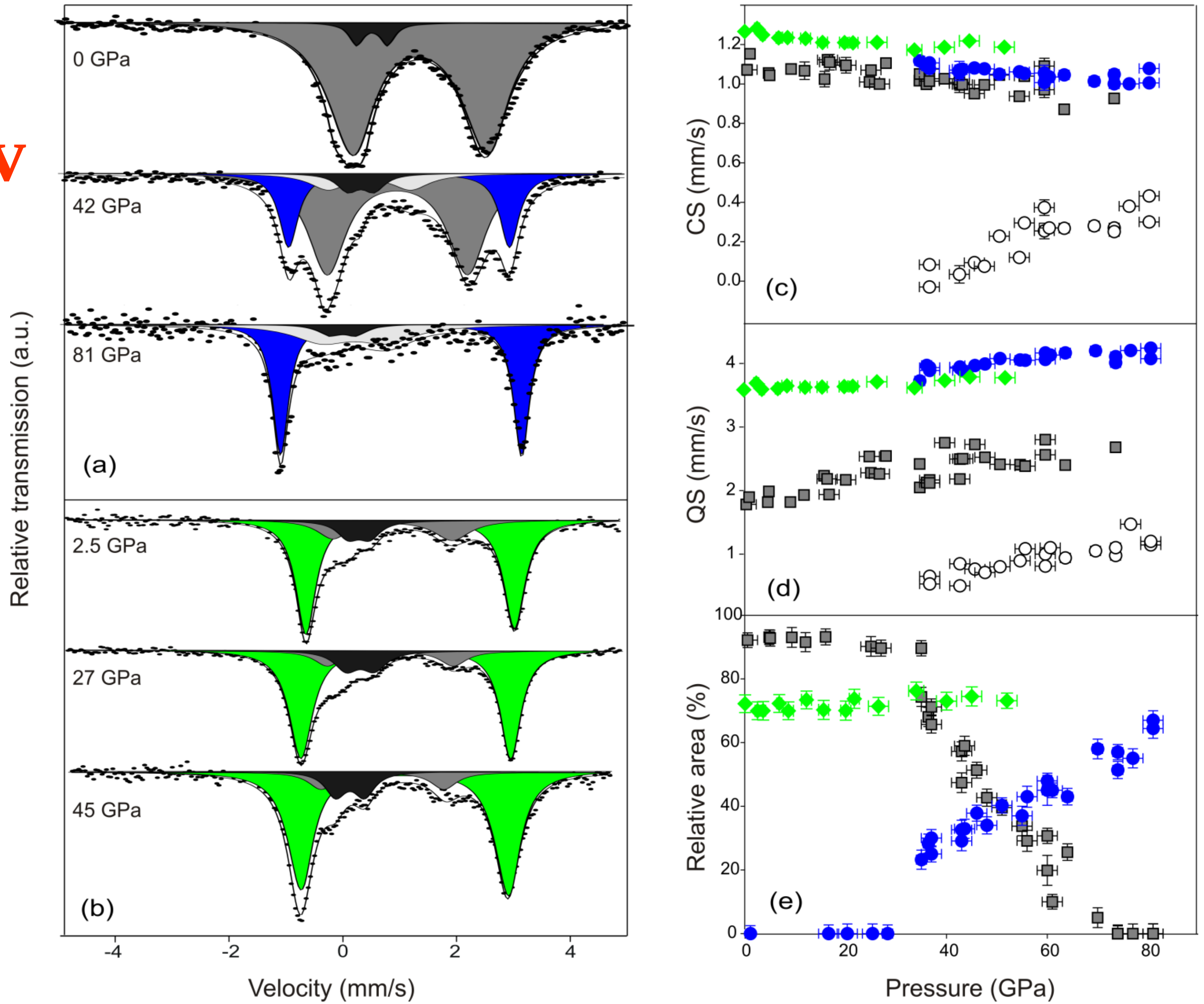

Narygina et al., Phys. Chem. Minerals, 2011

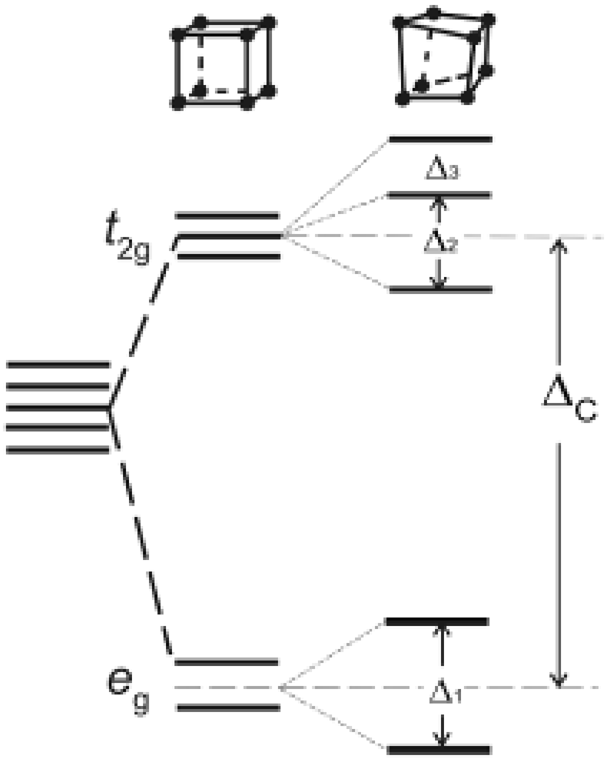

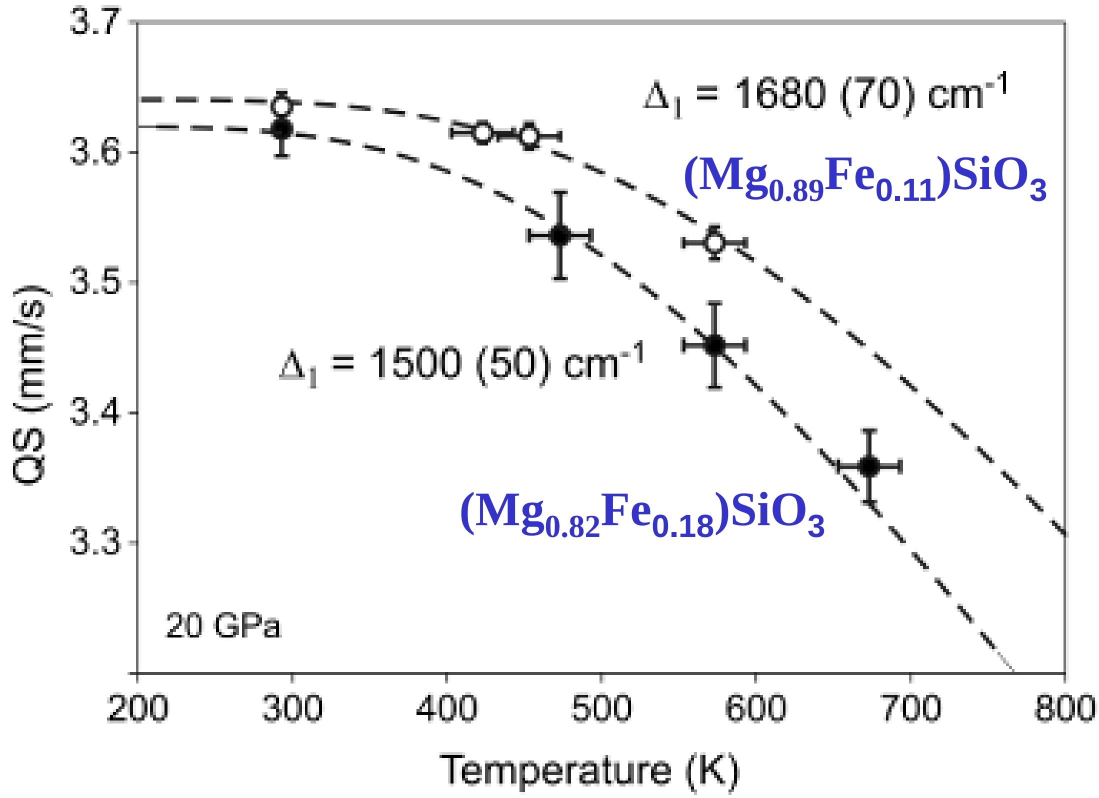

$$QS(T) = QS(0)\left(\frac{1 - e^{-\Delta_1/kT}}{1 + e^{-\Delta_1/kT}}\right)$$

Narygina et al., Phys. Chem. Minerals, 2011

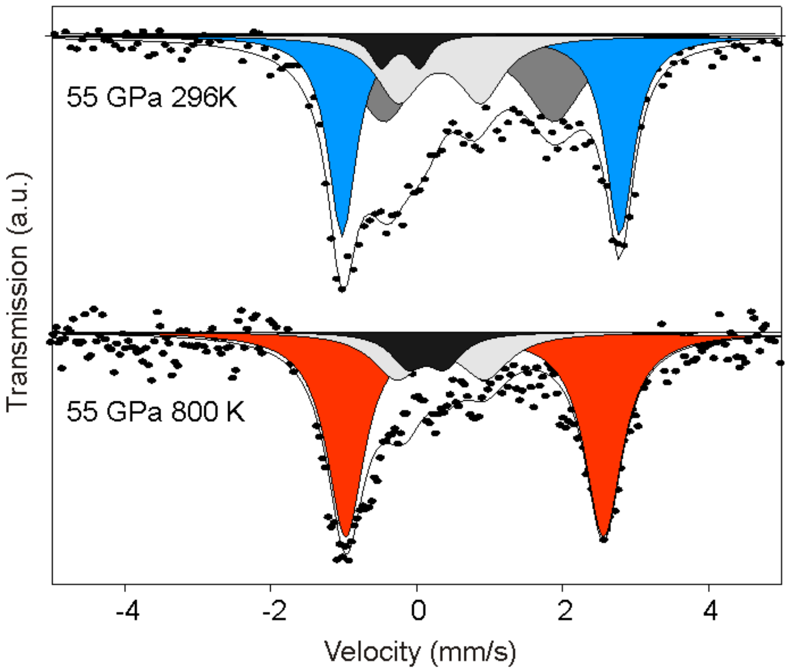

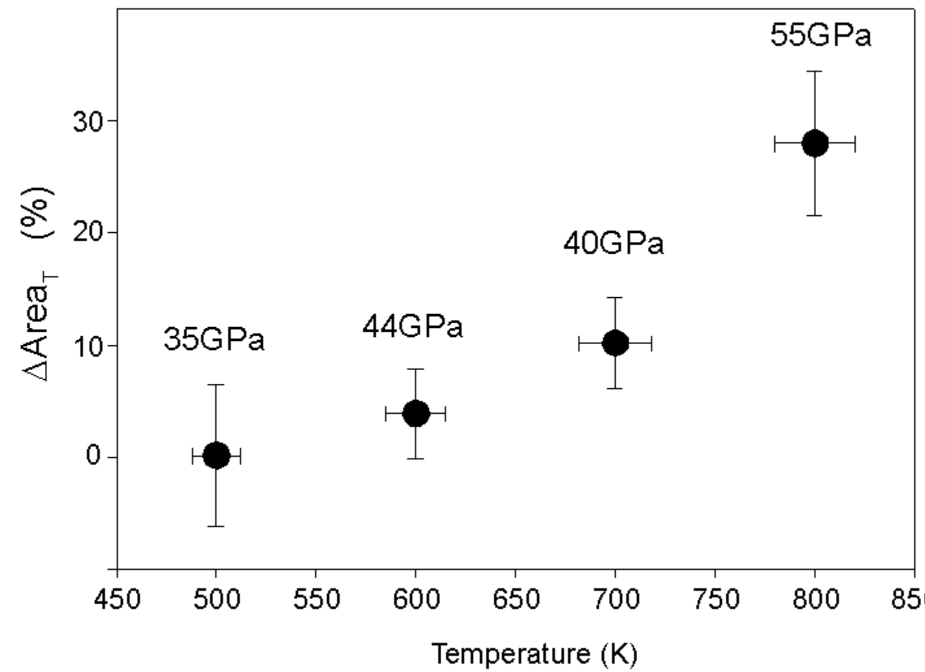

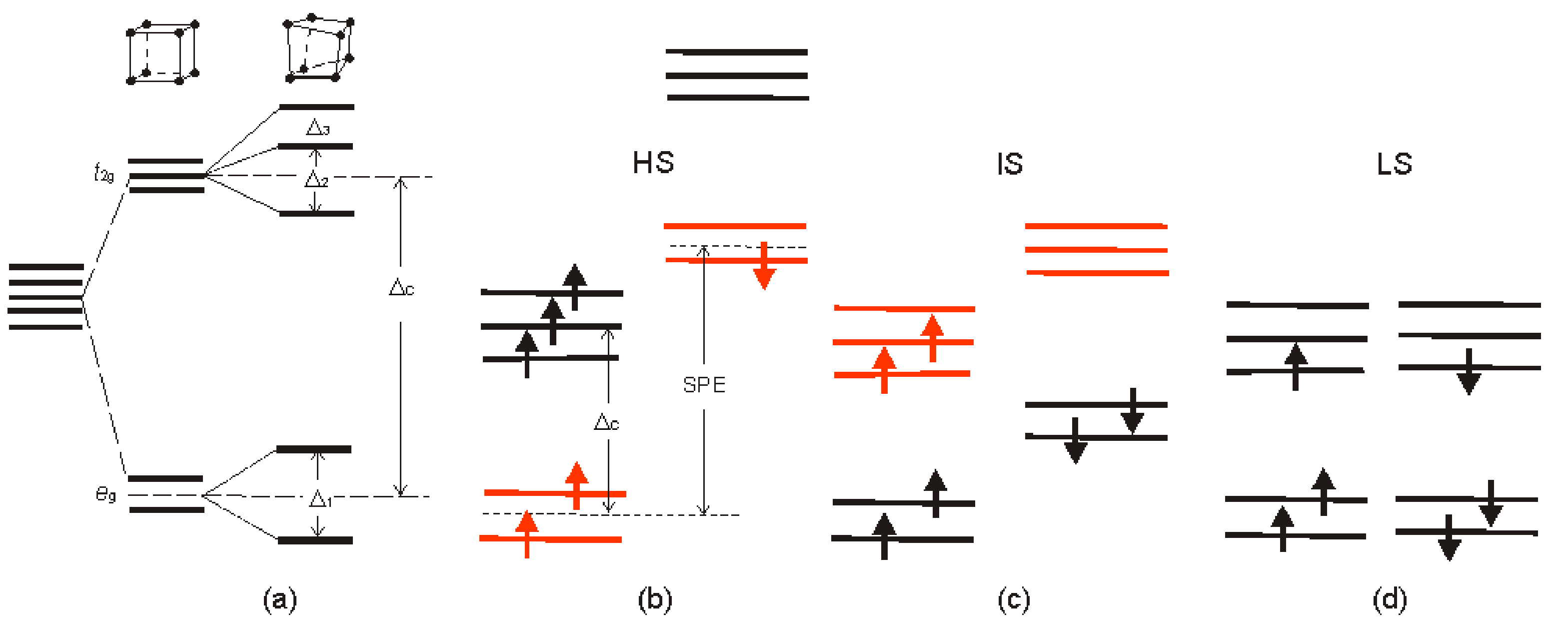

Narygina et al., Phys. Chem. Minerals, 2011

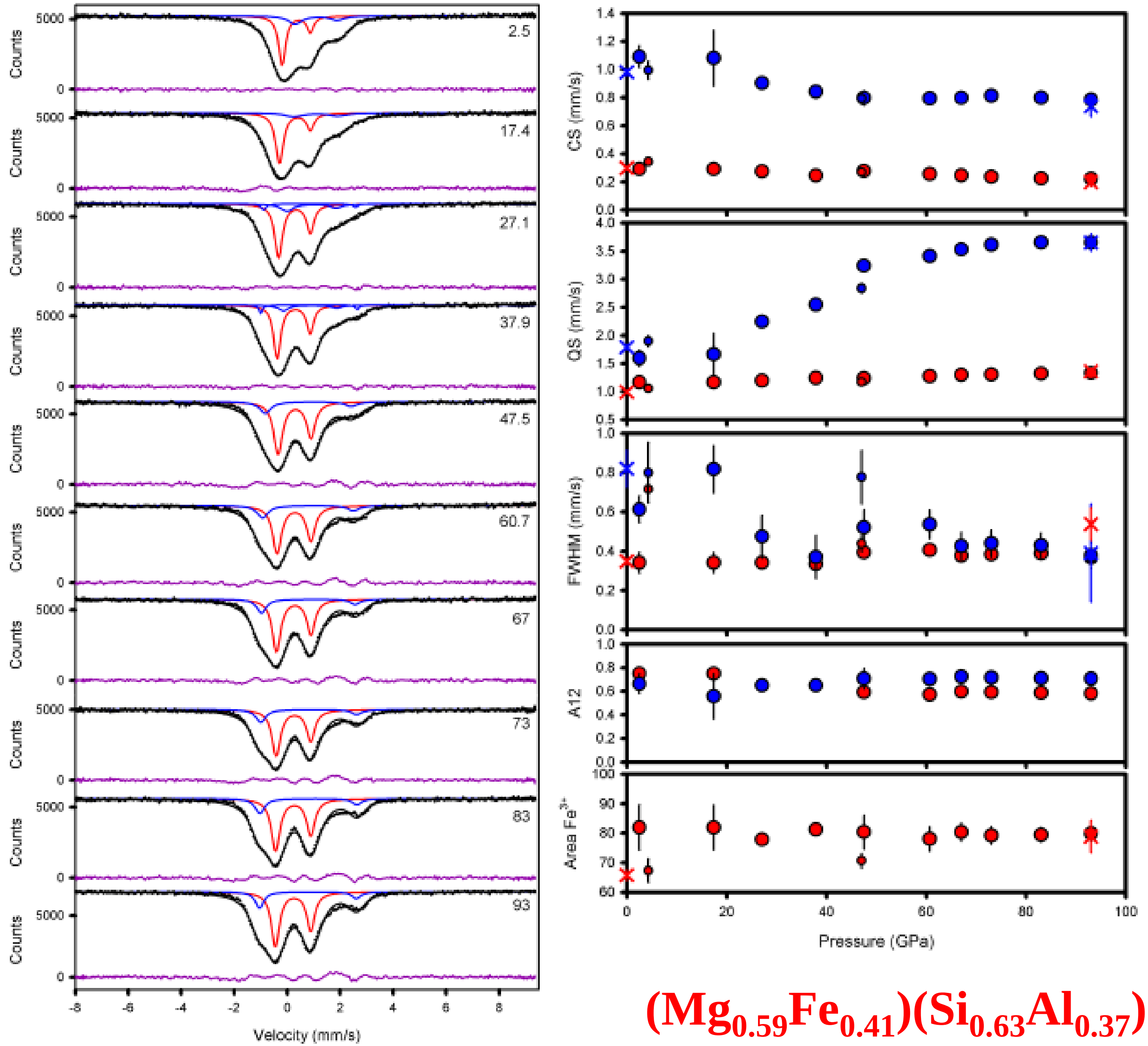

Potapkin et al., 2011

$(Mg_{0.59}Fe_{0.41})(Si_{0.63}Al_{0.37})O_3$ Pv

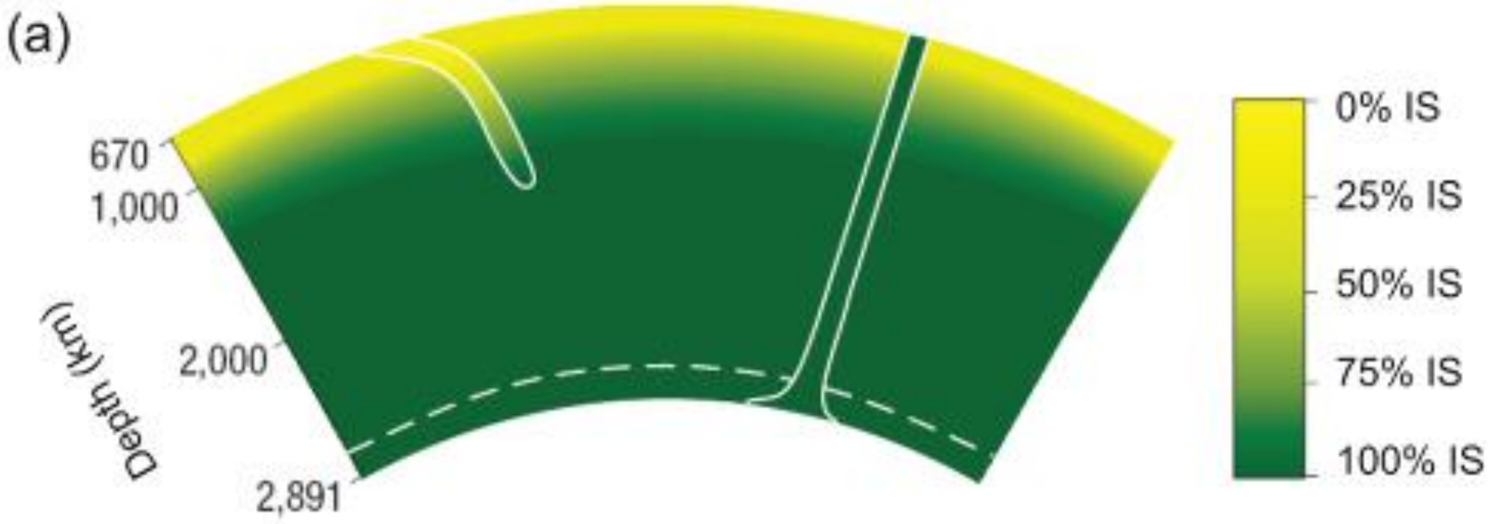

Pv

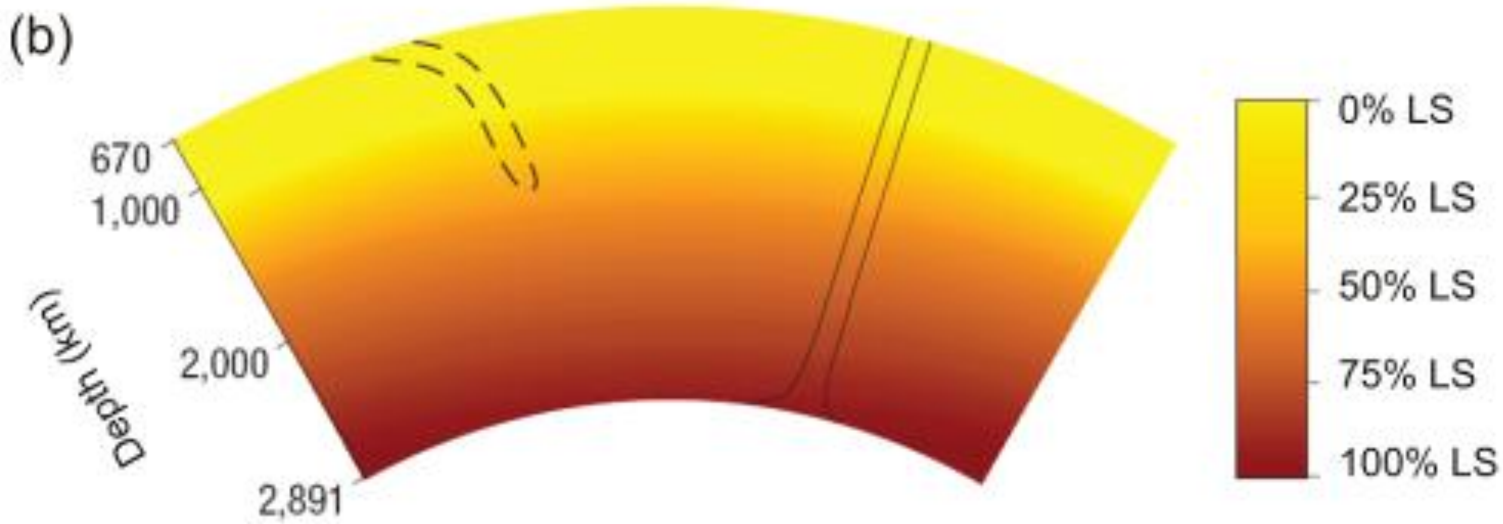

Fp

McCammon et al., 2008; Narygina, 2009, 2010

$(Mg_{0.59}Fe_{0.41})(Si_{0.63}Al_{0.37})O_3$

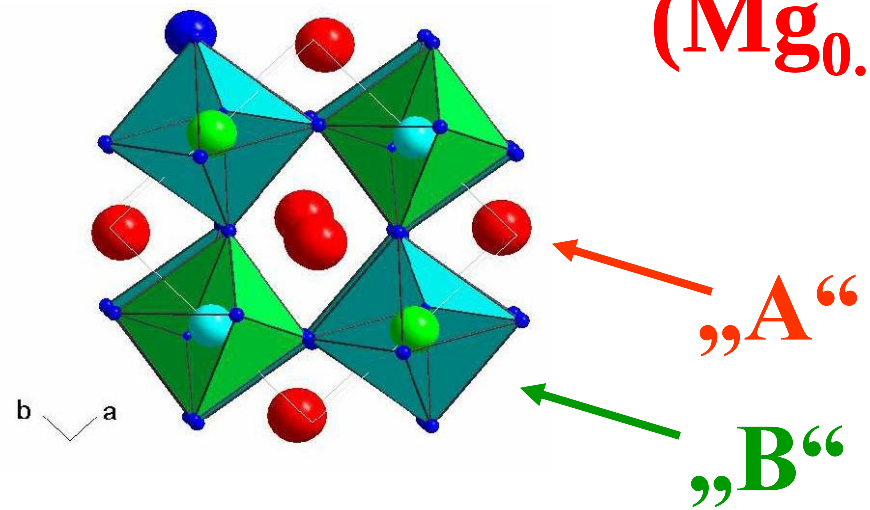

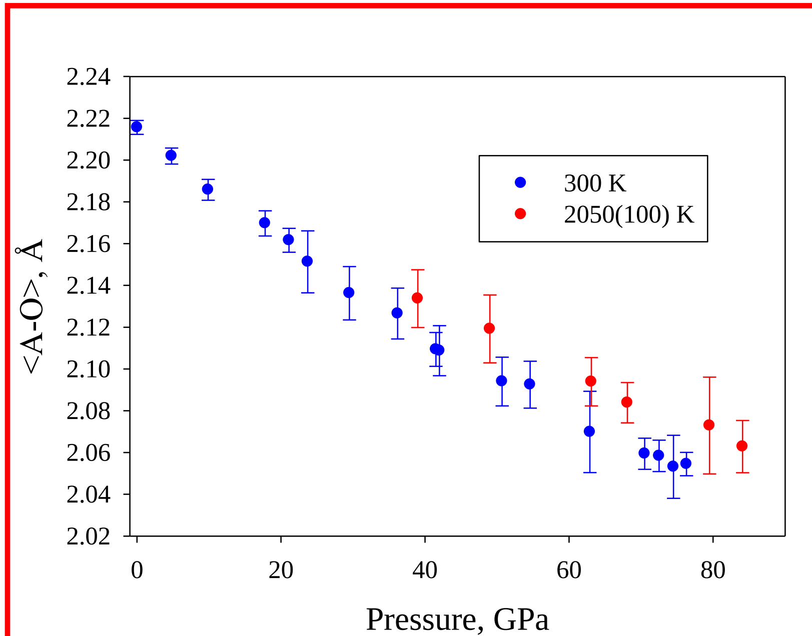

$(Mg_{0.88}Fe_{0.12})SiO_3$

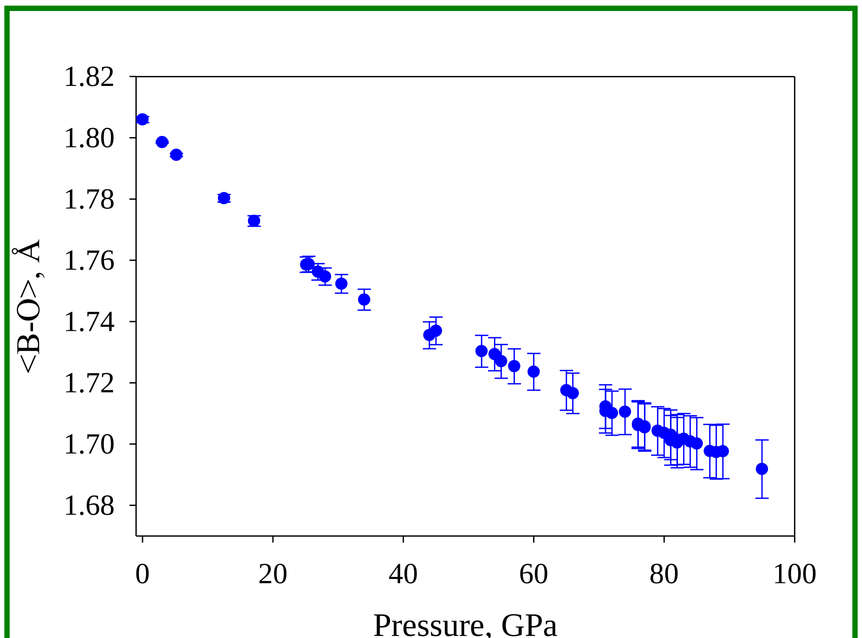

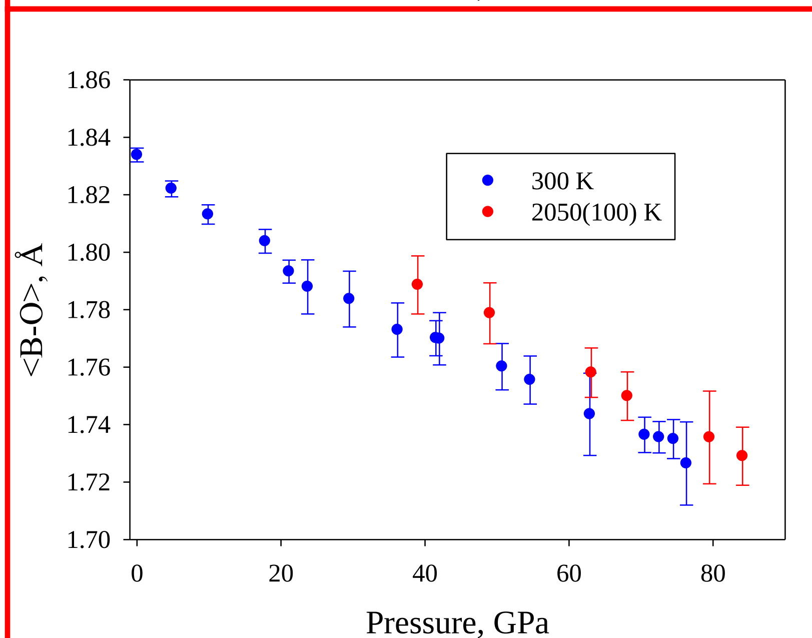

$(Mg_{0.88},Fe_{0.12})SiO_3$

$(Mg_{0.59},Fe_{0.41})(Si_{0.63}Al_{0.37})O_3$

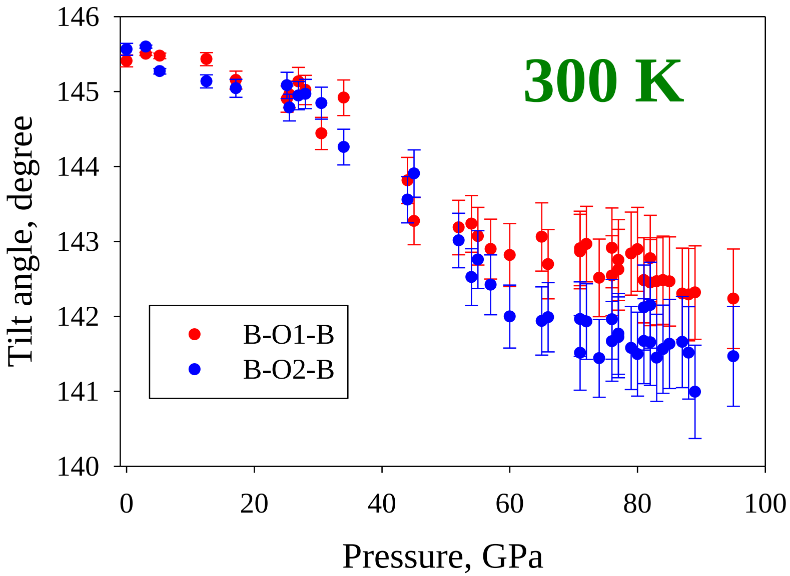

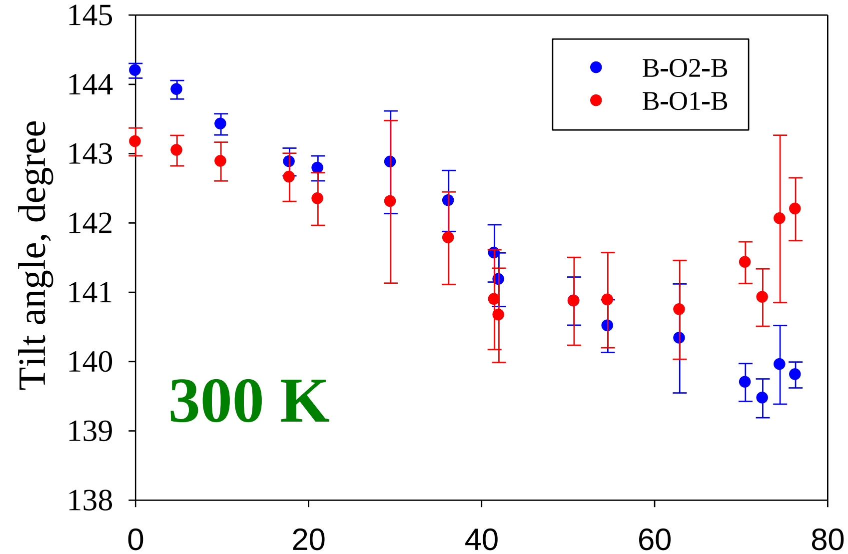

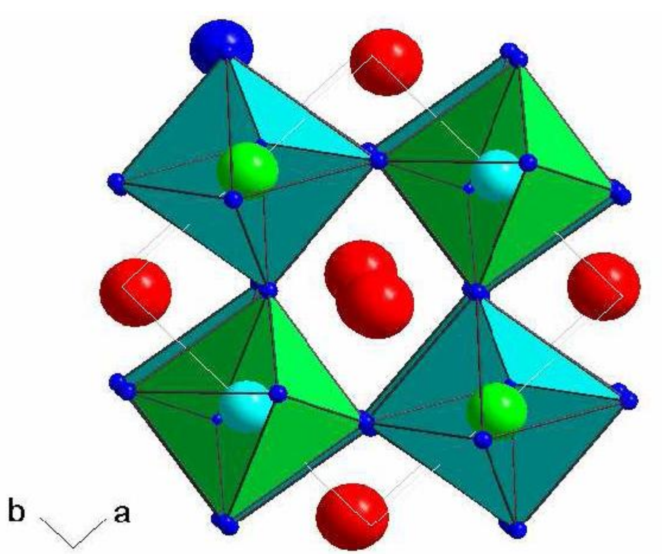

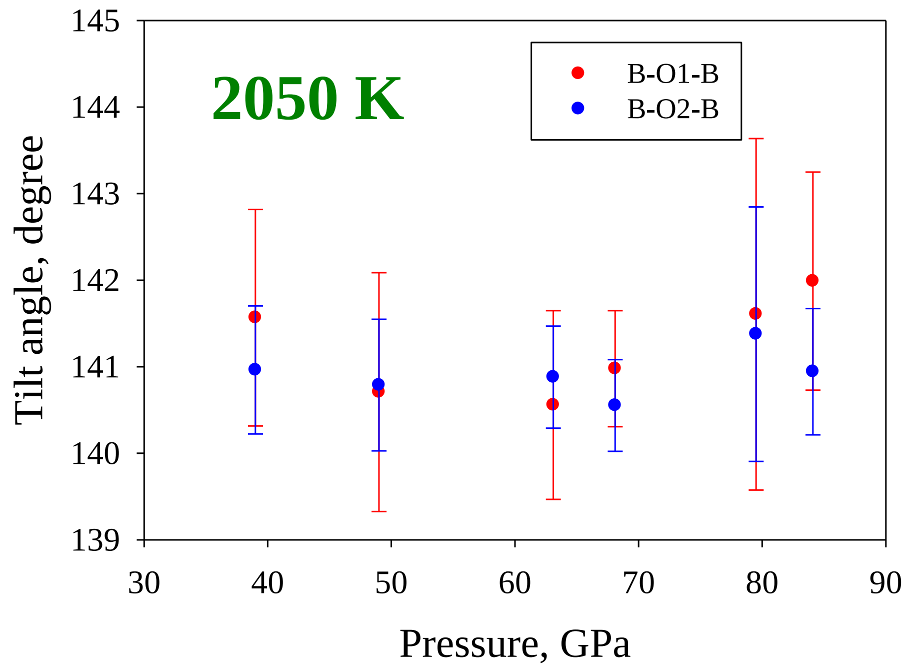

$(Mg_{0.59},Fe_{0.41})(Si_{0.63}Al_{0.37})O_3$

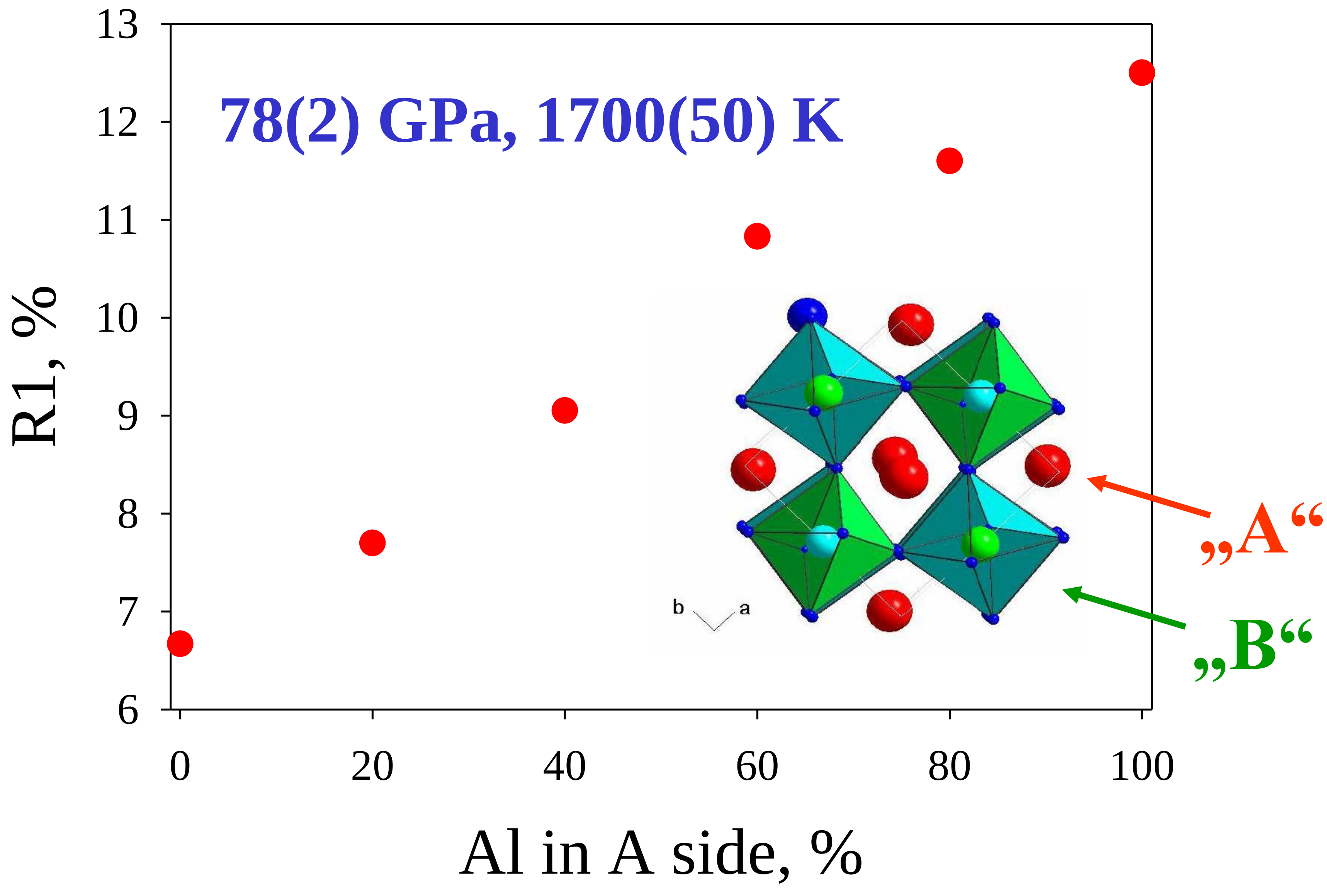

Thermal EoS of $(Mg_{0.88}Fe_{0.12})SiO_3$ Pv

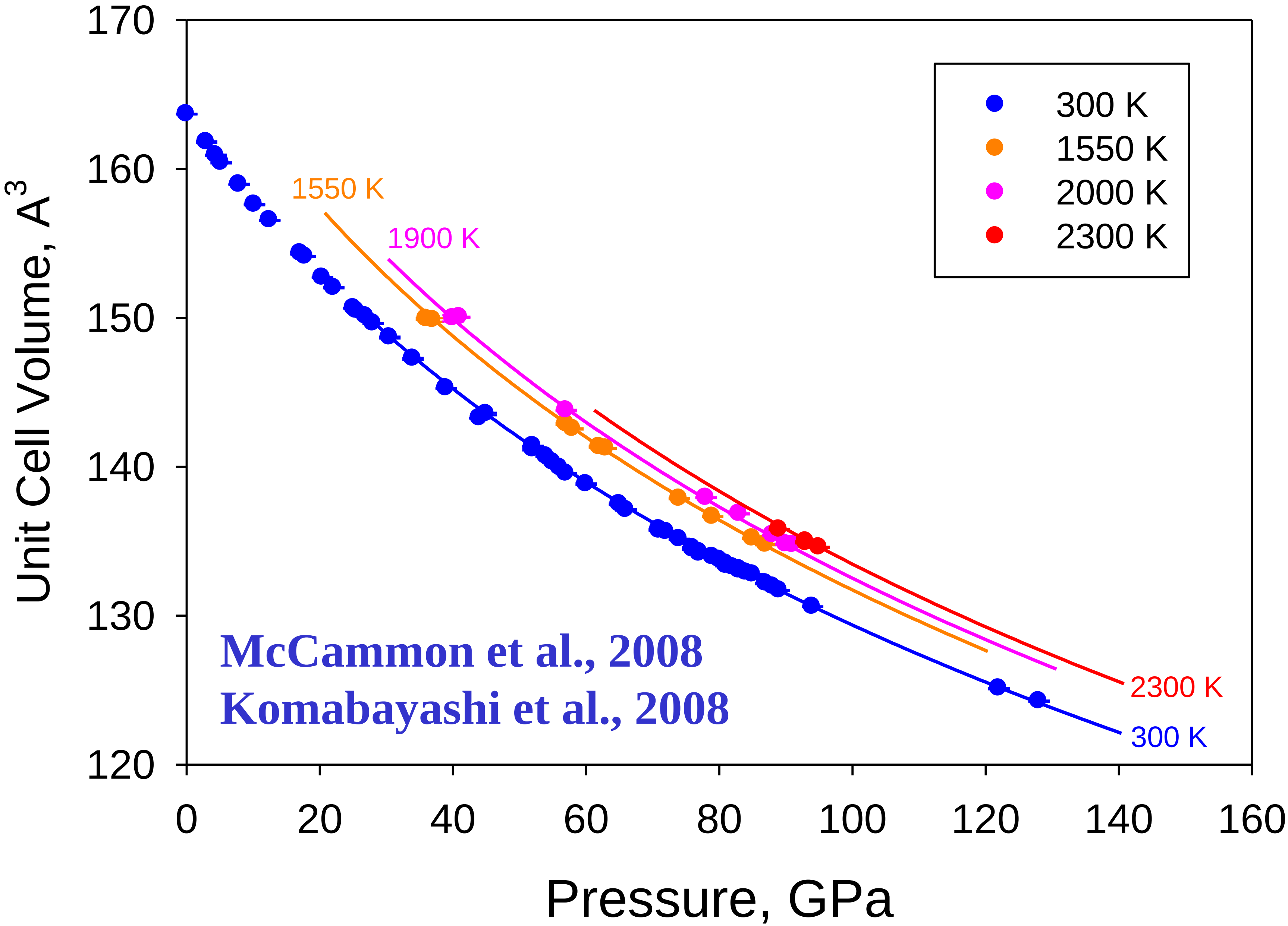

Thermal EoS of $(Mg_{0.59}Fe_{0.41})(Si_{0.63}Al_{0.37})O_3$ Pv

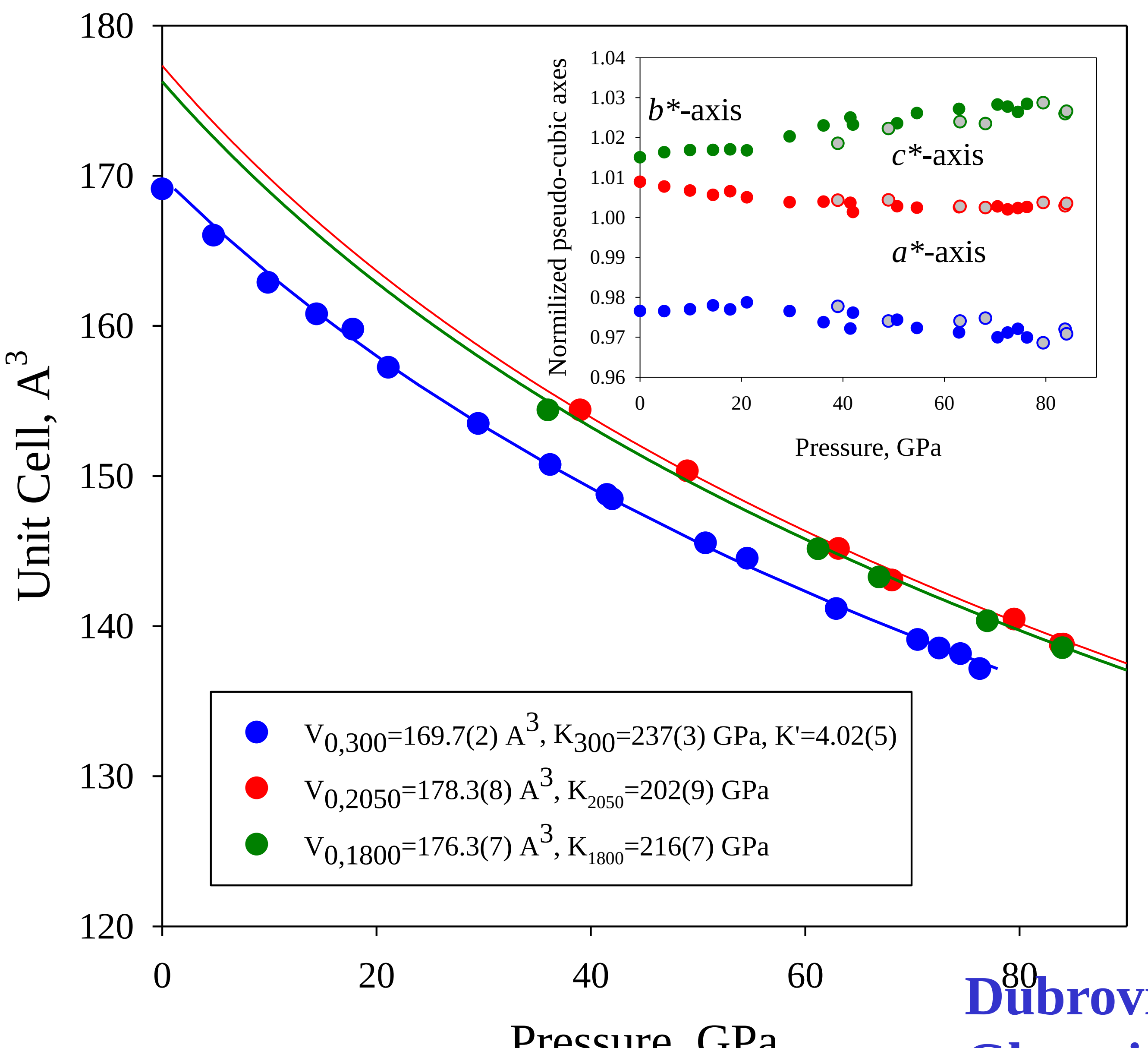

Dubrovinsky et al., 2010
Glazyrin et al., 2012

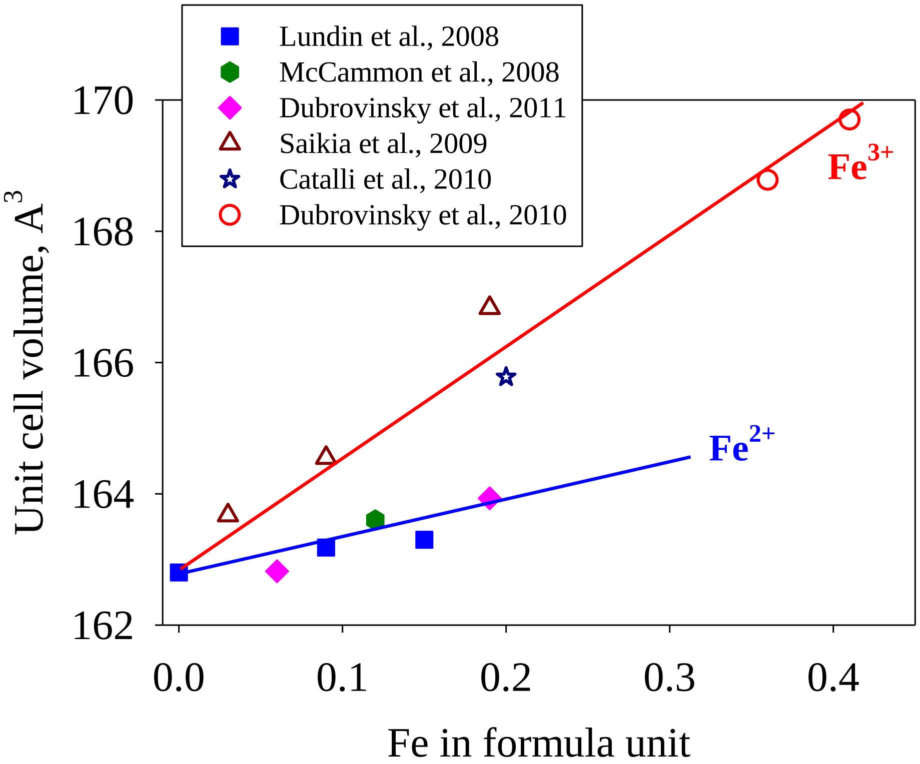

Towards of "universal" EoS of Pv?

$(Mg_{1-x}Fe^{2+}_xFe^{3+}_y)(Si_{1-y}Al_y)O_3$

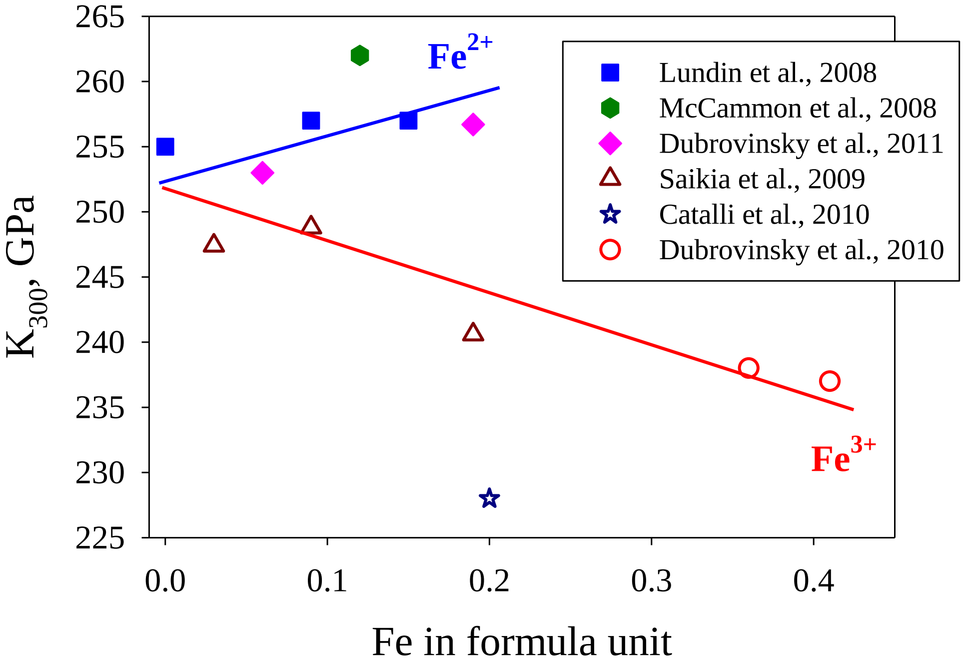

Mantle velocity profiles and tomography

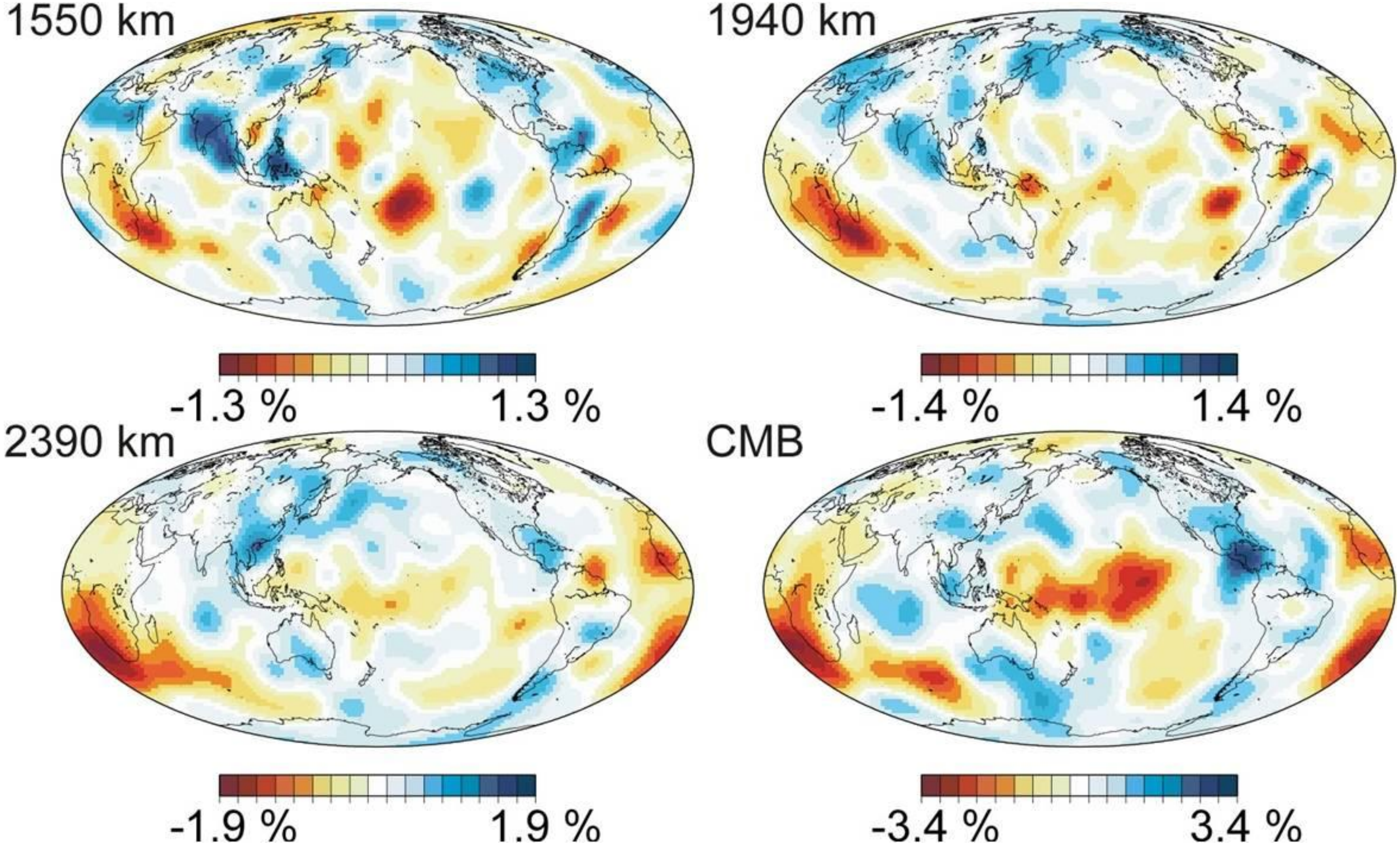

Takeuchi, N., 2007. J. Int., 169, 1153-1163

www.eri.u-tokyo.ac.jp/takeuchi/model/

Conclusions and perspectives

The most reliable information about crystal structures and their response to changes in pressure and temperature is obtained from single crystal diffraction experiments. We have developed a methodology to perform single crystal X-ray diffraction experiments in laser-heated DACs and demonstrated that structural refinements and accurate measurements of the thermal equation of state of metals, oxides, silicates from single crystal intensity data are possible at pressures up to megabars and temperatures of thousands degrees. New methodology was applied to study structural variations in ferropericlase and iron- and aluminum-bearing silicate perovskites at conditions of the Earth's lower mantle.

Acknowledgments:

PhD Students:

K. Glazyrin
E. Greenberg
E. Holbig
I. Kantor
A. Kantor
J. Liu
O. Narygina
E. Zarechnaya

Post-Docs and AvH Fellows

A. Kurnosov
A. Kuznetzov
V. Prakapenka
J. Rouquette
S. Ryosuke
C. Wegel
X. Wu

I. Abrikosov, LIU
G. Aquilanti, ESRF
W. Crichton, ESRF
N. Dubrovinskaia, UB
V. Dmitriev, SNBL
M. Hanfland, ESRF
C. McCammon, BGI
G. Steinle-Neumann, BGI
S. Pascarelli, ESRF

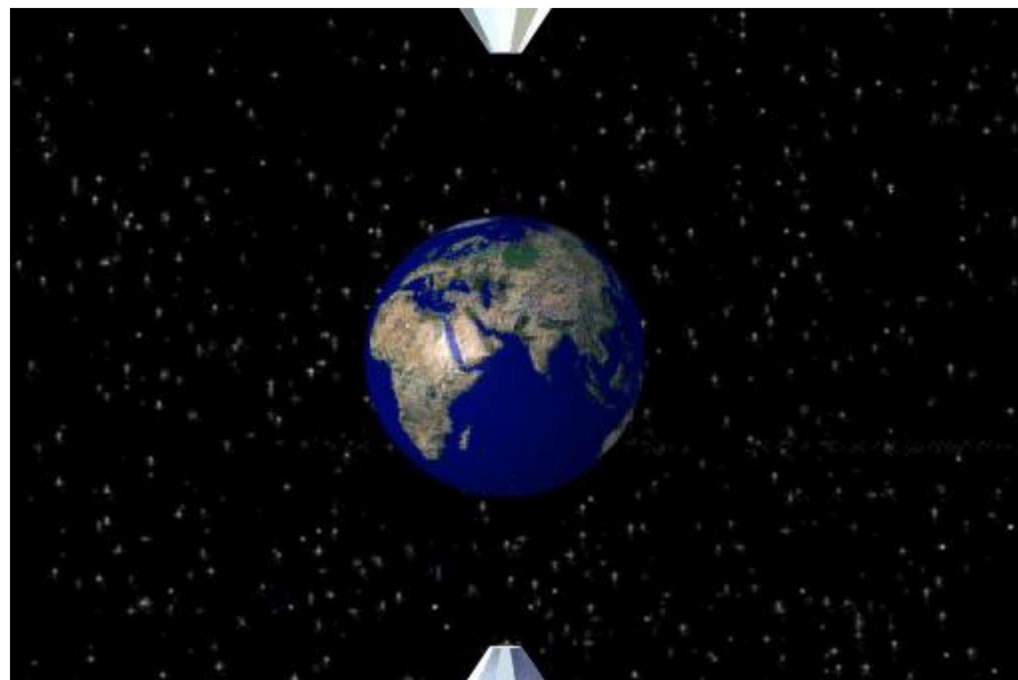

From EoS

$$\frac{K_S}{\rho} = V_P^2 - \frac{4}{3}V_S^2 = V_\Phi{}^2$$

$$\frac{G}{\rho} = V_S^2$$

???!!!

$$\frac{3}{V_D^3} = \frac{1}{V_P^3} + \frac{2}{V_S^3}$$

From NIS!!!

Laser heated DAC on ID18 beamline

(Nuclear Inelastic Scattering, NIS)

Dubrovinsky et al., 2009
Glazyrin et al., 2010

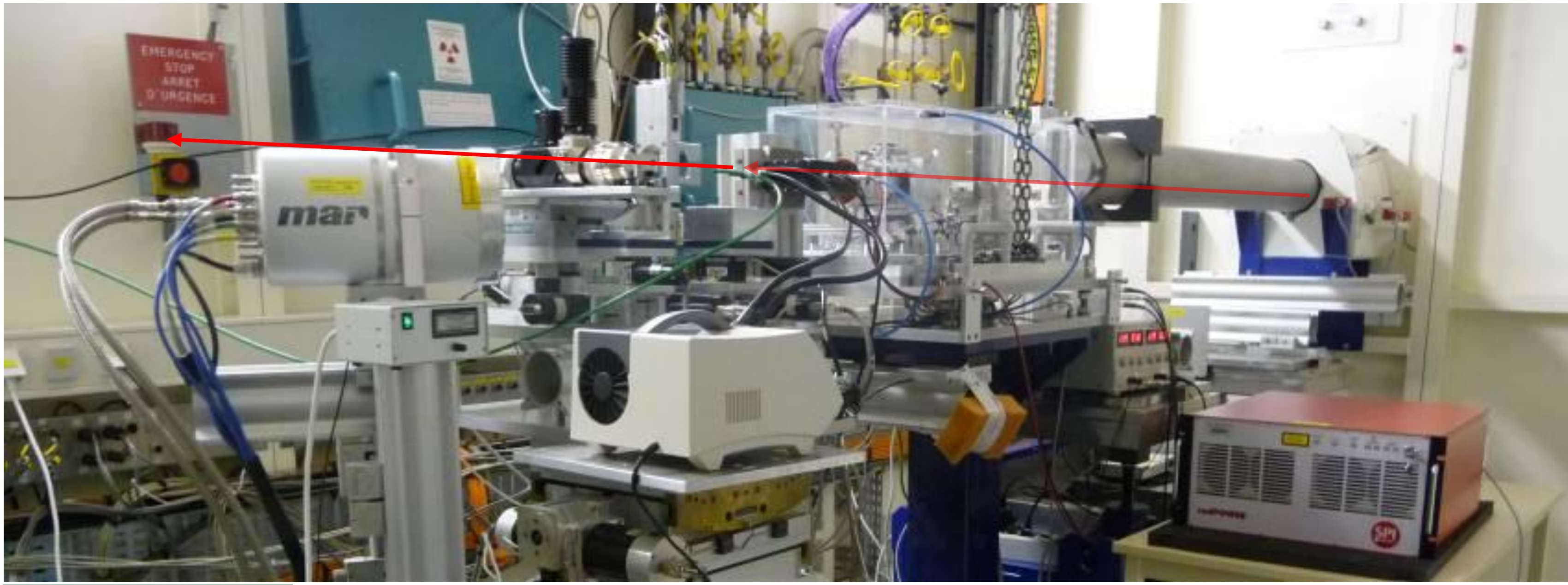

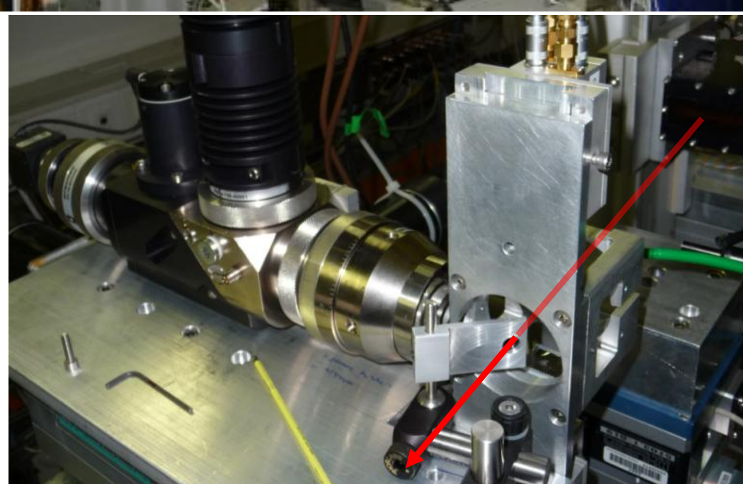

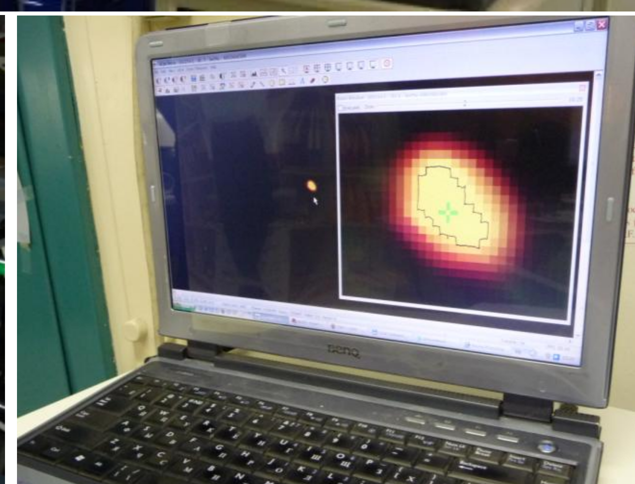

Mantle velocity…

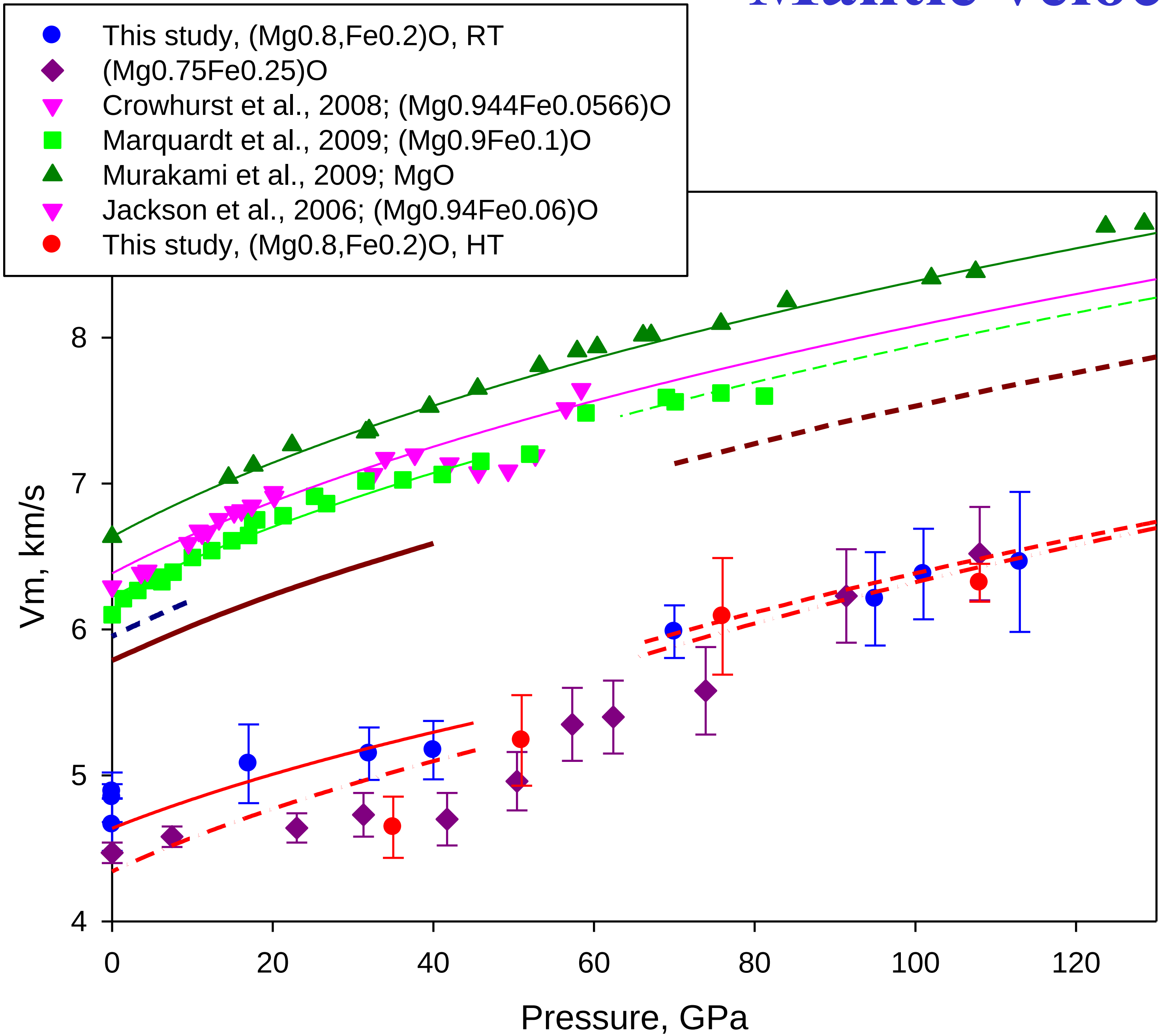

Mantle velocity, "Birch law"

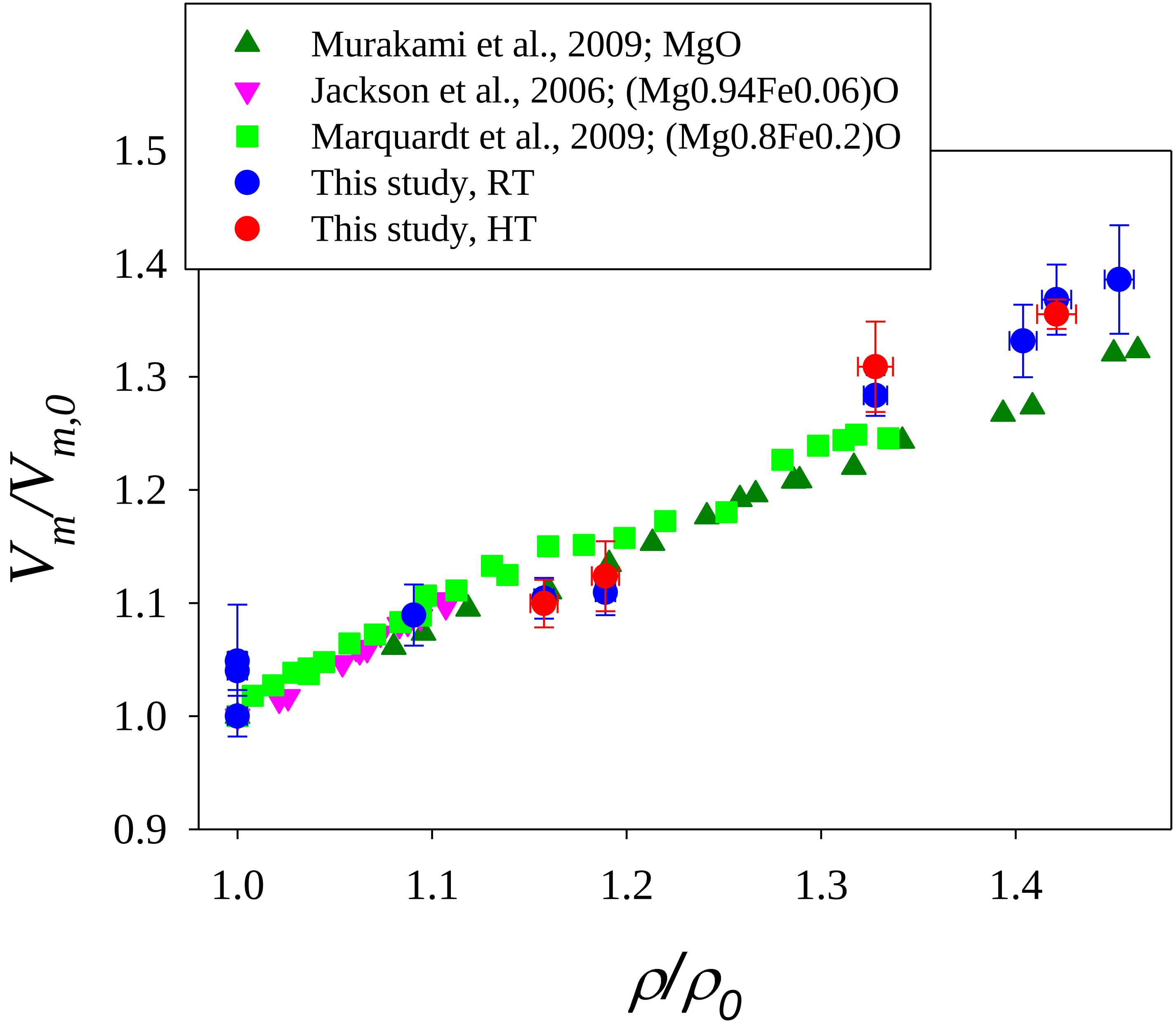

Mantle velocity, “Birch law”

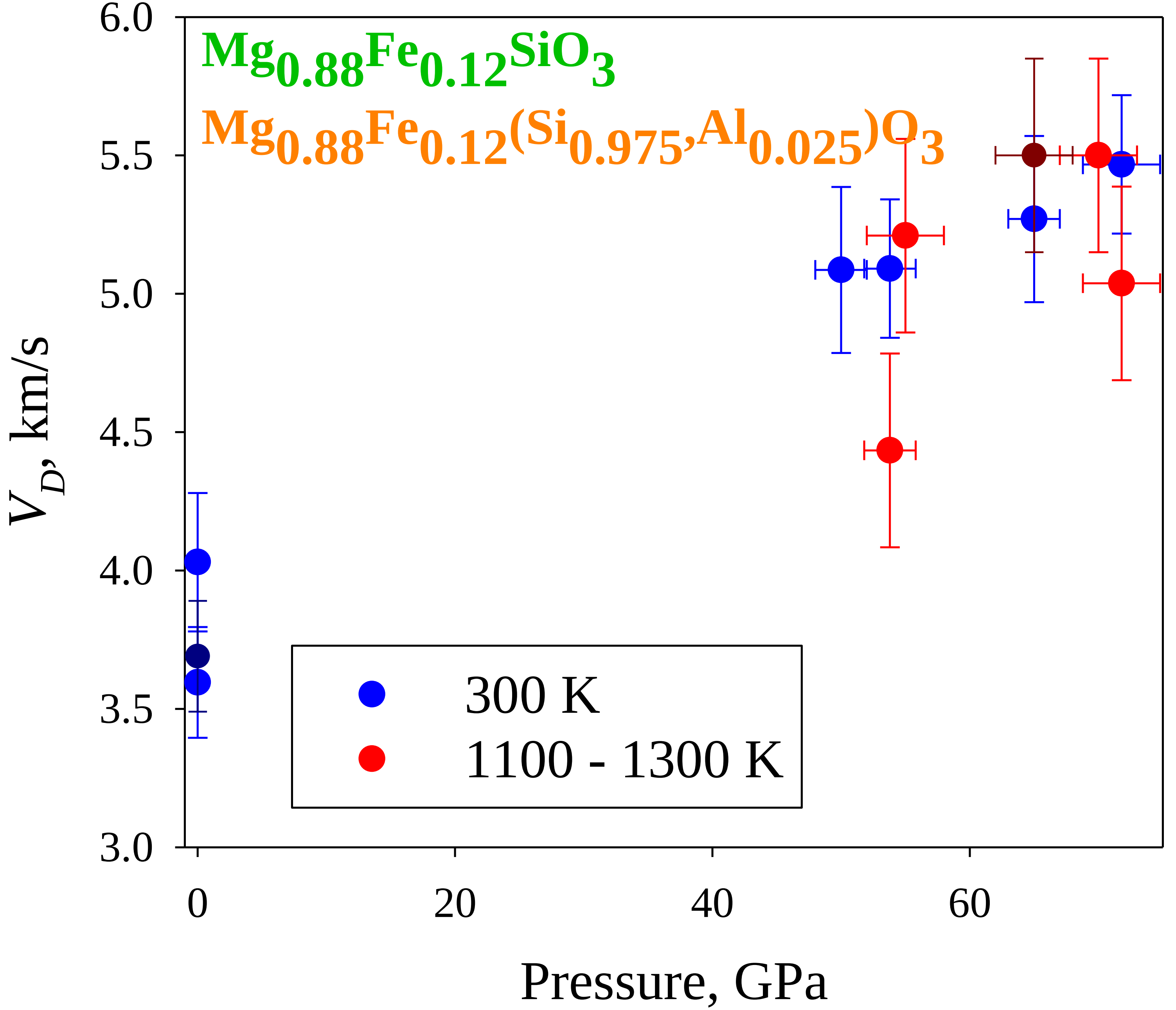

Mantle velocity, "Birch law"

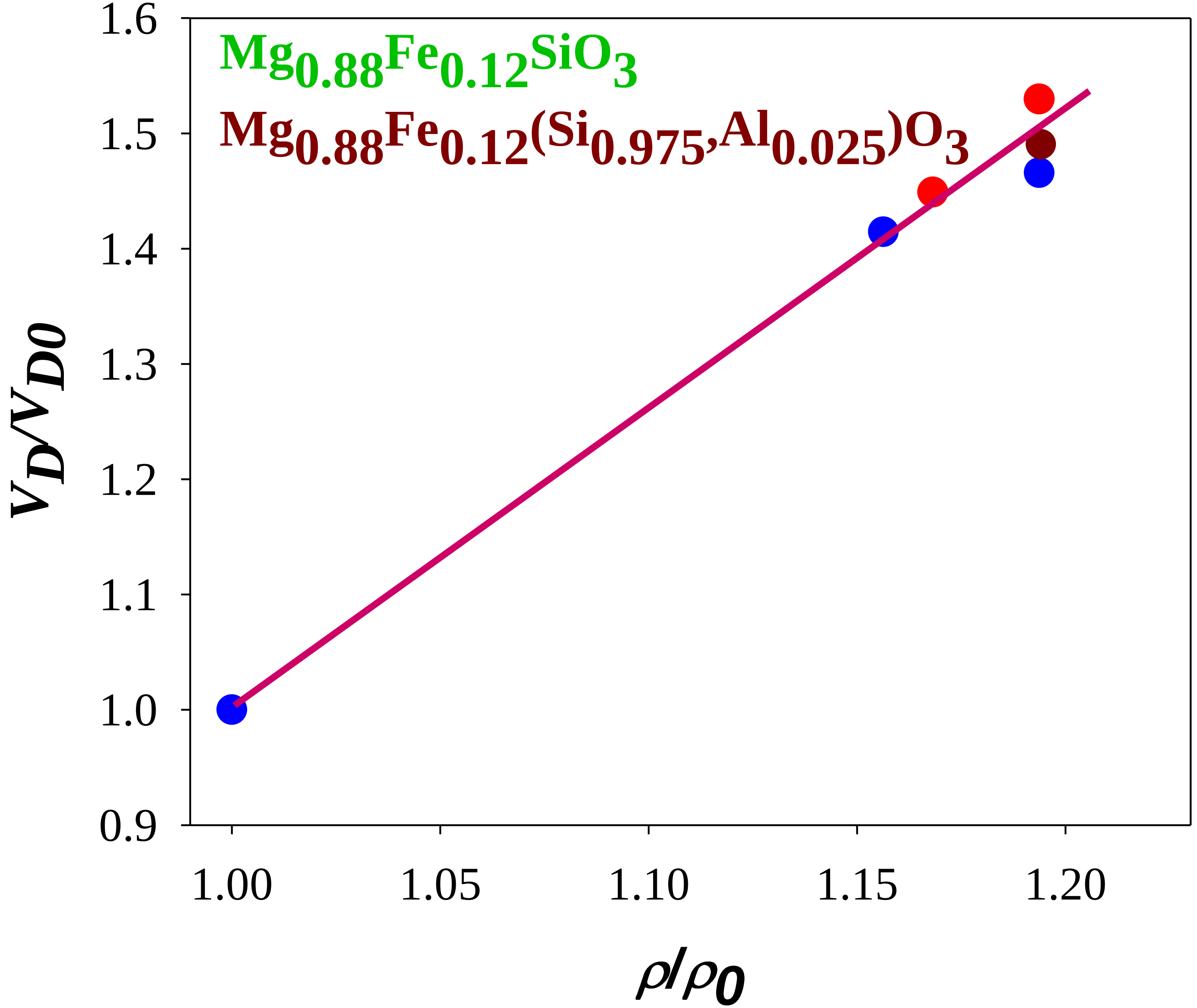

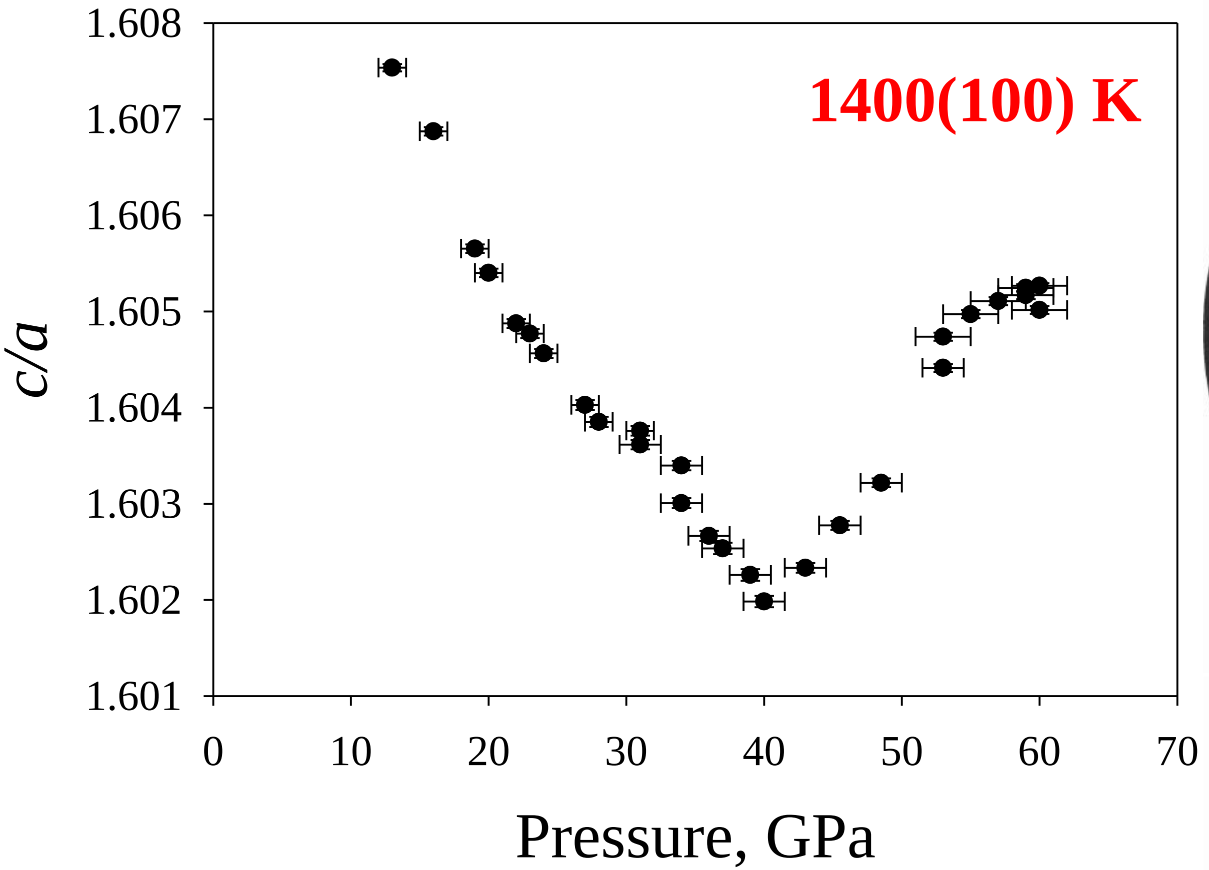

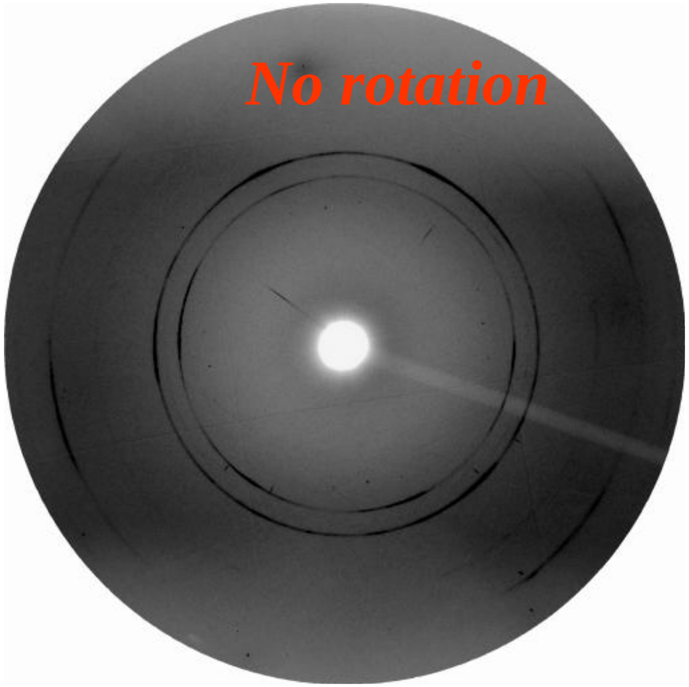

hcp-Fe in laser-heated DAC in He

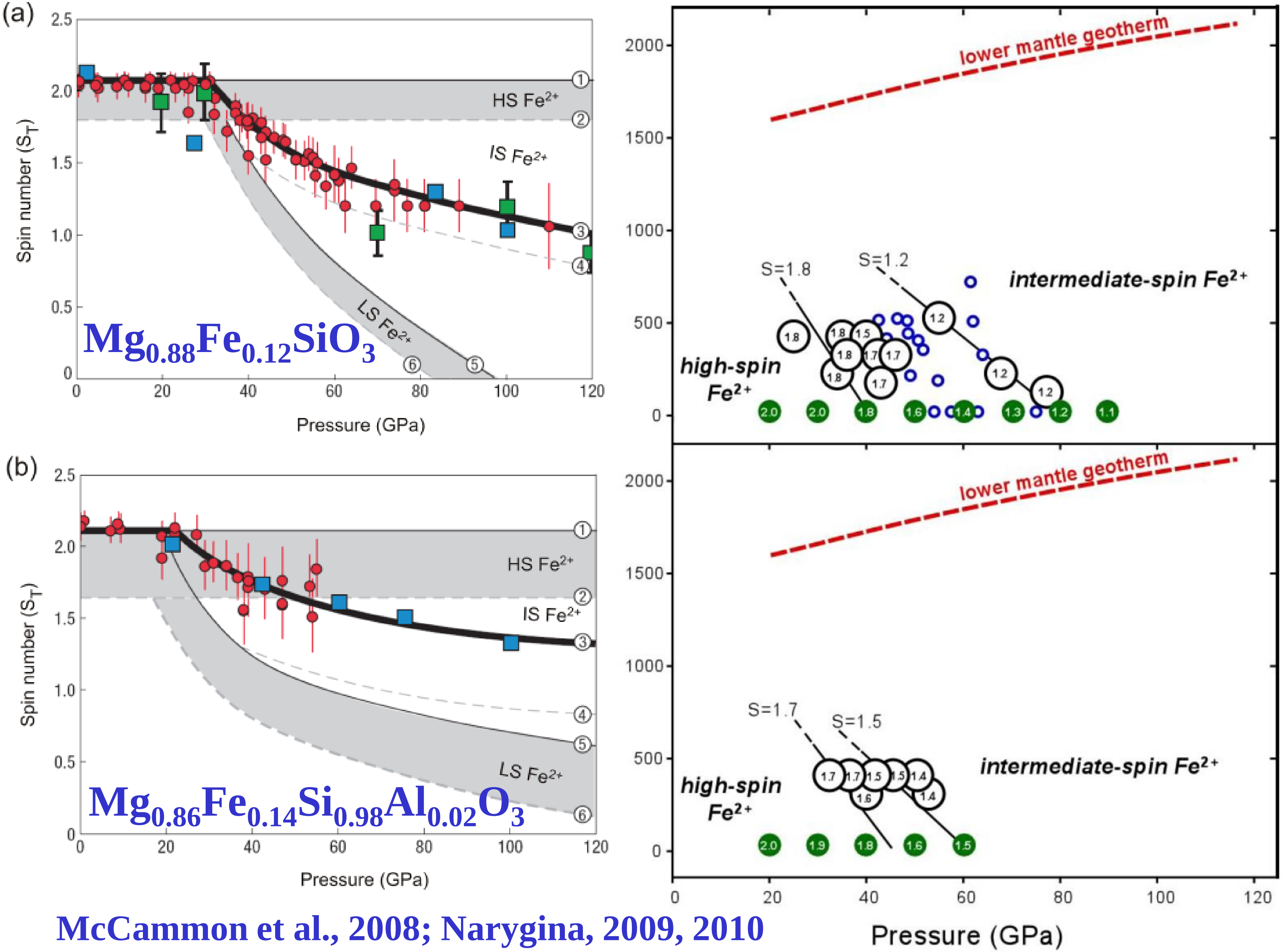

McCammon et al., 2008; Narygina, 2009, 2010

Fe_2O_3

Hematite, R3(-)c

Reflections: 45

R1: 4.4%

28.5(3) GPa

RT

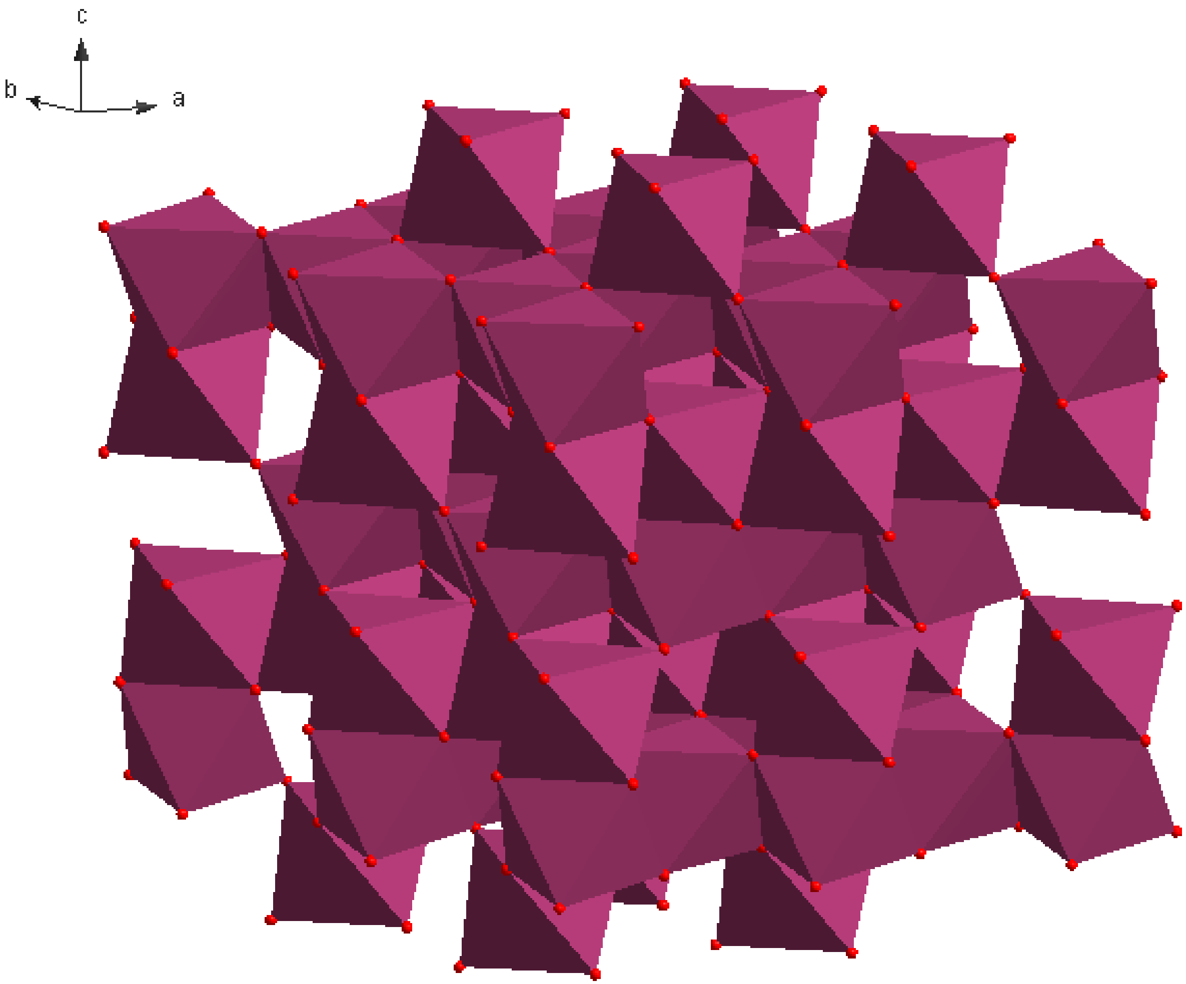

Fe_2O_3

Hematite, R3(-)c

Reflections: 26

R1: 8.8%

31.7(5) GPa

2250(50) K

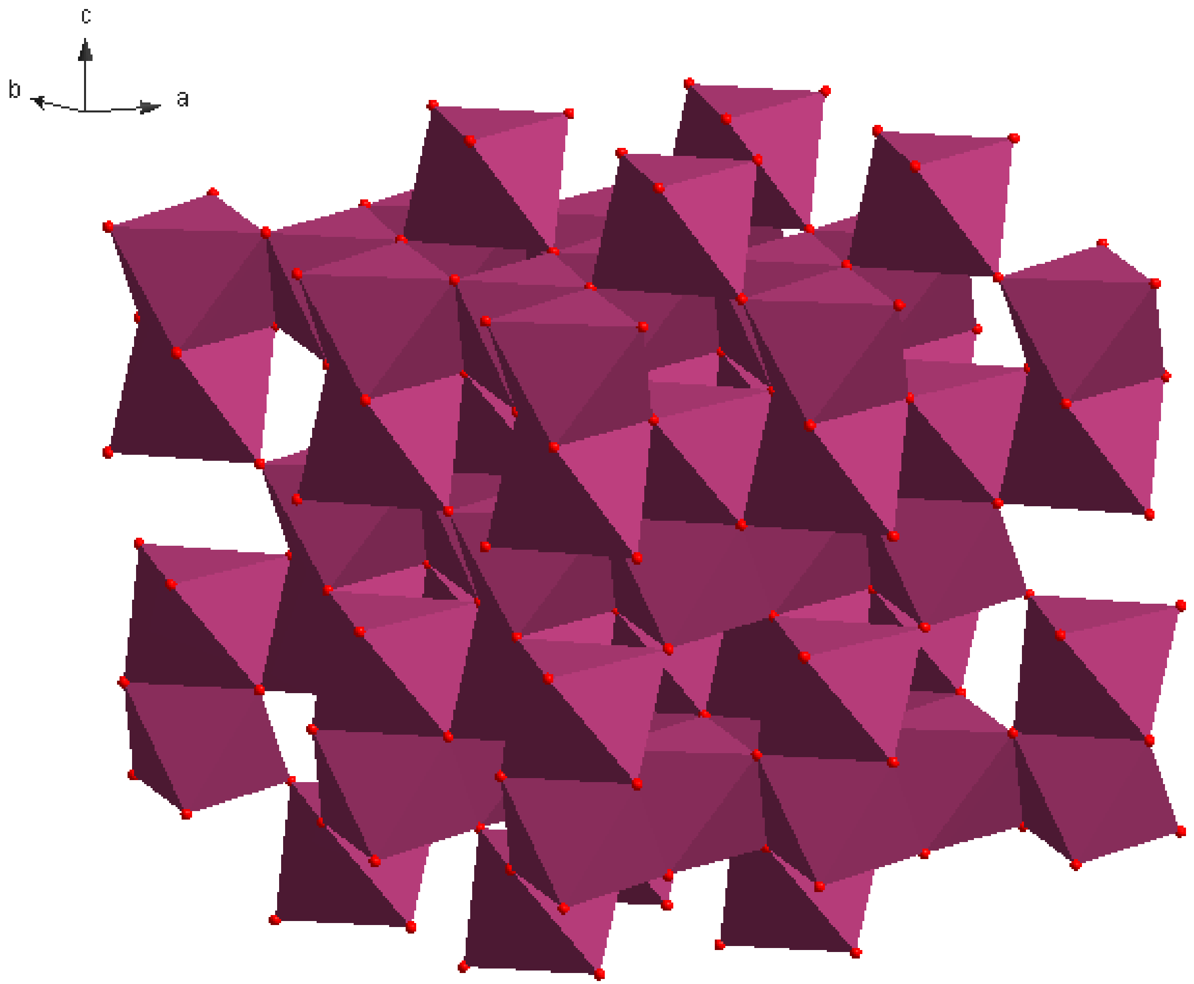

Fe_2O_3

Pbnm, #62

Reflections: 55

R1: 21.2%

```
Extinction symbol : Pbna

Candidate space groups :
------------------------------------------------------------------------------------
H-M symbol        #    Centric  Laue class    M  R(int)  N(obs)  CSD  ICSD   CFOM
------------------------------------------------------------------------------------
 P b n a    NS    60     yes      mmm         8  0.027       33  1740  193   1.336
------------------------------------------------------------------------------------

 -->>> Selected space group = P b n a

 Space groups are described under the Centric designator as :
   yes     - meaning centrosymmetric
   no      - meaning non-centrosymmetric with symmetry operators
             of the second kind (i.e. roto-inversions)
   chiral  - meaning non-centrosymmetric with only symmetry
             operators of the first kind (i.e. rotations & translations)

 Only space groups in the last category can support crystallisation
 of enantiomerically-pure configurationally stable chiral molecules,
 into ordered crystal structures.
```

Fe_2O_3

Pbna, #60

Reflections: 55

R1: 5.2%

40.4(5) GPa

2300(50) K

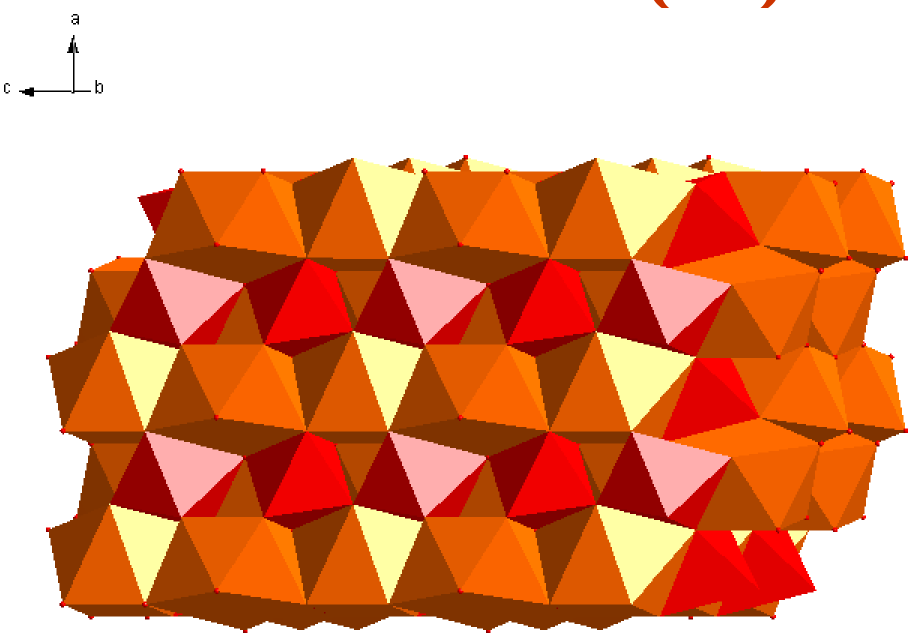

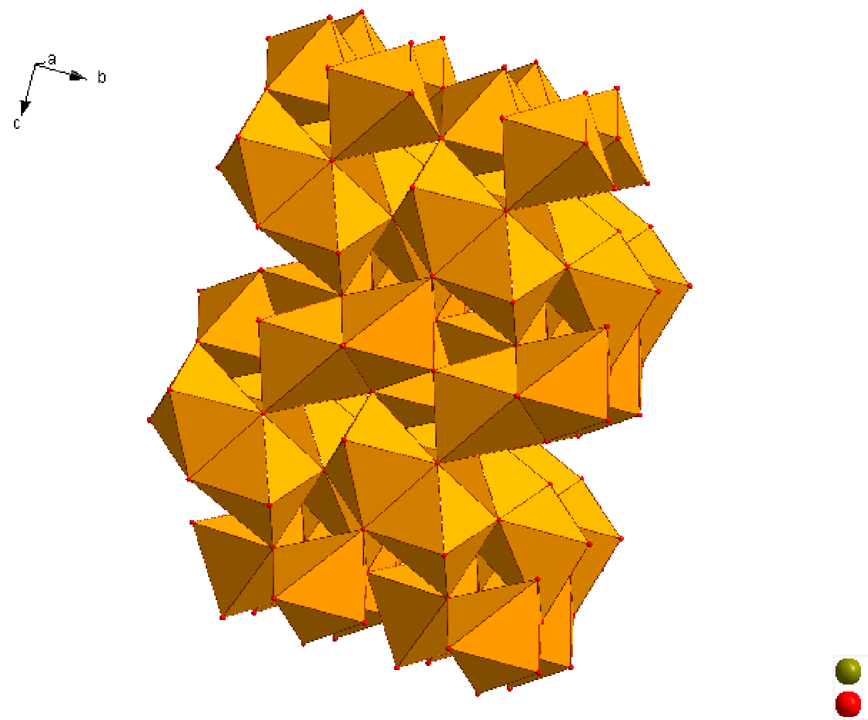

R. Boehler, 2009

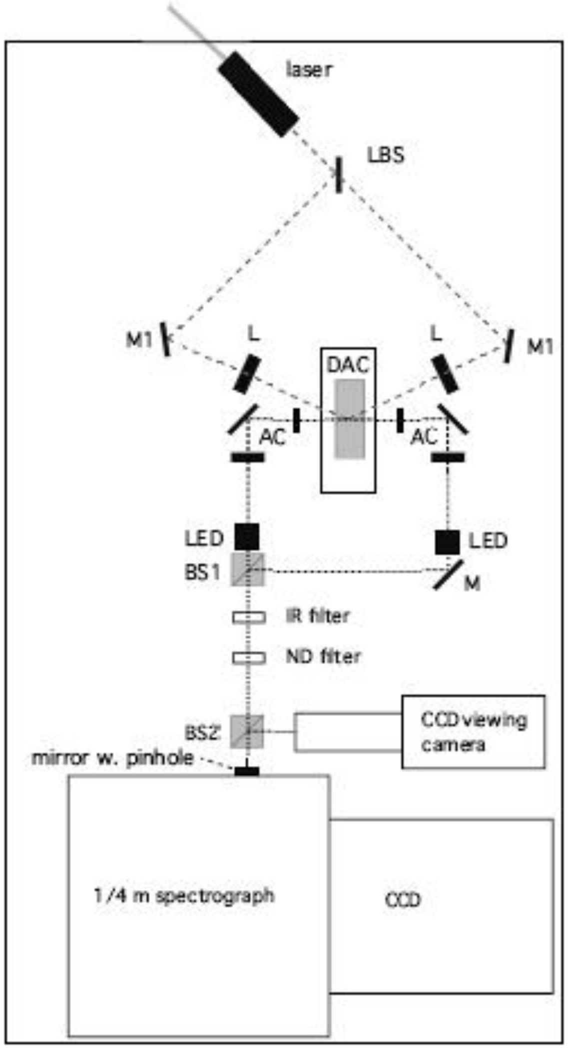

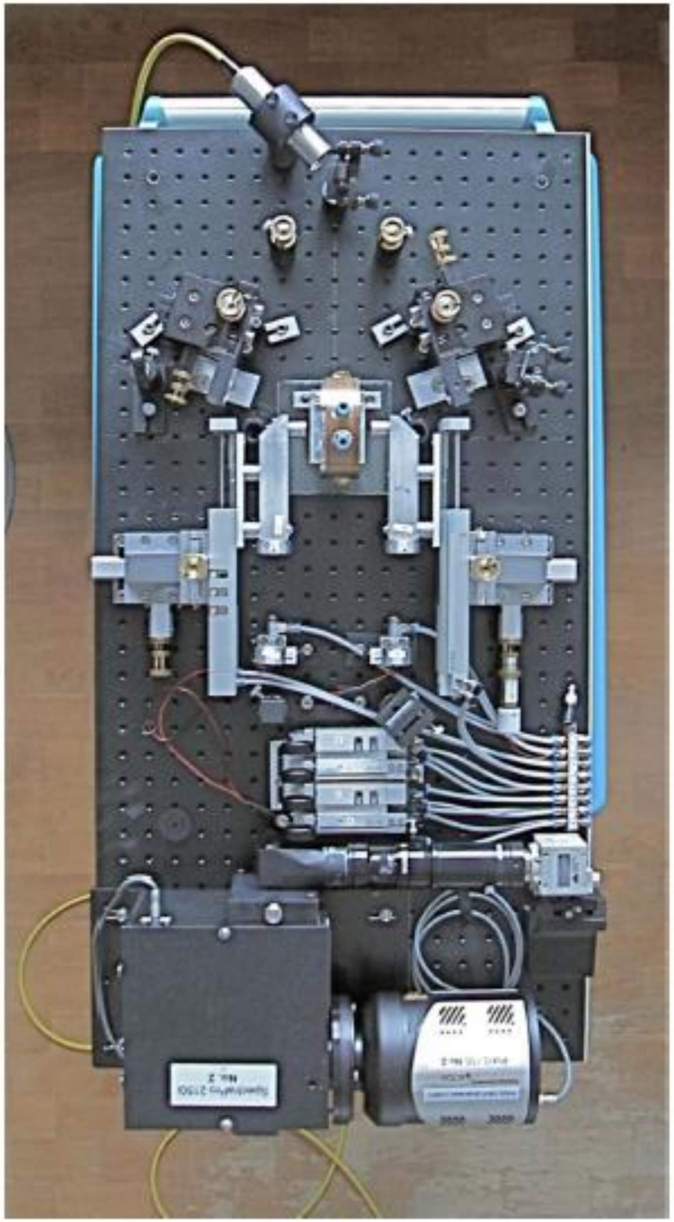

FIG. 1. (Color online) (A) Schematics of the layout and (B) photograph of the portable laser-heating stand (description see text).

Electrical Heating in DAC
Pressure above 300 GPa
Temperatures to 1200 K

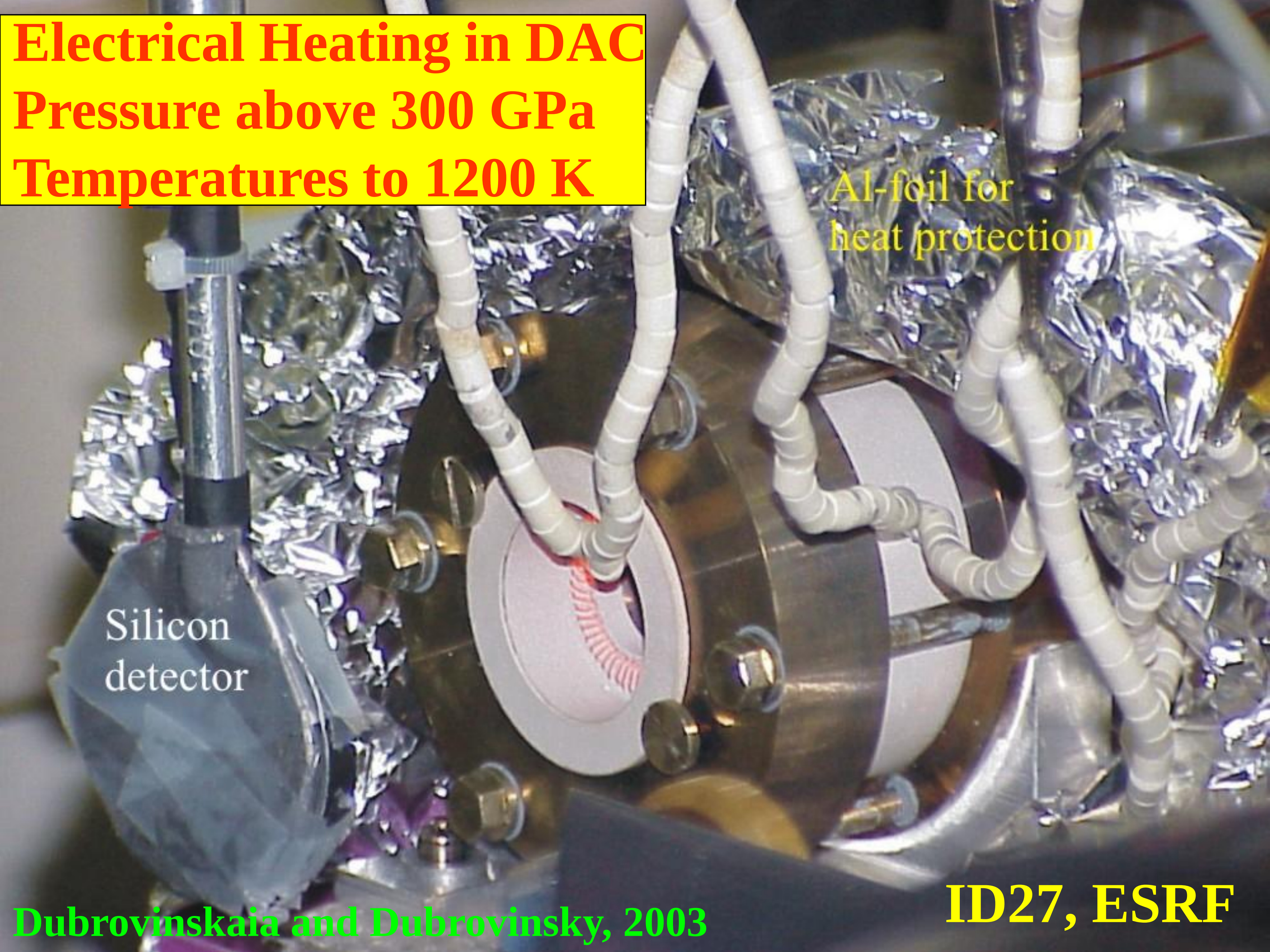

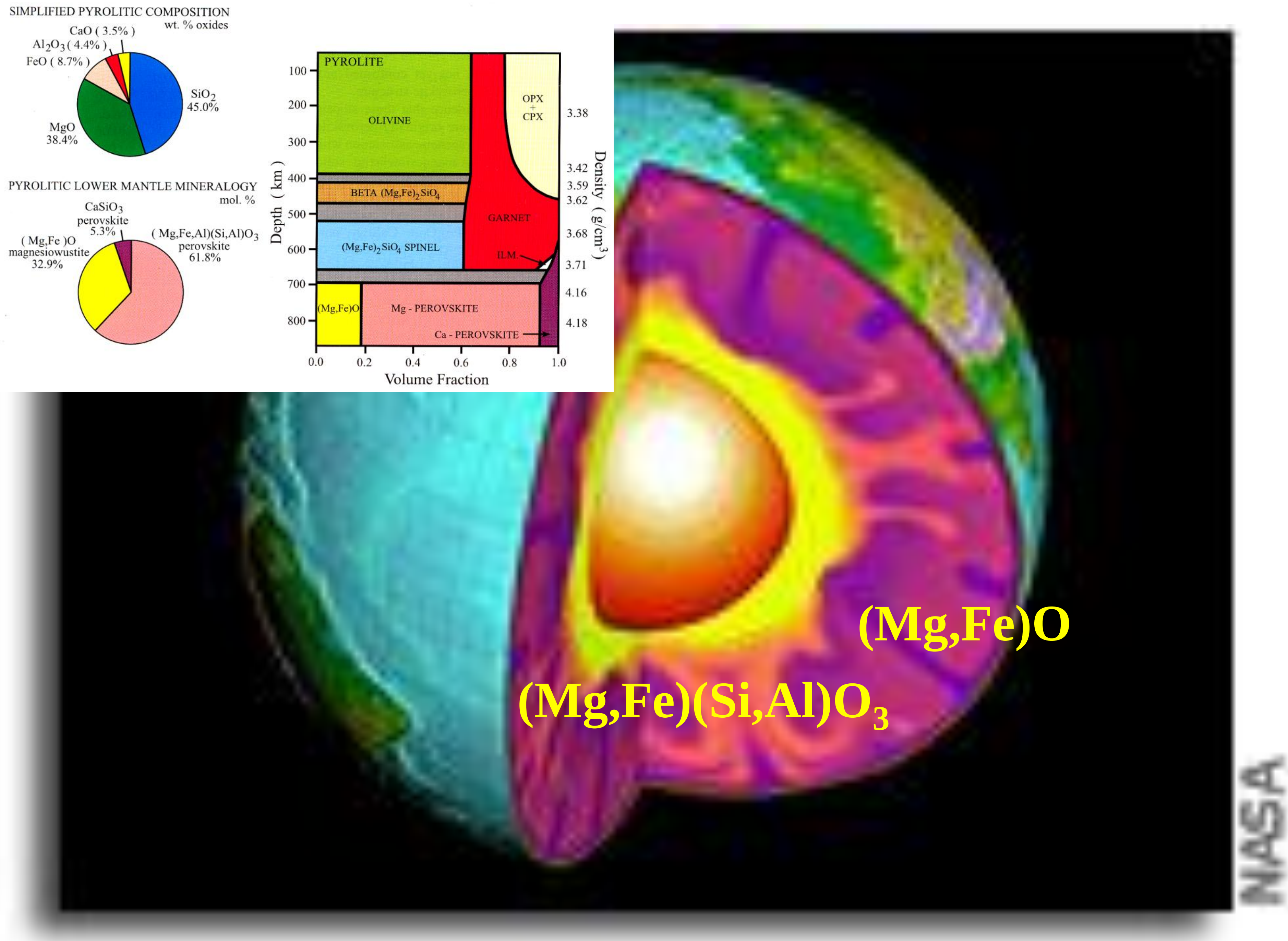
SIMPLIFIED PYROLITIC COMPOSITION
wt. % oxides
CaO (3.5%)
Al2O3 (4.4%)
FeO (8.7%)
SiO2 45.0%
MgO 38.4%
PYROLITIC LOWER MANTLE MINERALOGY
mol. %
CaSiO3 perovskite 5.3%
(Mg,Fe)O magnesiowustite 32.9%
(Mg,Fe,Al)(Si,Al)O3 perovskite 61.8%
PYROLITE
OLIVINE
OPX + CPX
BETA (Mg,Fe)2SiO4
GARNET
(Mg,Fe)2SiO4 SPINEL
ILM.
(Mg,Fe)O
Mg - PEROVSKITE
Ca - PEROVSKITE
Depth (km)
100
200
300
400
500
600
700
800
Density (g/cm3)
3.38
3.42
3.59
3.62
3.68
3.71
4.16
4.18
0.0
0.2
0.4
0.6
0.8
1.0
Volume Fraction
(Mg,Fe)O
(Mg,Fe)(Si,Al)O3
NASA

Thermal EoS of $(Mg_{0.8}Fe_{0.2})O$

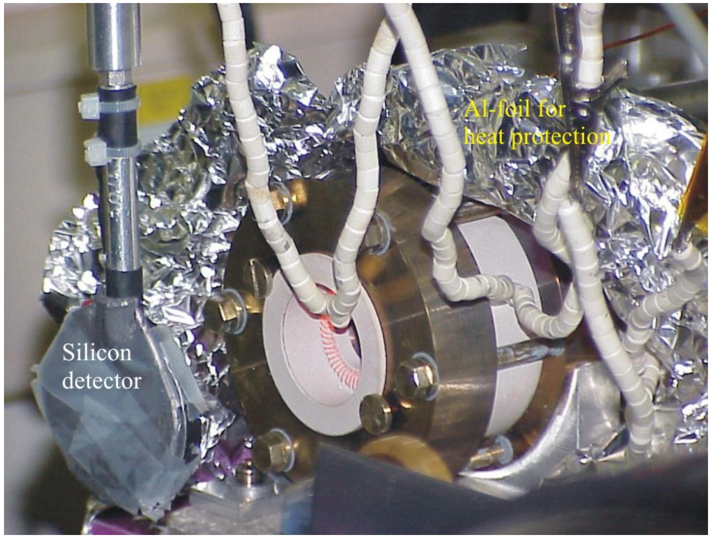

Powder Diffraction

External Electrical and Laser Heating

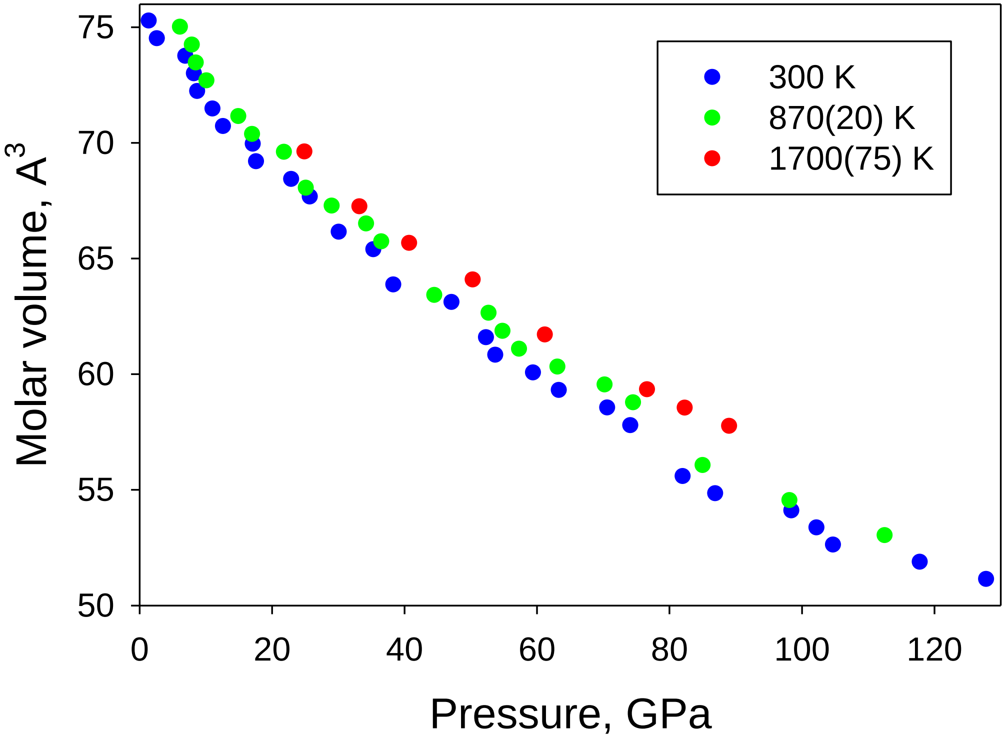

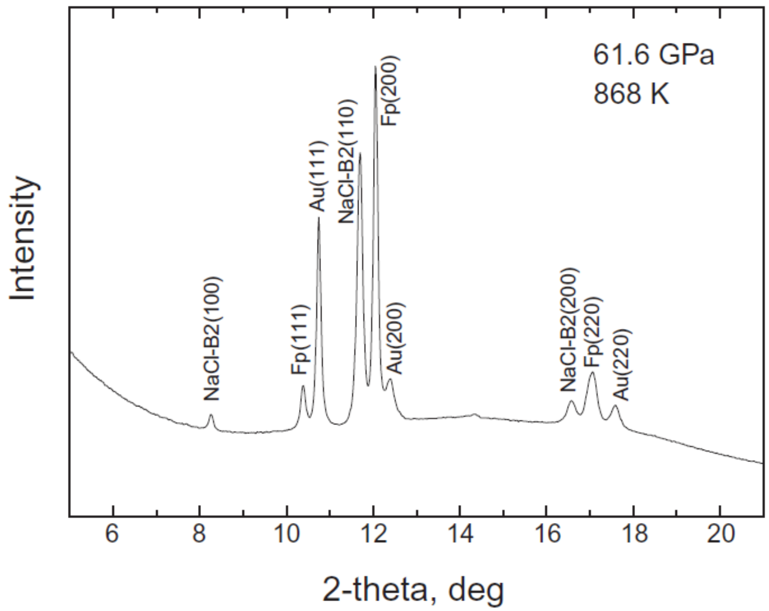

Thermal EoS of $(Mg_{0.8}Fe_{0.2})O$

Powder Diffraction

External Electrical and Laser Heating

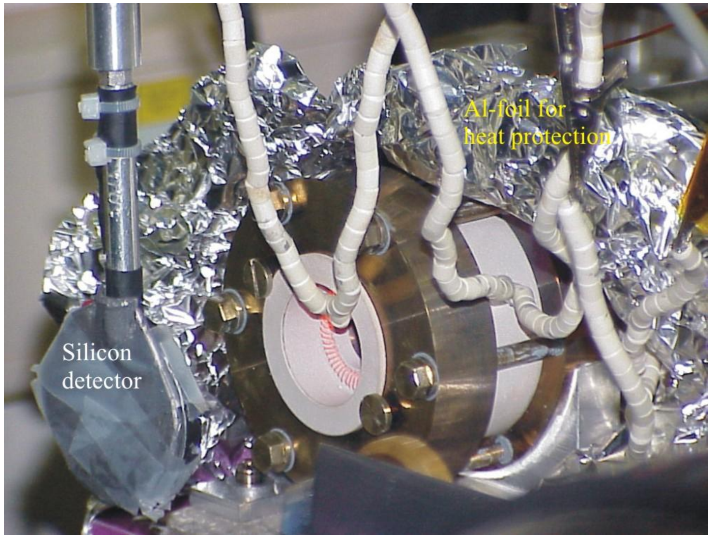

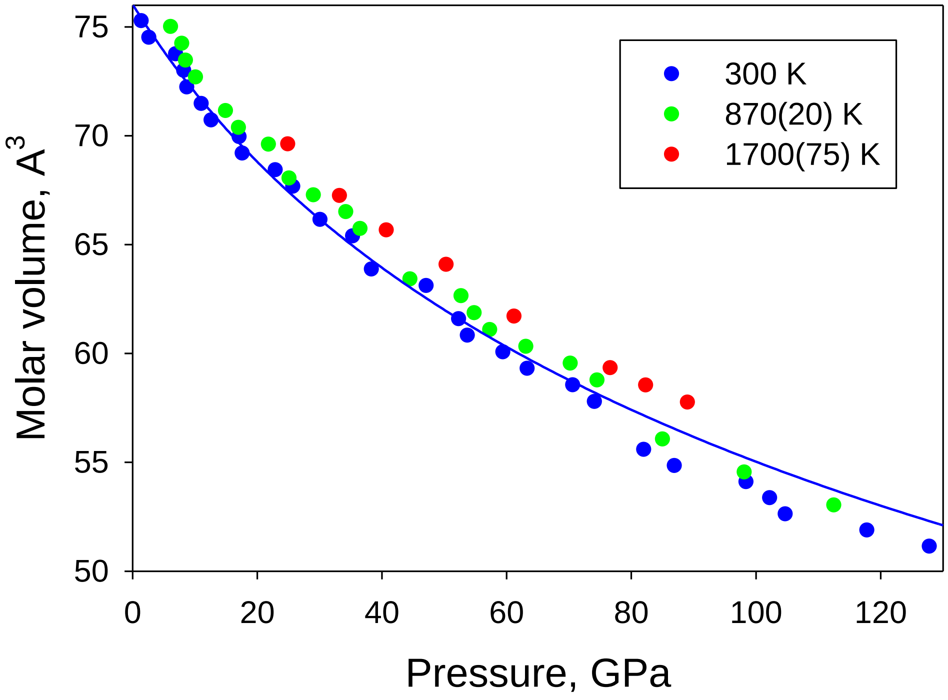

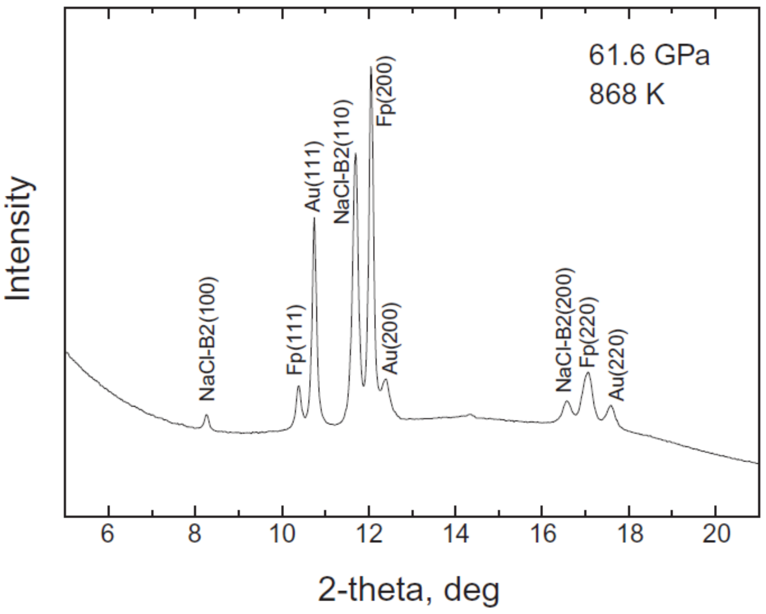

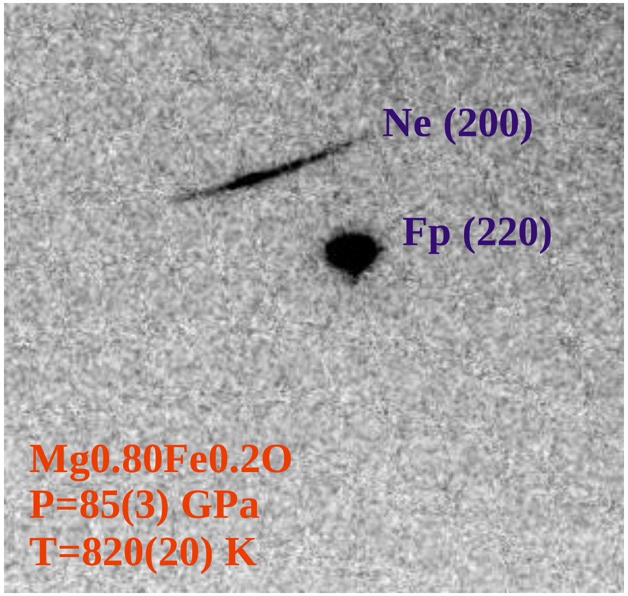

Thermal EoS of $(Mg_{0.8}Fe_{0.2})O$

Single Crystal Diffraction

External Electrical and Laser Heating

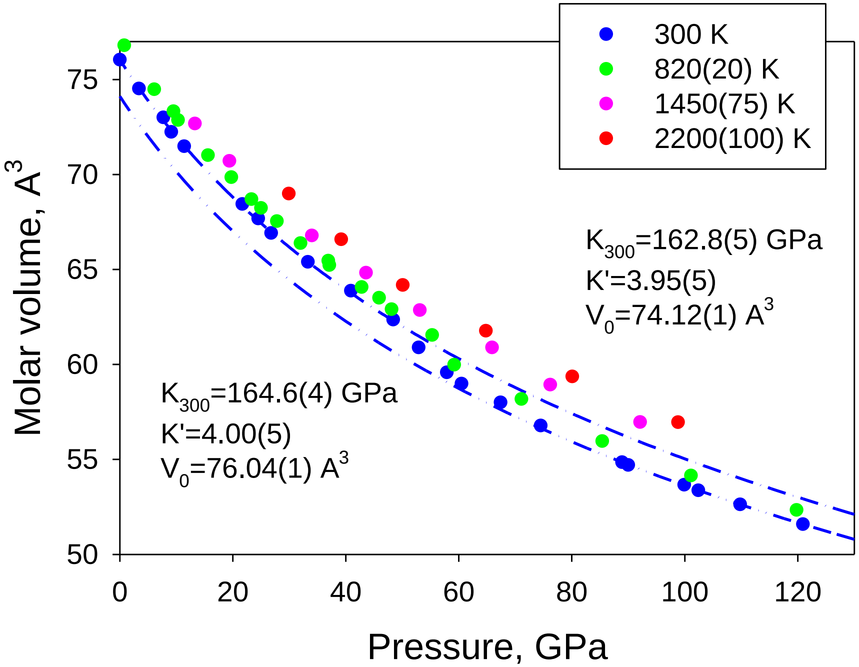

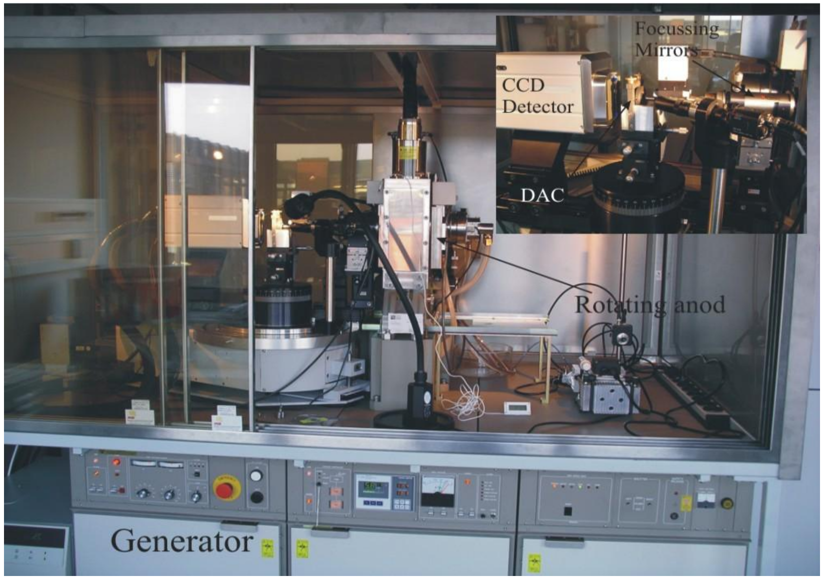

Dubrovinsky et al., 2004

Thermal EoS of Fp

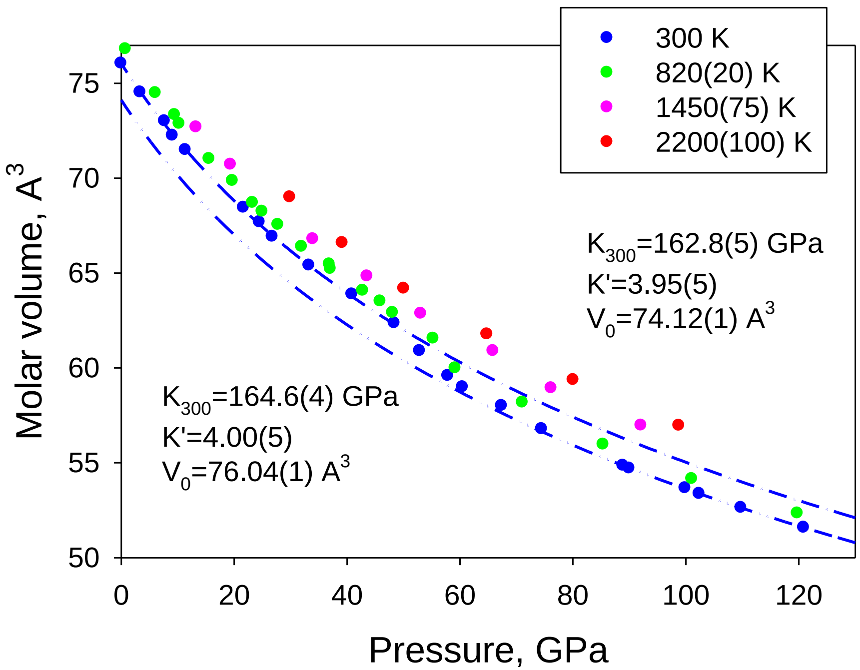

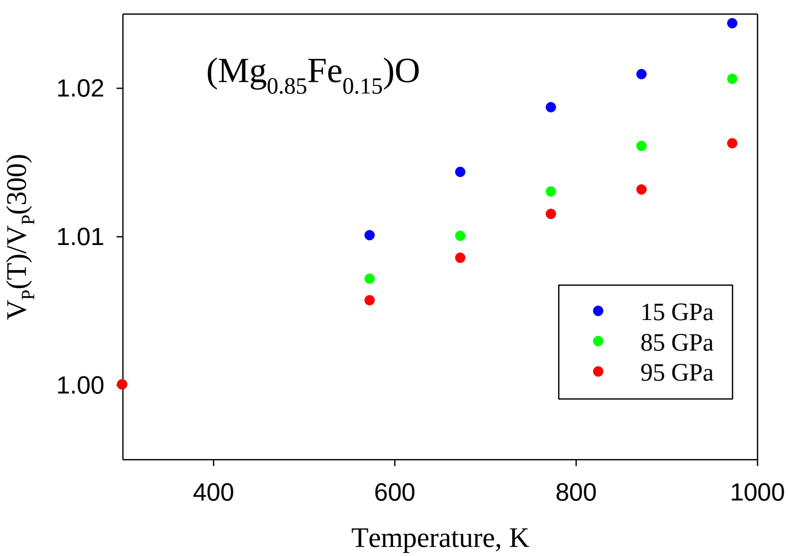

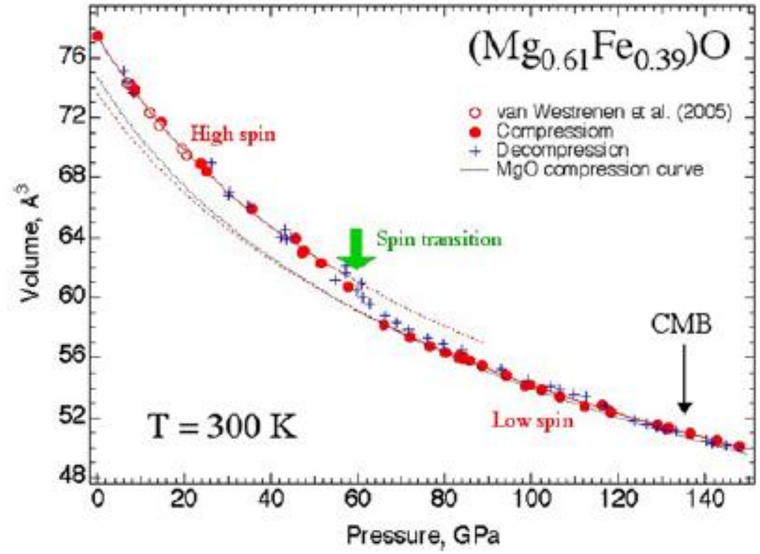

GEOPHYSICAL RESEARCH LETTERS, VOL. 34, L17307, doi:10.1029/2007GL030712, 2007

Click Here for Full Article

Spin transition and equations of state of (Mg, Fe)O solid solutions

Yingwei Fei,[1] Li Zhang,[1] Alexandre Corgne,[1,2] Heather Watson[1,3], Angele Ricolleau,[1] Yue Meng,[4] and Vitali Prakapenka[5]

JOURNAL OF GEOPHYSICAL RESEARCH, VOL. 112, B10212, doi:10.1029/2006JB004730, 2007

Click Here for Full Article

Effects of Fe spin transition on the elasticity of (Mg, Fe)O magnesiowüstites and implications for the seismological properties of the Earth's lower mantle

S. Speziale,[1,5] V. E. Lee,[1] S. M. Clark,[2] J. F. Lin,[3] M. P. Pasternak,[4] and R. Jeanloz[1]

Elasticity of (Mg,Fe)O Through the Spin Transition of Iron in the Lower Mantle

J. C. Crowhurst,[1*] J. M. Brown,[2] A. F. Goncharov,[3] S. D. Jacobsen[4]

Dubrovinsky et al., 2010

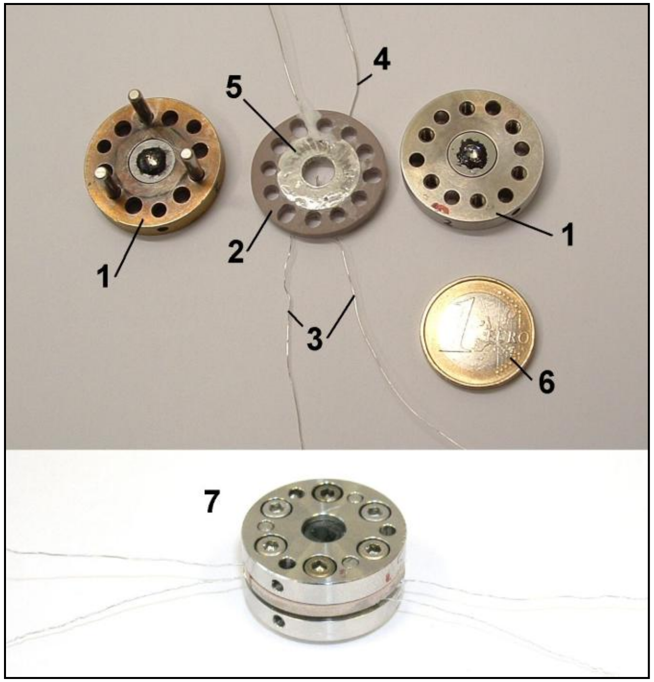

Heating assembly for high *P, T* Mössbauer measurements:

1 – diamond anvil cell,
2 – ceramic heater,
3 – thermocouple,
4 – platinum wires,
5 – mica for electrical isolation,
6 – one Euro coin for scale,
7 – entire assembly.

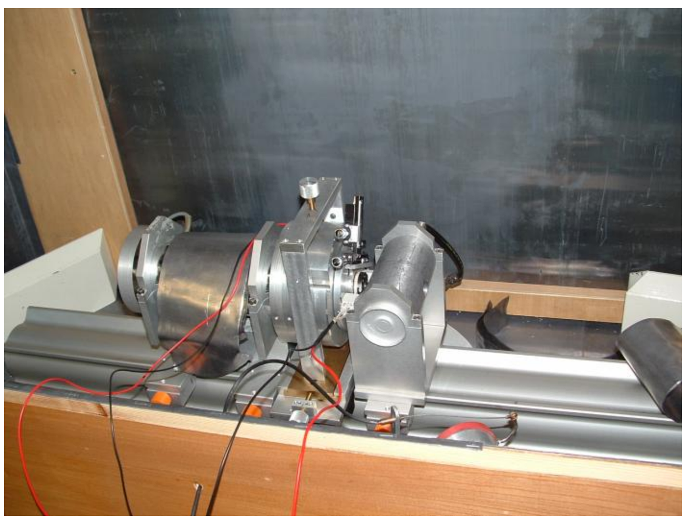

Mössbauer spectrometer

Micro-Raman spectrometer

Dubrovinskaia and Dubrovinsky, 2003

$(Mg_{0.88}Fe_{0.12})SiO_3$

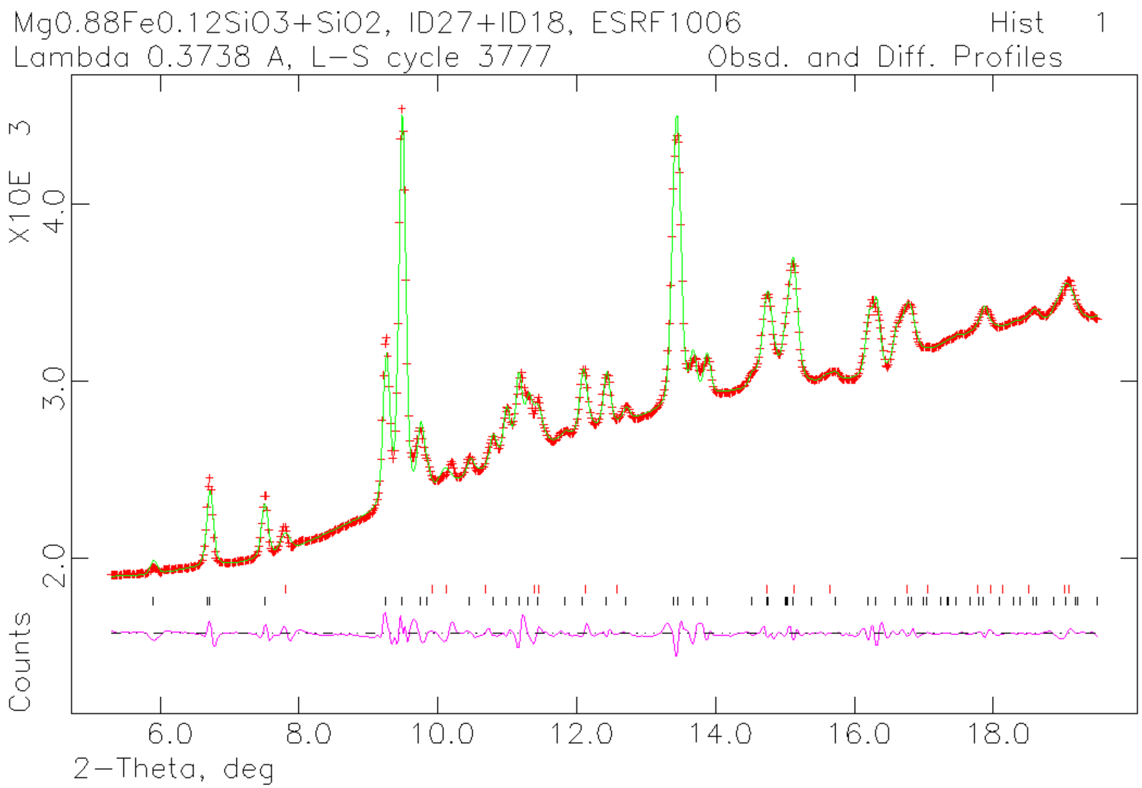

Mouse (keyboard): Left(H) - Height, Right(W) - Location Both(X) - exit

112(3) GPa
2200(50) K

LETTERS

Stable intermediate-spin ferrous iron in lower-mantle perovskite

C. McCAMMON[1*], I. KANTOR[1†], O. NARYGINA[1], J. ROUQUETTE[1†], U. PONKRATZ[2], I. SERGUEEV[2], M. MEZOUAR[2], V. PRAKAPENKA[3] AND L. DUBROVINSKY[1]

```
Lattice constants are
 a =  4.4060(7)  b =  4.6310(5)  c =  6.3992(9)
 Alpha =  90      Beta =  90     Gamma =  90
cell volume = 130.570(31)
```

Name	X	Y	Z	Ui/Ue*100	Site sym	Mult	Type	Seq	Fractn
MG1	0.9820(13)	0.0698(7)	0.250000	8.2(4)	M(001)	4	MG	1	0.882(15)
SI2	0.000000	0.500000	0.000000	1.68(19)	-1	4	SI	2	1.0000
O3	0.0896(18)	0.4848(19)	0.250000	2.20(31)	M(001)	4	O	3	1.0000
O4	0.6923(16)	0.3021(11)	0.0622(12)	1.41(20)	1	8	O	4	1.0000
FE5	0.9820(13)	0.0698(7)	0.250000	3.7(4)	M(001)	4	FE	5	0.118(15)
FE6	0.000000	0.500000	0.000000	2.50	-1	4	FE	6	0.0000

Thermal EoS of $(Mg_{0.88}Fe_{0.12})SiO_3$ Pv

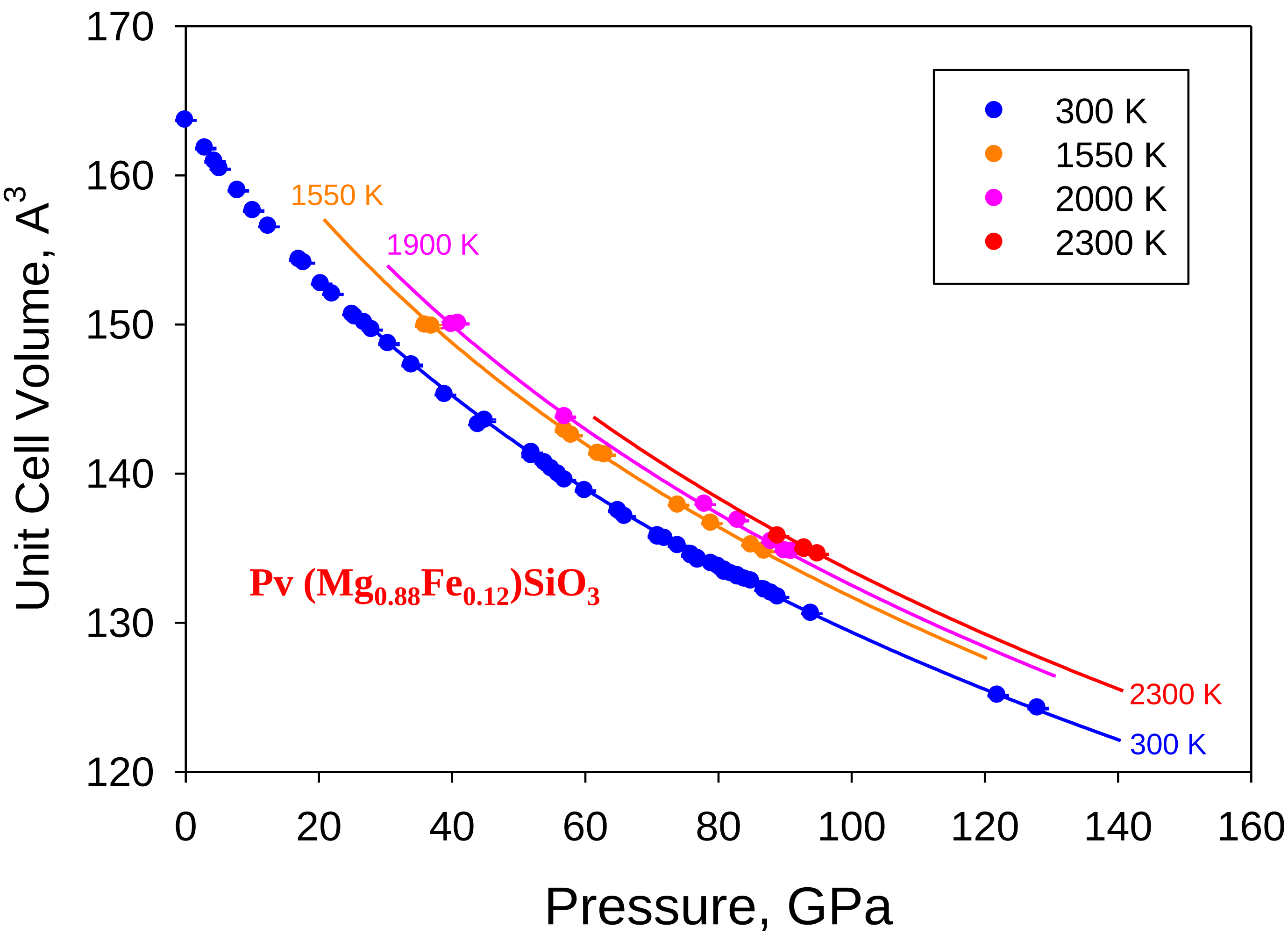

Simultaneous volume measurements of post-perovskite and perovskite in $MgSiO_3$ and their thermal equations of state

Tetsuya Komabayashi [a,*], Kei Hirose [a,b], Emiko Sugimura [a], Nagayoshi Sata [b], Yasuo Ohishi [c], Leonid S. Dubrovinsky [d]

Earth and Planetary Science Letters 265 (2008) 515–524

LETTERS

Stable intermediate-spin ferrous iron in lower-mantle perovskite

C. McCAMMON[1*], I. KANTOR[1†], O. NARYGINA[1], J. ROUQUETTE[1†], U. PONKRATZ[2], I. SERGUEEV[2], M. MEZOUAR[2], V. PRAKAPENKA[3] AND L. DUBROVINSKY[1]

Crystal Chemistry of Pv

PRL 95, 025503 (2005) PHYSICAL REVIEW LETTERS week ending 8 JULY 2005

General Rules for Predicting Phase Transitions in Perovskites due to Octahedral Tilting

R. J. Angel,* J. Zhao, and N. L. Ross

Virginia Tech Crystallography Laboratory, Department of Geosciences, Virginia Tech, Blacksburg, Virginia 24060, USA

(Received 29 April 2005; published 8 July 2005)

Recent experiments on several oxide perovskites reveal that they undergo tilt phase transitions to higher-symmetry phases on increasing pressure and that $dT_c/dP < 0$, contrary to a general rule previously proposed for such zone-boundary transitions. We show that the negative slope of the phase boundary is a consequence of the octahedra in these perovskites being more compressible than the extra-framework cation sites. Conversely, when the octahedra are stiffer than the extra-framework cation sites, the phase transition temperatures increase with increasing pressure, $dT_c/dP > 0$.

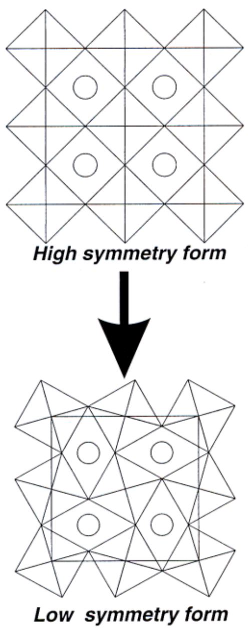

FIG. 1. Perovskites are comprised of a framework of BX_6 octahedra with *A* cations (shown as spheres) occupying the interstices within the framework. The aristotype structure is cubic and shows no octahedral tilting (top). If the octahedra are completely rigid, the only way in which the unit-cell volume can be reduced is by introducing tilts of the octahedra (bottom).

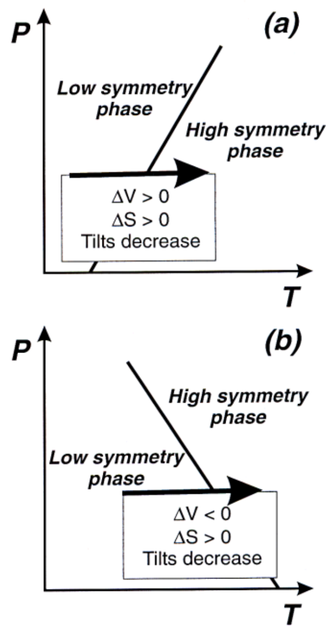

FIG. 2. Schematic *P-T* phase diagrams for perovskites. (a) $dT_c dP > 0$ when the octahedra are more rigid than the AX_{12} site. (b) $dT_c/dP < 0$ when the octahedra are less rigid than the AX_{12} site.

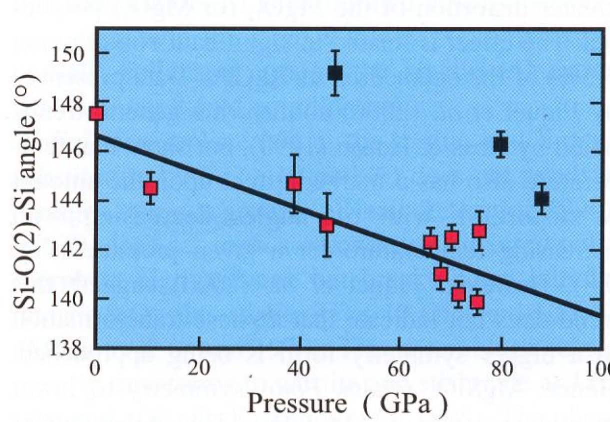

Fig. 9.8. Si-O(2)-Si bond angles for $MgSiO_3$-perovskite as a function of pressure and temperature. Data points collected at room temperature (red symbols) are from Fiquet *et al.* (2000) and Ross & Hazen (1990); those at high temperature and high pressure (black symbols) are from Fiquet *et al.* (2000).

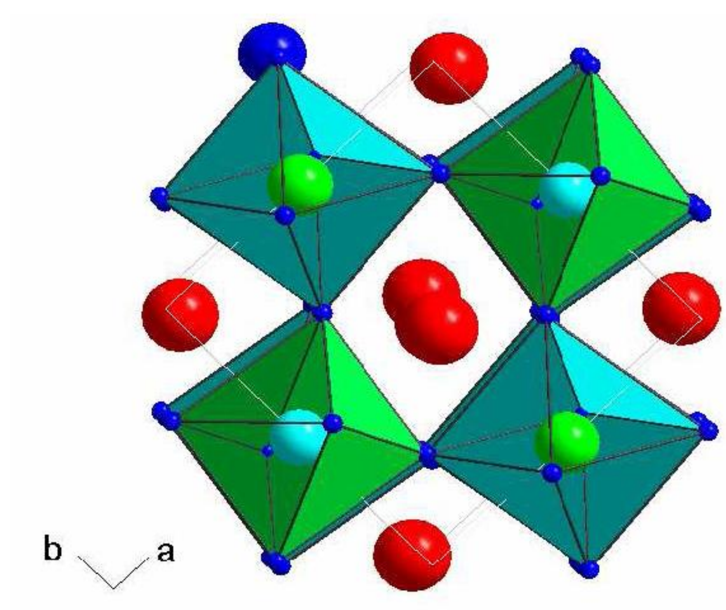

Iron Partitioning Between Pv and Fp

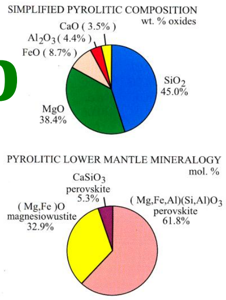

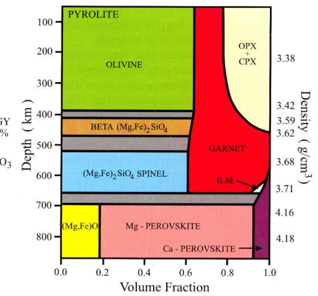

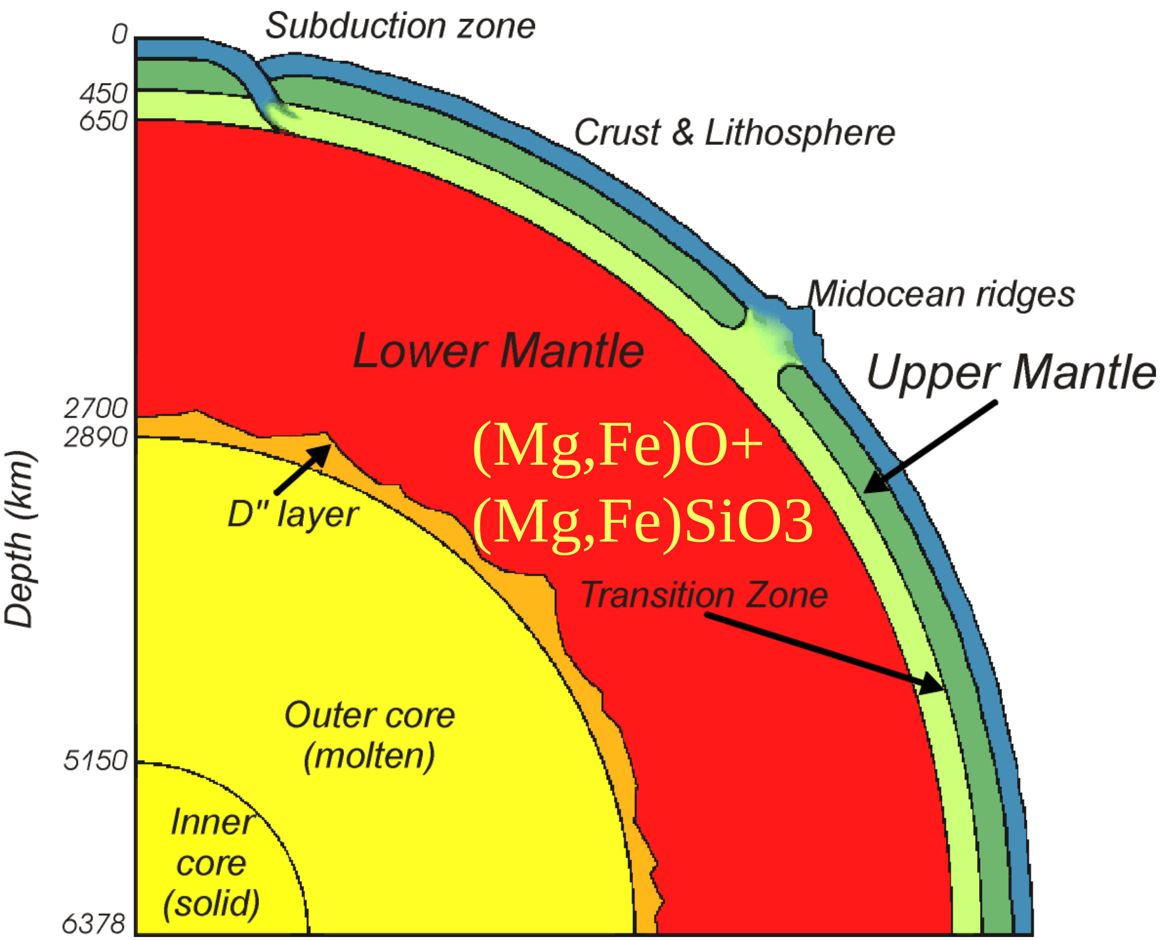

$$K_D = \left(\frac{X_{Fe}}{X_{Mg}}\right)^{Pv} \Big/ \left(\frac{X_{Fe}}{X_{Mg}}\right)^{Fp}$$

$$X_{Fe} = \frac{[FeO]}{[FeO]+[MgO]}$$

$(Mg,Fe)_2SiO_4 \rightarrow (Mg,Fe)SiO_3 + (Mg,Fe)O$

Rw Pv Fp

X-ray Absorption Near-Edge Spectroscopy

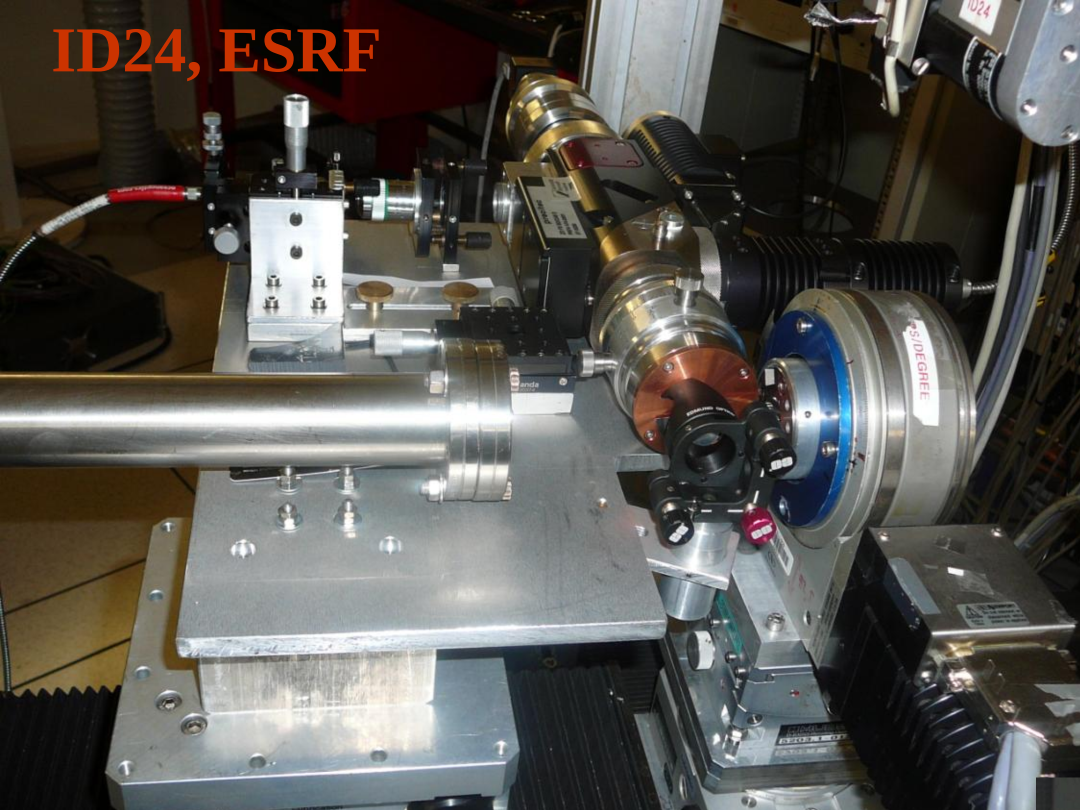

research papers

Journal of
Synchrotron
Radiation
ISSN 0909-0495

Received 10 December 2008

Development of micro-XANES mapping in the diamond anvil cell

Giuliana Aquilanti,[a]* Sakura Pascarelli,[a] Olivier Mathon,[a] Manuel Muñoz,[b] Olga Narygina[c] and Leonid Dubrovinsky[c]

high pressure

Journal of
Synchrotron
Radiation
ISSN 0909-0495

Received 9 June 2009
Accepted 25 September 2009

Portable laser-heating system for diamond anvil cells

L. Dubrovinsky,[a]* K. Glazyrin,[a] C. McCammon,[a] O. Narygina,[a] E. Greenberg,[a] S. Übelhack,[a] A. I. Chumakov,[b] S. Pascarelli,[b] V. Prakapenka,[c] J. Bock[d] and N. Dubrovinskaia[e]

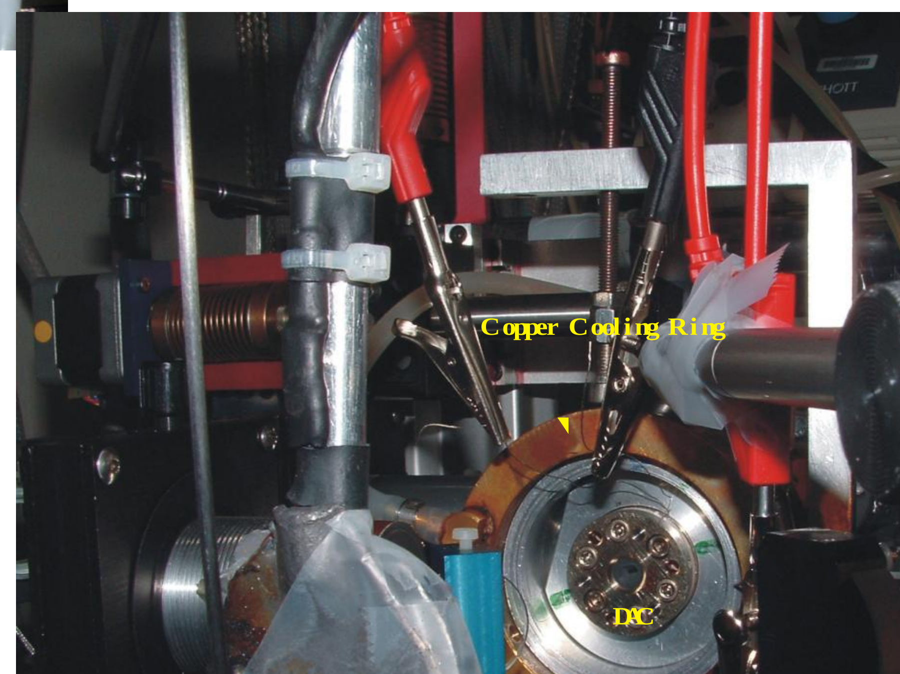

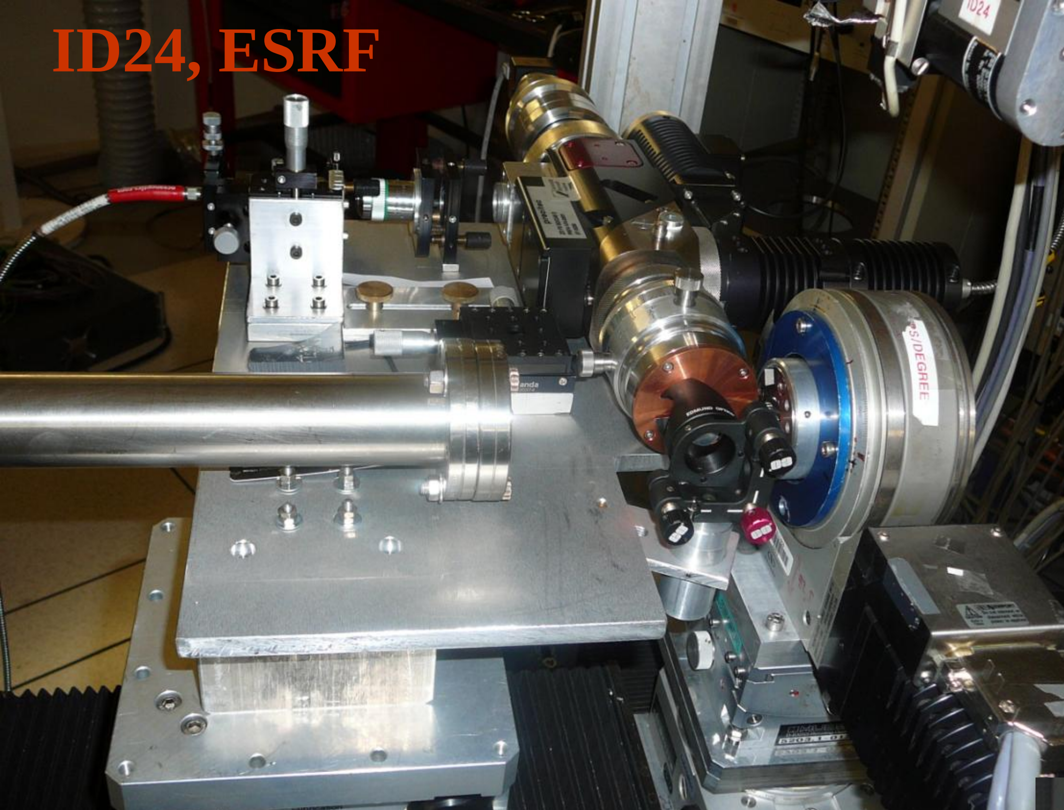

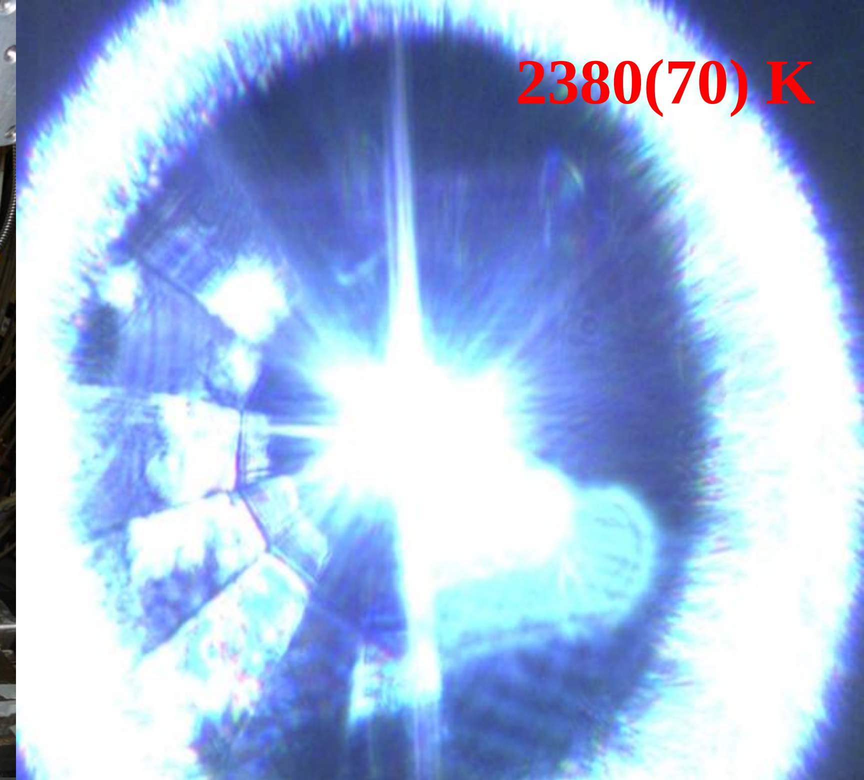

research papers

Journal of
Synchrotron
Radiation
ISSN 0909-0495

Received 10 December 2008

Development of micro-XANES mapping in the diamond anvil cell

Giuliana Aquilanti,[a]* Sakura Pascarelli,[a] Olivier Mathon,[a] Manuel Muñoz,[b] Olga Narygina[c] and Leonid Dubrovinsky[c]

high pressure

Journal of
Synchrotron
Radiation
ISSN 0909-0495

Received 9 June 2009
Accepted 25 September 2009

Portable laser-heating system for diamond anvil cells

L. Dubrovinsky,[a]* K. Glazyrin,[a] C. McCammon,[a] O. Narygina,[a] E. Greenberg,[a] S. Übelhack,[a] A. I. Chumakov,[b] S. Pascarelli,[b] V. Prakapenka,[c] J. Bock[d] and N. Dubrovinskaia[e]

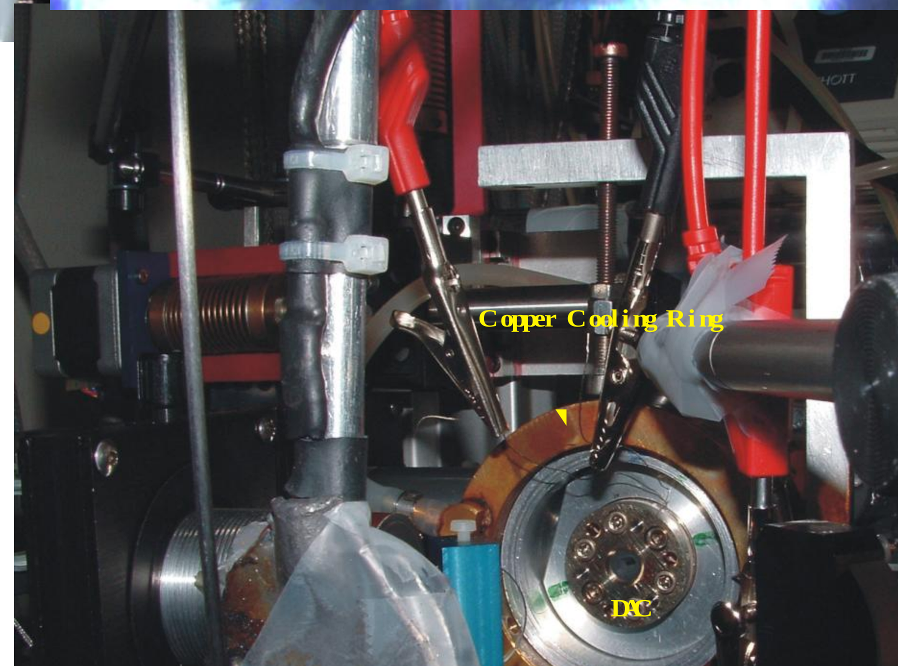

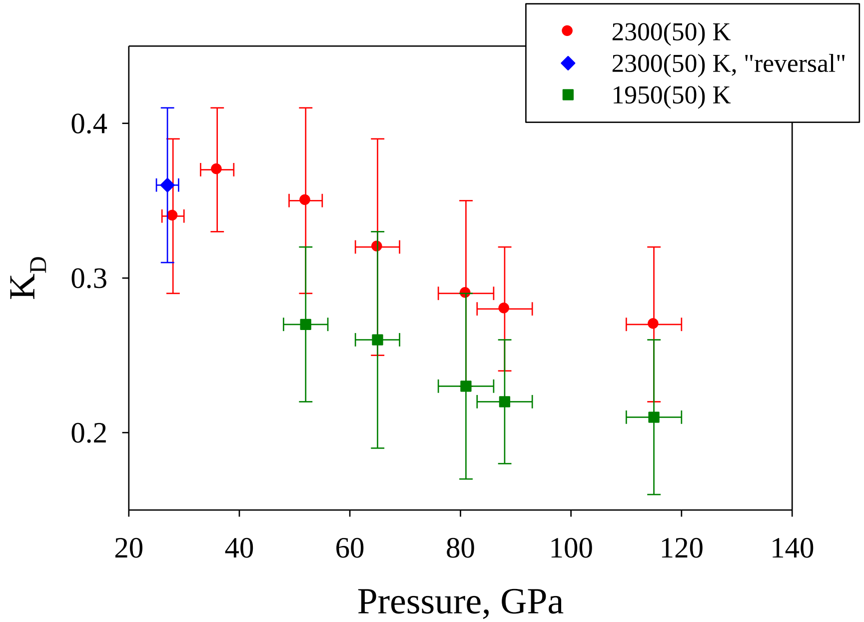

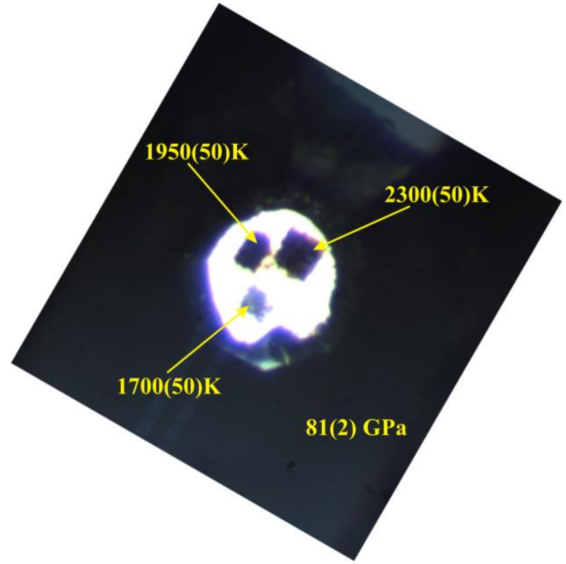

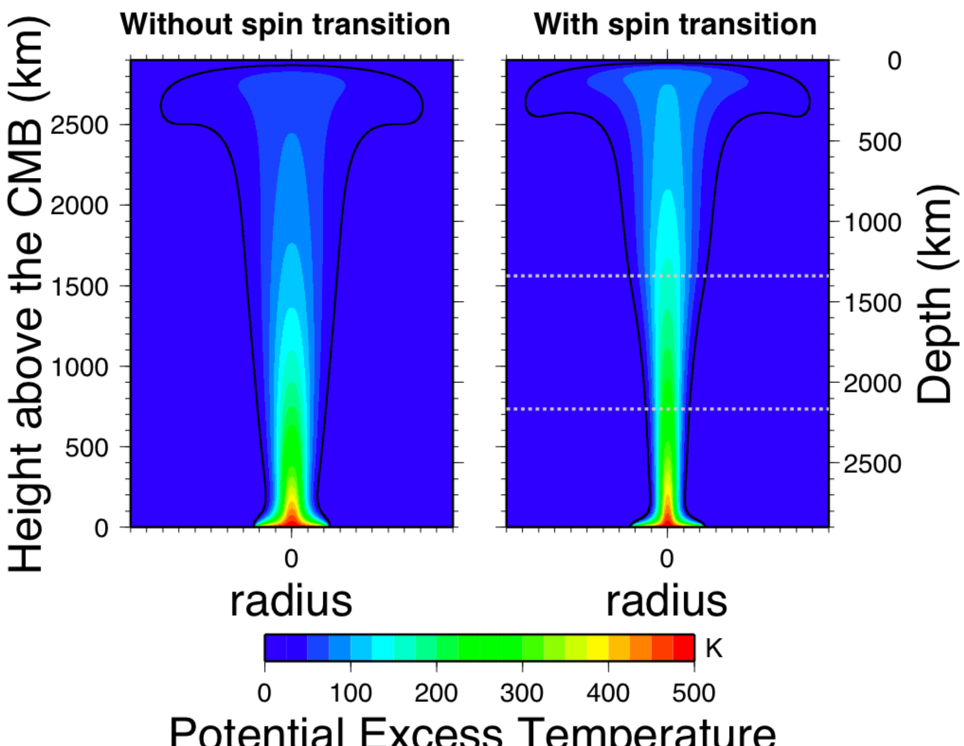

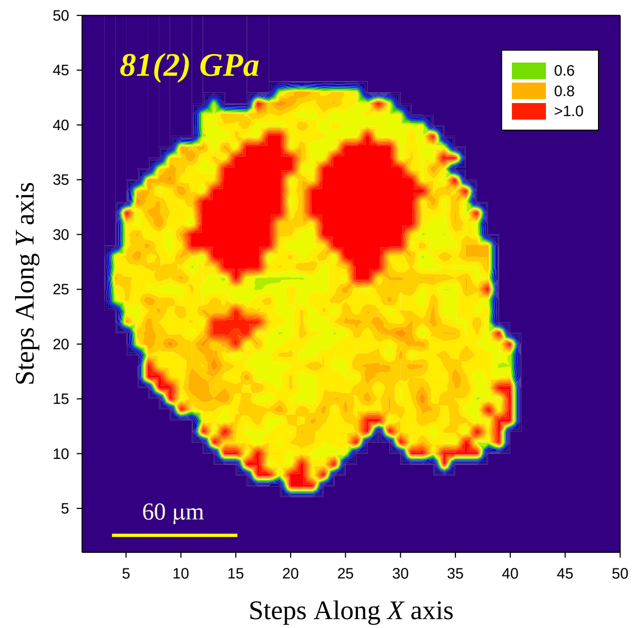

Narygina et al., 2010

Single Crystal Diffraction at Megabar Pressure Range

- High-Temperature

(a) External electrical heating

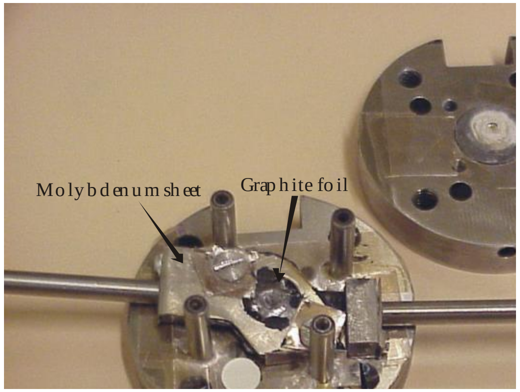

(b) Laser heating

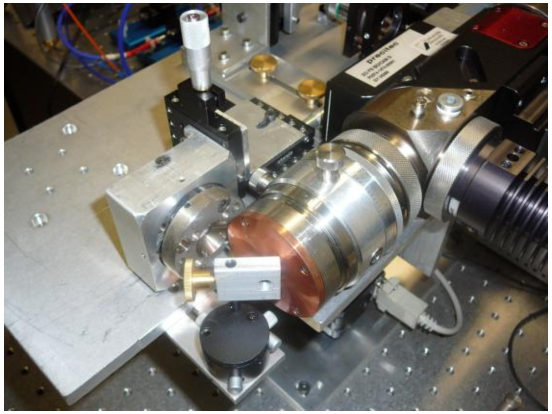

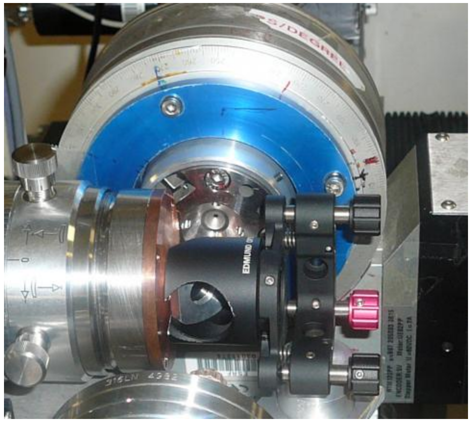

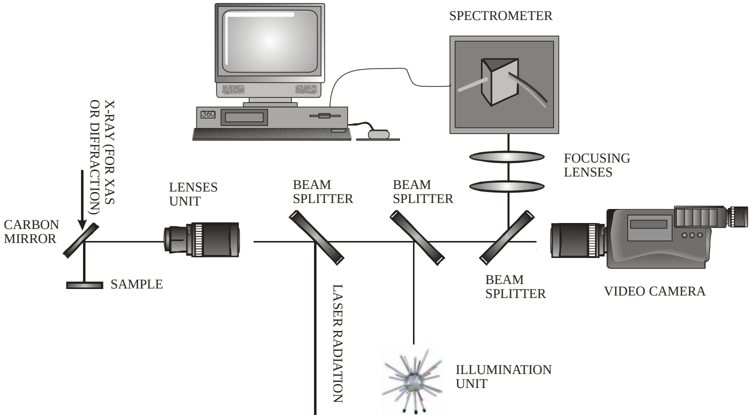

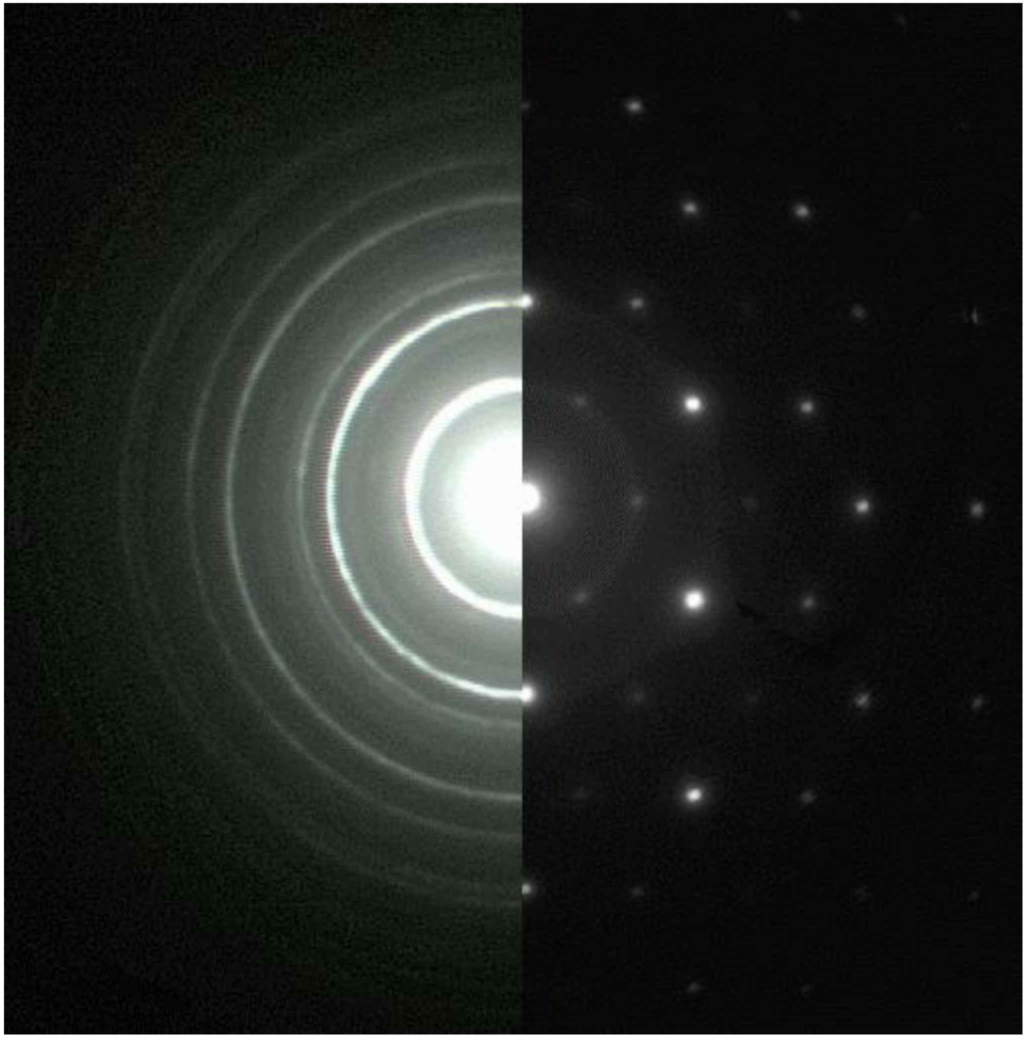

Cr_2O_3

Nuclear forward scattering (synchrotron Mössbauer) of $(Mg_{0.88}Fe_{0.12})SiO_3$ Pv

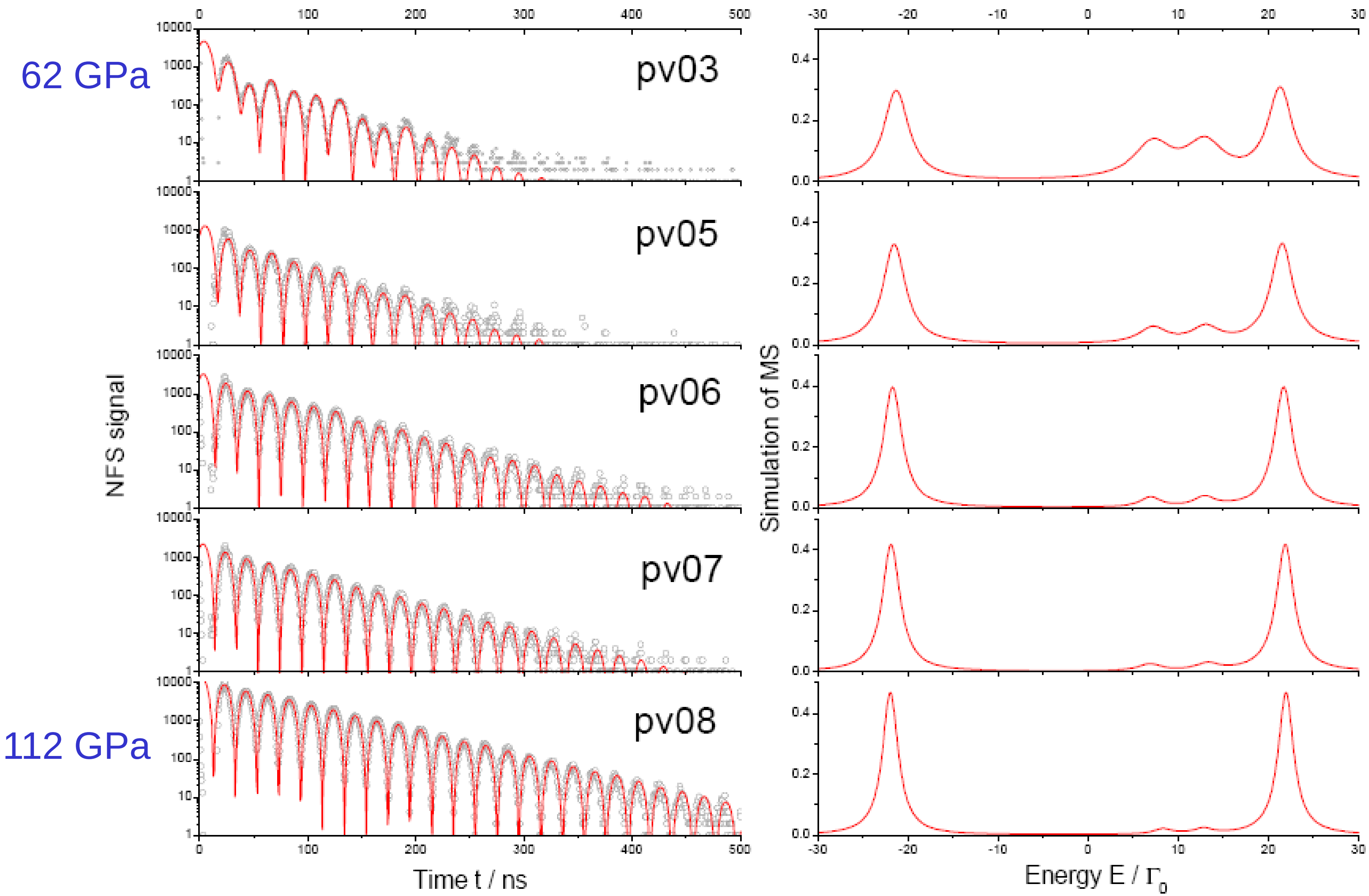

McCammon et al., 2008; Narygina, 2009, 2010

Crystal Chemistry of Pv

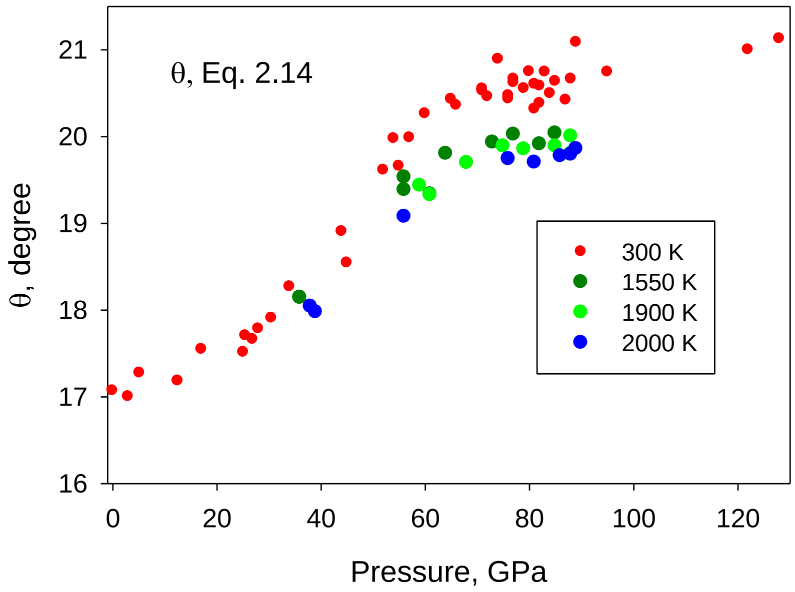

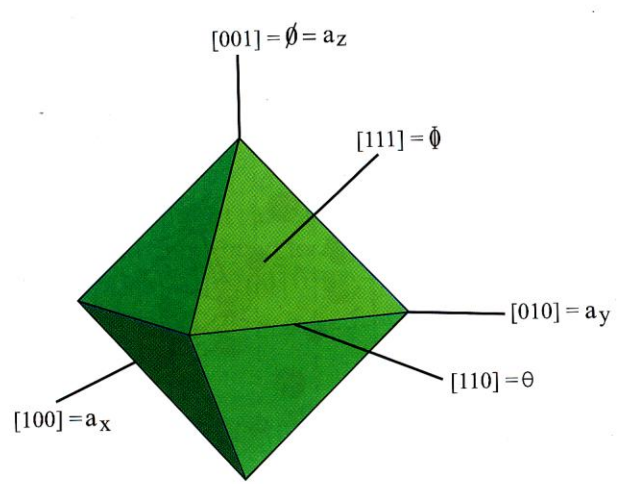

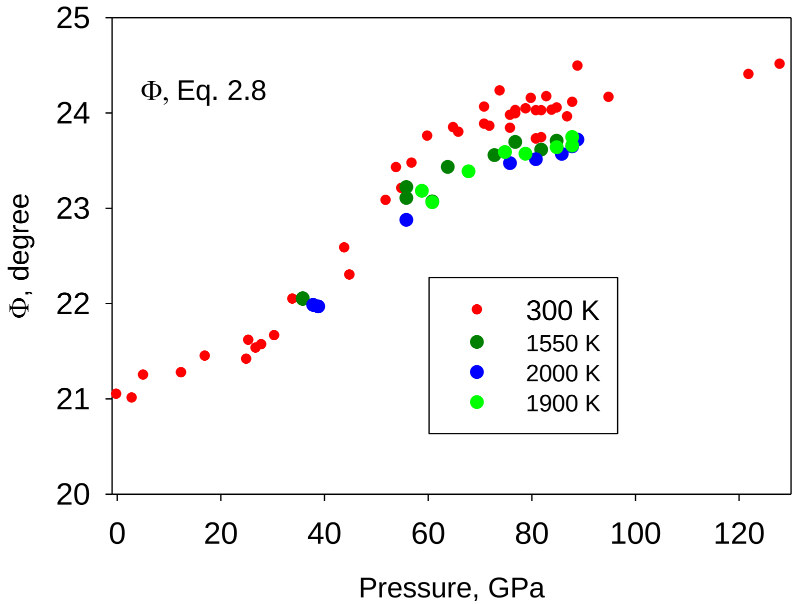

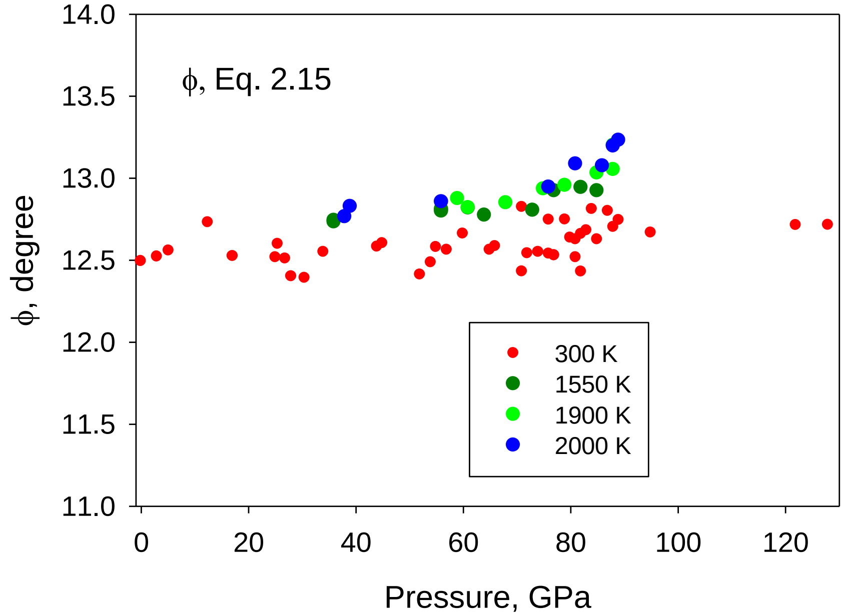

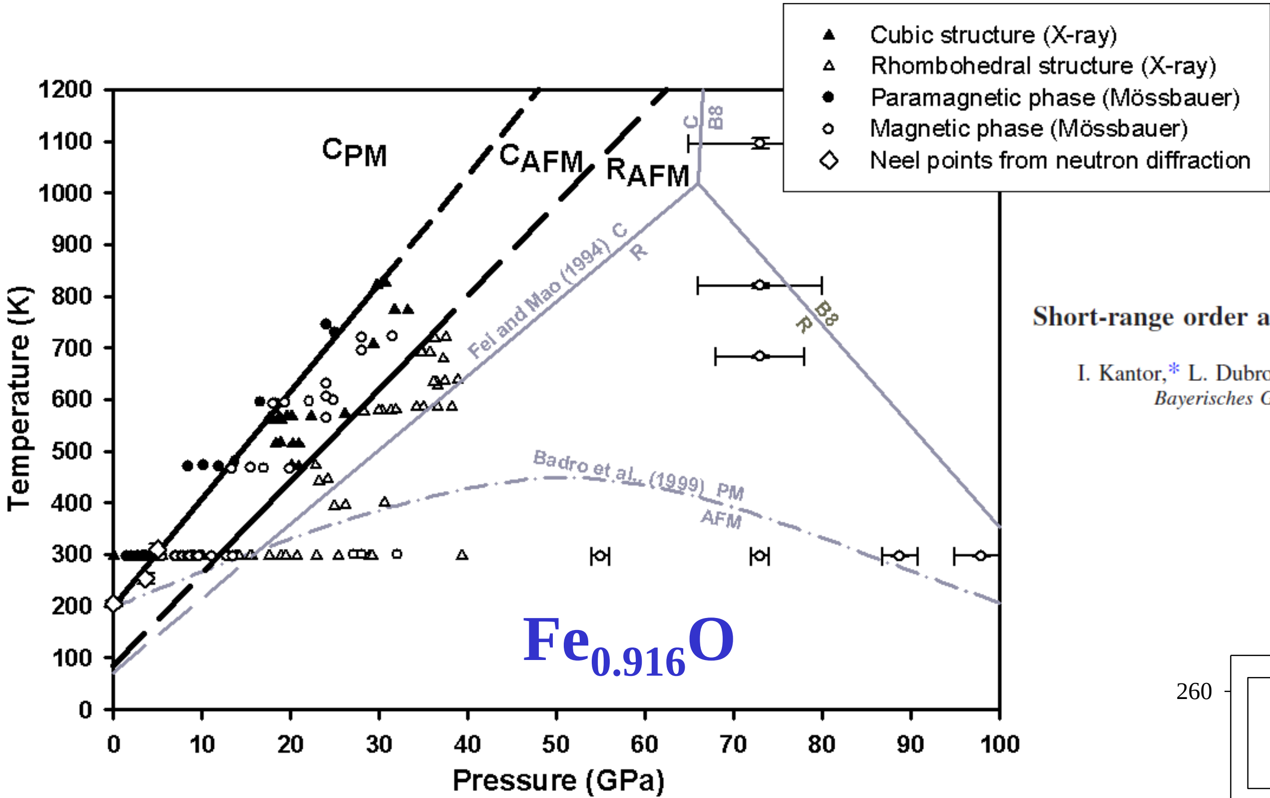

PHYSICAL REVIEW B **80**, 014204 (2009)

Short-range order and Fe clustering in $Mg_{1-x}Fe_xO$ under high pressure

I. Kantor,* L. Dubrovinsky, C. McCammon, G. Steinle-Neumann, and A. Kantor
Bayerisches Geoinstitut, Bayreuth University, 95440 Bayreuth, Germany

VOLUME 93, NUMBER 21 PHYSICAL REVIEW LETTERS week ending 19 NOVEMBER 2004

Pressure-Induced Magnetization in FeO: Evidence from Elasticity and Mössbauer Spectroscopy

Anastasia P. Kantor,[1,2] Steven D. Jacobsen,[3,1] Innokenty Yu. Kantor,[1] Leonid S. Dubrovinsky,[1] Catherine A. McCammon,[1] Hans J. Reichmann,[4] and Igor N. Goncharenko[5]

Phase Transitions,
Vol. 80, Nos. 10–12, October–December 2007, 1151–1163

Taylor & Fran
Taylor & Francis Group

FeO and MnO high-pressure phase diagrams: relations between structural and magnetic properties

I. KANTOR*†, L. DUBROVINSKY†, C. MCCAMMON†, N. DUBROVINSKAIA†‡, I. GONCHARENKO§, A. KANTOR†,

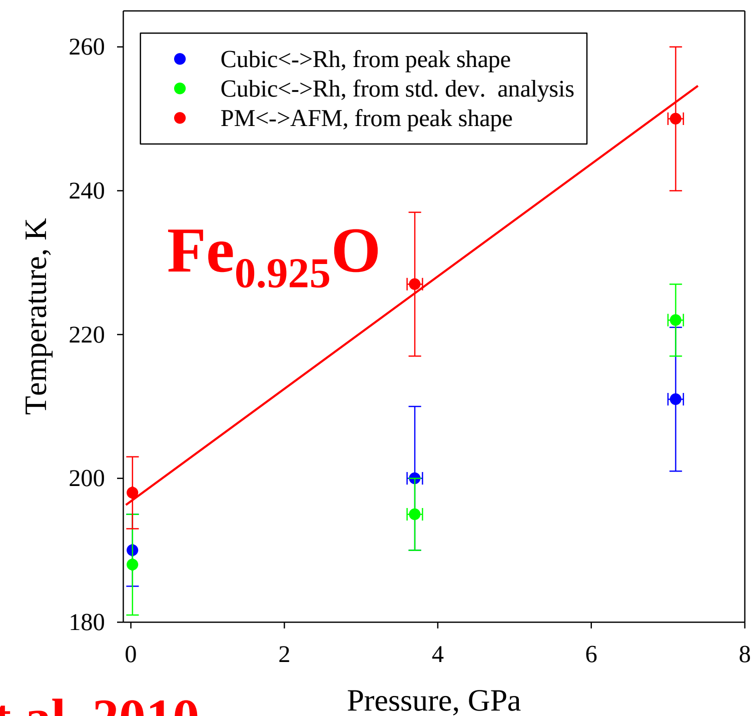

Glazyrin et al, 2010

Z. Kristallogr. **223** (2008) 461–464 / **DOI** 10.1524/zkri.2008.0049

Monoclinic FeO at high pressures

Innokenty Kantor*[,I,II], Alexander Kurnosov[I], Catherine McCammon[I] and Leonid Dubrovinsky[I]

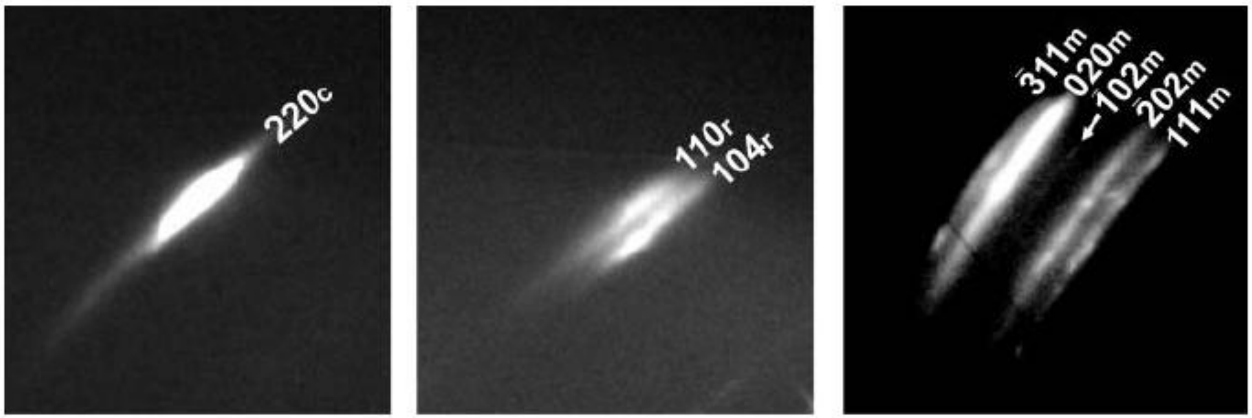

Fig. 1. Pressure evolution of the cubic 220 reflection. Left – cubic phase at 11.6 GPa (just below the trigonal distortion pressure). Middle – trigonal phase at 24.6 GPa with two reflections (104 and 110 in the trigonal setting). Right – monoclinic phase at 75.5 GPa with five reflections (111, $\bar{2}$02, $\bar{1}$02, 020, and $\bar{3}$11).

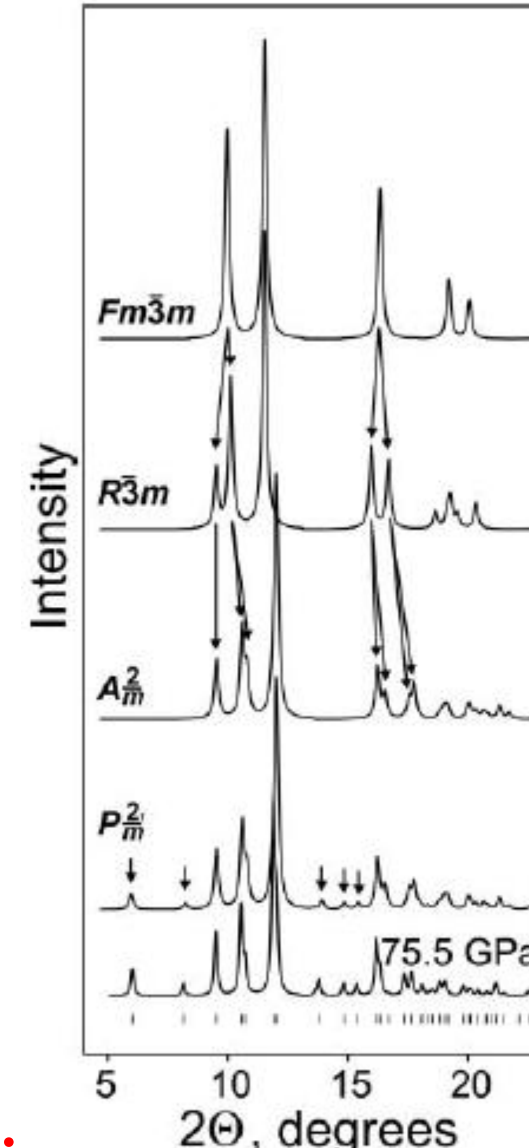

75(1) GPa

After laser heating

Stable intermediate-spin ferrous iron in lower-mantle perovskite

C. McCAMMON[1]*, I. KANTOR[1†], O. NARYGINA[1], J. ROUQUETTE[1†], U. PONKRATZ[2], I. SERGUEEV[2], M. MEZOUAR[2], V. PRAKAPENKA[3] AND L. DUBROVINSKY[1]

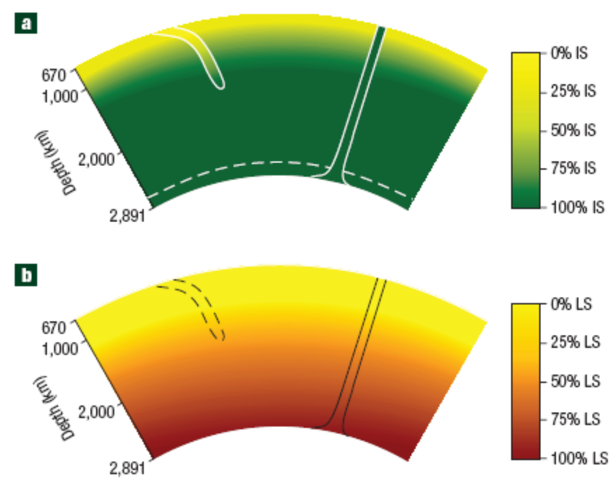

Figure 3 Estimated Fe^{2+} spin-state distribution in the lower mantle. a, Silicate perovskite variation estimated from our data, previous XES data[1,2] and current thermal models[17–19]. The greatest contrast occurs in the uppermost region, and no spin transition is expected at the base of the mantle in the postperovskite phase[10]. **b**, (Mg,Fe)O variation on the basis of previous data[26] shows the greatest contrast in spin state to occur in the middle part of the lower mantle. Slab mineralogy excludes (Mg,Fe)O and the temperature effect is small in the uppermost and lowermost regions of the lower mantle[26].

ESRF

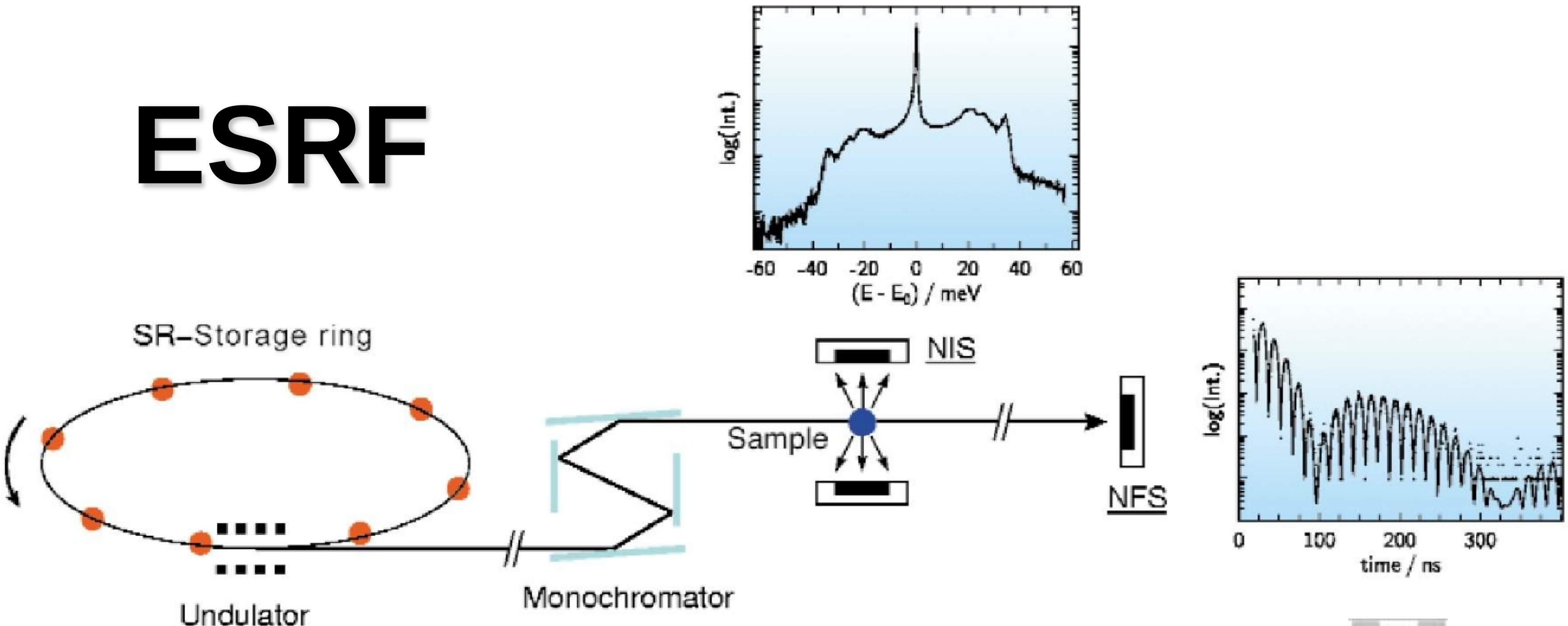

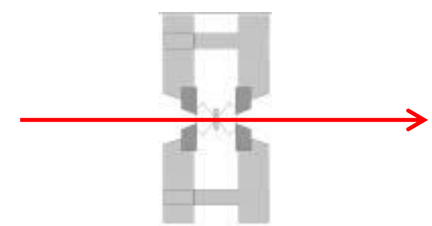

nuclear forward scattering

Mantle velocity profiles and tomography

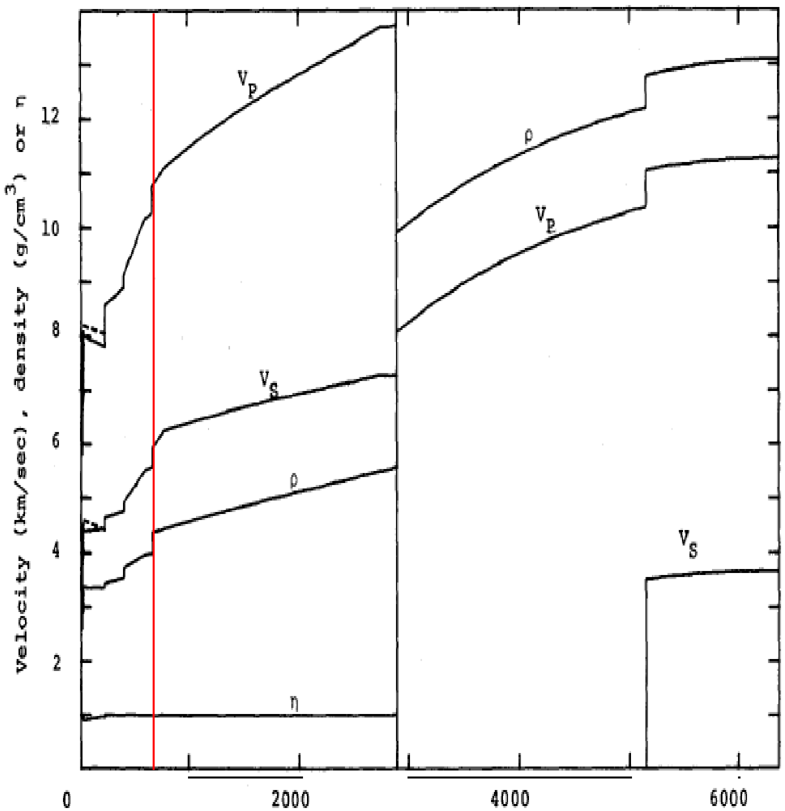

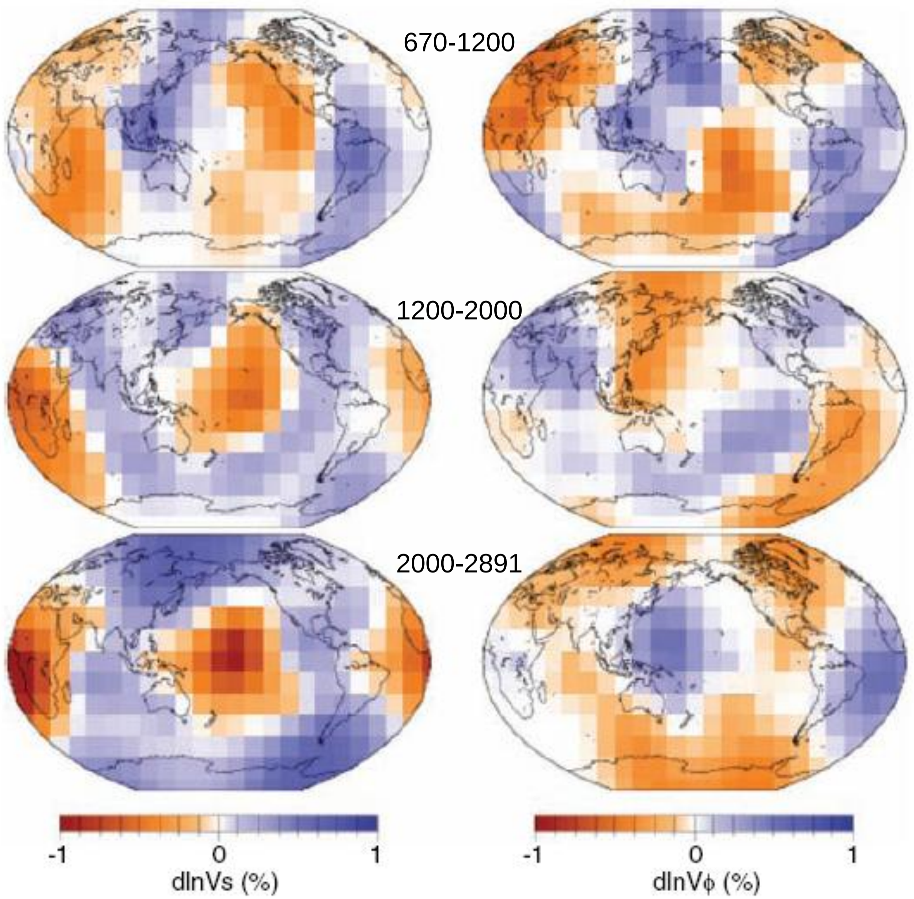

Dziewonski and Anderson (1981)

Trampert et al. 2004

www.eri.u-tokyo.ac.jp/takeuchi/model/

Possible effects of Fe^{2+} spin crossover important for geophysics

Rapid change in Fe partitioning between major phases: (Mg,Fe)O ferropericlase and $(Mg,Fe)SiO_3$ perovskite.

2 MAY 2003 VOL 300 SCIENCE www.sciencemag.org

Iron Partitioning in Earth's Mantle: Toward a Deep Lower Mantle Discontinuity

James Badro,[1] Guillaume Fiquet,[1] François Guyot,[1]
Jean-Pascal Rueff,[2] Viktor V. Struzhkin,[3] György Vankó,[4]
Giulio Monaco[4]

"... at pressures greater then 70 GPa or at depths greater than 2000 km, perovskite would then be completely iron-free, and any iron would be transferred into ferropericlase"

GEOPHYSICAL RESEARCH LETTERS, VOL. 32, L19301, doi:10.1029/2005GL023257, 2005

Fe-Mg partitioning between (Mg, Fe)SiO_3 post-perovskite, perovskite, and magnesiowüstite in the Earth's lower mantle

Yusuke Kobayashi,[1] Tadashi Kondo,[1] Eiji Ohtani,[1] Naohisa Hirao,[1]
Nobuyoshi Miyajima,[2] Takehiko Yagi,[2] Toshiro Nagase,[3] and Takumi Kikegawa[4]

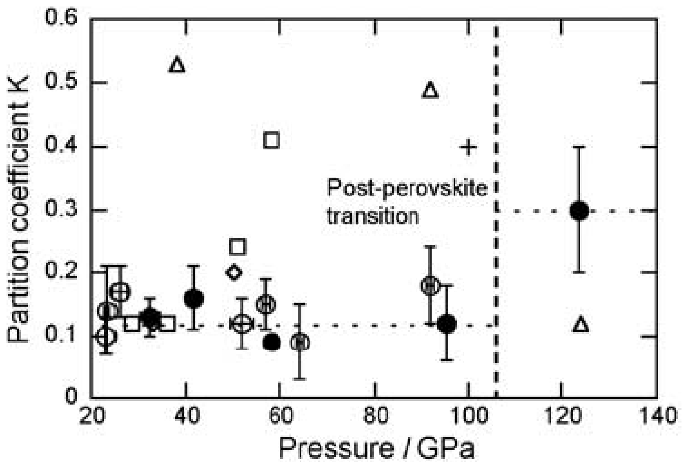

Figure 3. Pressure versus Fe-Mg partition coefficients between Pv and Mw, $K^{Pv/Mw}$ = $(FeO/MgO)_{Pv}/(FeO/MgO)_{Mw}$, and PPv and Mw, $K^{PPv/Mw}$ = $(FeO/MgO)_{PPv}/(FeO/MgO)_{Mw}$ compared with previous studies. Open and solid circles represent K values in this study from XRD and ATEM, respectively. Open diamonds, *Mao et al.* [1997] at 1500 K; open squares, *Andrault* [2001] at 2200 K; plus, *Kesson et al.* [2002]; open triangles, *Murakami et al.* [2005]. All K values in this figure have been obtained from Al-free system except *Murakami et al.* [2005].

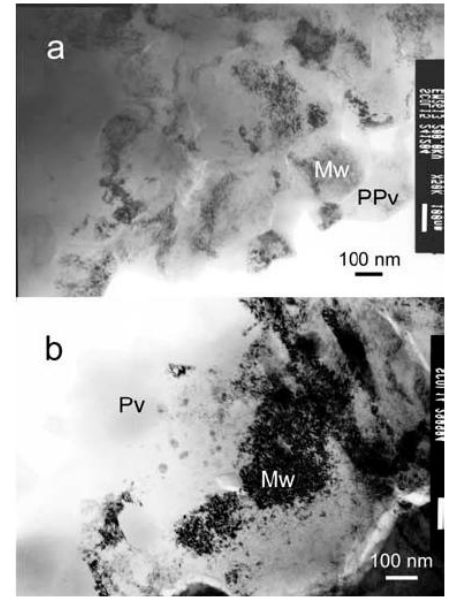

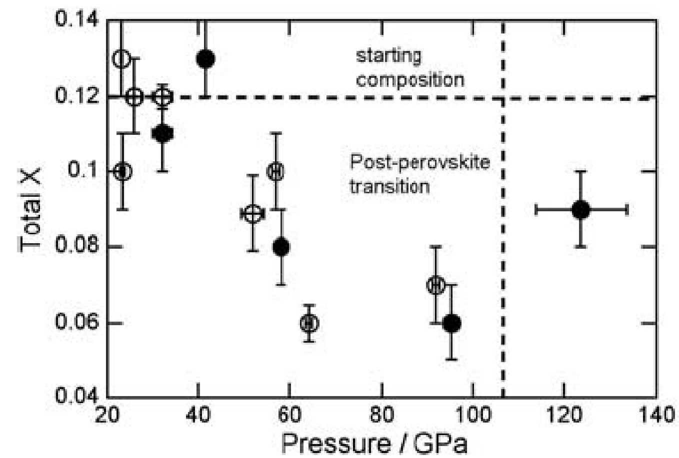

Figure 4. Total X [FeO/(FeO + MgO) in molar ratio] calculated from each X of PPv or Pv and Mw. Open and solid circles represent total X obtained from XRD and that from ATEM, respectively.

Available online at www.sciencedirect.com
ScienceDirect
EPSL
Earth and Planetary Science Letters xx (2008) xxx–xxx
www.elsevier.com/locate/epsl

Element partitioning between magnesium silicate perovskite and ferropericlase: New insights into bulk lower-mantle geochemistry

Anne-Line Auzende [a,*], James Badro [a,b], Frederick J. Ryerson [b], Peter K. Weber [b], Stewart J. Fallon [b], Ahmed Addad [c], Julien Siebert [b], Guillaume Fiquet [a]

[a] IPGP, IMPMC, Université Paris VI & Paris VII, CNRS, Department of Mineralogy, campus Boucicaut, 140 rue de Lourmel, 75015 Paris, France
[b] LLNL, Energy and Environment, Experimental geophysics, University of California, Livermore, CA 94550, United States
[c] LSPES, CNRS, Université des Sciences et Technologies de Lille, Cité scientifique, 59655 Villeuneuve d'Ascq, France

Received 12 July 2007; received in revised form 18 January 2008; accepted 3 February 2008

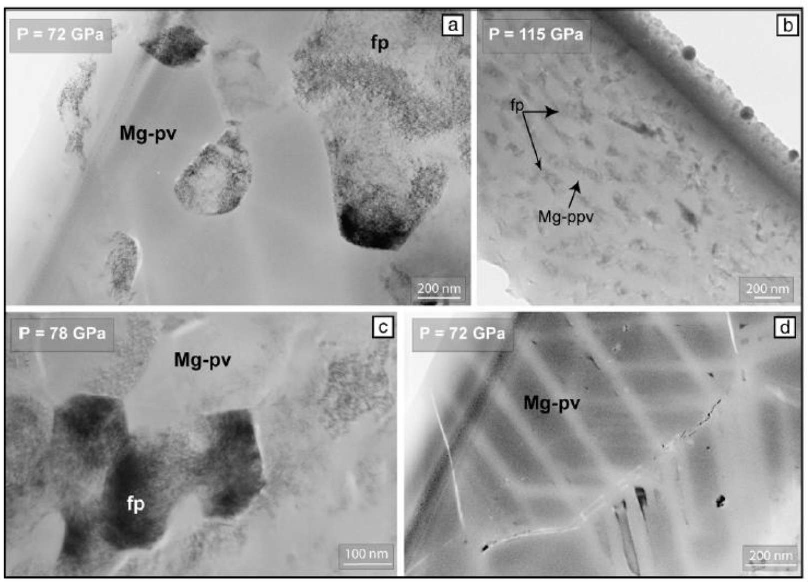

Fig. 2. TEM micrographs of mineralogical assemblages synthesized in a laser-heated diamond anvil cell at high pressures and high temperatures along the Earth geotherm. a) Amorphous pv and fp grains in Pv-04 synthesized at 72 GPa, b) same assemblage in a run conducted at 115 GPa, enlightening the pressure effect on the grain size, c) equilibrium texture in Pv-06, d) Amorphous pv showing the ghosts of the twin structures.

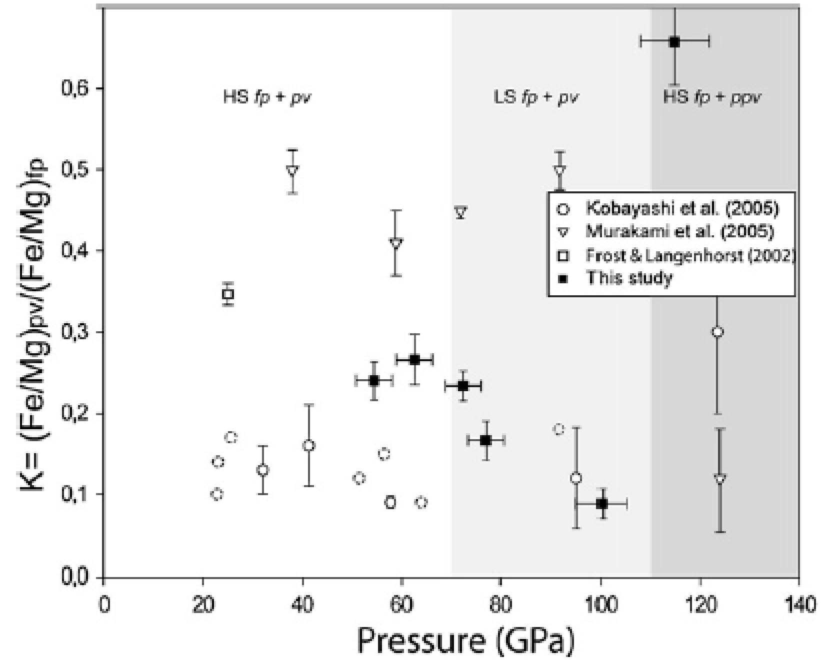

Fig. 4. Fe–Mg exchange coefficients between pv (or ppv) and fp plotted as a function of pressure. The coefficients published by Murakami et al. (2005) and Kobayashi et al. (2005) are reported for information. The three grey-shaded fields emphasize the stability fields of the successive coexisting phases: HS or LS fp+pv (Badro et al., 2003) and LS fp+ppv (Murakami et al., 2004).

Table 1
Experimental conditions

Run	*P* (Gpa)	*T* (K)	Duration of heating [at peak *T*] (min)
Pv_08	55	2450	23 [18]
Pv_05	63	2450	11 [5]
Pv_04	72	2000	27 [9]
Pv_06	78	2200	11 [7]
Pv_13	100	2150	24 [11]
Pv_14	115	2200	7 [6]

ID24: Energy dispersive XAS beam-line at ESRF

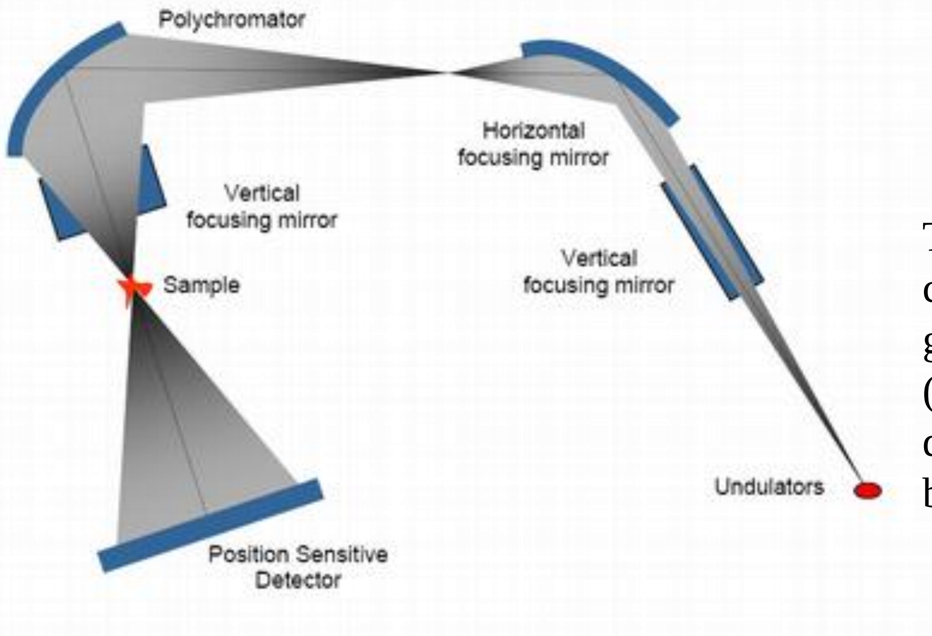

The complete optical scheme adopted on ID24, consisting in a pair of mirrors in a Kirkpatrick Baez geometry (VFM1 and HFM) and the polychromator (PLC). A second vertically focusing mirror (VFM2) downstream the polychromator is used to refocus the beam on the sample

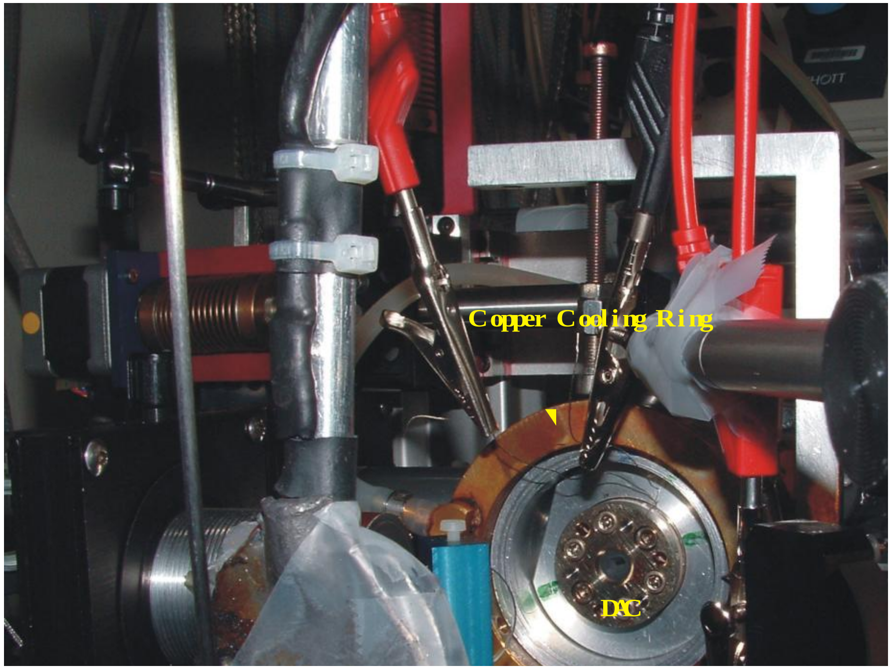

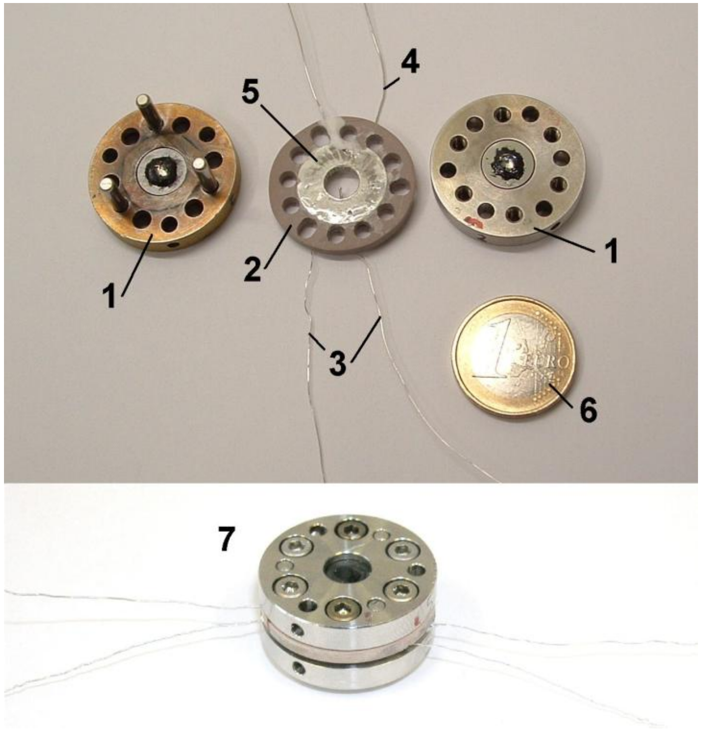

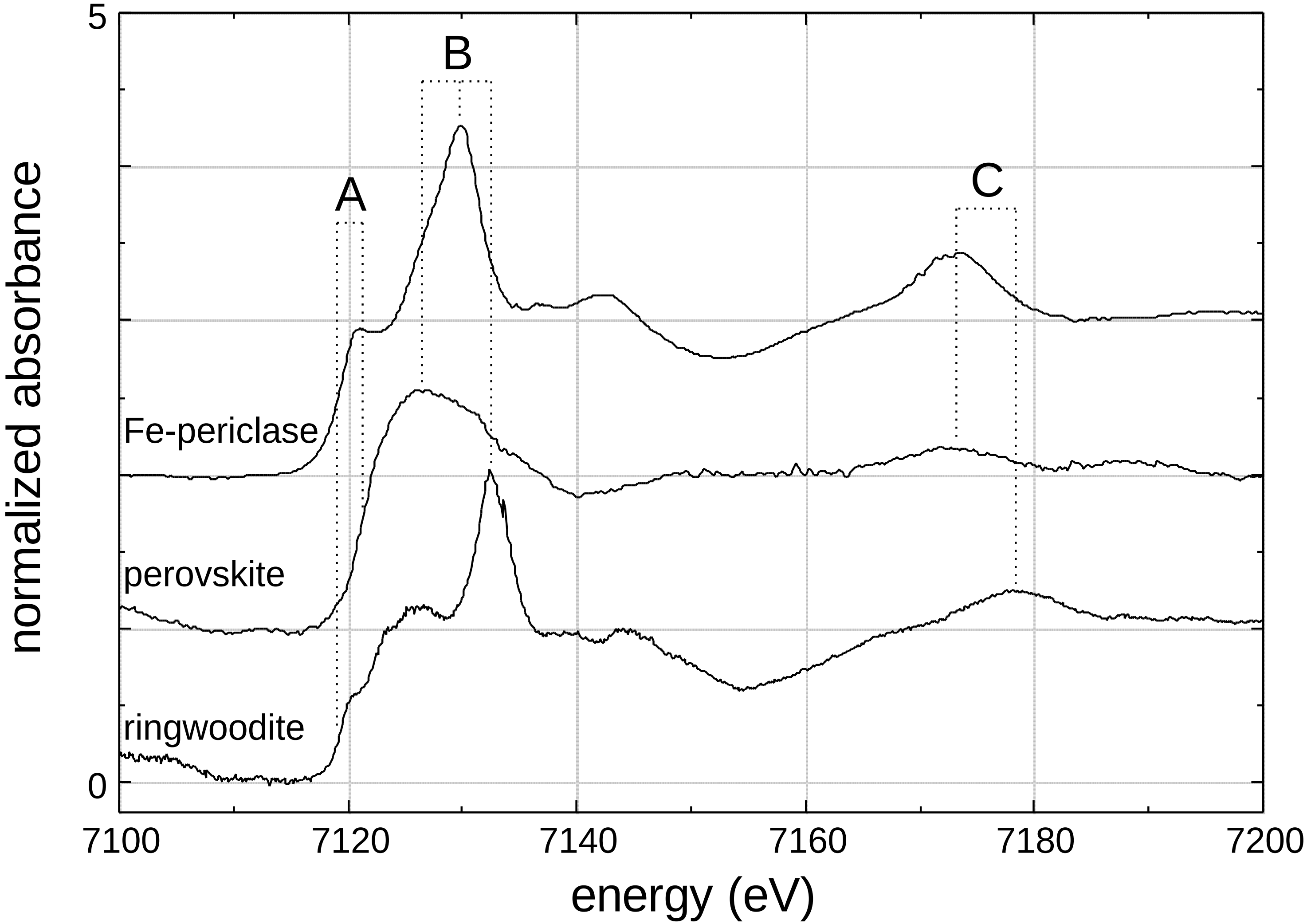
normalized absorbance
energy (eV)
5
0
7100
7120
7140
7160
7180
7200
A
B
C
Fe-periclase
perovskite
ringwoodite

24-26 GPa

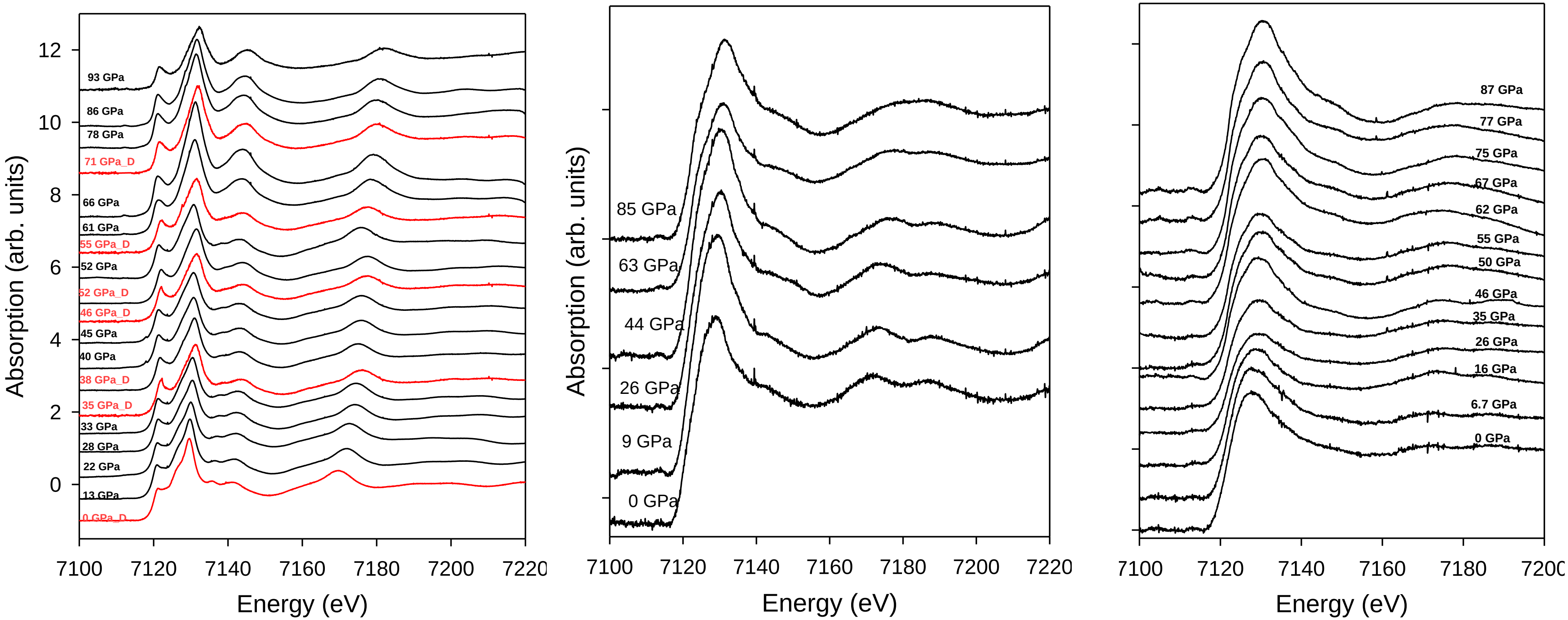

$(Mg_{0.88}Fe_{0.12})O$
$(Mg_{0.80}Fe_{0.20})O$

P ~ 100 GPa

$(Mg_{0.88}Fe_{0.12})SiO_3$

P ~ 105 GPa

$(Mg_{0.86}Fe_{0.14})(Si_{0.975}Al_{0.025})O_3$

P ~ 90 GPa

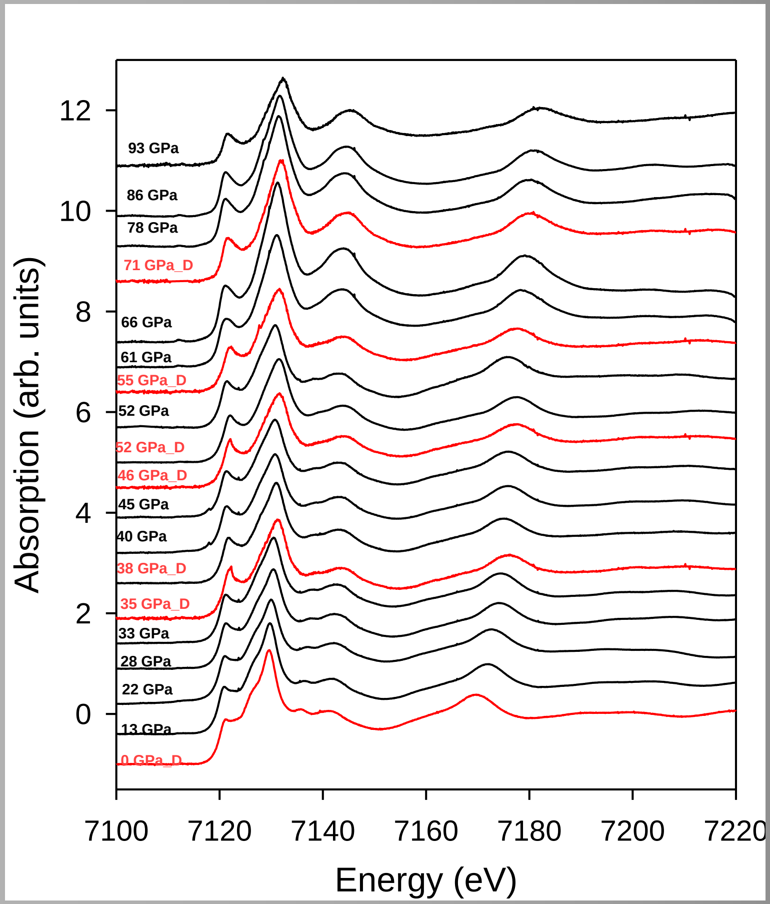

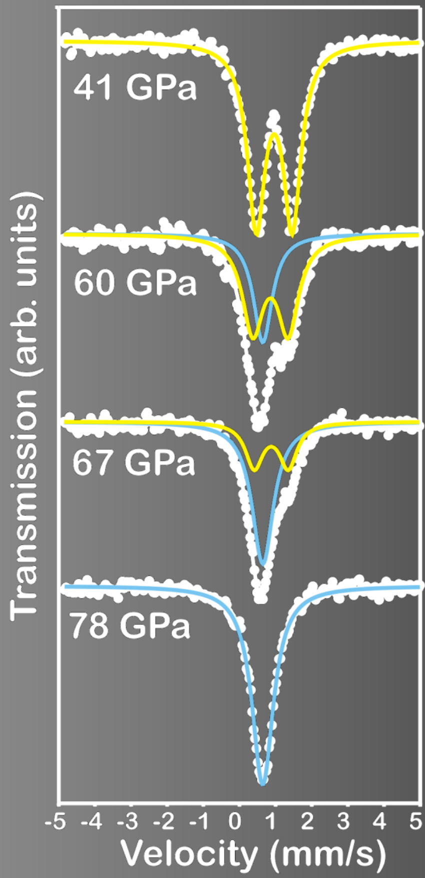

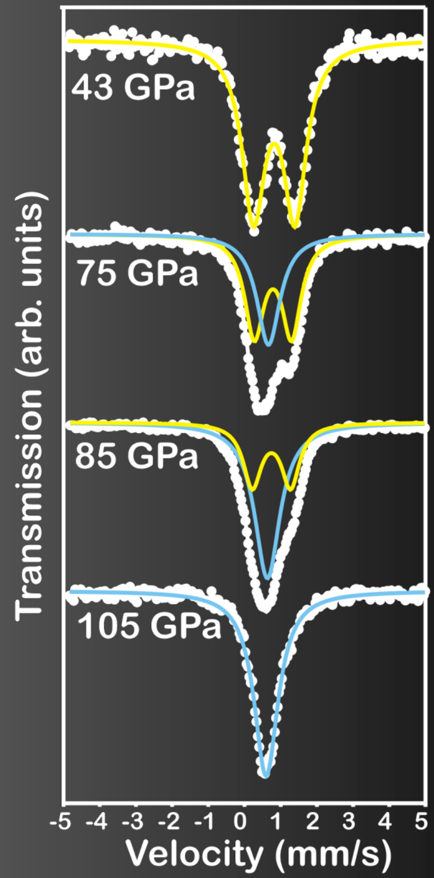

$(Mg_{0.95}Fe_{0.05})O$ $(Mg_{0.80}Fe_{0.20})O$

$(Mg_{0.88}Fe_{0.12})O$
$(Mg_{0.80}Fe_{0.20})O$

Kantor et al., 2007
Narygina et al., 2008

$(Mg_{0.88}Fe_{0.12})SiO_3$

$(Mg_{0.86}Fe_{0.14})(Si_{0.975}Al_{0.025})O_3$

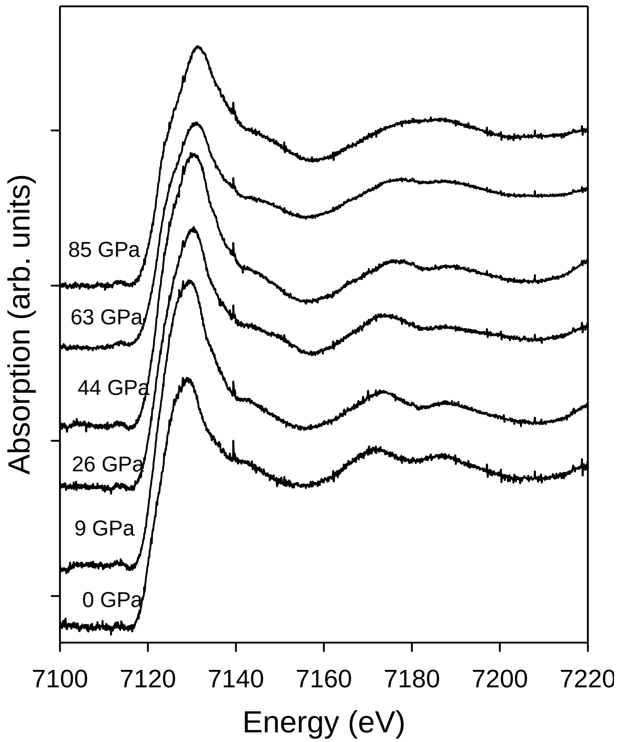

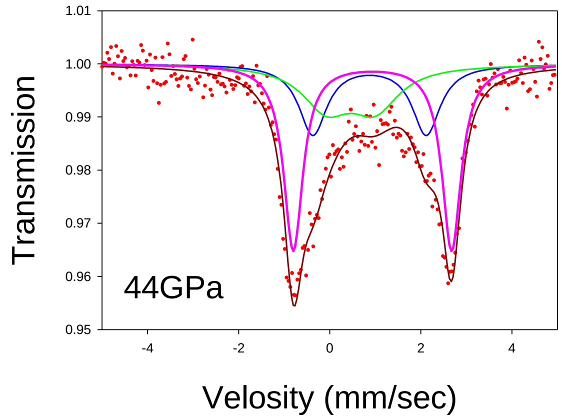

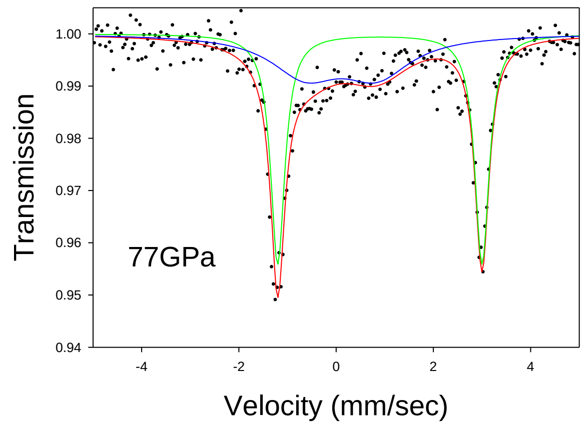

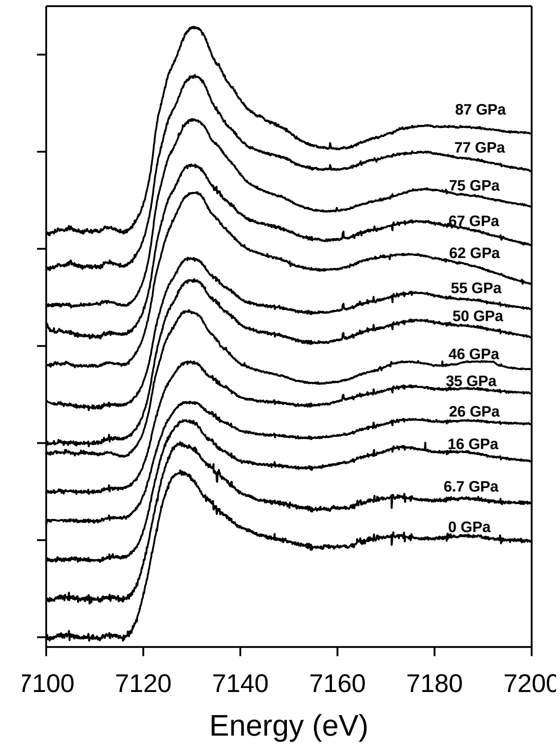

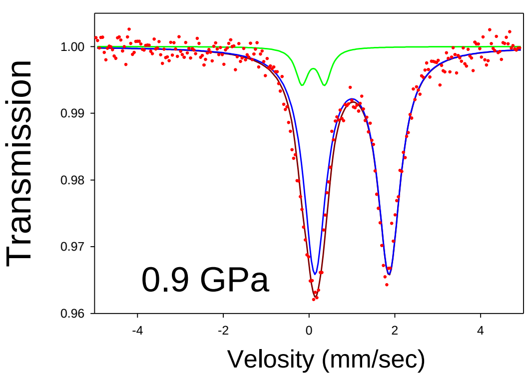

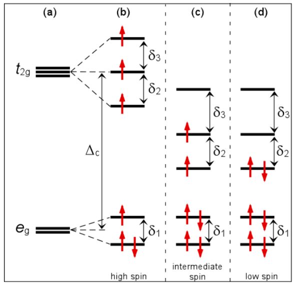

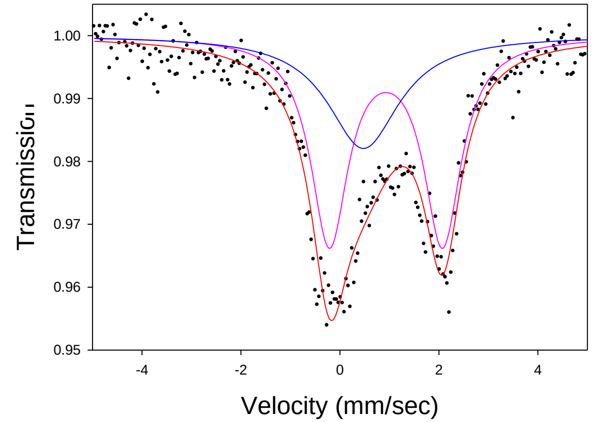

$(Mg_{0.88}Fe_{0.12})SiO_3$

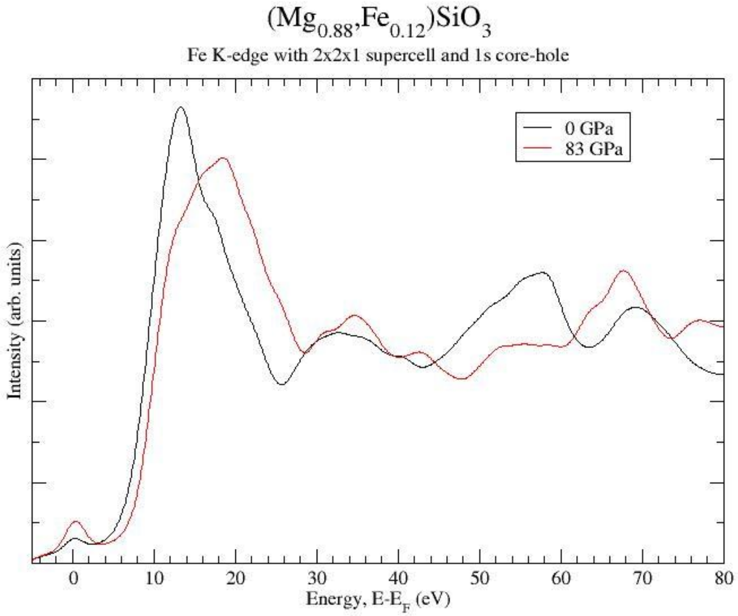

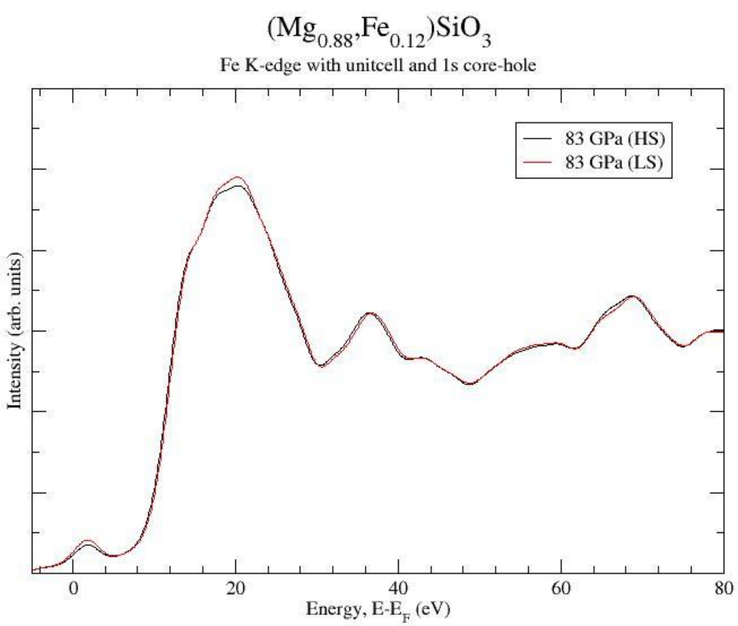

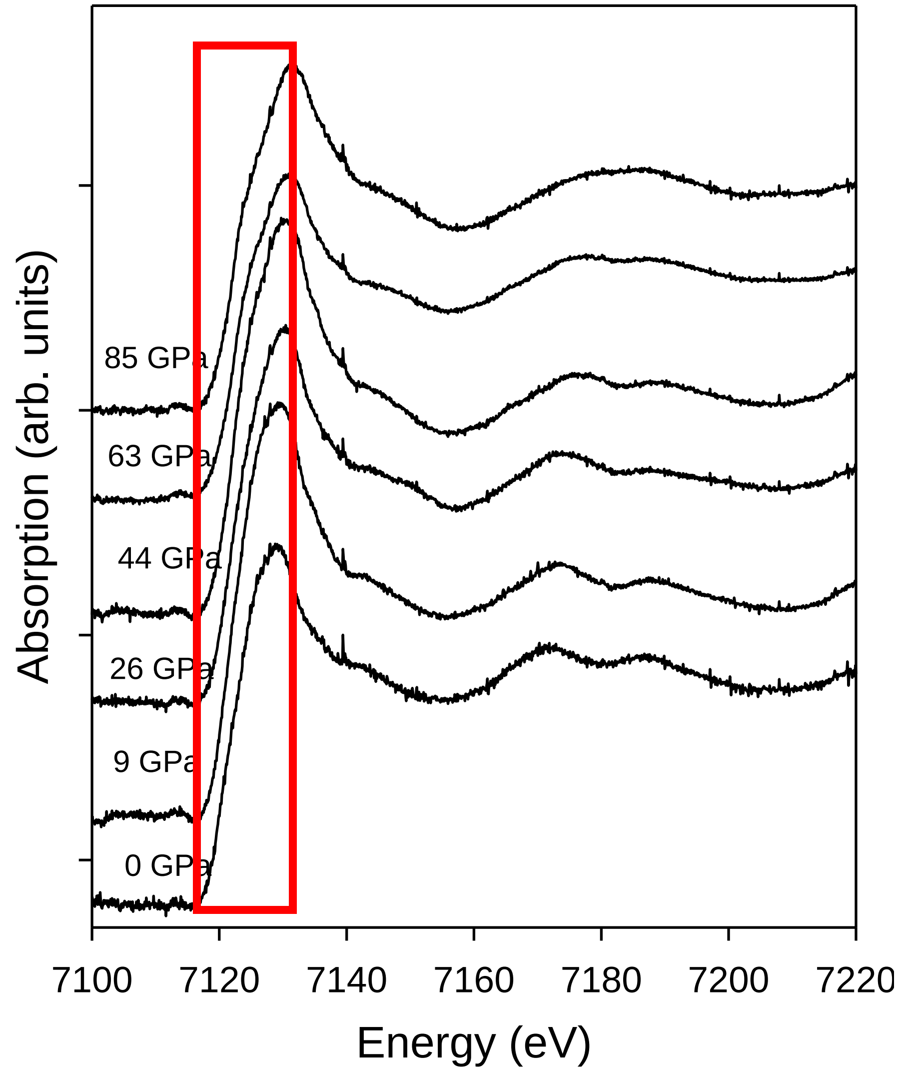

M. Mattesini et al., 2008

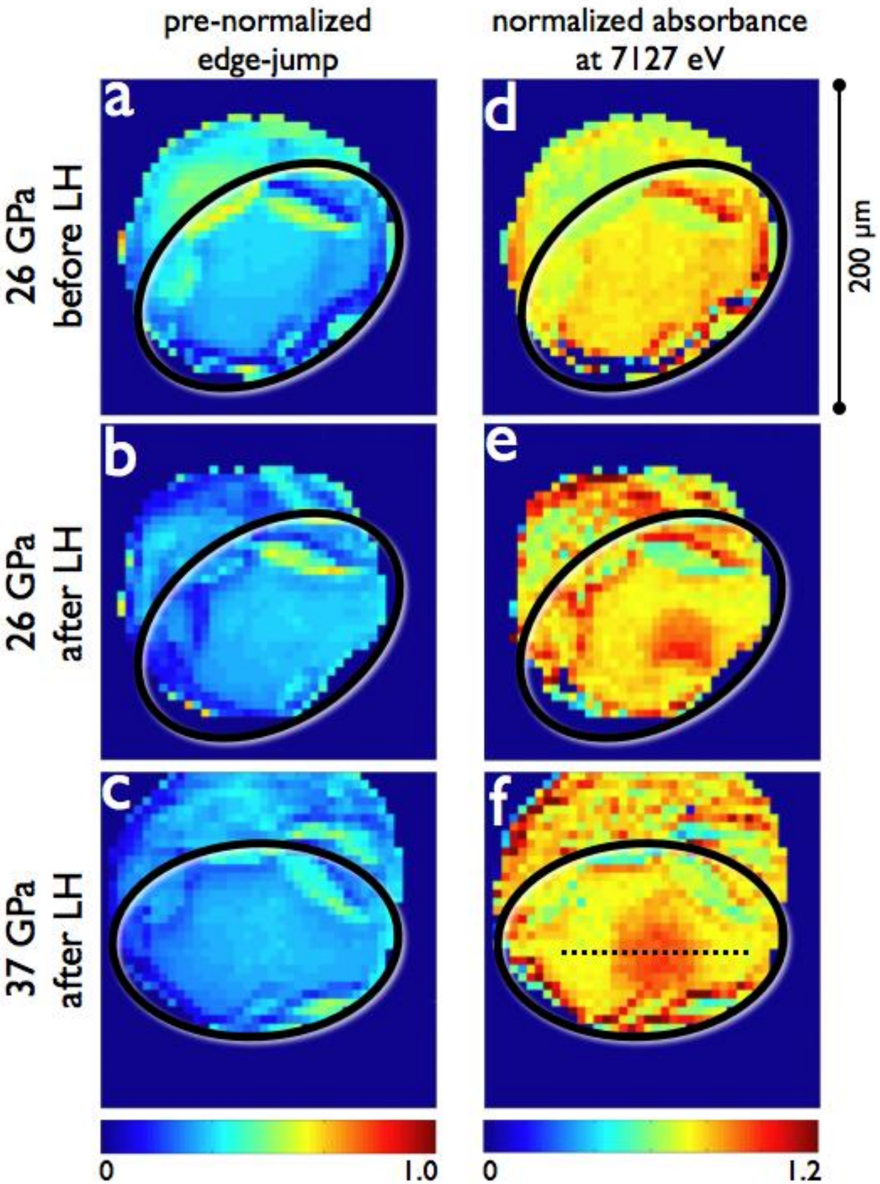
pre-normalized
edge-jump
normalized absorbance
at 7127 eV
a
b
c
d
e
f
26 GPa
before LH
26 GPa
after LH
37 GPa
after LH
200 µm
0
1.0
0
1.2

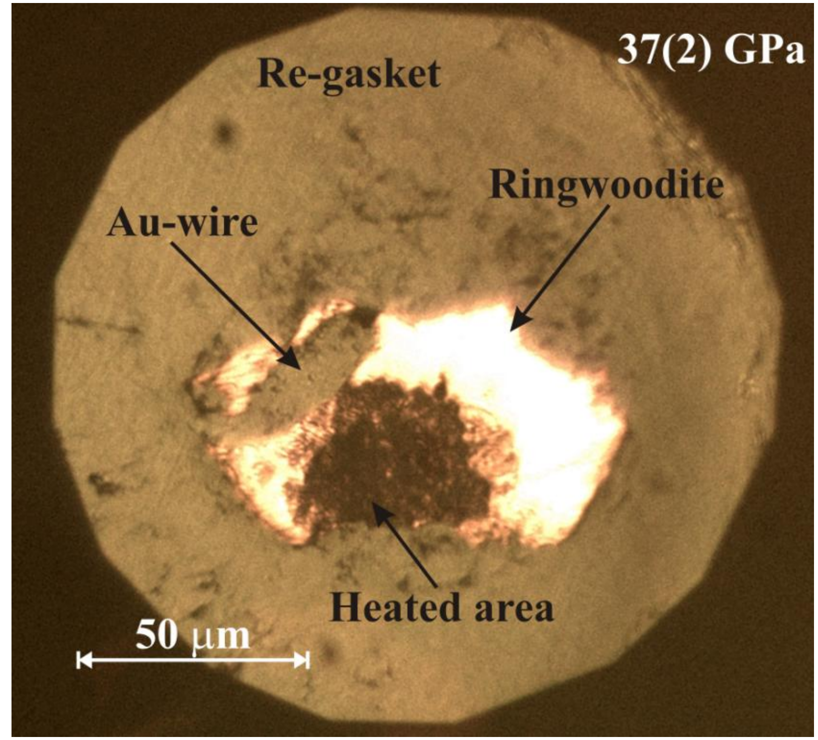
37(2) GPa
Re-gasket
Ringwoodite
Au-wire
Heated area
50 µm

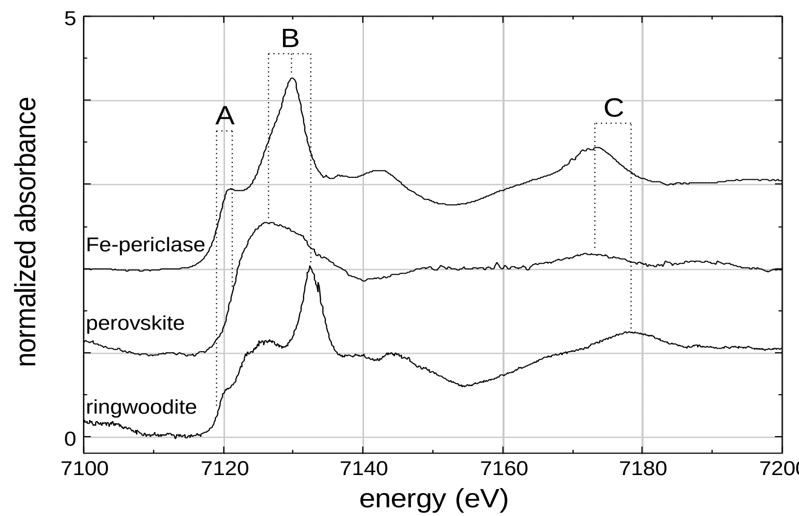
5
0
A
B
C
Fe-periclase
perovskite
ringwoodite
normalized absorbance
7100
7120
7140
7160
7180
7200
energy (eV)

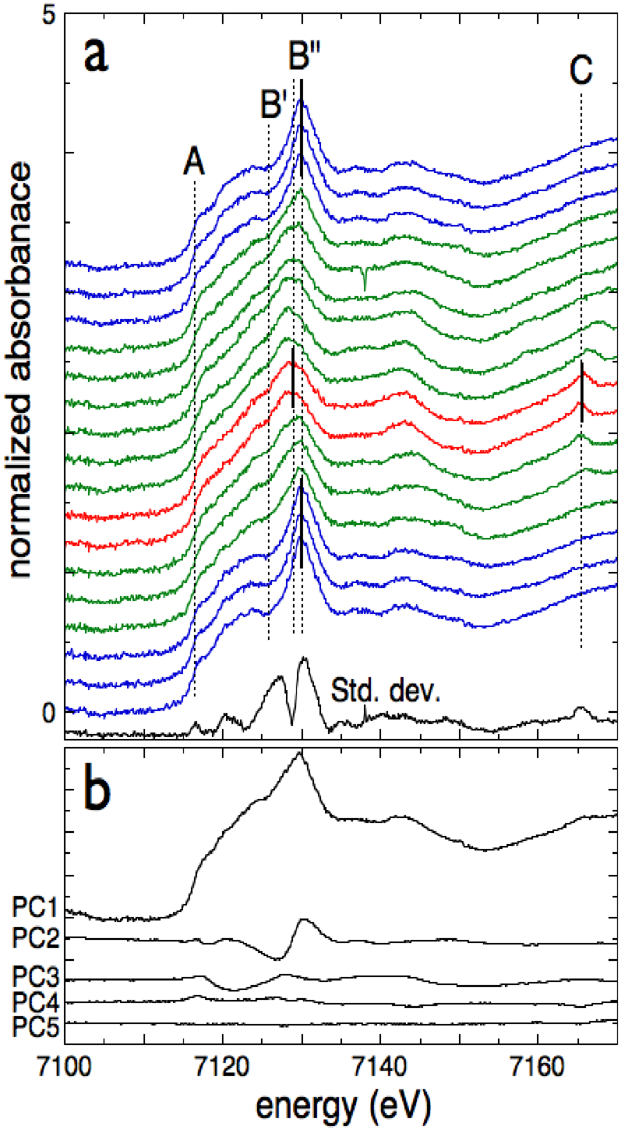

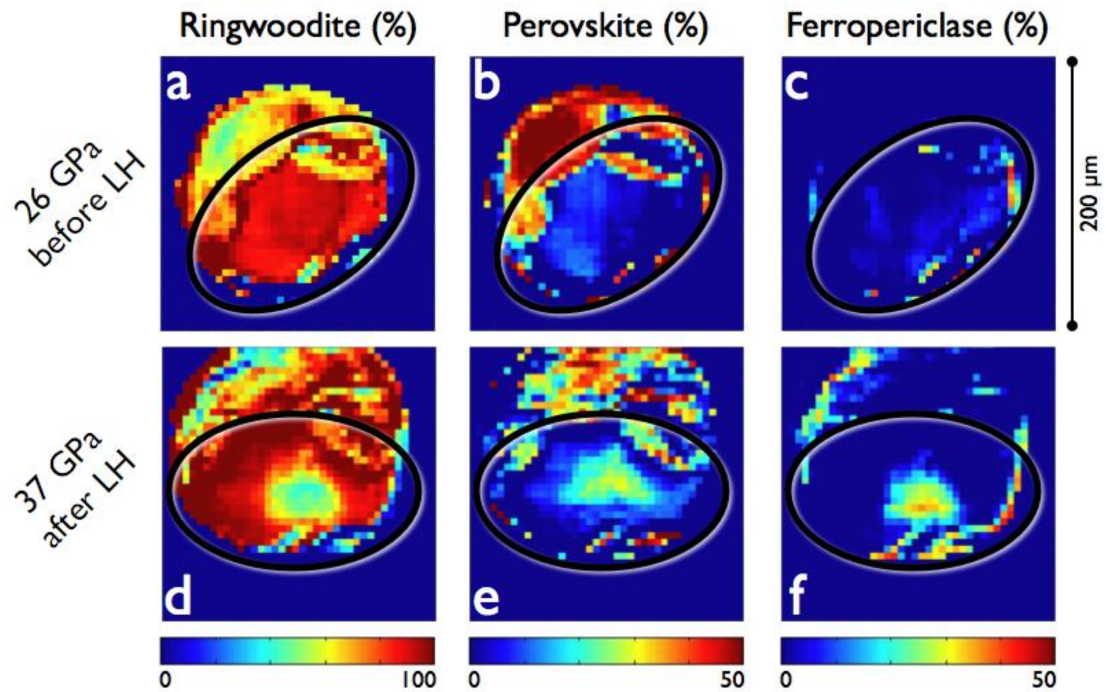

Concentration maps of ringwoodite, perovskite and ferropericlase, for the sample at 26 GPa before laser heating, (a, b and c, respectively) and for the sample at 37 GPa after laser heating (d, e and f, respectively). Note that the sample in the pressure chamber is surrounded with a black line.

M. Munoz et al., 2008

37 GPa

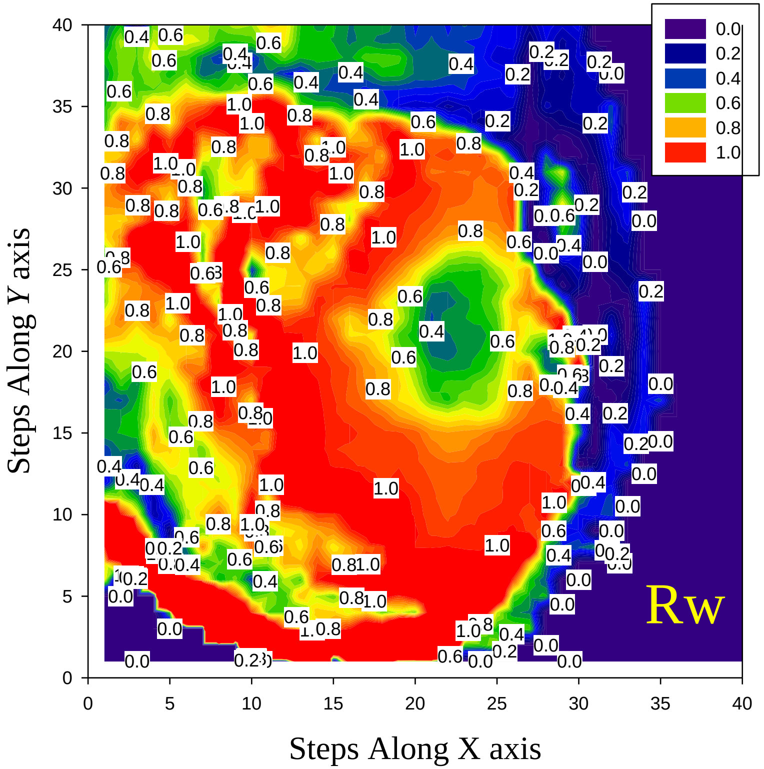
Steps Along Y axis
Steps Along X axis
0 5 10 15 20 25 30 35 40
0.0
0.2
0.4
0.6
0.8
1.0
Rw

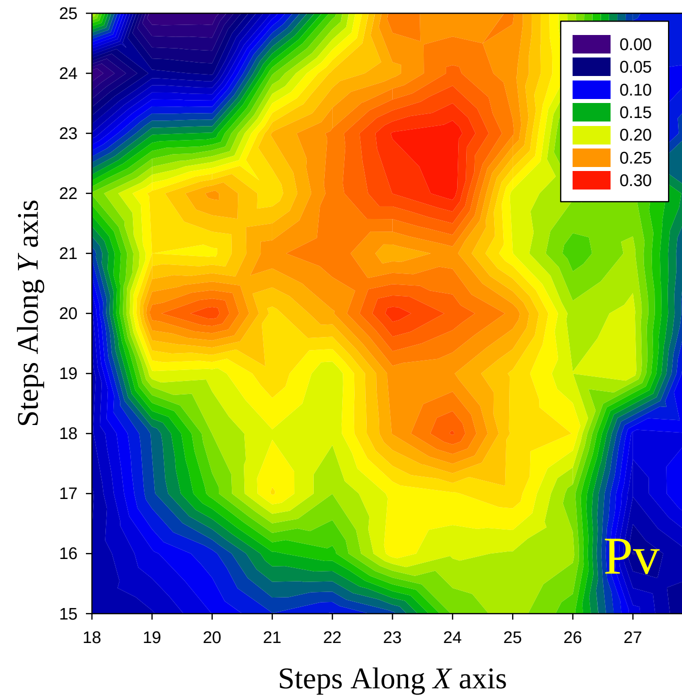
Steps Along Y axis
Steps Along X axis
18 19 20 21 22 23 24 25 26 27 28
15 16 17 18 19 20 21 22 23 24 25
0.00
0.05
0.10
0.15
0.20
0.25
0.30
Pv

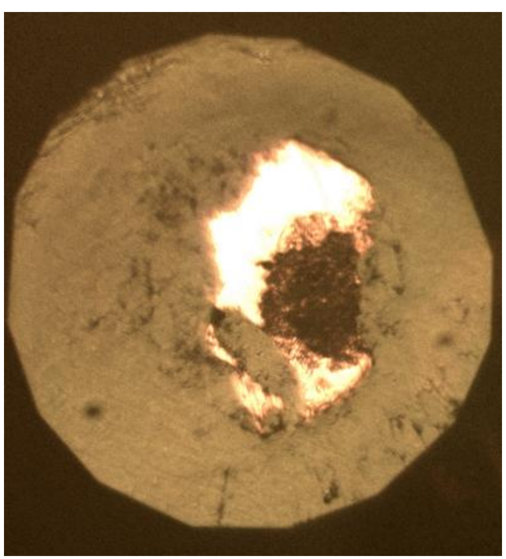

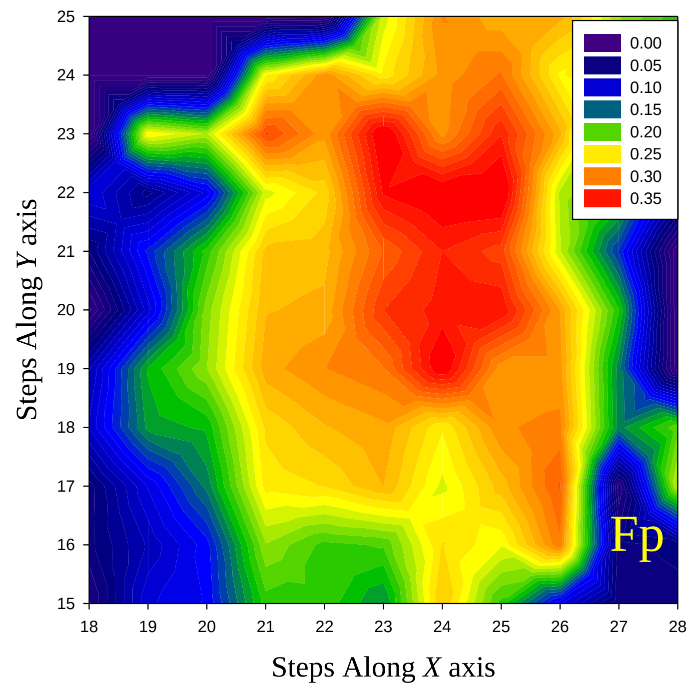
Steps Along Y axis
Steps Along X axis
18 19 20 21 22 23 24 25 26 27 28
15 16 17 18 19 20 21 22 23 24 25
0.00
0.05
0.10
0.15
0.20
0.25
0.30
0.35
Fp

37 GPa

RP

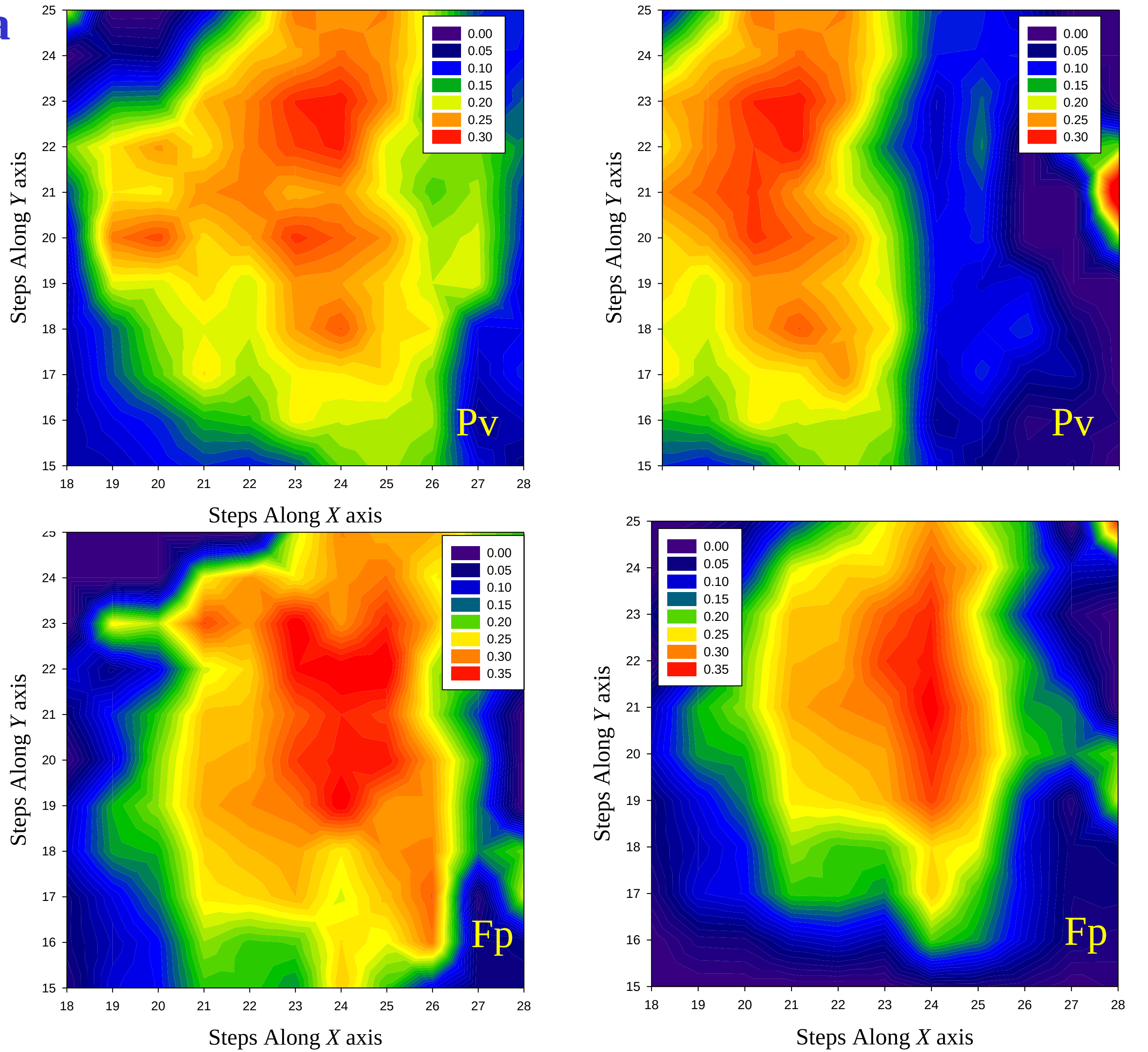

Steps Along Y axis
Steps Along X axis
0.00
0.05
0.10
0.15
0.20
0.25
0.30
0.35
Pv
Pv
Fp
Fp

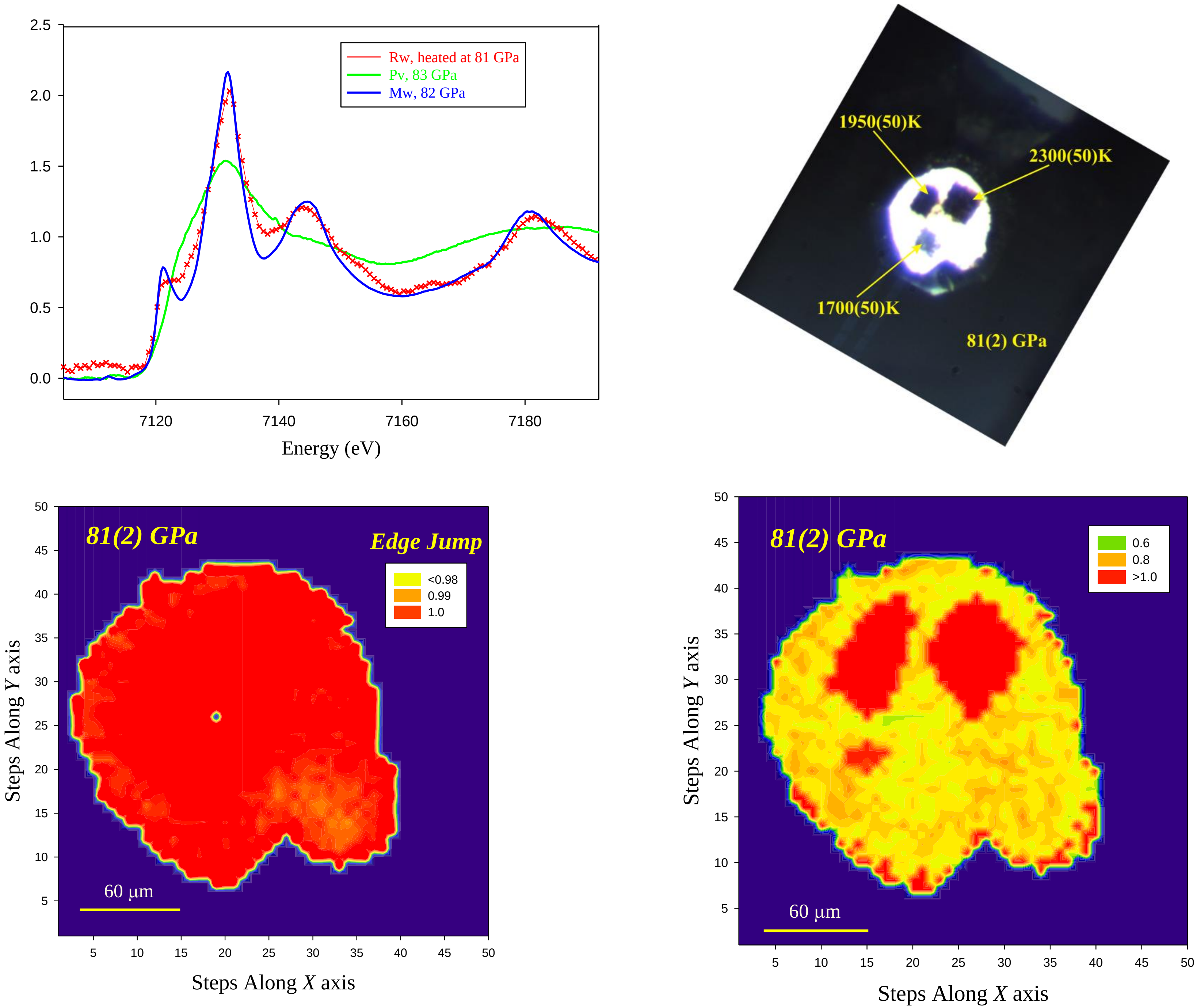

Rw, heated at 81 GPa
Pv, 83 GPa
Mw, 82 GPa
Energy (eV)
1950(50)K
2300(50)K
1700(50)K
81(2) GPa
81(2) GPa
Edge Jump
<0.98
0.99
1.0
60 µm
Steps Along Y axis
Steps Along X axis
81(2) GPa
0.6
0.8
>1.0
60 µm
Steps Along Y axis
Steps Along X axis

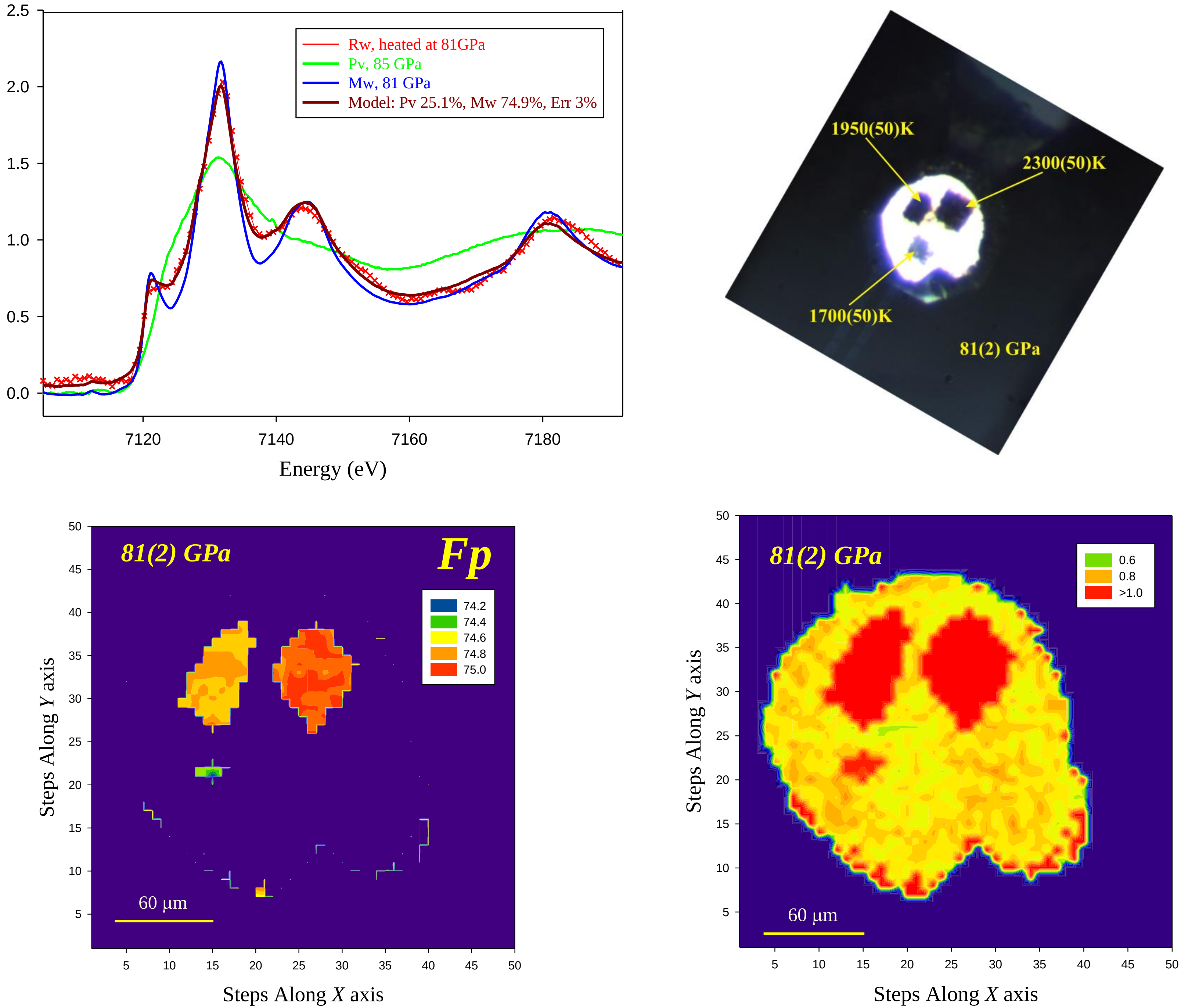

Rw, heated at 81GPa
Pv, 85 GPa
Mw, 81 GPa
Model: Pv 25.1%, Mw 74.9%, Err 3%
Energy (eV)
1950(50)K
2300(50)K
1700(50)K
81(2) GPa
81(2) GPa
Fp
74.2
74.4
74.6
74.8
75.0
60 µm
Steps Along Y axis
Steps Along X axis
81(2) GPa
0.6
0.8
>1.0
60 µm
Steps Along Y axis
Steps Along X axis

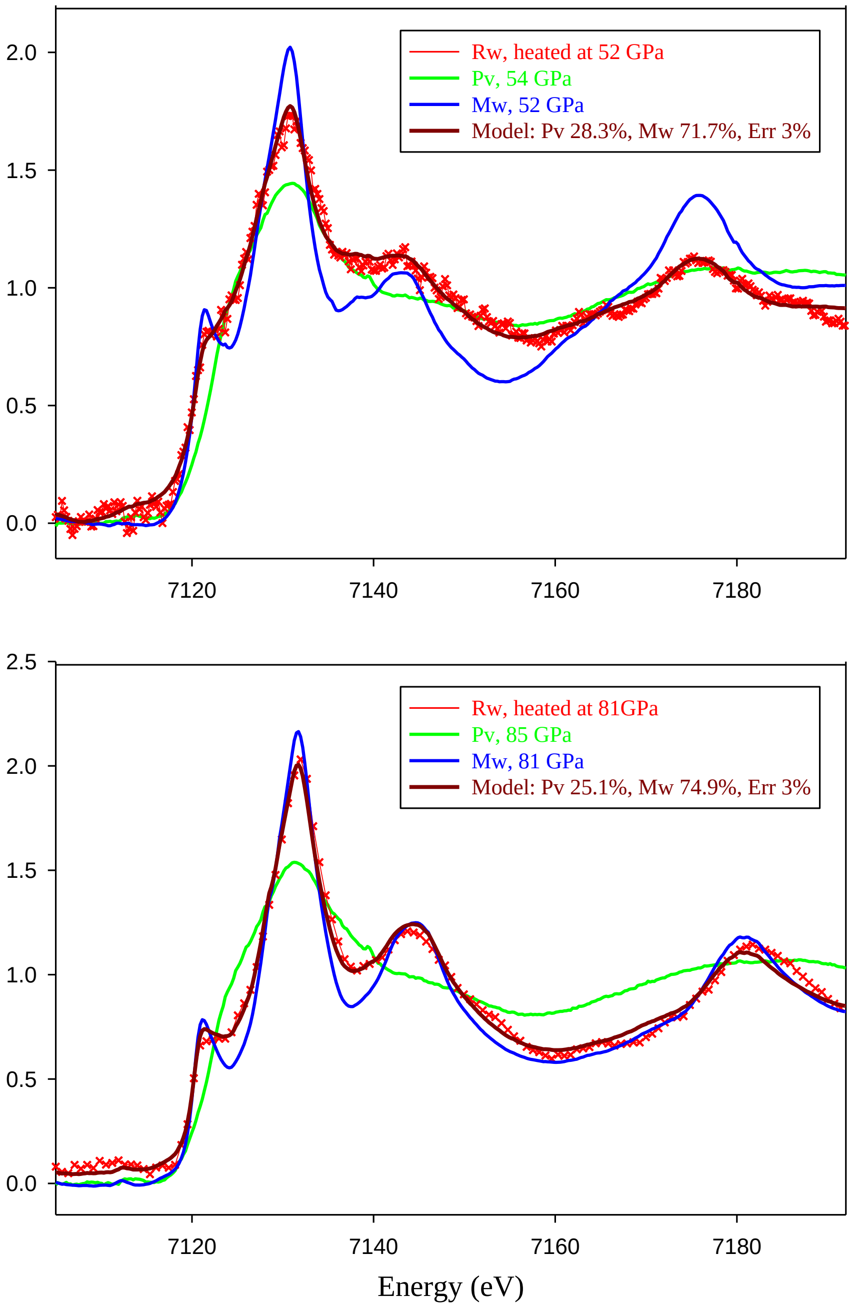

$$K_D = \left(\frac{X_{Fe}}{X_{Mg}}\right)^{Pv} \Big/ \left(\frac{X_{Fe}}{X_{Mg}}\right)^{Fp}$$

$$X_{Fe} = \frac{[FeO]}{[FeO]+[MgO]}$$

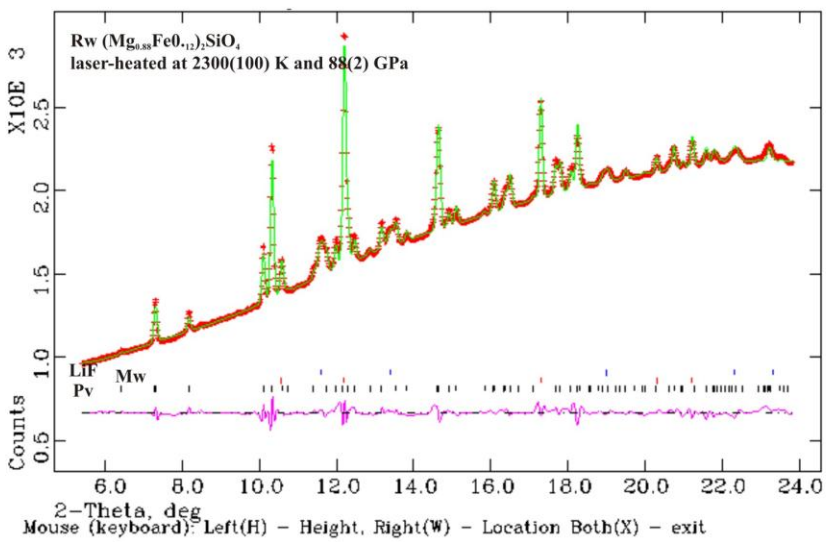

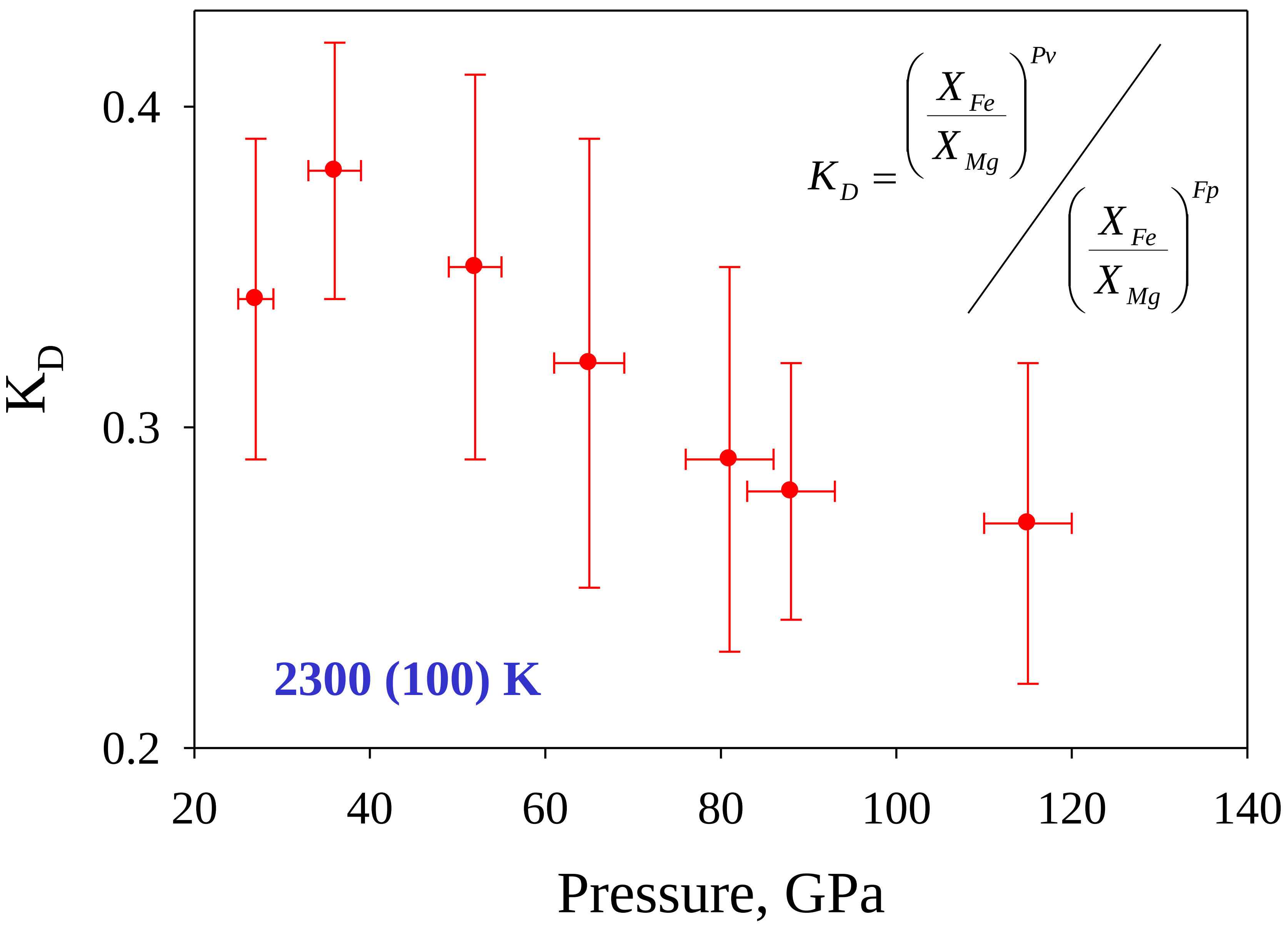

0.4
0.3
0.2
K_D
20
40
60
80
100
120
140
Pressure, GPa
2300 (100) K
$K_D = \left(\frac{X_{Fe}}{X_{Mg}}\right)^{Pv} \Big/ \left(\frac{X_{Fe}}{X_{Mg}}\right)^{Fp}$

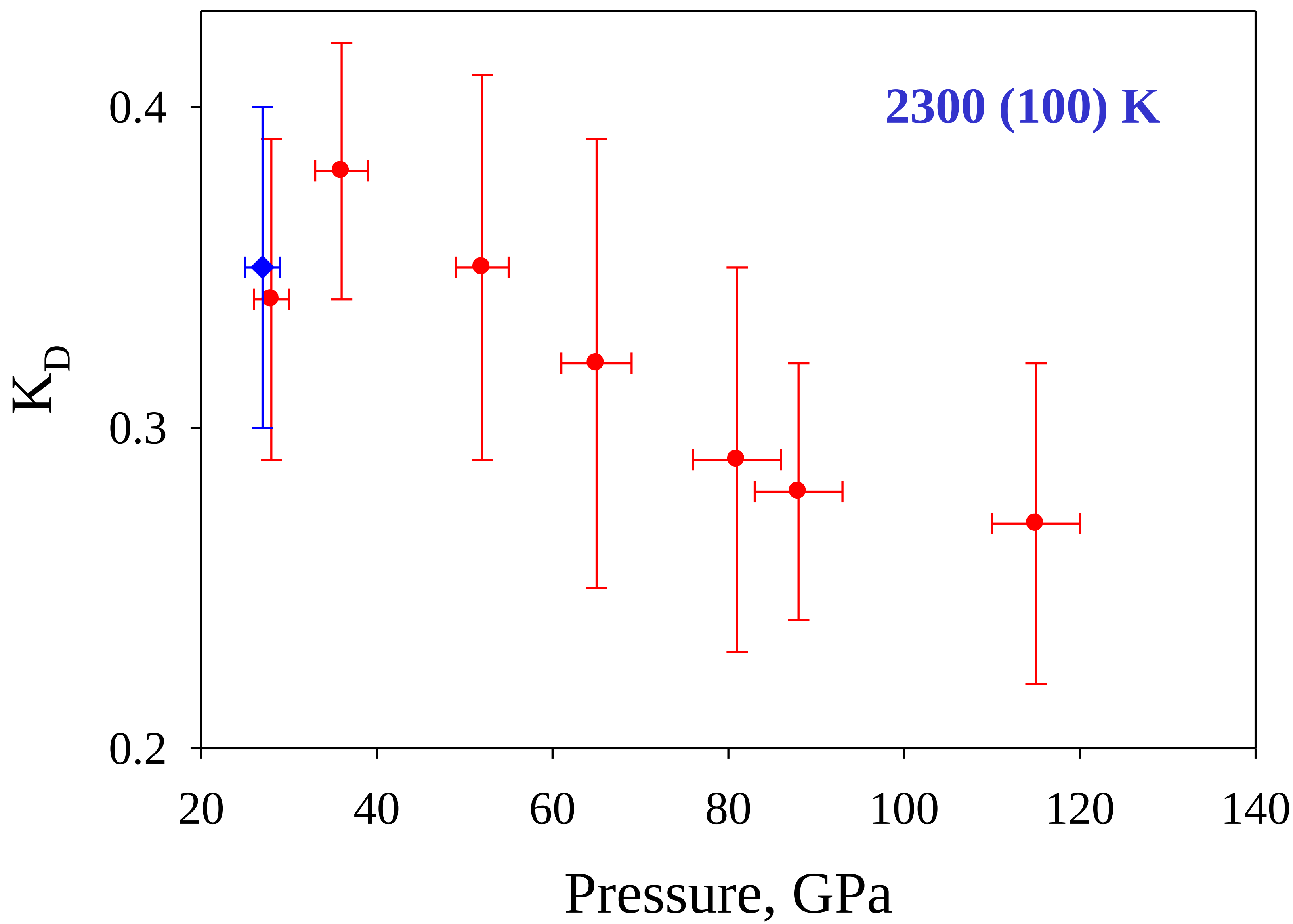

2300 (100) K
0.4
0.3
0.2
K_D
20
40
60
80
100
120
140
Pressure, GPa

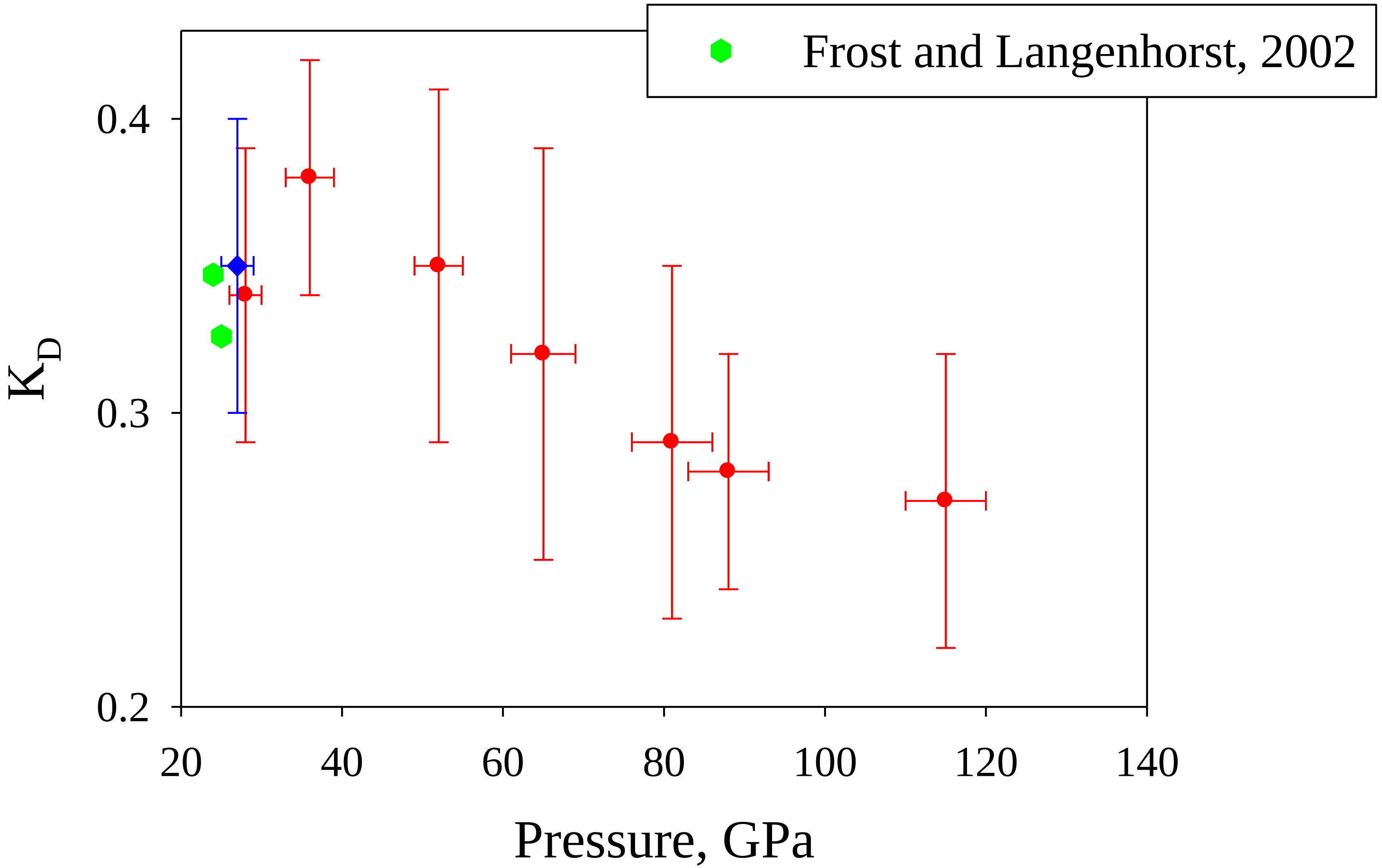

Frost and Langenhorst, 2002
0.4
0.3
0.2
K_D
20
40
60
80
100
120
140
Pressure, GPa

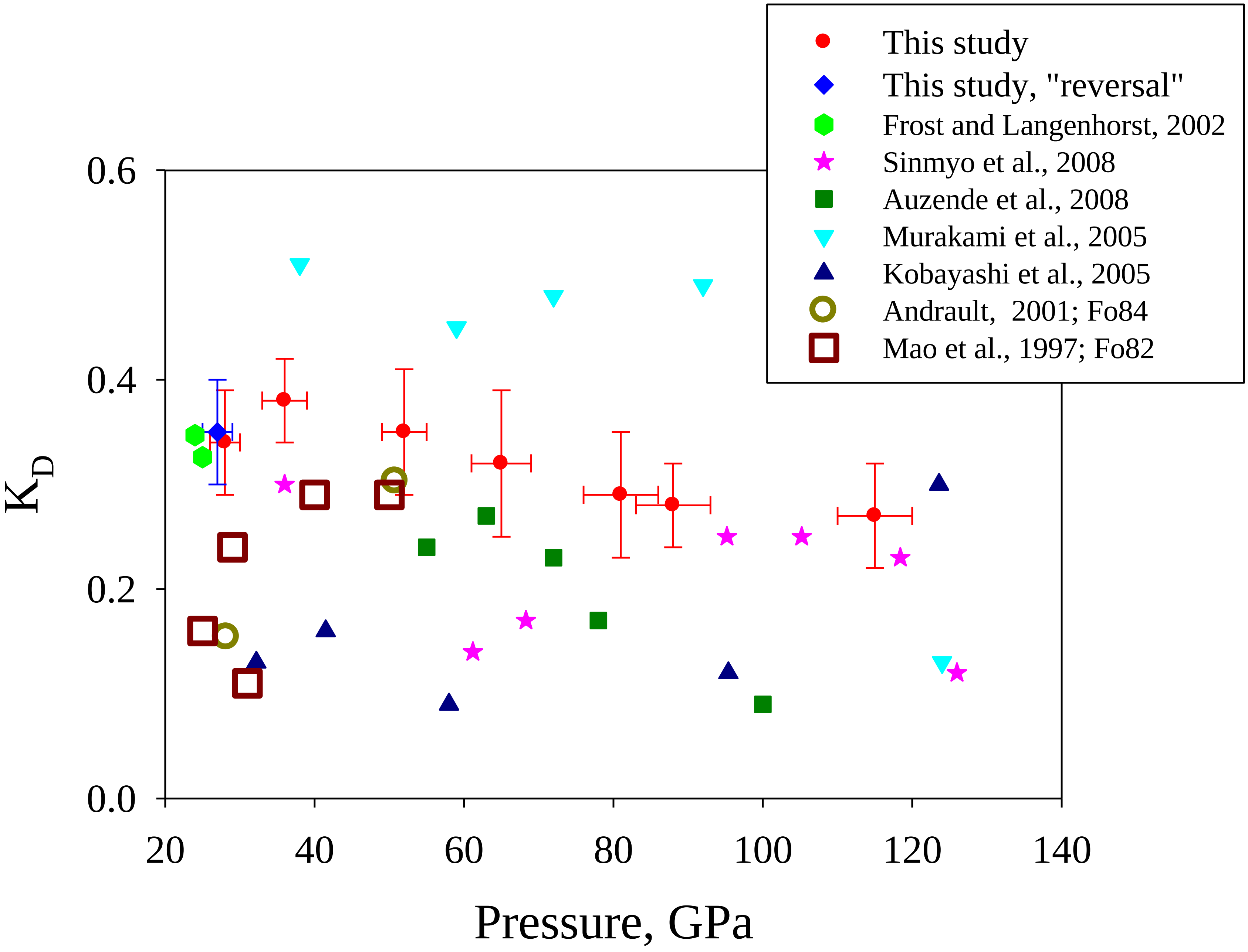

This study
This study, "reversal"
Frost and Langenhorst, 2002
Sinmyo et al., 2008
Auzende et al., 2008
Murakami et al., 2005
Kobayashi et al., 2005
Andrault, 2001; Fo84
Mao et al., 1997; Fo82
K_D
0.0
0.2
0.4
0.6
20
40
60
80
100
120
140
Pressure, GPa

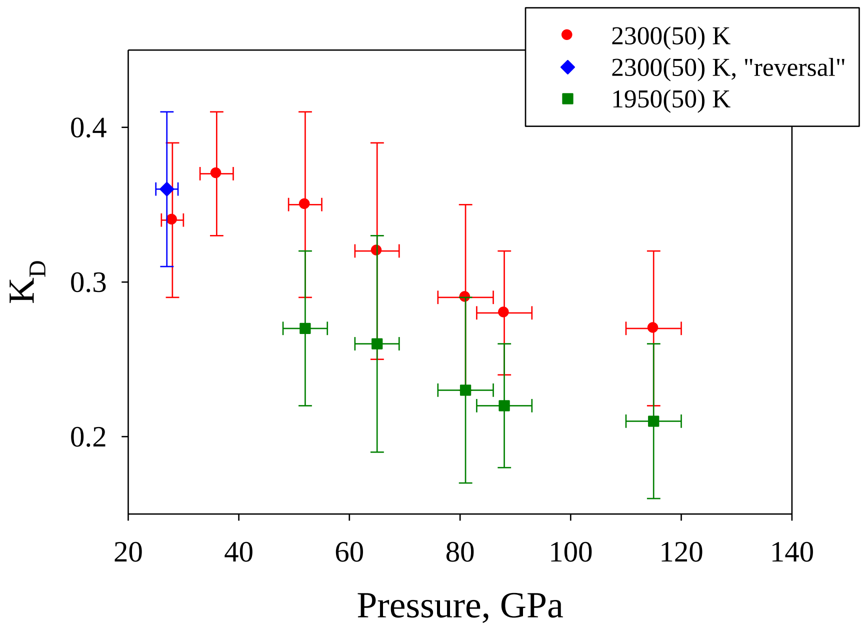

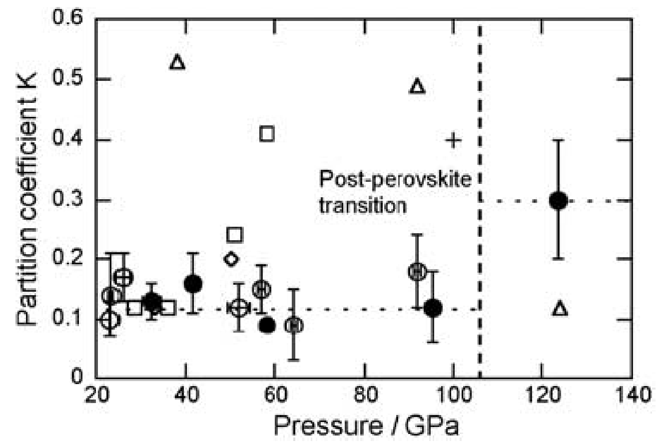

Figure 3. Pressure versus Fe-Mg partition coefficients between Pv and Mw, $K^{Pv/Mw}$ = $(FeO/MgO)_{Pv}/(FeO/MgO)_{Mw}$, and PPv and Mw, $K^{PPv/Mw}$ = $(FeO/MgO)_{PPv}/(FeO/MgO)_{Mw}$ compared with previous studies. Open and solid circles represent *K* values in this study from XRD and ATEM, respectively. Open diamonds, *Mao et al.* [1997] at 1500 K; open squares, *Andrault* [2001] at 2200 K; plus, *Kesson et al.* [2002]; open triangles, *Murakami et al.* [2005]. All *K* values in this figure have been obtained from Al-free system except *Murakami et al.* [2005].

Iron Partitioning in Earth's Mantle: Toward a Deep Lower Mantle Discontinuity

James Badro,[1] Guillaume Fiquet,[1] François Guyot,[1] Jean-Pascal Rueff,[2] Viktor V. Struzhkin,[3] György Vankó,[4] Giulio Monaco[4]

"... at pressures greater then 70 GPa or at depths greater than 2000 km, perovskite would then be completely iron-free, and any iron would be transferred into ferropericlase"

$$K_D = \left(\frac{X_{Fe}}{X_{Mg}}\right)^{Pv} \Bigg/ \left(\frac{X_{Fe}}{X_{Mg}}\right)^{Fp}$$

2 MAY 2003 VOL 300 SCIENCE www.sciencemag.org

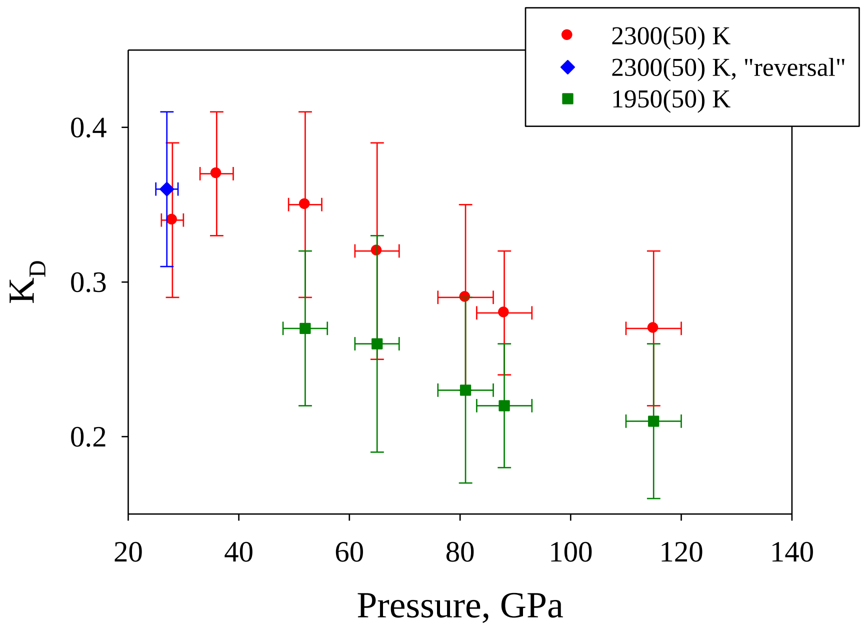

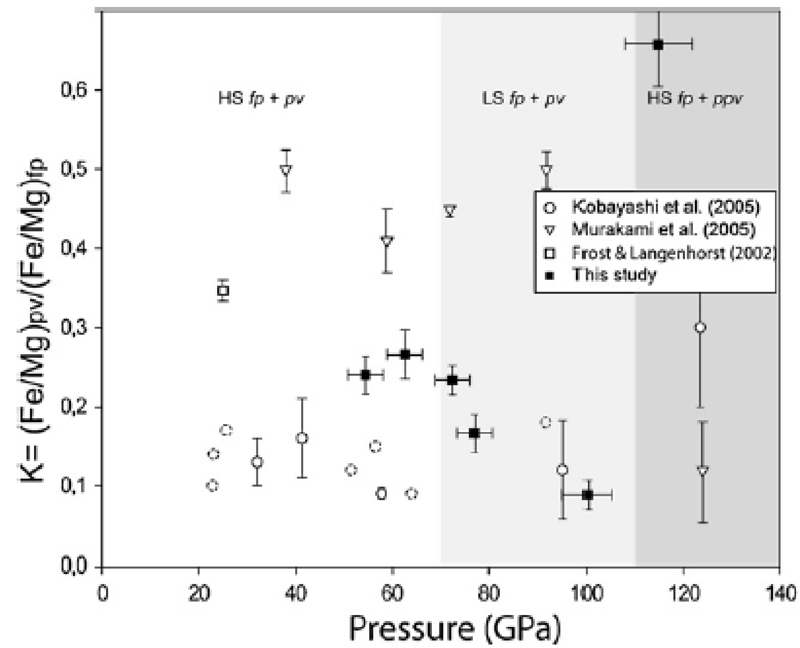

Fig. 4. Fe–Mg exchange coefficients between pv (or ppv) and fp plotted as a function of pressure. The coefficients published by Murakami et al. (2005) and Kobayashi et al. (2005) are reported for information. The three grey-shaded fields emphasize the stability fields of the successive coexisting phases: HS or LS fp+pv (Badro et al., 2003) and LS fp+ppv (Murakami et al., 2004).

Iron Partitioning in Earth's Mantle: Toward a Deep Lower Mantle Discontinuity

James Badro,[1] Guillaume Fiquet,[1] François Guyot,[1] Jean-Pascal Rueff,[2] Viktor V. Struzhkin,[3] György Vankó,[4] Giulio Monaco[4]

"... at pressures greater then 70 GPa or at depths greater than 2000 km, perovskite would then be completely iron-free, and any iron would be transferred into ferropericlase"

$$K_D = \left(\frac{X_{Fe}}{X_{Mg}}\right)^{Pv} \Big/ \left(\frac{X_{Fe}}{X_{Mg}}\right)^{Fp}$$

2 MAY 2003 VOL 300 SCIENCE www.sciencemag.org

GEOPHYSICAL RESEARCH LETTERS, VOL. 32, L19301, doi:10.1029/2005GL023257, 2005

Fe-Mg partitioning between (Mg, Fe)SiO_3 post-perovskite, perovskite, and magnesiowüstite in the Earth's lower mantle

Yusuke Kobayashi,[1] Tadashi Kondo,[1] Eiji Ohtani,[1] Naohisa Hirao,[1]
Nobuyoshi Miyajima,[2] Takehiko Yagi,[2] Toshiro Nagase,[3] and Takumi Kikegawa[4]

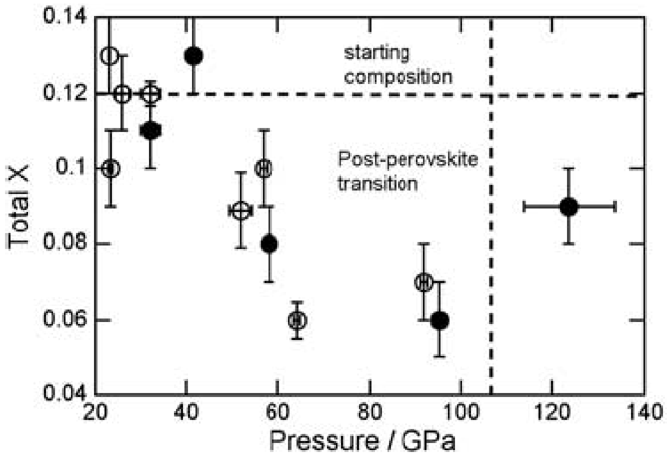

Figure 4. Total *X* [FeO/(FeO + MgO) in molar ratio] calculated from each *X* of PPv or Pv and Mw. Open and solid circles represent total *X* obtained from XRD and that from ATEM, respectively.

ARTICLE IN PRESS
EPSL-09155; No of Pages 11
ELSEVIER
Available online at www.sciencedirect.com
ScienceDirect
Earth and Planetary Science Letters xx (2008) xxx–xxx
EPSL
www.elsevier.com/locate/epsl

Element partitioning between magnesium silicate perovskite and ferropericlase: New insights into bulk lower-mantle geochemistry

Anne-Line Auzende [a,*], James Badro [a,b], Frederick J. Ryerson [b], Peter K. Weber [b], Stewart J. Fallon [b], Ahmed Addad [c], Julien Siebert [b], Guillaume Fiquet [a]

[a] IPGP, IMPMC, Université Paris VI & Paris VII, CNRS, Department of Mineralogy, campus Boucicaut, 140 rue de Lourmel, 75015 Paris, France
[b] LLNL, Energy and Environment, Experimental geophysics, University of California, Livermore, CA 94550, United States
[c] LSPES, CNRS, Université des Sciences et Technologies de Lille, Cité scientifique, 59655 Villeneuve d'Ascq, France

Received 12 July 2007; received in revised form 18 January 2008; accepted 3 February 2008

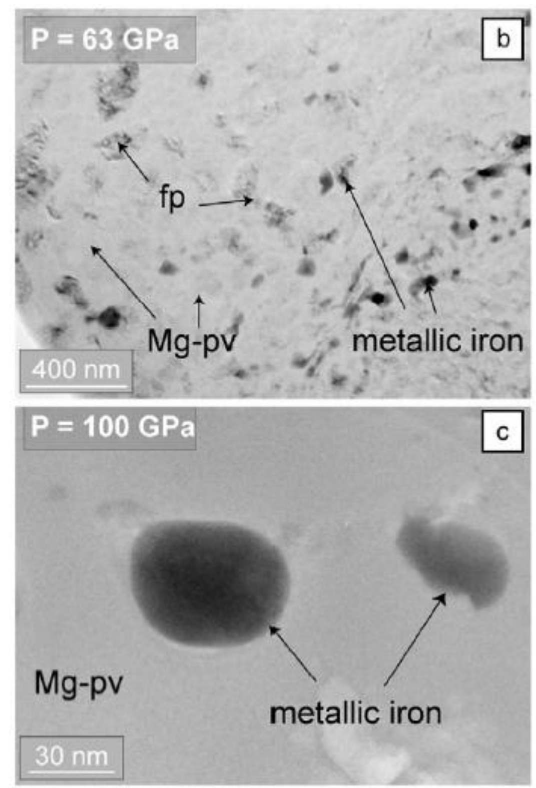

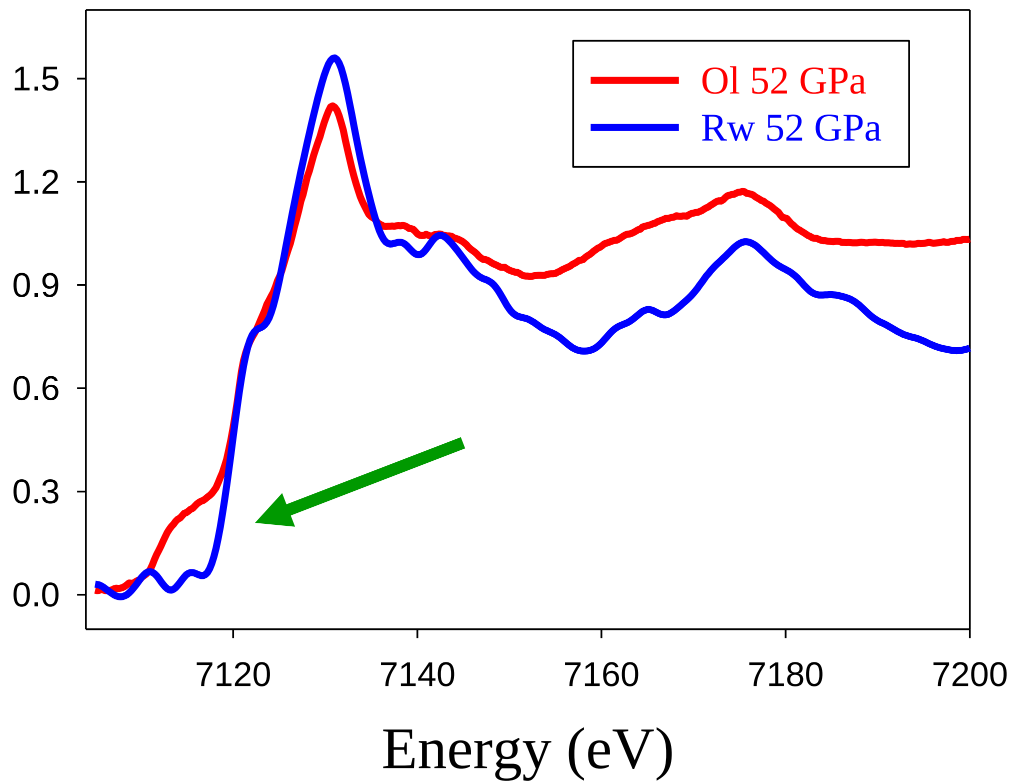

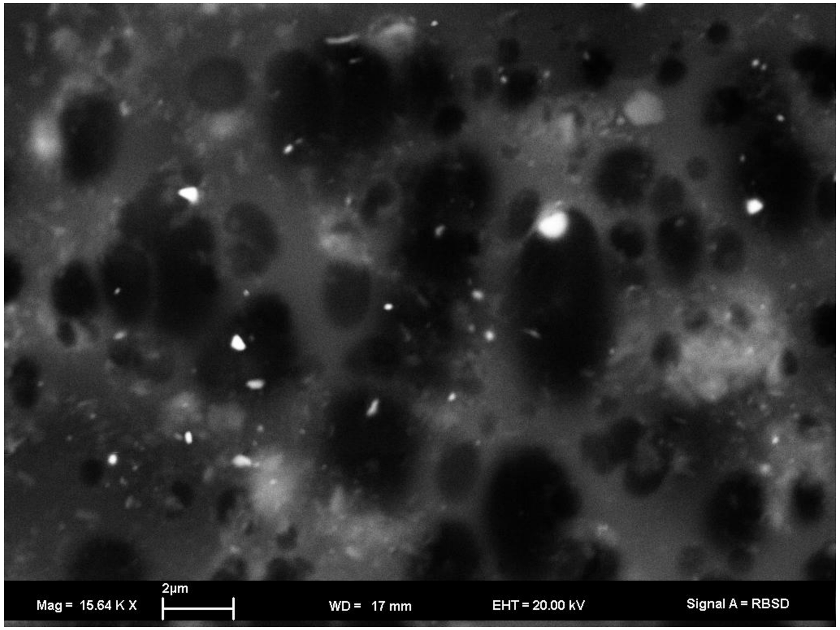

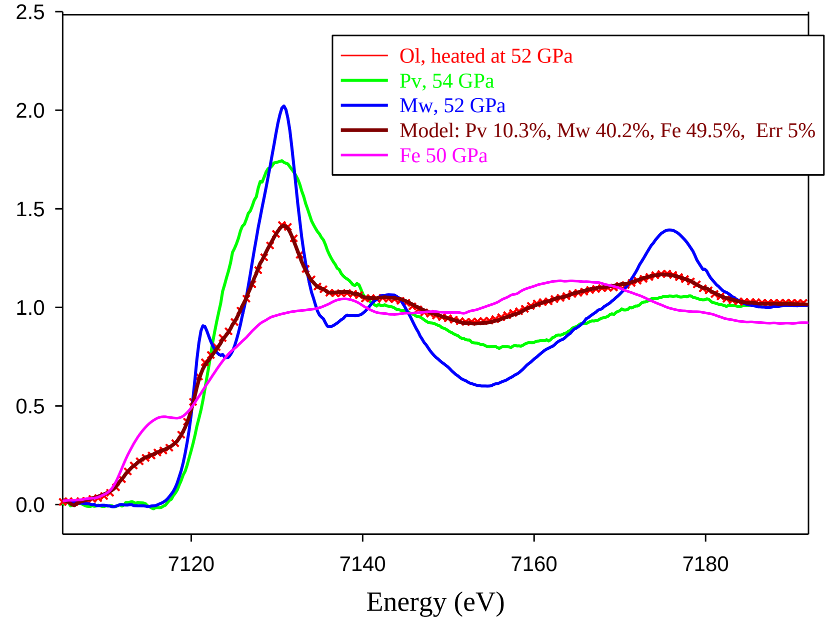

Olivine, laser-heated at 52(2) GPa

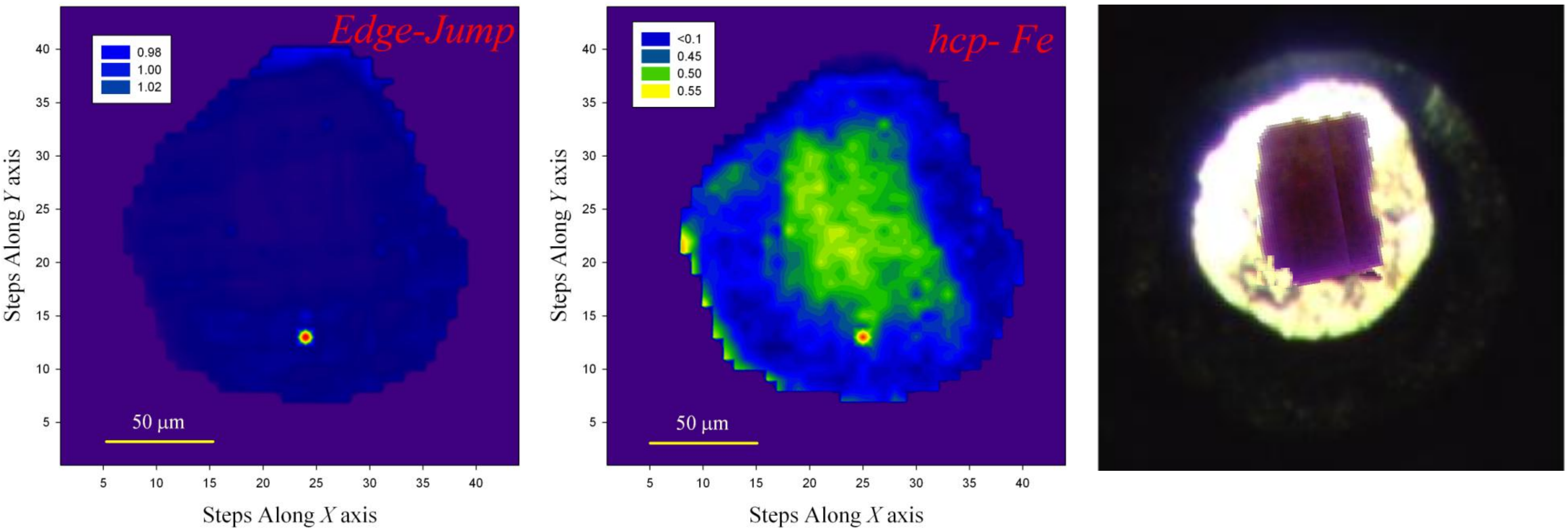

Olivine $(Mg_{0.88}Fe_{0.12})_2SiO_4$,
Laser heated at 52 GPa and 2300 K

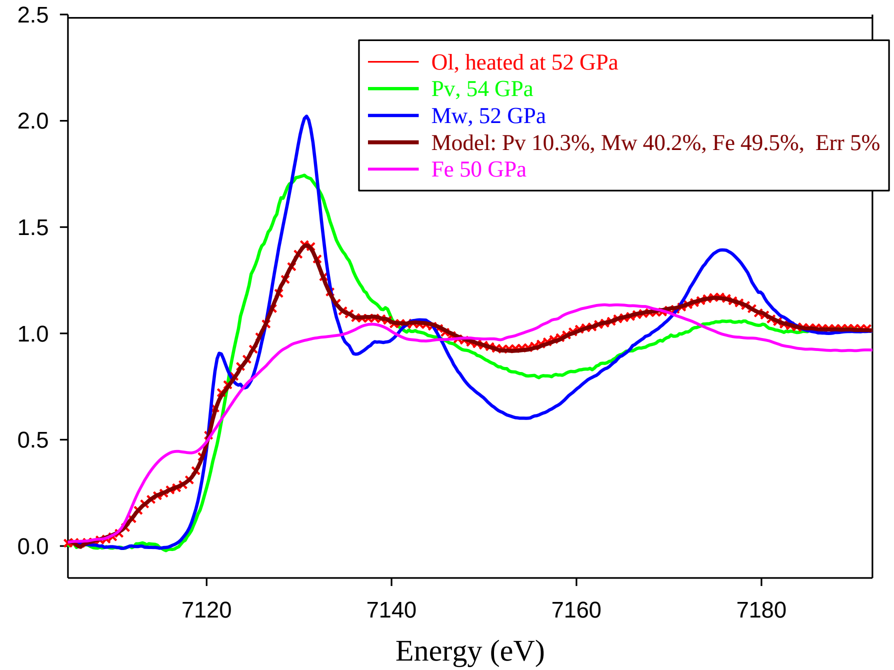

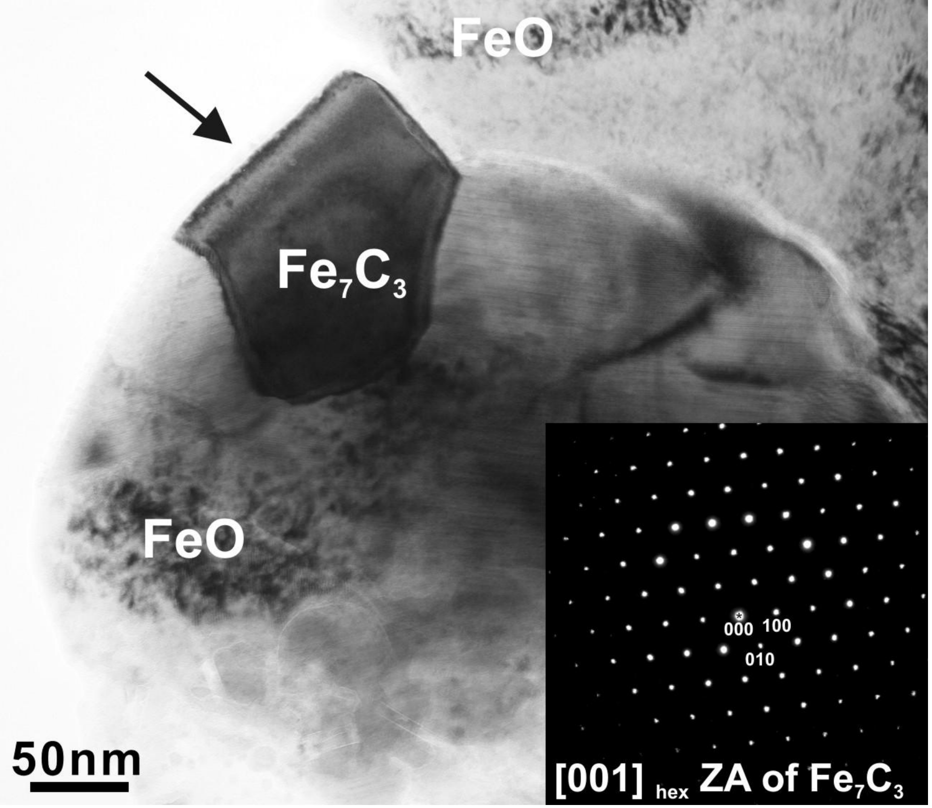

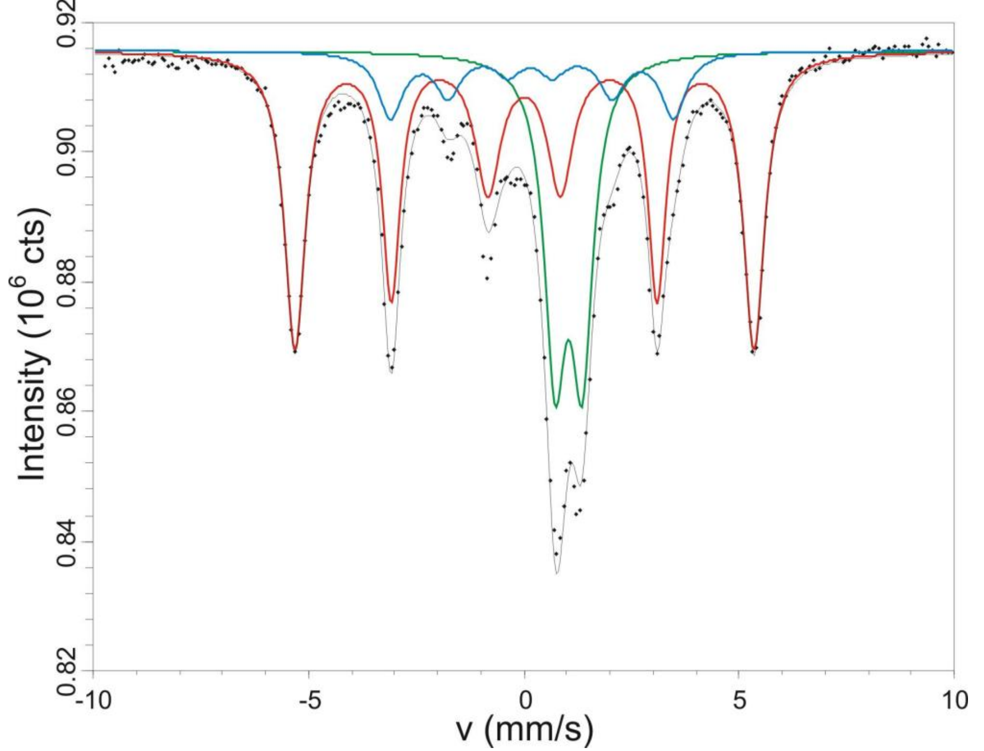

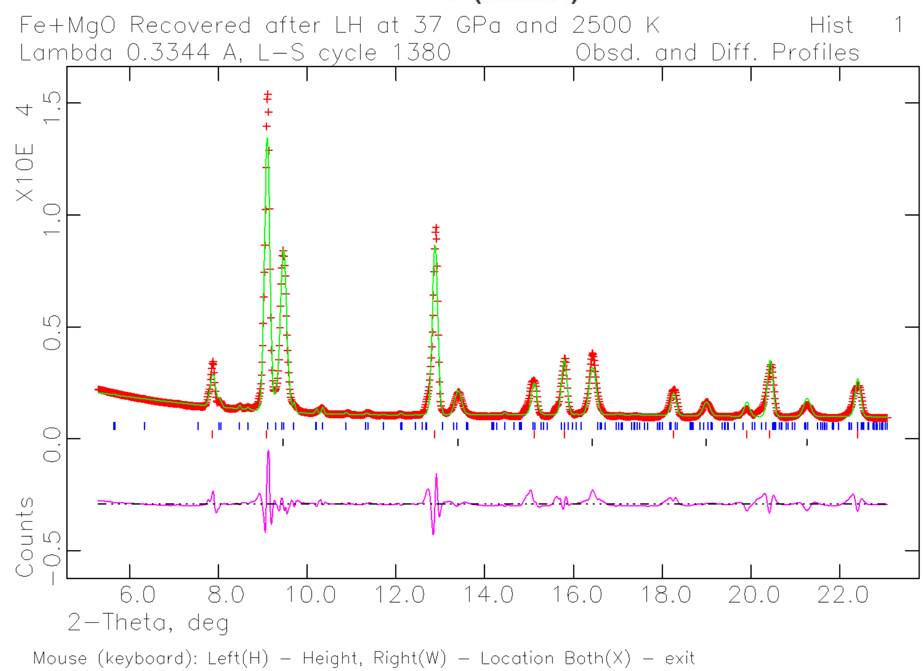

Fe+MgO
Recovered after heating
at 2700(100) K and 72(3) GPa

Rw+Graphite, laser-heated at 35(3) GPa and 2200(100) K

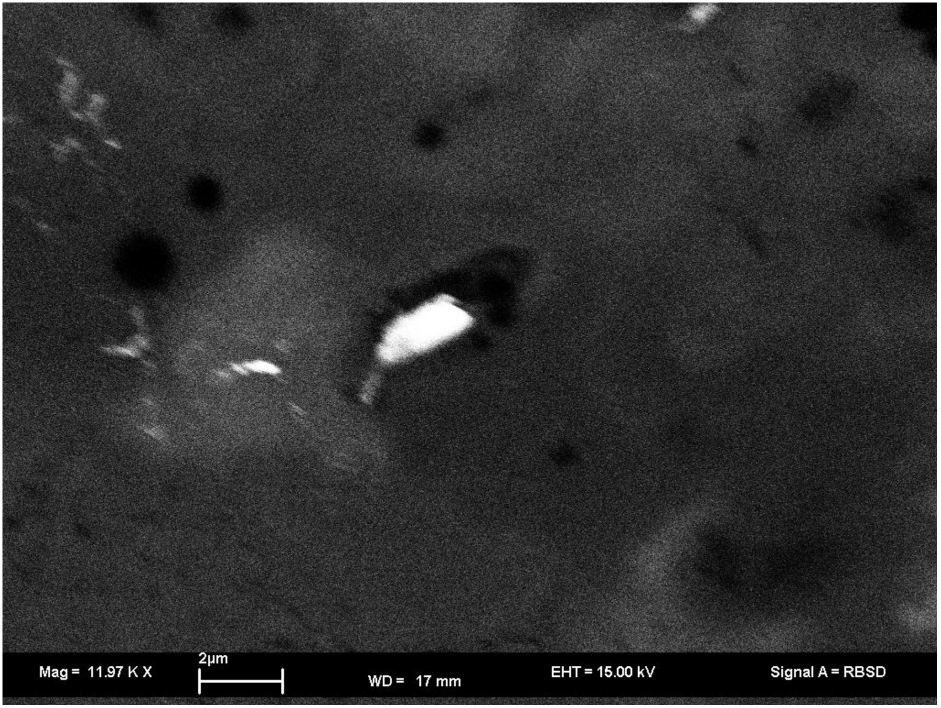

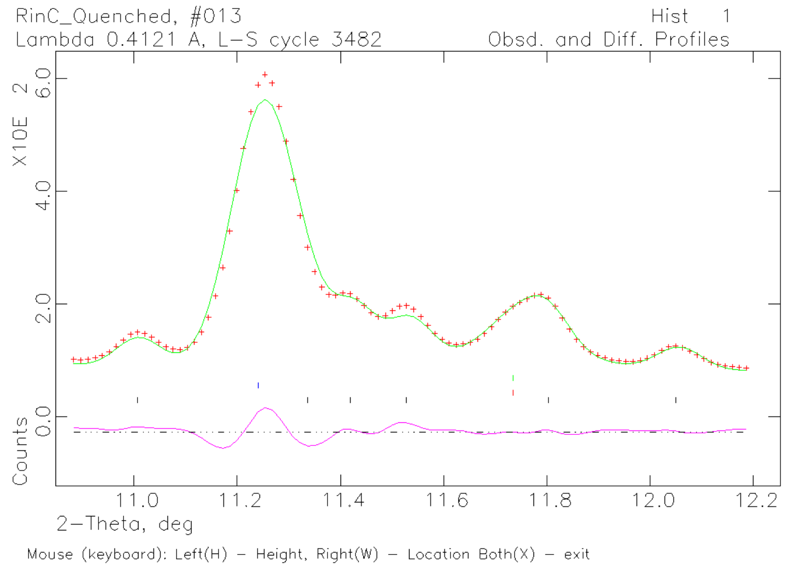

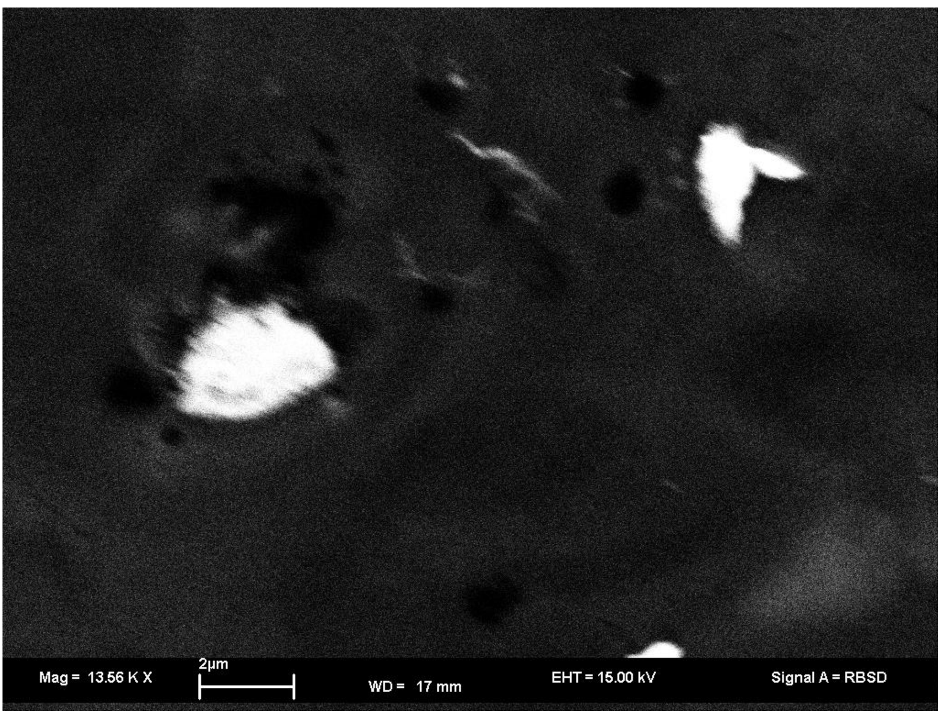

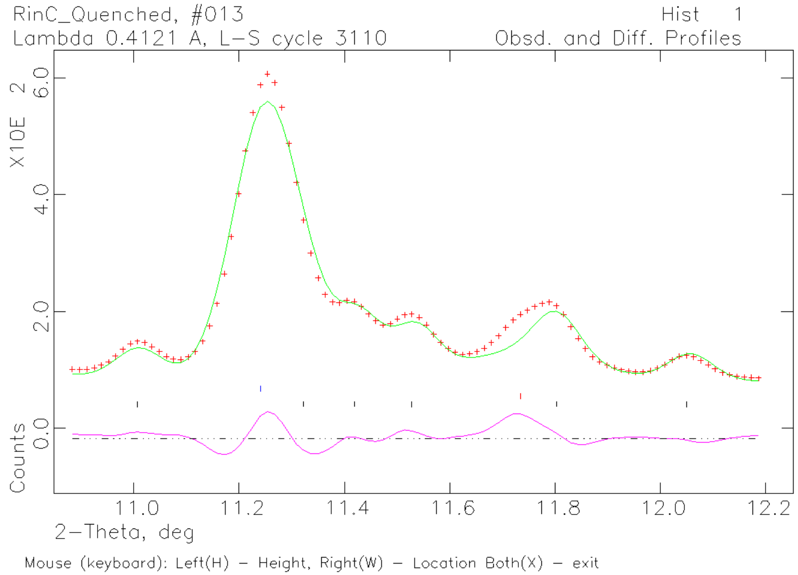

$[MgSiO_3]^{Pv} + [FeO]^{Fp} \longleftrightarrow [FeSiO_3]^{Pv} + [MgO]^{Fp}$

$RT\ln K_D = -\Delta H + T\Delta S - P\Delta V$

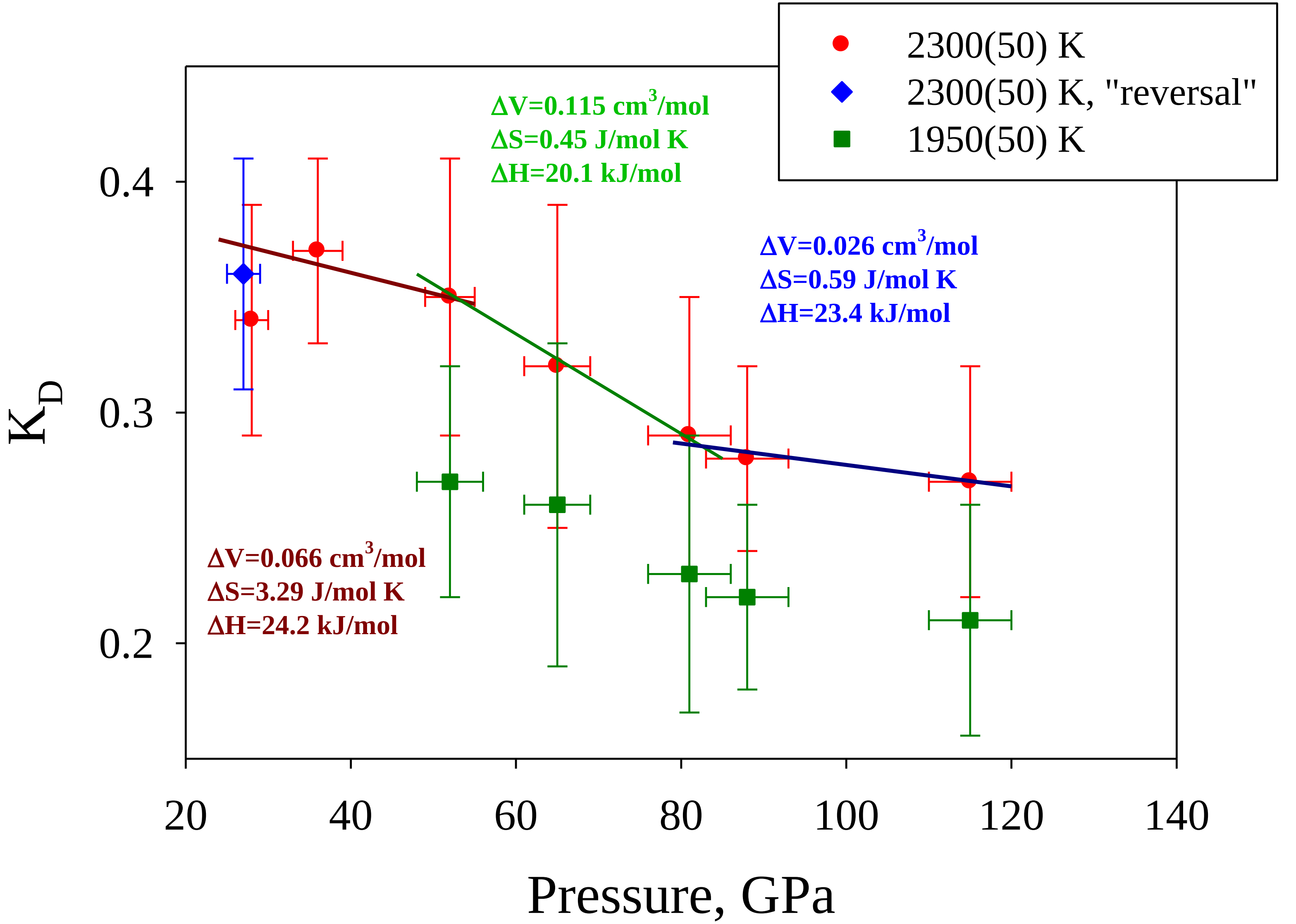

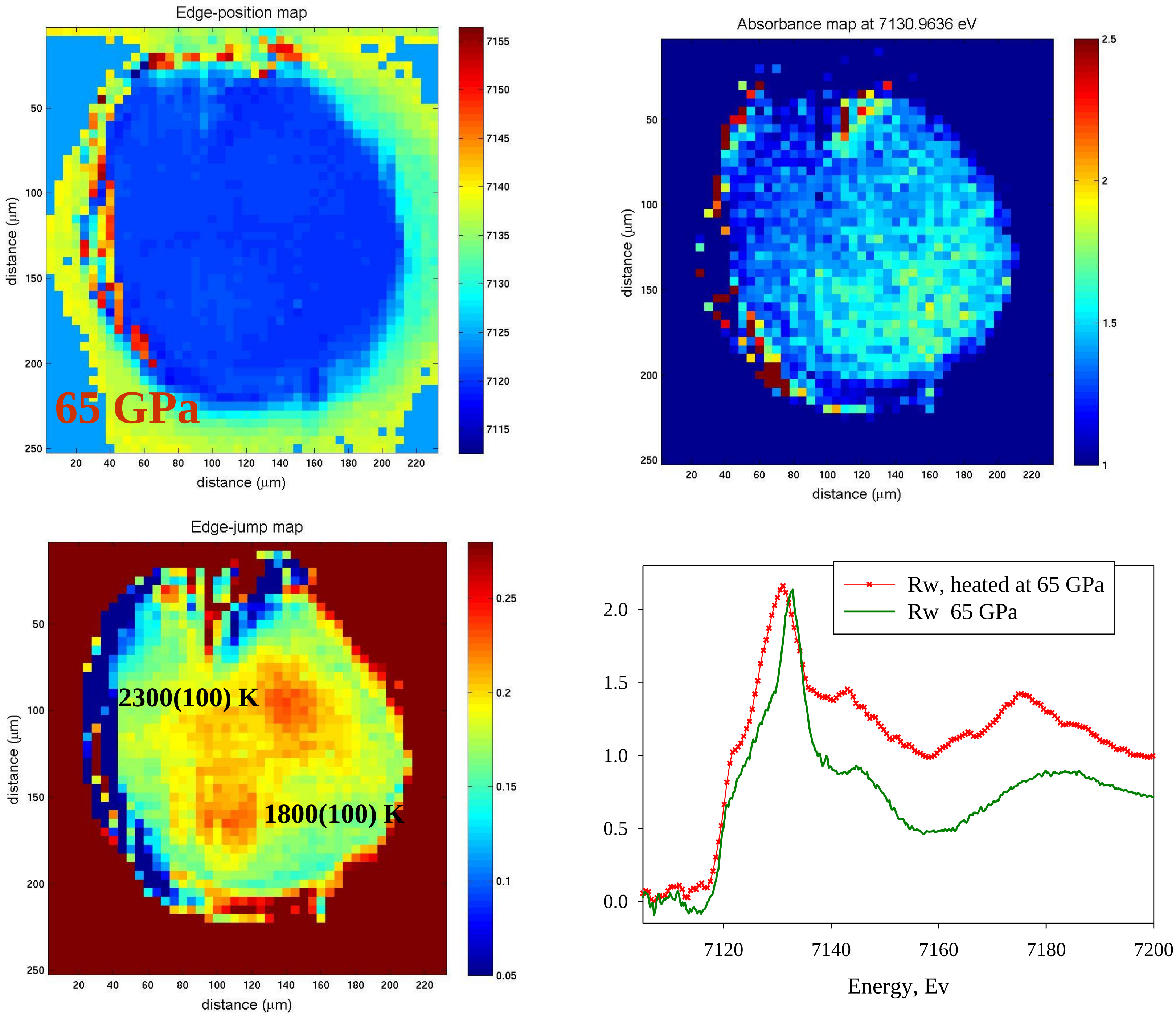

Edge-position map
65 GPa
distance (µm)
distance (µm)
Absorbance map at 7130.9636 eV
distance (µm)
distance (µm)
Edge-jump map
2300(100) K
1800(100) K
distance (µm)
distance (µm)
Rw, heated at 65 GPa
Rw 65 GPa
Energy, Ev

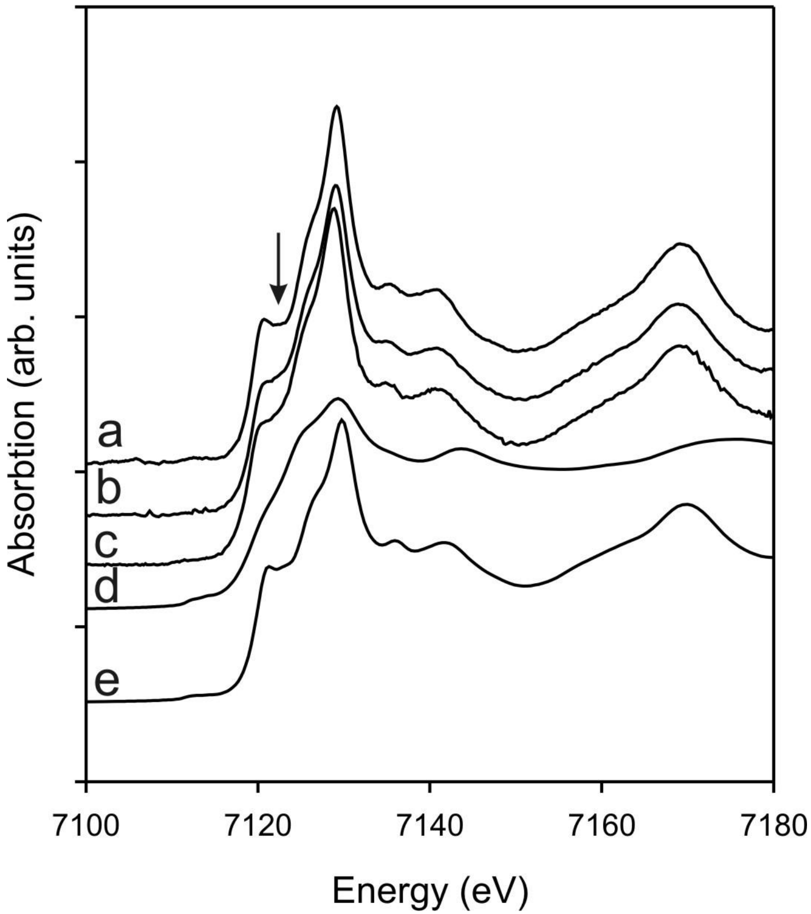

Fe K-edge XANES spectra of (Mg,Fe)O and FeO. a) Fe5 sample after compression; b) Fe13 sample after compression; c) Fe25 sample after compression; d) FeO wüstite sample. e) starting Fe13 material. The arrow indicates the region of major changes in the XANES spectra.

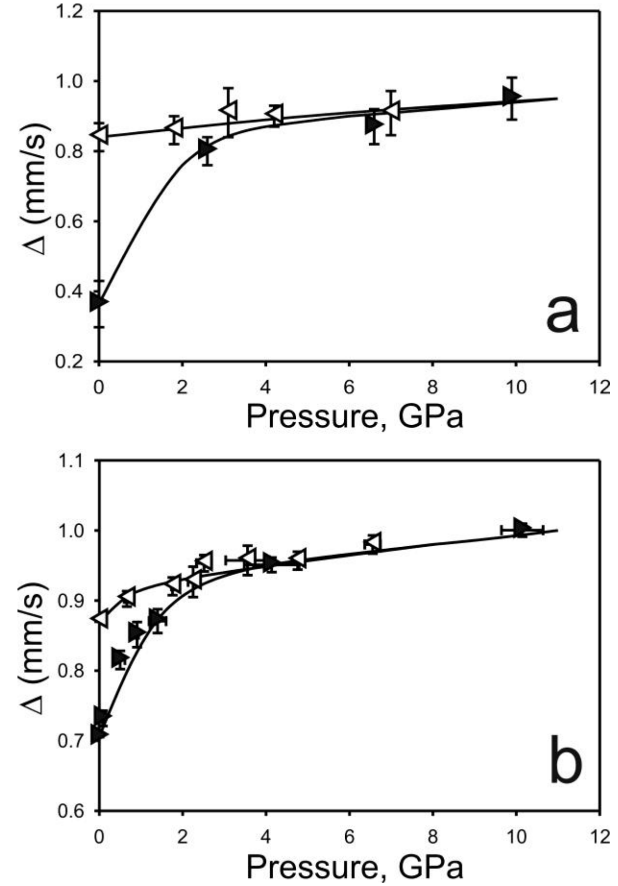

Pressure dependence of the quadrupole splitting of Fe5 and Fe20 samples (a and b, respectively). Black triangles pointing to the right are compression points, while white triangles pointing to the left are decompression points.

Kantor et al., 2007; 2008

Stability and Phase Transition(s)

Science 22 November 1996:
Vol. 274. no. 5291, pp. 1357 - 1359
DOI: 10.1126/science.274.5291.1357

‹ Prev | Table of

REPORTS

Stability of Perovskite ($MgSiO_3$) in the Earth's Mantle

Surendra K. Saxena, Leonid S. Dubrovinsky, Peter Lazor, Yngve Cerenius, Patrik Häggkvis
Michael Hanfland, Jingzhu Hu

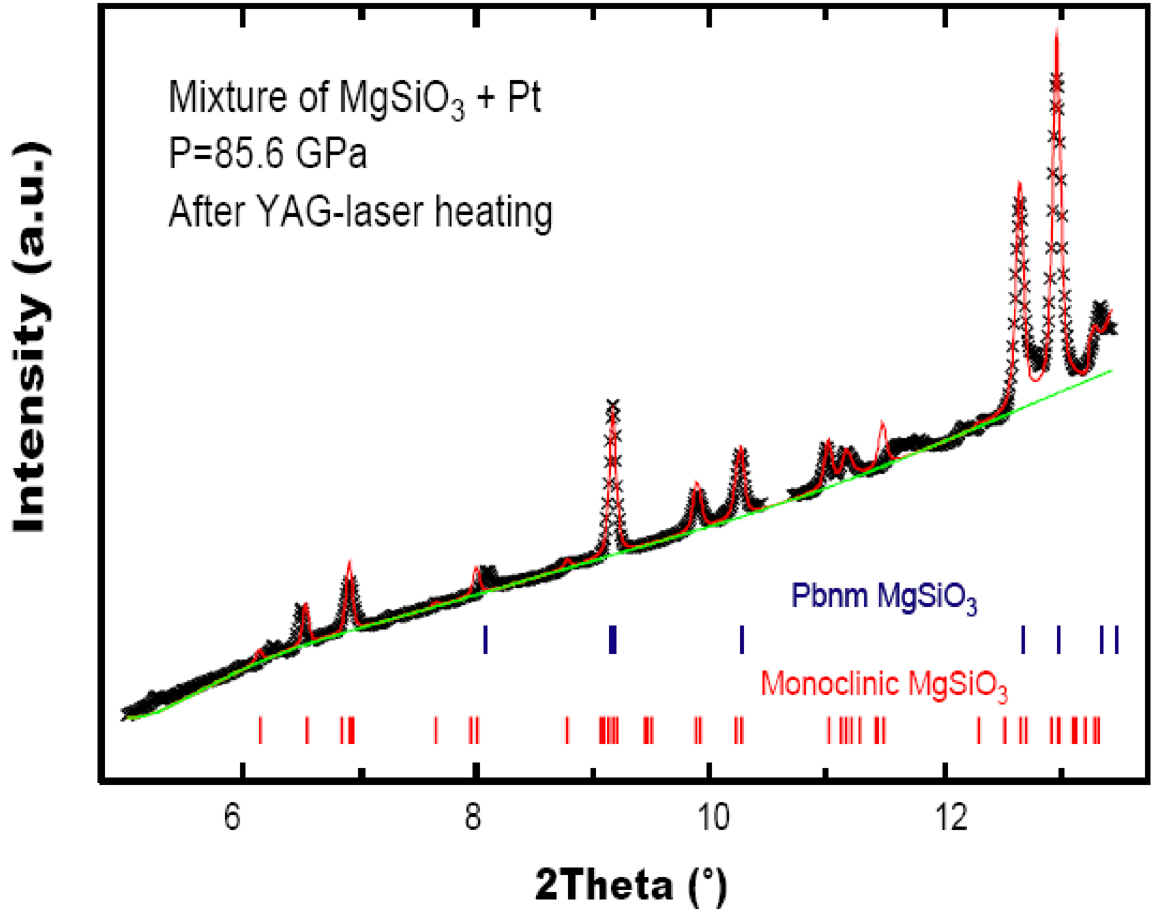

Science 23 June 1995:
Vol. 268. no. 5218, pp. 1743 - 1745
DOI: 10.1126/science.268.5218.1743

ARTICLES

High-Temperature Phase Transition and Dissociation Perovskite at Lower Mantle Pressures

Charles Meade [1], Ho Kwang Mao [1], and Jingzhu Hu [1]

D. Andrault, 2007

Science 28 September 2001:
Vol. 293. no. 5539, pp. 2437 - 2440
DOI: 10.1126/science.1061235

‹ Prev | Table of Contents |

REPORTS

Stability and Structure of $MgSiO_3$ Perovskite to 2300-Kilometer Depth in Earth's Mantle

Sang-Heon Shim,[1*†] Thomas S. Duffy,[1] Guoyin Shen[2]

Results: optical absorption spectroscopy

(Mg$_{0.88}$Fe$_{0.12}$)O crystal

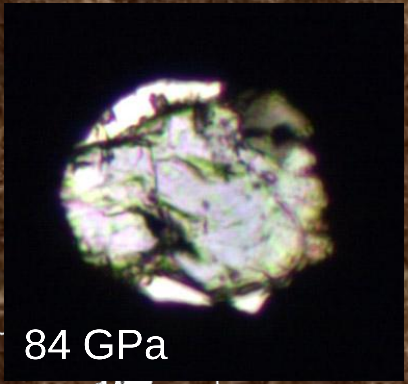

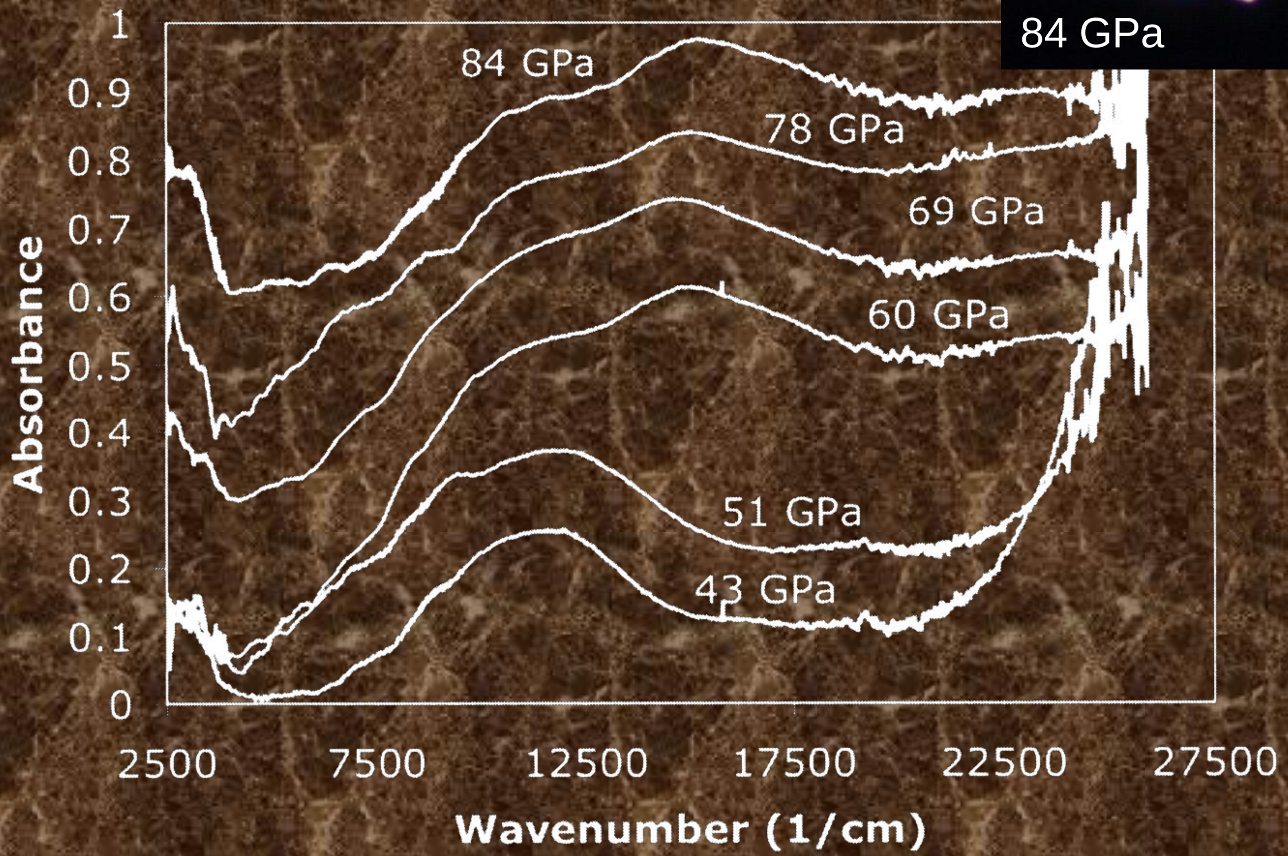

Optical absorption spectroscopy: literature data

Reduced Radiative Conductivity of Low-Spin (Mg,Fe)O in the Lower Mantle

A. F. Goncharov, V. V. Struzhkin, S. D. Jacobsen

SCIENCE 312, 1205 (2006)

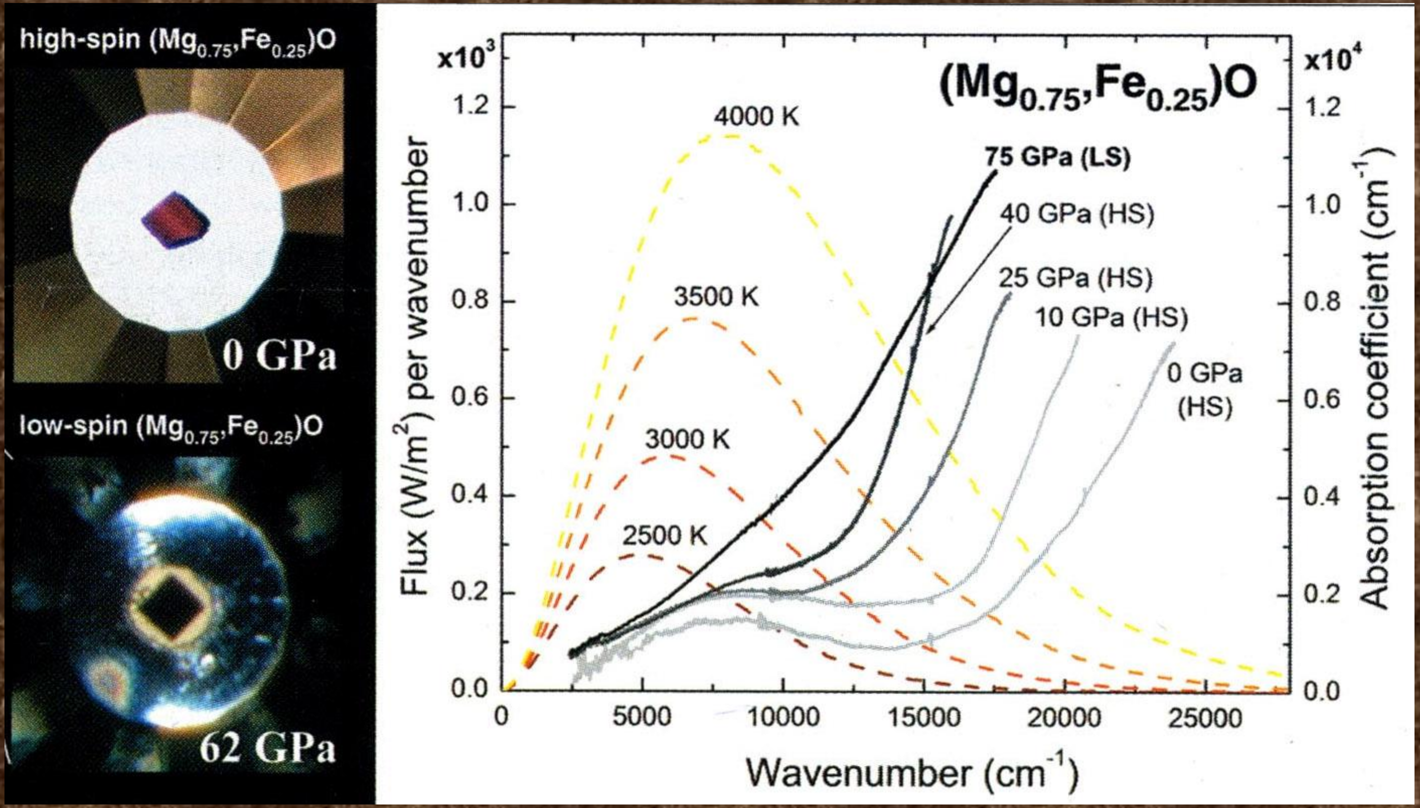

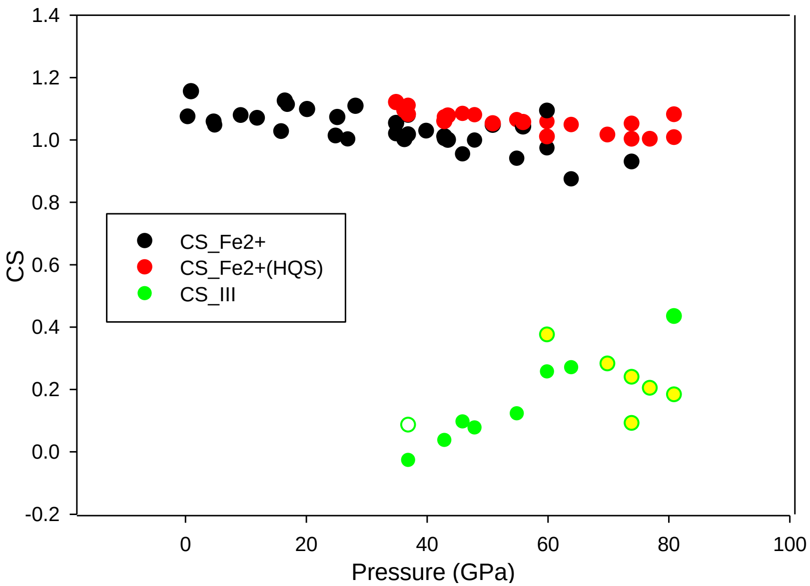
CS
CS_Fe2+
CS_Fe2+(HQS)
CS_III
Pressure (GPa)

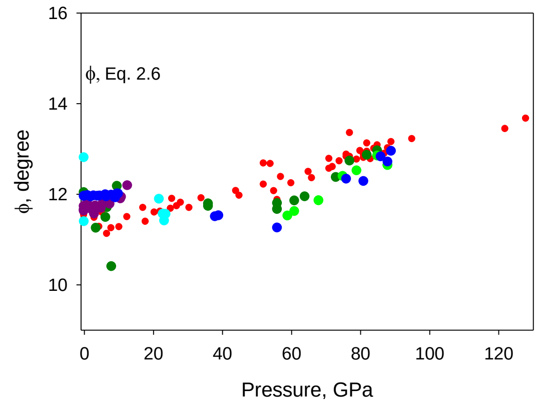
ϕ, Eq. 2.6
ϕ, degree
Pressure, GPa

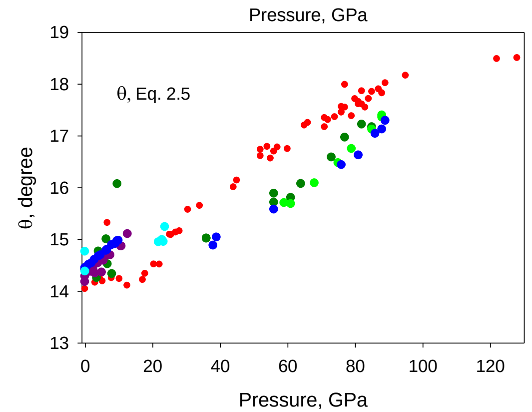
Pressure, GPa
θ, Eq. 2.5
θ, degree
Pressure, GPa

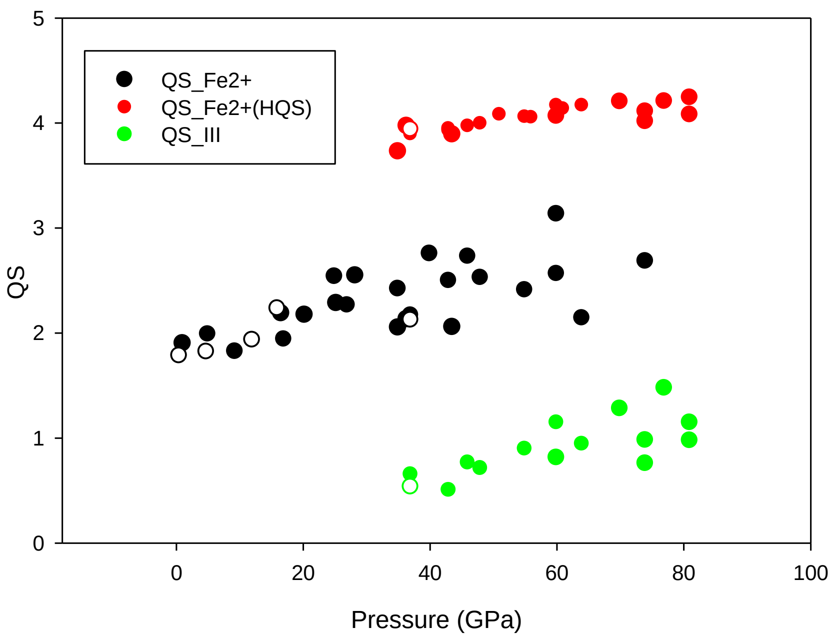
QS
QS_Fe2+
QS_Fe2+(HQS)
QS_III
Pressure (GPa)

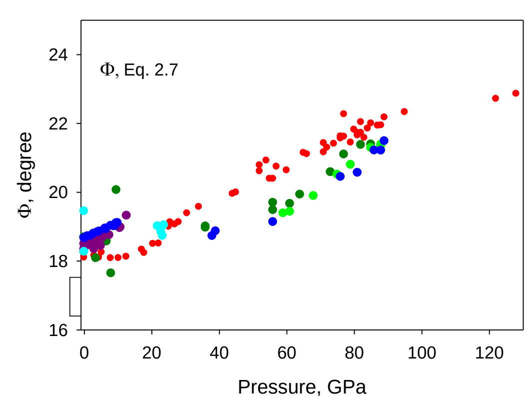
Φ, Eq. 2.7
Φ, degree
Pressure, GPa

$(Mg_{0.85}Fe_{0.15})O$, 85-90 GPa

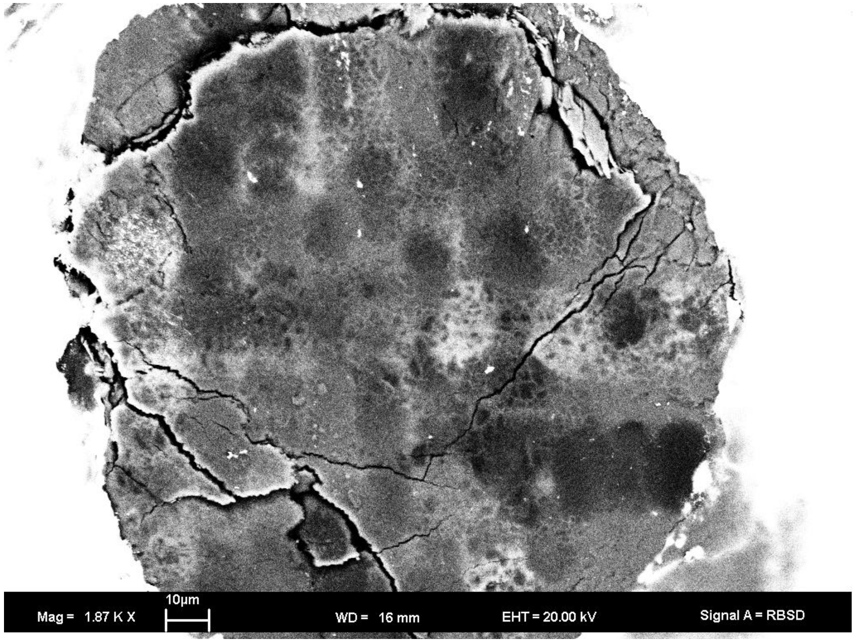

$(Mg_{0.875}Fe_{0.125})O$

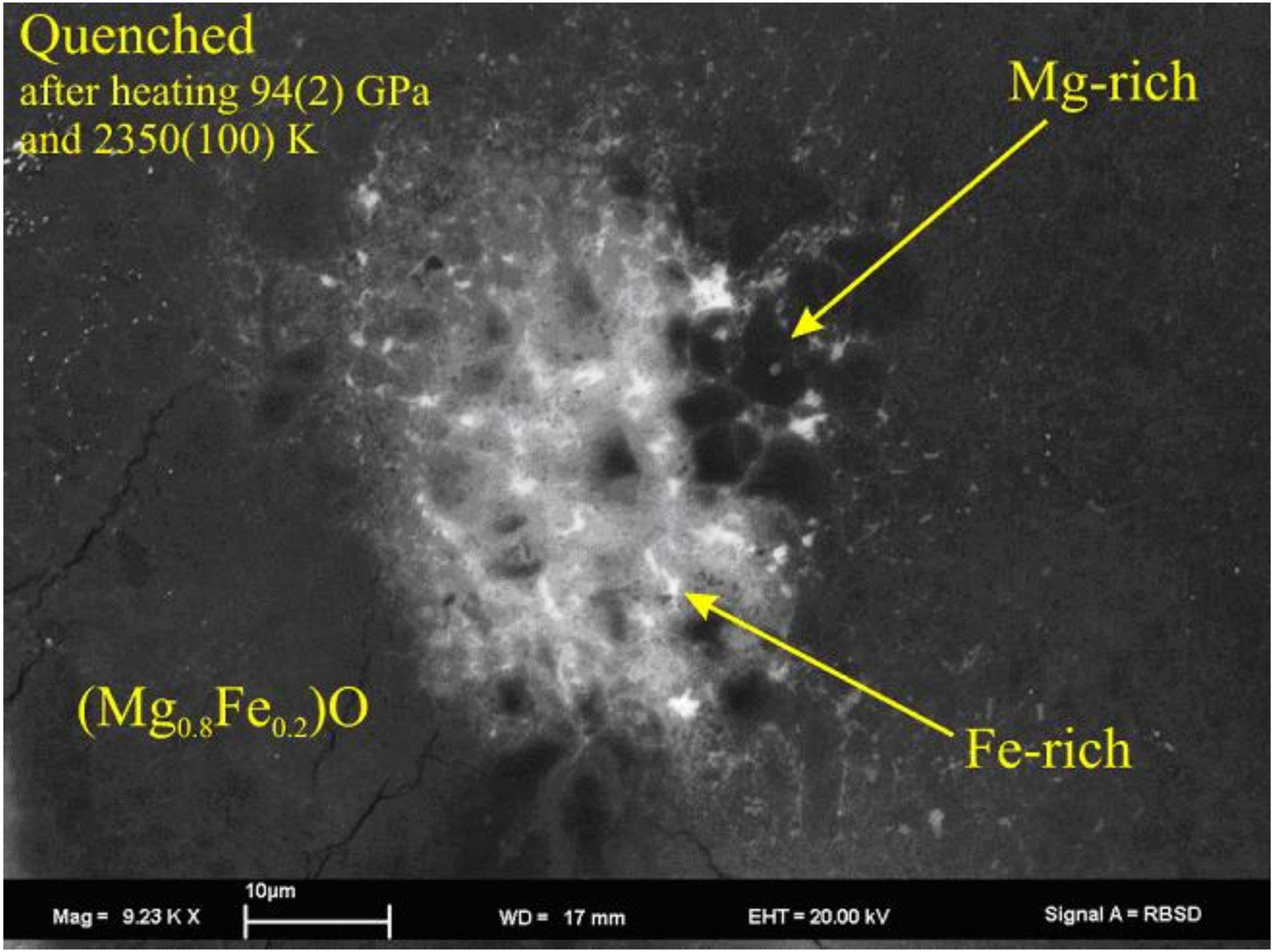
Quenched
after heating 94(2) GPa
and 2350(100) K
Mg-rich
$(Mg_{0.8}Fe_{0.2})O$
Fe-rich
Mag = 9.23 K X
10µm
WD = 17 mm
EHT = 20.00 kV
Signal A = RBSD

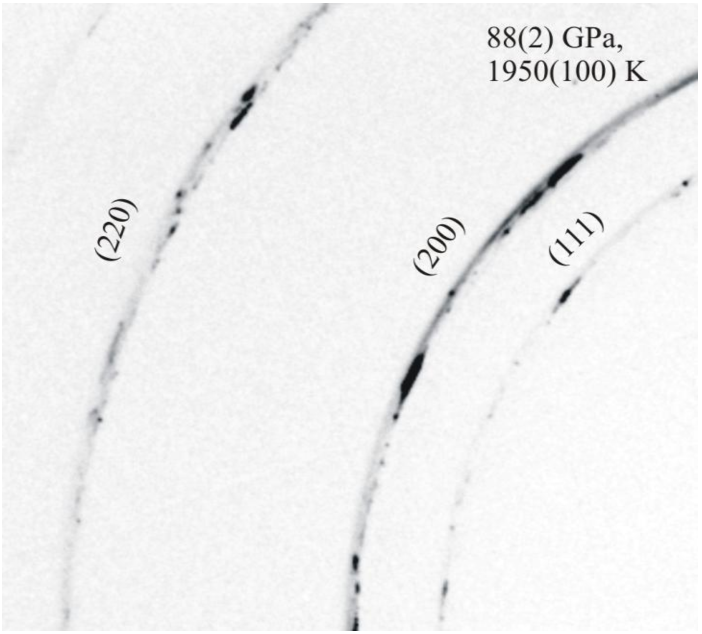
88(2) GPa,
1950(100) K
(220)
(200)
(111)

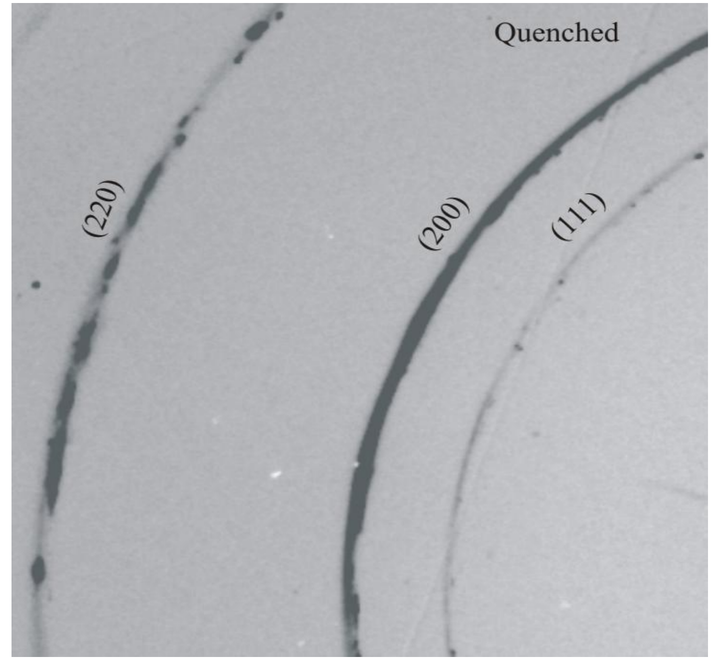
Quenched
(220)
(200)
(111)

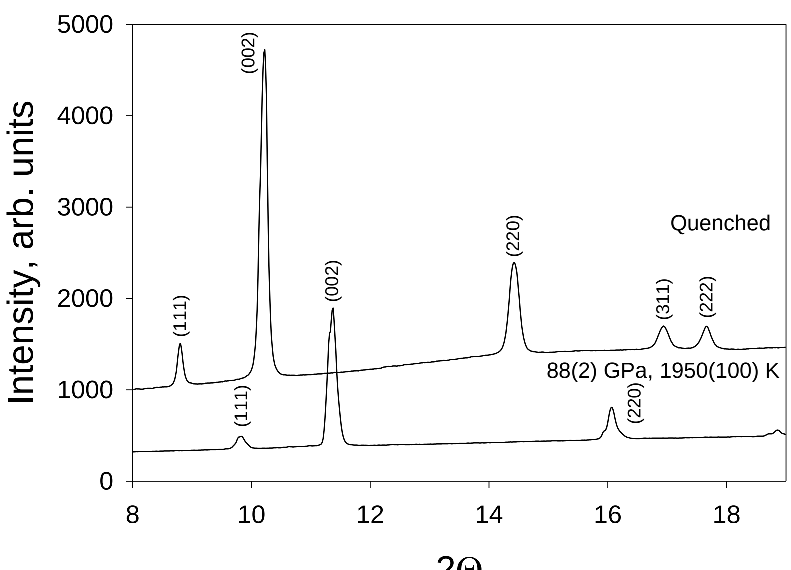
Intensity, arb. units
2Θ
Quenched
88(2) GPa, 1950(100) K
(111)
(002)
(002)
(220)
(311)
(222)
(111)
(220)

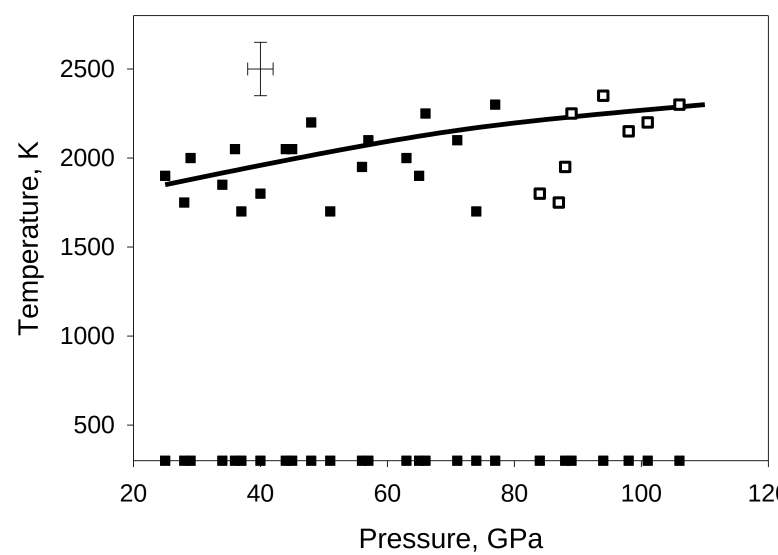
Temperature, K
Pressure, GPa

Fei and Mao, 1994

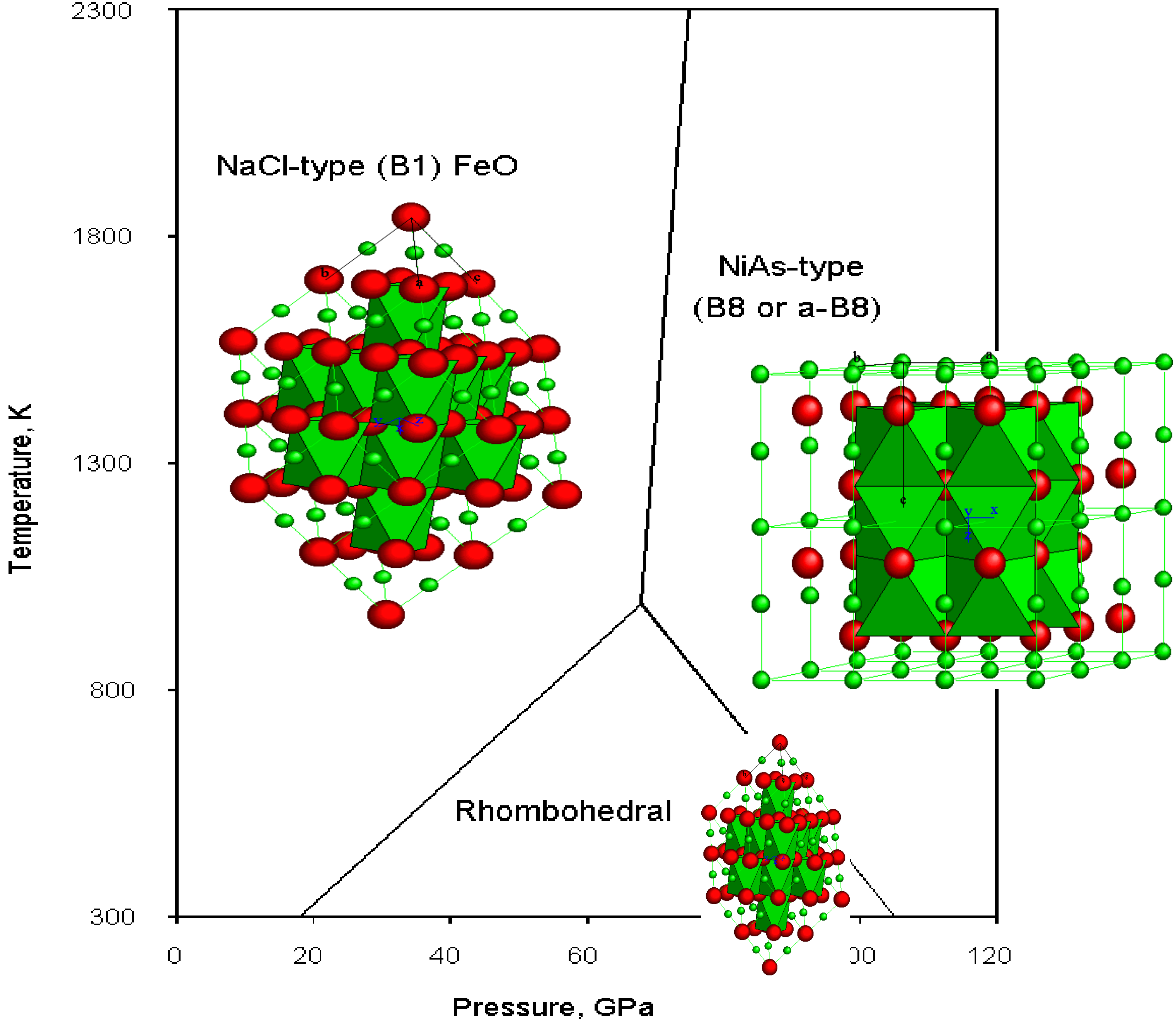

Dubrovinsky et al., 2001
Kondo et al., 2004
Kantor et al., 2008

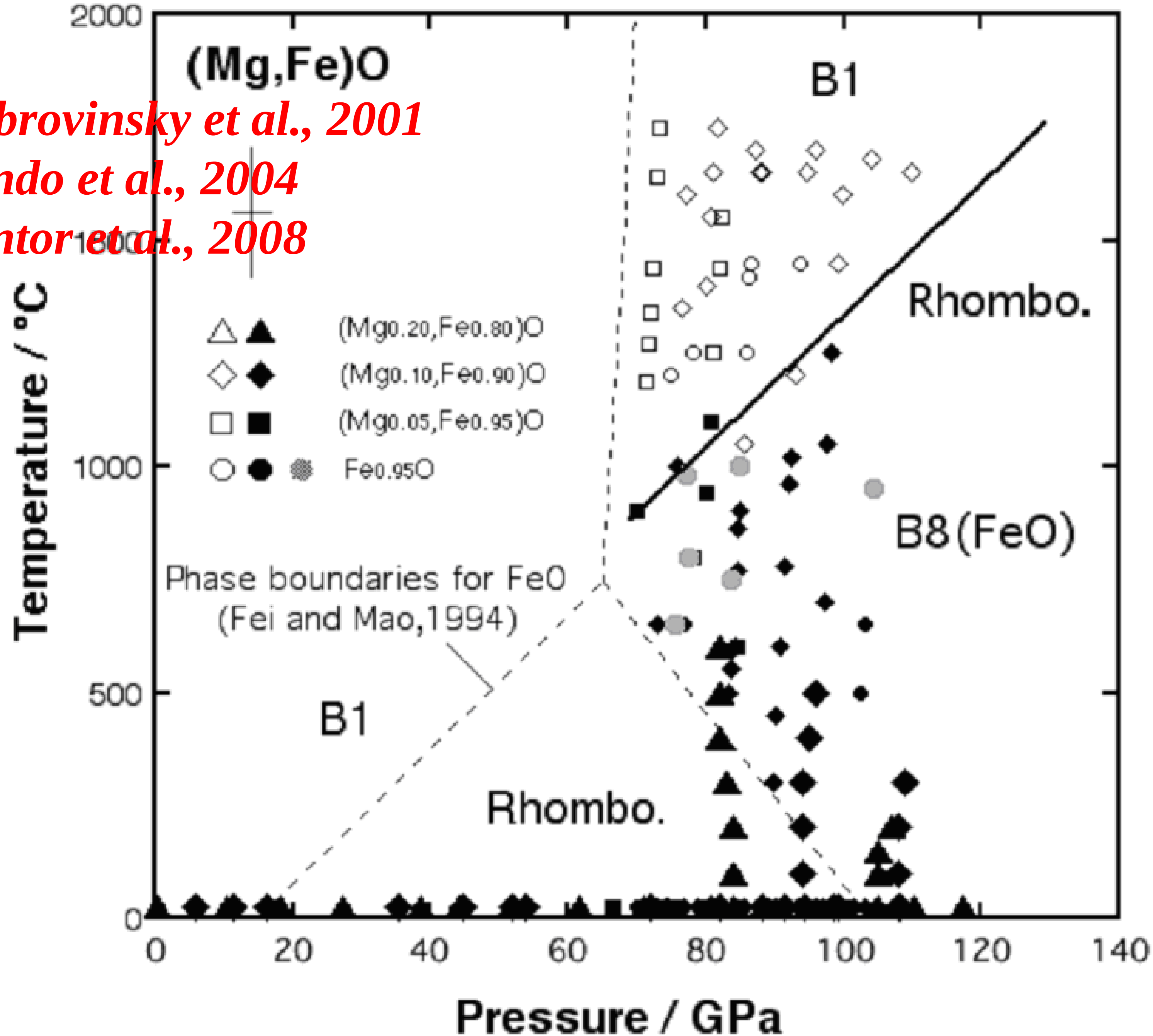

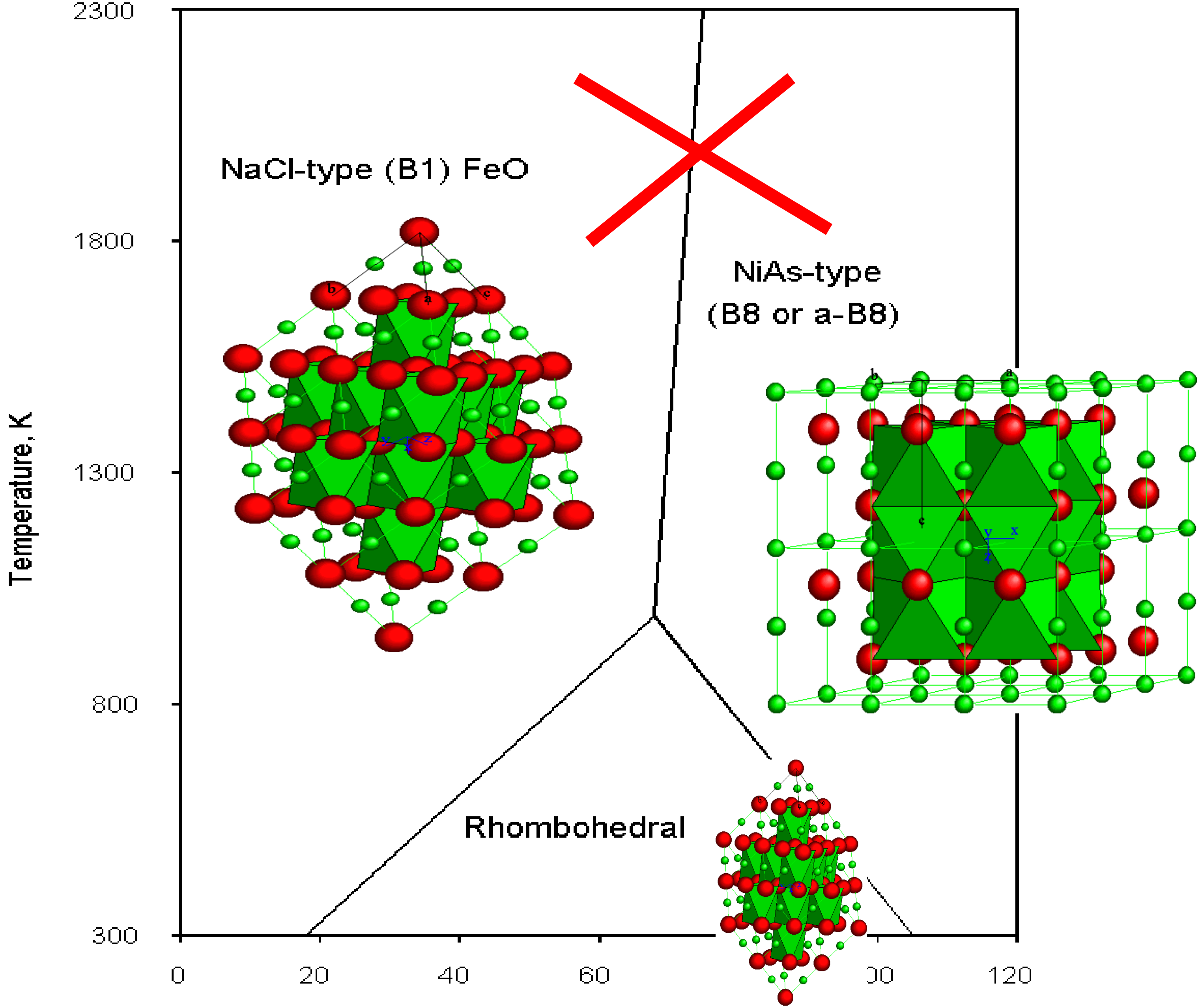
2300
1800
1300
800
300
Temperature, K
0
20
40
60
00
120
Pressure, GPa
NaCl-type (B1) FeO
NiAs-type
(B8 or a-B8)
Rhombohedral

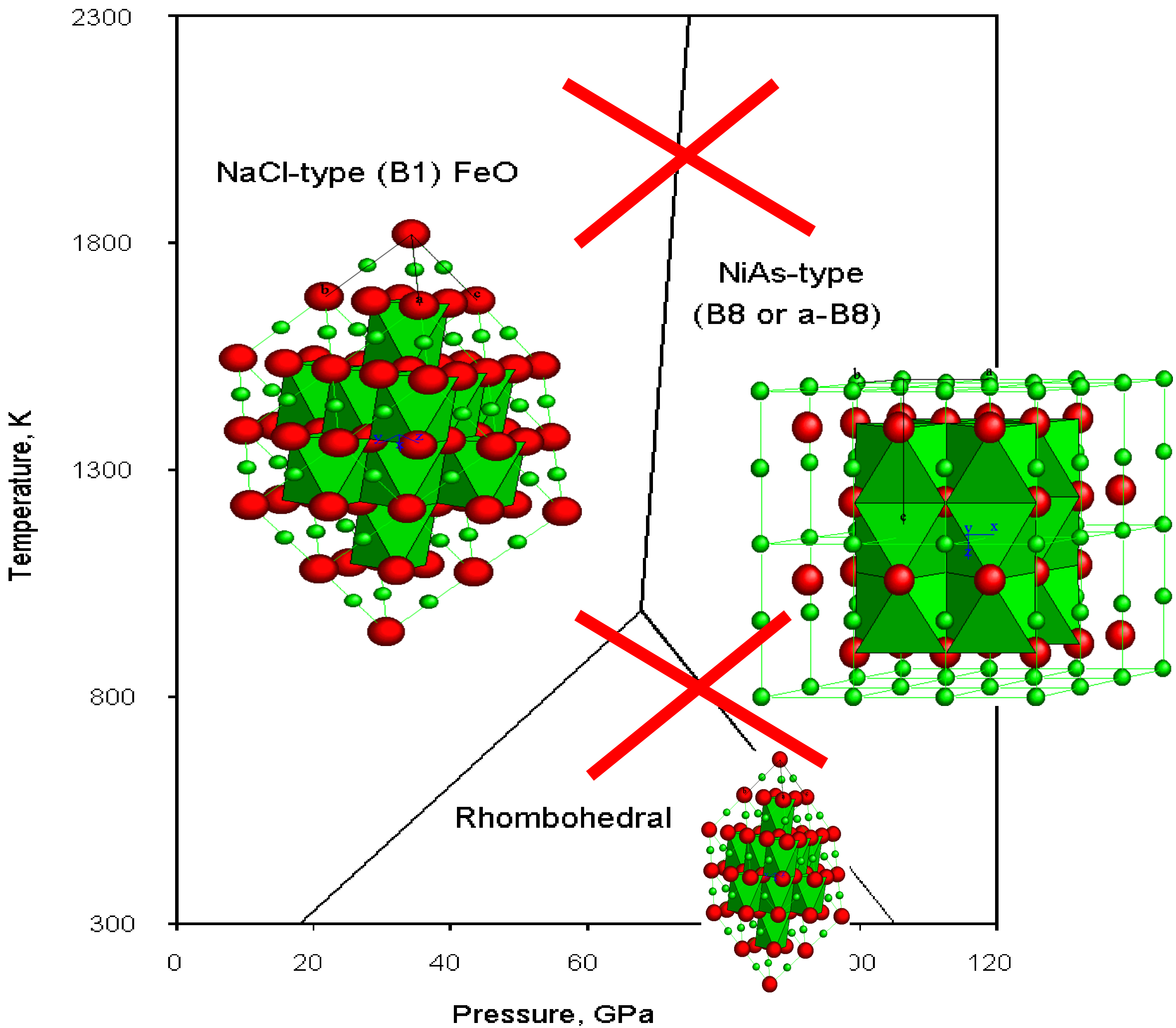

2300
1800
1300
800
300
0
20
40
60
00
120
Temperature, K
Pressure, GPa
NaCl-type (B1) FeO
NiAs-type
(B8 or a-B8)
Rhombohedral

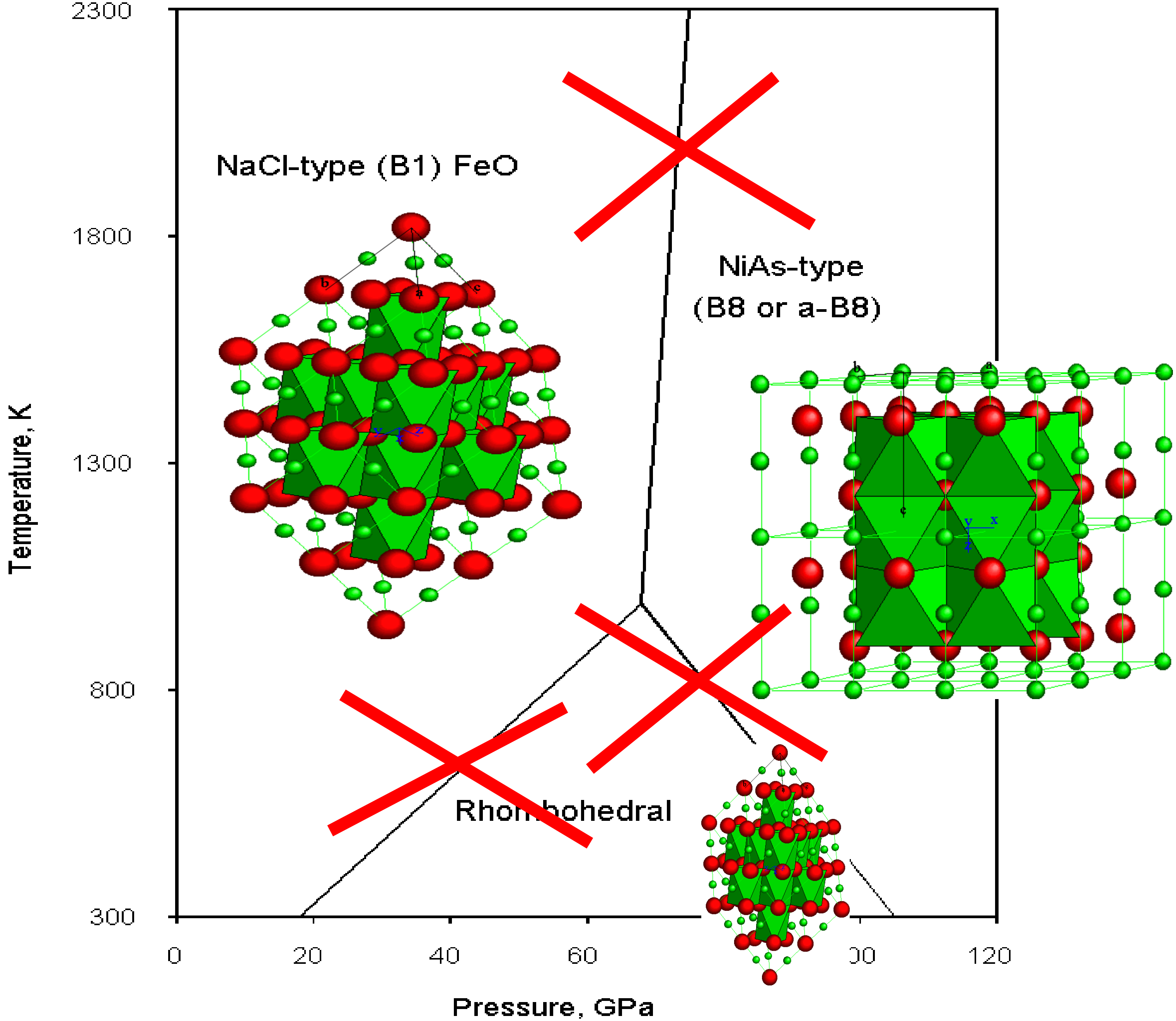

2300
1800
1300
800
300
Temperature, K
NaCl-type (B1) FeO
NiAs-type
(B8 or a-B8)
Rhombohedral
0
20
40
60
120
Pressure, GPa